Ollscoil na hÉireann, Corcaigh

National University of Ireland, Cork

An investigation of the role of ACTN1 in platelet formation and of platelet function in myeloma.

Thesis presented by

Leanne Rose O'Sullivan

for the degree of

Doctor of Philosophy

University College Cork

School of Biochemistry & Cell Biology

Head of School/Department: Dr. Justin McCarthy

Supervisors: Dr. Paul Young & Prof. Mary Cahill

2021

Table of Contents

Table of Contents 1

Declaration 7

Acknowledgements 8

Abbreviations 10

Abstract 14

1.0 Introduction 16

1.1 General Overview of Platelets 16

1.1.1 Platelet Count 16

1.1.2 Platelet Size 17

1.1.3 Platelet Lifespan 17

1.1.4 Platelet Production 18

1.1.4.1 Models of Platelet Production 18

1.1.5 Resting Platelet Structure 19

1.1.5.1 The Platelet Cytoskeleton 20

1.1.5.2 Organelles 21

1.1.5.3 Exosomes & Microparticles 24

1.1.5.4 Open Canalicular System 24

1.1.6 Platelets in Clot Formation 25

1.1.7 Platelets in Immunity & Inflammation 26

1.1.7.1 Interaction with Microbes 26

1.1.7.2 Interaction with the Endothelium in Inflammation 28

1.1.7.3 Platelets in Autoimmune Disorders 28

1.1.7.4 Platelet-Leucocyte Interactions 29

1.2 Platelets in an Inherited Bleeding Disorder : Actinin-1 33

1.2.1 The Actin Cytoskeleton 33

1.2.2 Overview of Actinin Isoforms 35

1.2.2 Functions of Actinin 38

1.2.2.1 Adhesion Sites 38

1.2.2.2 Cell Motility 38

1.2.2.3 Endocytosis & Exocytosis 39

1.2.2.4 Cytokinesis 39

1.2.2.5 Sarcomeric Z Disc 40

1.2.2.6 CNS Synapses 41

1.2.3 Actinin Structure 41
1.2.3.1 Actin Binding Domain 42
1.2.3.2 Rod Domain 42
1.2.3.3 Calmodulin-Like Domain 44
1.2.4 Actinin Interaction with Actin 44
1.2.5 Actinin Regulation 45
1.2.5.1 Calcium 46
1.2.5.2 Proteases 46
1.2.5.3 Phosphatidylinositols 46
1.2.5.4 Phosphorylation 47
1.2.5.5 Mechanosensory Regulation 48
1.2.6 Actinin Related Diseases 48
1.2.6.1 Focal Segmental Glomerulosclerosis (FSGS) 48
1.2.6.2 Athletic Performance 49
1.2.6.3 Myopathies 50
1.2.6.4 Cancer 51
1.2.6.5 Autoimmune Disease 52
1.2.6.6 Congenital Macrothrombocytopenia (CMTP) 53
1.2.7 Actinin In Platelets 55
1.3 Acquired Platelet Dysfunction in Cancer : Multiple Myeloma 56
1.3.1 Features of Platelet Function 56
1.3.1.1 Activation 56
1.3.1.3 Aggregation 61
1.3.1.3 Adhesion 62
1.3.2 Platelets in Cancer 62
1.3.2.1 Platelets in Tumour Growth & Progression 62
1.3.2.2 Tumour Protection by Platelets 63
1.3.2.3 Tumour-Educated Platelets 64
1.3.2.4 Cancer & Thrombosis 64
1.3.3 Treatment of Platelet Dysfunction 65
1.3.3.1 Anti-Platelet Therapies 65
1.3.3.2 Prohaemostatic Therapies 67
1.4 Thesis Overview 68
2.0 Investigation of Calmodulin-Like and Rod Domain Mutations Suggests Common Molecular Mechanism for α-Actinin-1-Linked Congenital Macrothrombocytopenia 69
2.1 Introduction 69

2.2 Methods 72
2.2.1 Actinin-1 cDNA Constructs 72
2.2.2 Protein Expression & Purification 73
2.2.3 Thermal Shift Assays 73
2.2.4 Isothermal Calorimetry 74
2.2.5 Actin Co-Sedimentation Assays 74
2.2.6 Cytoskeletal Purification Assays 75
2.2.7 Immunofluorescence Studies 76
2.2.8 Statistical Analysis 77
2.3 Results 78
2.3.1 Expression & Purification of CaM-domain and Full Length Actinin-1 Proteins 78
2.3.2 Actinin-1 CaM-Like Domains with CMTP-Causing Mutations Have Decreased Thermal Stability But Maintain Calcium Binding Ability. 80
2.3.3 Calcium Binding Affinity of Actinin-1 CaM-like Domains is Not Dramatically Affected by the G764S and R752Q CMTP-Causing Mutations. 82
2.3.4 CMTP-Causing Mutations in the Rod and CaM-like Domain Enhance the F-actin Bundling Ability of Actinin-1. 84
2.3.4 CMTP-causing mutations in the CaM-like domain of actinin-1 increase the stability of its association with the actin cytoskeleton in cells. 87
2.4 Discussion 91
2.4.1 CaM-like Domain Mutations 93
2.4.2 Rod Domain Mutations 95
3.0 Assessment of Actinin in Platelet Production 98
3.1 Introduction 98
3.1.1 Overview of Platelet Formation 98
3.1.2 Megakaryocyte Podosomes and Their Role in Platelet Formation 100
3.1.3 Actinin in Megakaryocytes 103
3.1.4 Megakaryocytic Cell Models 104
3.1.5 The Cytoskeleton in Platelet Function 105
3.1.5.2 Platelet Actin Nodules 107
3.1.6 Actinin in Platelets 107
3.1.6.1 Actinin Isoforms in Platelets 107
3.1.6.2 Actinin Localisation in the Platelet 108
3.1.6.3 Regulation of Actinin in Platelets 109
3.1.6.4 Actinin Interaction With Platelet Signalling Molecules 110
3.1.6.5 Actinin in Platelet Activation 113
3.2 Methods 114

3.2.1 Culture of MEG-01, CMK and HEK293FT Cells 114
3.2.2 Culture and Differentiation of Primary Murine Megakaryocytes 114
3.2.3 Staining of Suspension Cells 115
3.2.4 Transfection of CMK & MEG-01 Cells 115
3.2.4.1 Optimisation of Nucleofection using MEG-01 Cells 115
3.2.4.2 Nucleofection of CMK Cells 116
3.2.4.3 Trial of Various Electroporation Buffers 116
3.2.4.4 Optimisation of Electroporation using MEG-01 Cells 116
3.2.4.5 Transfection of CMK & MEG-01 Cells. 116
3.2.5 Transfection of Primary Cells 117
3.2.5.1 Transfection of Primary Cells with Lipofectamine-2000 117
3.2.5.2 Electroporation of Primary Cells 118
3.2.5.3 Nucleofection of Primary Cells 118
3.2.6 Lentiviral Infection of Primary Murine Megakaryocytes 118
3.2.6.1 Lentivirus Constructs 118
3.2.6.2 Optimisation of Transfection of HEK293FT Cells 119
3.2.6.3 Optimisation of lentiviral plasmid concentration ratios for virus production. 120
3.2.6.4 Optimisation of Lentivirus Production 121
3.2.6.5 Concentration of the Lentivirus 122
3.2.6.6 Assessment of Lentiviruses by Infection of HEK293FT cells 122
3.2.7 Infection of Primary Murine Megakaryocytes 124
3.2.8 Analysis of Actinin-1 and Actinin-4 in Platelets and Megakaryocytic Cell lines. 126
3.2.8.1 Protein Expression and Purification 126
3.2.8.2 Quantification of Actinin-1 and Actinin-4 by Western Blot 127
3.2.8.3 Pull-down of Actinin-1 and Actinin-4 from CMK cells 128
3.2.8.4 Immunofluorescent Imaging of Actinin-1 and Actinin-4 128
3.2.8.5 Assessment of Ploidy in Actinin-1 Transfected MEG-01 Cells 129
3.2.9 Analysis of Actinin-1 and Actinin-4 Heterodimers 130
3.2.9.1 Expression & Purification of Actinin-1 and Actinin-4 proteins 130
3.2.9.2 Nickel Column Purification 131
3.2.9.3 Amylose Column Purification 131
3.2.9.4 Analysis of Heterodimers expressed in BL21 E. *coli* by Native PAGE 131
3.2.9.5 Expression of Actinin-2 Rod Heterodimers in HEK293 Cells 132
3.3 Results 134
3.3.1 Transfection of MEG-01 and CMK cells 134
3.3.2 CMTP Mutations Do Not Affect MEG-01 Cell Ploidy 136

3.3.3 Actinin-1 and Actinin-4 Are Present in MEG-01, CMK and Human Platelets at Varying Concentrations....142
3.3.4 Actinin-1 / Actinin-4 Interacting Proteins....145
3.3.5 Actinin is Present in Proplatelets and Podosomes in Primary Megakaryocytes....146
3.3.5.1 Optimisation of Antibodies for Immunofluorescent Staining....147
3.3.5.2 Actinin is Present in Proplatelets and Podosomes in Primary Megakaryocytes....147
3.3.6 Transfection of Primary Murine megakaryocytes....156
3.3.7 Lentiviral Infection of Primary Murine Megakaryocytes....158
3.3.8 Production of Actinin-1 and Actinin-4 Heterodimers....160
3.4 Discussion....166
4.0 Platelet Hyperactivation in Multiple Myeloma is also Evident in Patients with Premalignant Monoclonal Gammopathy of Undetermined Significance....173
4.1 Introduction....173
4.2 Methods....176
4.2.1 Patient Recruitment....176
Healthy Control Selection....176
4.2.2 Assessment of Platelet Activation Status and Reactivity by Flow cytometry....179
4.2.3 Washed Platelet Preparation....180
4.2.4 Reticulated Platelet Quantification....180
4.2.5 Analysis of Platelet-Associated Immunoglobulin (PAIg)....181
4.2.6 Quantification of FcγRIIa in Washed Platelets....181
4.2.7 Statistical Analysis....181
4.3 Results....183
4.3.1 Platelets are Hyper-Activated in MGUS and Multiple Myeloma Patients....183
4.3.2 Marker-Specific Changes in Platelet Responsiveness in MGUS and MM Patients. 185
4.3.3 Platelet – Leucocyte Aggregates (PLA) and *In-vitro* Formation of PLA are Unaltered in MGUS and Myeloma Patients....187
4.3.4 Increased Platelet-Associated Immunoglobulin (PAIg) in a Subset of MGUS and SM/MM Patients....187
4.3.5 SM/MM Patients Have Increased Cleavage of Platelet FcγRIIa Receptor....189
4.3.6 Fibrinogen Levels Are Elevated in MGUS and MM Patients....191
4.4 Discussion....193
4.5 Supplementary Results....198
5.0 Platelet Hyperactivation and Hyporesponsiveness at Diagnosis in Multiple Myeloma Persists During Treatment Initiation....209
5.1 Introduction....209

5.2 Methods 213
5.2.1 Patient Recruitment 213
5.2.2 Assessment of Platelet Activation Status and Reactivity by Flow Cytometry 214
5.2.3 Washed Platelet Preparation 215
5.2.4 Reticulated Platelet Quantification 215
5.2.5 Quantification of Thrombopoietin 216
5.2.6 Statistical Analysis 216
5.3 Results 217
5.3.1 Platelet Hyperactivation and Hyporesponsiveness Persist Post-Treatment. 217
5.3.2 Platelet-Leucocyte Aggregates and Reticulated Platelet Levels Increase Post-Treatment. 219
5.4 Discussion 222
5.5 Supplementary Results 227
6.0 Overall Discussion & Conclusion 233
7.0 Bibliography 235
8.0 Appendix 291

Declaration

This is to certify that the work I am submitting is my own and has not been submitted for another degree, either at University College Cork or elsewhere. All external references and sources are clearly acknowledged and identified within the contents. I have read and understood the regulations of University College Cork concerning plagiarism and intellectual property.

Acknowledgements

I would like to thank my supervisor Dr. Paul Young for the opportunity to work in his lab and his support over the last number of years. I would like to thank my supervisor Prof. Mary Cahill for her guidance and encouragement throughout the project. I thank them sincerely for their patience, kindness, and consistent support.

I would also like to thank Gerardene Meade-Murphy for her guidance on the project and her encouragement over the years. Thank you also to the technical staff; Pat, Noreen, Jenny, and Trish, who have been a huge support throughout my project. I would like to thank other PIs in the School of Biochemistry & Cell Biology, particularly Dr. Kellie Dean, Dr. Justin McCarthy, Dr. Tommie McCarthy, and Dr. Tom Moore, for their support and feedback throughout the project. I would also like to thank researchers in CancerResearch@UCC for their support throughout the project, particularly Sharon McKenna and Tracey O'Donovan for flow cytometry advice and Maura Bendix for her assistance with electroporation experiments.

I would like to thank my colleagues in the lab for their support and friendship. Thank you especially to Julia Samson, Averil Kiely and Joan Lenihan for their support and friendship throughout my time in the lab.

I would like to thank the staff at Cork University Hospital, particularly the haematology consultants Dr. Vitaliy Mykytiv and Dr. Oonagh Gilligan, haematology nursing staff and phlebotomy staff for their work in recruiting patients for the study and collecting samples. Thank you to Dr. Maeve Crowley for her insight and feedback on a manuscript detailing results of the study, which was published in Thrombosis Research. I would also like to thank staff in the haematology laboratory particularly Mary Ring, Dr. Norma Reidy, Ber Murphy, Seamus Hayes and Damien Hennessy for providing laboratory space, IT support and flow cytometry advice. I would also like to thank the patients and healthy volunteers who kindly provided samples for this research study. Their participation was critical to the study and I am grateful for their commitment to this research.

I would like also to thank my family, especially my parents, grandparents, and siblings, particularly to Lara for her work on illustrations in the thesis. I thank them for their support throughout the project. I thank Seán for his encouragement and invaluable support. I also

thank my close friends Seán, Ciarán, Aoife, Claire and Laura for their support and friendship throughout the project.

I would also like to acknowledge the Irish Research Council - Government of Ireland Postgraduate Scholarship Programme (Project ID: GOIPG/2017/952), Translational Research Access Programme, UCC and the Haematology Association of Ireland for funding this project.

Abbreviations

ABD	Actin-Binding Domain
ABS	Actin-Binding Sites
ADAM10	A Disintegrin And Metaloprotease 10
ADAM17	A Disintegrin And Metaloprotease 17
ADP	Adenosine Diphosphate
ALP	Actin-associated LIM Protein
AML	Acute Myeloid Leukaemia
AMR	Ashwell-Morell Receptor
AP-3	Adaptor Protein Complex 3
APS	Antiphospholipid Syndrome
Arp	Actin-Related Protein
BLOC	Biogenesis of Lysosome-related Organelle Complex
BPD	Bleeding & Platelet Disorders
CaM	Calmodulin-like
CBV	Coxsackie B Virus
CCL5 (Rantes)	C-C Motif Chemokine Ligand 5
CH	Calponin Homology
CLEC2	C-type lectin-Like type II Receptor
CMV	Cytomegalovirus
CR3	Complement Receptor 3
CXCL	C-X-C Motif Chemokine Ligand
DCM	Dilated Cardiomyopathy
DIC	Disseminated Intravascular Coagulopathy
DVT	Deep Vein Thrombosis
ECL	Enhanced Chemiluminescence
EGF	Epidermal Growth Factor
EMCV	Encephalomyocarditis Virus
EMT	Epithelial–Mesenchymal Transition
FSGS	Focal Segmental Glomerulosclerosis
GPCR	G-protein Coupled Receptors
GWAS	Genome-Wide Association Study
HCM	Hypertrophic Cardiomyopathy

HER2	Human Epidermal Growth Factor Receptor 2
HIV	Human Immunodeficiency Virus
HMBG1	High-Mobility Box Group 1
HNP1	Human Neutrophil Peptide 1
HTS	High-Throughput Sequencing
ICAM	Intercellular Cell Adhesion Molecule
IFNγ	Interferon γ
IGF1	Insulin-like Growth Factor
IPD	Inherited Platelet Disorder
IT	Information Technology
JAK1	Janus Kinase 1
JAK2	Janus Kinase 2
KRAS	Kirsten Rat Sarcoma 2 Viral Oncogene Homolog
LPA	Lysophosphatidic Acid
LTA	Light-Transmission Aggregometry
MGUS	Monoclonal Gammopathy of Undetermined Significance
MHC	Major Histocompatibility Complex
MK	Megakaryocyte
MPTP	Mitochondrial Permeability Transition Pore
MPV	Mean Platelet Volume
MM	Multiple Myeloma
MYH9	Myosin Heavy Chain IIA
MYH-9	Myosin Heavy Chain
NBEAL2	Neurobeachin-Like 2
NET	Neutrophil Extracellular Traps
NIH	National Institute of Health
NK Cell	Natural Killer Cell
NKG2DL	Natural Killer Group 2D Ligand
NMDA	N-methyl D-Aspartate
NSAID	Non-steroidal Anti-inflammatory Drug
OCS	Open Canalicular System
PAR	Protease-Activated Receptors
PDGF	Platelet-Derived Growth Factor
PFA-100	Platelet Function Analyser 100

PGE2	Prostaglandin E_2
PIP2	Phosphatidylinositol 4,5-Biphosphate
PIP3	PtdIns (3,4,5,)-P3
polyP	Polyphosphate
PS	Phosphatidylserine
PSGL	P-selectin Glycoprotein Ligand
RA	Rheumatoid Arthritis
ROS	Reactive Oxygen Species
S1P	Sphingosine 1-phosphate
SLE	Systemic Lupus Erythematosus
SNARE	Soluble-N-Ethyl-Malemide-Sensitive
SNV	Single-Nucleotide Variant
SR	Spectrin-like Repeat
STAT3	Signal Transducer and Activator of Transcription 3
TC	Thrombocidin
TCIPA	Tumour-Cell Induced Platelet Aggregation
TEV	Tobacco Etch Virus
TFPI	Tissue Factor Pathway Inhibitor
TGFβ	Transforming Growth Factor β
TLR	Toll-Like Receptor
TNF- α	Tumour Necrosis Factor α
tPMP-1	Thrombin-Induced Platelet Microbicidal Protein
TPO	Thrombopoietin
TRAP	Thrombin Receptor Activating Peptide
VAMP	Vesicle-Associated Membrane Protein
VCAM	Vascular Cell Adhesion Molecule
VEGF	Vascular Endothelial Growth Factor
VLK	Vertebrate Lonesome Kinase
VTE	Venous Thromboembolism
VUS	Variant of Undetermined Significance
VWF	Von Willebrand Factor
WAS	Wiskott-Aldrich Syndrome
WASP	Wiskott-Aldrich Syndrome Protein
WAVE	WASP-family Verprolin-Homologous Protein

WES	Whole Exome Sequencing
WIP	WASP Interacting Protein

Abstract

Platelet dysfunction may be inherited or acquired. In this study platelet dysfunction was assessed in both contexts; the inherited platelet disorder ACTN1-related Congenital Macrothrombocytopenia (CMTP) and the acquired prothrombotic state in Multiple Myeloma (MM).

Actinin-1 is a widely-expressed actin binding protein but mutations have a tissue-specific impact, causing CMTP, characterised by low platelet count and large platelet size. It was previously shown that mutations in the actin-binding domain of actinin-1 increase the affinity of actinin-1 for actin filaments. In this study, nine mutations in rod domain and calcium-binding CaM-like domain were assessed in terms of their impact on actin binding and calcium binding. It was shown that calcium binding was not significantly affected by mutations in the CaM-like domain, although thermal stability was slightly decreased, and mutations in both the rod and CaM-like domain increased actinin's ability to bundle actin filaments *in-vitro*. Thus, CMTP-causing actinin-1 mutations outside the actin-binding domain also increase actin association, suggesting a common molecular mechanism underlying actinin-1 related CMTP.

The tissue specific functions of actinin-1 in platelet production were explored. Megakaryocyte maturation in terms of polyploidy was assessed in CMK and MEG-01 cell lines expressing mutant actinin-1 but no significant disruption was noted. Primary murine megakaryocytes were used to image WT actinin-1 and actinin-4 in two key structural features of platelet production; podosomes and proplatelets. It was shown that more actinin-1 was expressed in platelets and megakaryocytic cell lines than actnin-4, possibly explaining the tissue-specific impact of actinin-1 mutations. The presence of actinin-1/4 heterodimers has not been explored in these cells and a method to assess actinin-1/actinin-4 heterodimers was optimised. It was also shown that integrin αIIβ3 interacts with actinin-4 or actinin-1/4 heterodimers, implying that this is not an actinin-1 specific interaction. Consideration of actinin isoform specific functions is of value in future study to determine the role actinin-1 plays in platelet production.

In the second part of this project, platelet activation status was assessed in myeloma patients. Thrombotic events are common in patients with multiple myeloma (MM),

smouldering myeloma (SM) and monoclonal gammopathy of undetermined significance (MGUS). In the present study, multiparameter analysis of platelet activation and responsiveness was investigated by flow cytometry in patients with MGUS, SM/MM and healthy controls (HCs). The median platelet surface levels of CD63, annexin V and PAC-1 antibody (specific for activated integrin αIIbβ3) binding were significantly elevated in patients with MGUS versus the HCs. In all, 74% of MGUS and 38% of SM/MM patients had one or more elevated marker of platelet activation, compared to 19% of the HCs. Marker-specific hyporesponsiveness of platelets to agonist [adenosine diphosphate (ADP), thrombin receptor-activating peptide 6] stimulation *in-vitro* was observed, with significantly reduced surface levels of P-selectin in response to ADP in patients with MGUS. Platelet-associated immunoglobulins were elevated in a subset of patients. A subset of patients were also analysed after two months of anti-myeloma treatment and anti-thrombotic therapies where prescribed. The hyperactive, hyporesponsive state was not significantly altered at this timepoint post diagnosis. However, a significant elevation in reticulated platelets and platelet-leucocyte aggregates was found. As risk assessment models evolve to include novel laboratory parameters, these observations suggest that further investigation of the predictive and prognostic value of platelet activation markers in such patients is warranted.

Overall this project contributes to what is known about actinin-1 related CMTP, as mutations outside the actin binding domain appear to also increase actinin's ability to bundle actin filaments. The impact of this gain-of-function disruption remains to be determined and several features of platelet production which involve actinin-1 are highlighted for further study in this project. Platelet dysregulation was demonstrated as a feature of MM, SM and pre-malignant MGUS and could be explored as a potential indicator of thrombotic risk in these patients in future study.

1.0 Introduction

Platelets are anucleate blood cells, released into the vasculature by megakaryocytes in the bone marrow and lungs. Their main function is to adhere to injured blood vessel endothelium and form aggregates (platelet plugs) which prevent blood loss. Their role in other physiological and disease processes is increasingly being recognised. Normal platelet count and function are essential, with dysregulation causing both clotting and bleeding disorders. This overview will describe the structure, formation, and functions of platelets in haemostasis and the immune system. I will then introduce two platelet-related disorders which are the focus of my study; the inherited platelet disorder Actinin-1 related Congenital Macrothrombocytopenia (CMTP) and the acquired platelet dysfunction recognised in Multiple Myeloma.

1.1 General Overview of Platelets

1.1.1 Platelet Count

A general reference range for platelet count is 150-400 x 10^9 cells/L, while variation due to sex and age is observed (Biino et al., 2013). Platelet count is highest in infants, decreases throughout childhood and stabilises at puberty before decreasing again in old age (Biino et al., 2013). From puberty, women have a higher platelet count than men but this difference reduces in old age (Biino et al., 2013). In addition to age and gender, genetic influence on platelet count exists and studies have identified several loci significantly associated with both platelet count and size, reviewed here (Eicher *et al.,* 2018). A meta-analysis of Genome-wide Association Studies (GWAS) identified 68 loci associated with platelet count and mean platelet volume (MPV) (Gieger et al., 2011). A set of 423 non-coding variants in megakaryocyte super-enhancers associated with these parameters and platelet function was also compiled from megakaryocyte-matched epigenomic data (Petersen et al., 2017). The INTERVAL (Moore et al., 2014) and UK biobank cohorts were used to assess 175,000 volunteers for single nucleotide variants (SNVs) associated with platelet formation (Astle et al., 2016).

A reduction of normal count by 70% has been shown to be required to impact bleeding time in mice, suggesting that the number of platelets in circulation is not a major determinant of thrombus formation (Morowski et al., 2013). In humans, thrombocytopenia is common in the clinical setting but severe haemorrhage is rare in the absence of platelet function defects or inflammation (Morowski et al., 2013; Neunert et al., 2008). Paradoxically, patients with immune thrombocytopenia may bleed but also have an increased risk of thrombotic events (Nørgaard et al., 2012). Platelet count is maintained in a steady state by controlled production and clearance (Grozovsky et al., 2015). Changes in platelet count can occur in response to infection or inflammation (Grozovsky et al., 2015).

1.1.2 Platelet Size

Platelets are the small (2-5 µm in diameter) anucleate blood cells that have a lifespan in the circulation of 7-10 days in humans (van der Meijden *et al.*, 2019). MPV may indicate platelet maturity, as younger cells are generally larger and more reactive, but MPV is influenced by sample type, processing techniques and equipment used, hindering its use clinically (Eicher *et al.,* 2018). Platelet count and size are reportedly inversely proportional (Eicher *et al.,* 2018). Heterogeneity in size exists in the platelet population and individual platelets undergo dynamic changes in size and shape while circulating (Baaten *et al.,* 2017). MPV has been demonstrated to be a predictor of thrombosis but both increased MPV (Jensvoll *et al.,* 2014; Kostrubiec et al., 2010) and decreased MPV (Ferroni et al., 2014; Riedl et al., 2017) have been reported to increase risk.

1.1.3 Platelet Lifespan

Platelets circulate for 7-10 days in the peripheral blood (Koupenova et al., 2018). Platelets which have been recently released from the megakaryocyte are larger in size, contain more RNA and have a greater capacity to synthesise proteins (Lev, 2016). These younger platelets are termed reticulated platelets (RP) or the immature platelet fraction (IPF) (Lev, 2016). This comprises approximately 1-5% of all platelets (Baaten et al., 2017). RP RNA content can vary due to age, sex and ethnicity (Simon et al., 2014). Assessment of RP may be of clinical value as recent studies have demonstrated a reduced responsiveness to anti-platelet drugs in patients with higher platelet turnover, and increased IPF was reported to be an independent predictor of adverse cardiac events (Cesari et al., 2013; Freynhofer et al., 2015; Ibrahim et al., 2014). Platelets are removed from the circulation by several

mechanisms, reviewed by Baaten et al. (Baaten et al., 2017). Platelet undergo an apoptotic process characterised by mitochondrial dysfunction, phosphatidylserine (PS) exposure, caspase proteolytic activity and resistance to integrin activation. Clearance can also be triggered by activation. Aged platelets also become desialylated and are removed by Ashwell-Morell receptors (AMR) in the liver.

1.1.4 Platelet Production

1.1.4.1 Models of Platelet Production

Platelets are formed primarily in the bone interacts marrow by megakaryocytes (van der Meijden *et al.,* 2019), although platelet-forming megakaryocytes have also been identified in the mouse lung (Lefrançais et al., 2017). Megakaryocytes are large polyploid cells which are derived from haematopoietic stem cells (Cuenca-Zamora *et al.,* 2019). They become polyploid through the process of endomitosis, where DNA replication occurs in the absence of cell division(Mazzi et al. , 2018). Platelet-specific proteins and organelles are produced in the megakaryocyte (Cuenca-Zamora *et al.,* 2019).

Thrombopoietin (TPO), formed mainly by the liver, is a key regulator of megakaryocyte differentiation and platelet production and its role in platelet formation is discussed by Grozovsky (Grozovsky et al., 2015). TPO interacts with platelets and megakaryocytes via the MpI receptor. TPO is constitutively produced, with serum levels being dependent on uptake by platelets and megakaryocytes. As platelets age their glycoproteins become desialylated by sialidases and are cleared by the hepatic AMR. AMR signalling enhances hepatic TPO production via JAK2 activation and STAT3 phosphorylation which upregulates TPO mRNA expression. TPO levels are also influenced by IL-6 in inflammatory states through STAT3 and JAK1 signalling (Kaser et al., 2001). TPO and another stimulator of MK (megakaryocyte) growth, CXCL12, are also secreted by bone marrow stromal cells (Hodohara et al., 2000; Sugiyama et al., 2006). TPO regulating proteins, JAK2 and dynamin 2 are also involved in regulation of platelet production. In mice lacking MpI or JAK2 in megakaryocytes, thrombocytosis and megakaryocytosis occurred, indicating that TPO is dispensable for platelet production but necessary for differentiation of progenitor cells towards the MK lineage, while MpI binding of TPO by MK and platelets functions regulates platelet count (Meyer et al., 2014; Ng et al., 2014).

The process of platelet production is a topic of ongoing research. It was proposed that megakaryocytes migrate from the osteoblastic to vascular niches in the bone marrow to release platelets from processes called proplatelets through the sinusoidal endothelial layer into the vasculature (Machlus *et al.,* 2013). When proplatelets are formed, microtubules move from the centre of the cell to the cell cortex and the sliding of overlapping microtubules results in pseudopod formation and proplatelet extension (Cuenca-Zamora *et al.,* 2019). The microtubules also function to transport proteins and organelles along the proplatelet shaft to platelets in a random and bi-directional process (Cuenca-Zamora *et al.,* 2019).

1.1.5 Resting Platelet Structure

Platelets have a thick outer glycocalyx containing glycoproteins necessary for adhesion, activation and aggregation (Kunicki, 1989). The platelet lipid membrane is compressed into folds of the open canalicular system, which can be utilised to rapidly increase cell size during adhesion and spreading (Escolar *et al.,* 1989). The open canalicular system, derived from the demarcation membrane system in MK, consists of membrane folding creating tubular structures which extend into the cell, which allows trafficking of plasma proteins such as fibrinogen into α-granules and facilitates granule release (White *et al.*, 1987; Escolar *et al.*, 1989; Gremmel *et al.*, 2016).

The lipid bilayer contains tissue factor and negatively charged phosphatidyl serine (PS) in activated platelets creating a procoagulant surface which promotes thrombin generation (Gremmel *et al*., 2016). In the submembrane region, transmembrane receptors interact with signalling proteins and the platelet cytoskeleton (Hartwig *et al.*, 1991). The myosin and actin filaments of the cytoskeleton are important to facilitate platelet shape change during activation and translocate receptors across the platelet surface (White, 1969).

A microtubule ring lies near the cell membrane and is thought to maintain the cell's discoid shape (Behnke, 1965; Haydon *et al.*, 1965; Gremmel *et al.*, 2016). The cytosolic actin cytoskeleton provides a matrix which separates granules, lysosomes and vesicles in the cell (Escolar *et al.*, 1986; Gremmel *et al.*, 2016). Platelets contain secretory organelles (α-granules, dense granules, lysosomes), mitochondria, glycosomes, tubular inclusions (remnants of MK smooth endoplasmic reticulum) and electron dense chains and clusters (Gremmel *et al.*, 2016).

1.1.5.1 The Platelet Cytoskeleton

The platelet and megakaryocyte cytoskeleton consists of actin filaments and microtubules, comprised of α- and β-tubulin heterodimers. The microtubule component of the platelet cytoskeleton has been reviewed by Cuenca-Zamora et al. (Cuenca-Zamora *et al.,* 2019). Microtubules are hollow tubes of 25 µm in diameter, with polarised ends with different affinities for tubulin dimers. Microtubules are arranged in a circular coil, helping to maintain the platelet discoid shape, and become centralised when platelets are activated to allow the cell shape to change. Dynein and dynactin are microtubule-associated proteins that participate in the sliding of microtubules during this shape change, and in platelet formation. Kinesins are also associated with microtubules and have motor functions, aiding organelle transport and granule secretion. The quantity of β1-tubulin is reduced in those with certain β1-tubulin variants, and also in neonates, but a normal circular coil and discoid shape is observed. It is thought that age-related variation in β1-tubulin may be overcome by over-expression of other tubulin variants in neonates (Caparrós-Pérez et al., 2017). Mutations in β1-tubulin result in decreased and disorganised microtubules which do not form a circular coil and cause macrothrombocytopenia, due to impaired proplatelet formation (Burley *et al.,* 2018).

In resting platelets, a cortex of tightly packed actin filaments make up the actin cytoskeleton (Sorrentino et al., 2016). This resembles spokes of a wheel, with F-actin radiating from the membrane to cell centre and a dense spectrin rich membrane skeleton encases the actin core (Sorrentino et al., 2015). The platelet membrane skeleton also maintains the cell discoid shape and is made up of actin filament barbed ends (existing free or capped by Arp 2/3 or adducin) and spectrin (Patel-Hett et al., 2011). Spectrin strands link to the cytoplasmic actin filaments, forming a continuous ultrastructure (Patel-Hett et al., 2011). Megakaryocytes also have a spectrin membrane skeleton similar to platelets (Patel-Hett et al., 2011). Spectrin in megakaryocytes is critical for invaginated membrane system formaton, proplatelet extension and the maturation of preplatelets to platelets (Patel-Hett et al., 2011).

1.1.5.2 Organelles

Platelets lack a nucleus and their key functional organelles are the granules. Platelets also contain a dense tubular system, derived from the megakaryocyte smooth endoplasmic reticulum (Behnke, 1967; Gremmel *et al.*, 2016). Rough endoplasmic reticulum, is not present usually, but has been reported during phases of rapid platelet production such as immune thrombocytopenia, speculated to be derived from young MK (Gremmel et al., 2016; Ts'ao, 1971). Hexagonal electron-dense formations have also been reported in 2-22% of platelets, with frequency increasing with age, but their function is not known (White, 2002).

Figure 1.1.5.1

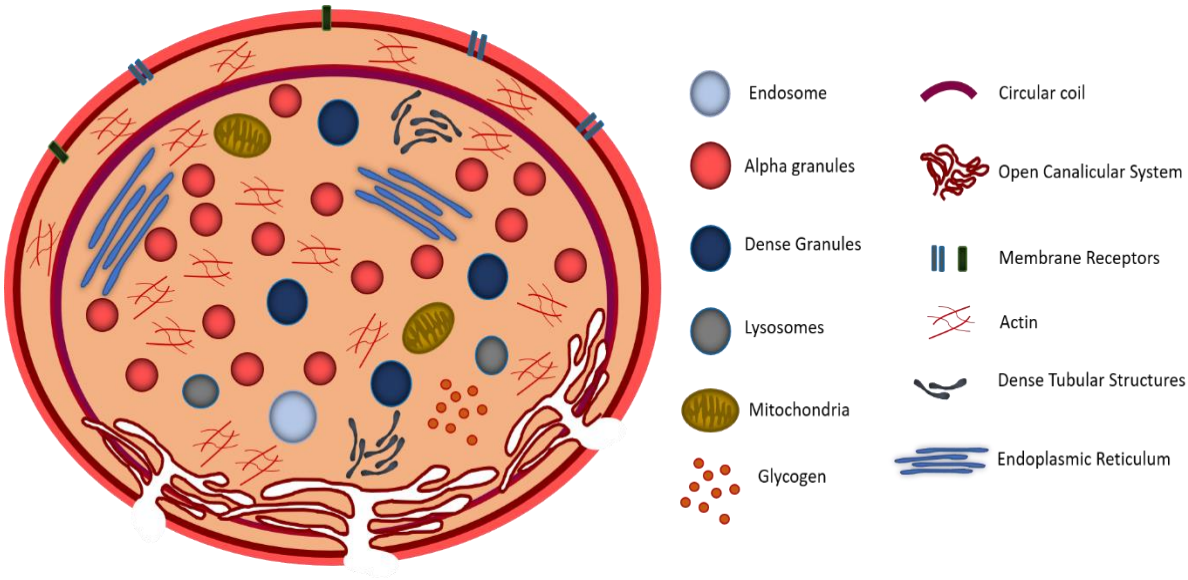

Figure 1.1.5.1: Representation of platelet structure and organelles present. *Figure illustrates a platelet in the resting state with key structural features highlighted. The platelet membrane extends into the open canalicular system and contains membrane receptors including integrins and G-protein coupled receptors (GPCR) . A microtubule circular coil maintains the cell's spherical shape. An actin cytoskeleton distributed throughout cell maintains the architecture of cell contents. Platelets contain various granules, lysosomes and endosomes.*

Granules

Platelet granule content supports haemostasis and other processes including inflammation, immune functions, angiogenesis and tumour growth (Joshi *et al.*, 2017). Granules are synthesised in the megakaryocyte but may mature in platelets in the circulation (Gremmel *et al*., 2016). Both platelet-synthesised and endocytosed proteins are moved to multivesicular bodies and then to α-granules and dense granules (Gremmel *et al.,* 2016). Granules synthesised in the megakaryocyte are delivered via proplatelets into platelets along microtubule tracks (Gremmel *et al*., 2016). Heterogeneity in granule content exists in the platelet population with alpha-granule rich, larger platelets being more reactive (Karpatkin, 1969; Vicic *et al.,* 1983; van der Meijden *et al.,* 2019). Granule content has been reviewed in detail (Gremmel *et al.,* 2016).

Alpha Granules

Platelet α-granules were described initially in the 1950s based on thin section electron microscopy studies, named for their large size and abundance (Yadav *et al.,* 2017). Platelets contain 50-80 α-granules which are separated by the actin cytoskeleton (King *et al.*, 2002; Gremmel *et al.*, 2016). Fusion of α-granules into larger organelles can occur *in-vitro* during platelet storage and *in-vivo* in platelet disorders including Paris Trousseau-Jacobsen syndrome (Krishnamurti *et al.*, 2001; Gremmel *et al*., 2016). Neurobeachin-like 2 (NBEAL2) protein is involved in the formation of α-granules, with defects in the protein causing grey platelet syndrome and resistance to arterial thrombosis (Deppermann et al., 2013). α-granules contain various proteins synthesised by the megakaryocyte including von Willebrand Factor (VWF), thrombospondin, P-selectin and coagulation Factor V (Gremmel et al., 2016). In addition, proteins such as fibrinogen may be taken up by the endocytic pathway by either megakaryocytes or platelets into α-granules (Gremmel et al., 2016). Granule membrane-associated proteins are found on the surface of activated platelets. This includes receptors which are already present on the surface of the platelet (αIIbβ3, GPVI, Fc receptors, GPIb-IX-V, tetraspanins and Glut-3) and those not present in resting platelets (P-selectin, CD109 and fibrocystin I) (Maynard *et al.*, 2007; Gremmel *et al.*, 2016). Receptors moved to the cell surface may also facilitate aggregation and adhesion. Released fibrinogen and VWF facilitate platelet aggregation (Gremmel *et al.*, 2016). α-granules also contain coagulation factors which contribute to secondary haemostasis and anti-thrombotic protein S and tissue-factor pathway inhibitor (TFPI) which aid regulation of thrombosis (Schwarz *et al.*, 1985; Novotny *et al.*, 1988; Gremmel *et al.*, 2016). The

contradictory presence of pro and anti-thrombotic factors in granules has led to the speculation that subpopulations of the granules exist within the platelet with distinct contents and functions (Yadav *et al.,* 2017). Spherical and tubular granules have been reported with distinct contents and varying presence in the platelet population (Van Nispen Tot Pannerden et al., 2010). Beyond haemostasis, α-granules also provide receptors for leucocyte and endothelial interaction and release pro-inflammatory factors, facilitating immune-modulating functions in platelets (Gremmel *et al.*, 2016). Released antimicrobial factors (CXCL4, CCL5 (RANTES), thymosin-β4, complement) also aid the immune system (Klinger *et al.,* 2002; Gremmel *et al.*, 2016). α-granules also have pro-angiogenic factors (VEGF, PDF, EGF, IGF) and anti-angiogenic factors (thrombospondin-1, angiostatin) (Gremmel *et al.*, 2016) which may be released differentially based on agonist stimulation (Italiano et al., 2008). Vertebrate Lonesome Kinase (VLK) tyrosine kinase is stored and released from α-granules, phosphorylates proteins extracellularly and is important for platelet aggregation (Bordoli et al., 2014; Revollo et al., 2021).

Dense Granules

Dense granule structure and content are detailed in a review by Gremmel et al. (Gremmel *et al.,* 2016). There are 3-5 dense granules per platelet. They contain ADP, ATP, uracil and guanine nucleotides, polyphosphates, histamine, serotonin, calcium, potassium and magnesium . Dense granules provide a source of calcium which is necessary for thrombosis . The granules originate from the endosomal system with biogenesis of lysosome-related organelle complexes (BLOCs) and AP-3 important for synthesis . The content of the granules becomes denser during platelet maturation as membrane pump activity increases . Membrane associated proteins include CD63, integrin αIIbβ3 and LAMP-2. ADP released from dense granules stimulates other platelets and serotonin supports platelet aggregation . pH in dense granules is maintained at pH 5.4 by a H^+ ATPase proton pump .

Lysosomes

Platelets contain 0-2 lysosomes, containing hydrolases, cathepsin D and E, LAMP-2 and CD63, which can be released with strong agonist stimulation (Gremmel *et al.,* 2016). Lysosomal release involves lysosome-related complex BLOC1-BLOC3 (Meng et al., 2015).

Endosomes

The endocytic pathway is mediated by membrane coat protein clathrin, adaptor proteins (AP-1, AP-2, AP-3), vesicle trafficking proteins (NSF, SNAREs) and GTPases (Dynamin 1-3, Cdc42, Arf6) (Gremmel *et al.,* 2016; Banerjee and Whitehert, 2017). Endocytosis is important to load granules with extracellular proteins, such as fibrinogen and VEGF, resensitising P2Y1 and P2Y12 receptors and regulating surface levels of C-type lectin-like receptor 2 (CLEC-2) and the thrombopoietin receptor (Banerjee & Whiteheart, 2017). Dynamins, which mediate endocytosis, also contribute to megakaryopoiesis, with mutations in Dynamin 2 and Dynamin 3 associated with MPV variation and macrothrombocytopenia (Benderet al., 2015; Nürnberg et al., 2012). Endocytosed material is stored in endosomes and may be degraded by integrating with lysosomes or recycled to the plasma membrane surface (Banerjee & Whiteheart, 2017).

1.1.5.3 Exosomes & Microparticles

The majority of circulating microparticles are platelet or megakaryocyte derived (Edelstein, 2017). This includes exosomes (40-100 nm) and microparticles (100-1000 nm) which resemble platelets containing RNA, cytokines, coagulation factors and eicosanoids (van der Meijden *et al.,* 2019). The vesicles may interact with other cells, particularly leucocytes and the endothelium (Varon & Shai, 2015) with their glycoprotein and ligand content varying depending on the age and activation status of the platelets from which they are derived (Vasina et al., 2013). Microparticles may have roles in inflammation and the immune response, tissue repair, angiogenesis and cancer metastasis, reviewed here (Varon & Shai, 2015).

1.1.5.4 Open Canalicular System

The open canalicular system (OCS) is a network of membrane channels within platelets that are connected to the cell surface membrane (Selvadurai et al., 2018). The OCS transfers molecules in and out of the cell and also provides a membrane reserve needed to increase the surface area of platelets upon activation (Selvadurai et al., 2018). Several inherited platelet disorders, including Bernard Soulier syndrome and MYH-9 related disorders, present with dilated and hypertrophic OCS (Selvadurai et al., 2018).

1.1.6 Platelets in Clot Formation

Platelets function mainly in preventing blood loss during vascular injury by rapidly adhering to the site of injury, forming aggregates and arresting bleeding (Stevens & McFadyen, 2019). Injured endothelium exposes extracellular matrix proteins such as collagen, vitronectin, fibronectin and laminin which bind VWF and receptors on the platelet surface (Koupenova *et al.*, 2018; Łukasik *et al.,* 2018). Additionally, the production of nitric oxide and prostacyclin by the endothelium, which keep the platelets in a resting state, is reduced (Koupenova et al., 2018). Adhesion of platelets to VWF or directly to collagen occurs via the GPIb and GPIa receptors respectively (Koupenova et al., 2018). Platelets then become activated, undergo shape change and release factors including thromboxane A2 and ADP which recruit, activate and stimulate aggregation of other platelets (Koupenova et al., 2018). Exposed tissue factor from damaged tissue also leads to thrombin generation and, in combination with activated platelets, leads to fibrinogen and fibrin accumulation at the site of injury (Koupenova et al., 2018). The platelet mass retracts, stabilising the clot (Koupenova et al., 2018). Platelets also interact with the coagulation system. Activated platelets expose phospholipids on their membrane, providing a negatively charged surface for coagulation factor complex assembly (Heemskerk *et al.,* 2002).

A contemporary model for haemostasis describes arterial thrombi as an ordered structure (Koupenova et al., 2018). The zone closest to the site of vascular injury (thrombus core) is rich in collagen, thrombin and fibrin and consists of highly activated, P-selectin exposing platelets (Agbani & Poole, 2017; Stevens & McFadyen, 2019). The outer layer (thrombus shell) includes platelets which remain in discoid shape, are not de-granulated and are in a low activation state, not expressing P-selectin (Koupenova et al., 2018; Stevens & McFadyen, 2019). The outer layer is permeable to plasma proteins and creates a gradient of thromboxane, ADP (Koupenova et al., 2018). A gradient of CXCL7 guides leucocytes to the site of injury through the thrombus (Ghasemzadeh et al., 2013). A procoagulant platelet subpopulation expose PS on their surface which binds tenase (Factor Xase) and prothrombinase to stimulate coagulation, while an aggregating subpopulation express activated integrin αIIbβ3 and bind fibrin to facilitate clot contraction into an impermeable cell mass (Agbani & Poole, 2017). High calcium concentrations that remain elevated allow PS externalisation, coagulation factor binding and integrin inactivation in procoagulant platelets while aggregating platelets experience intermittent calcium spikes and sustained integrin engagement (Agbani & Poole, 2017). Platelet age and oxidative stress may also influence subpopulations which arise (Agbani & Poole, 2017). The dynamics of thrombus

formation and the interaction of platelets with the coagulation pathway is likely dependent on whether it occurs in venous or arterial vasculature and also the shear rate ($\frac{\text{difference in velocity between layers of cells under flow}}{\text{distance between layers}}$) and shear stress (shear rate x blood viscosity) (Hathcock, 2006; van der Meijden & Heemskerk, 2019) . The shear rate in venous blood is lower (100 s^{-1}) than arterial (300-2800 s^{-1}), with platelet activation stimulated at high shear rates and interactions with other cells favoured at lower shear rates (Hathcock, 2006).

Venous thrombi generally develop on intact endothelium which has become inflamed in response to a triggering event and this process is detailed by Stevens & McFayden (Stevens & McFadyen, 2019). The inflamed endothelium releases adhesive VWF and P-selectin, which bind to platelets and leucocytes respectively. Neutrophils are recruited initially and release tissue factor and neutrophil extracellular traps (NETs) on activation, which may activate platelets and promote coagulation. Activated platelets release polyphosphate (polyP) from dense granules, which activate the Factor XII coagulation pathway and contribute to venous thromboembolism (VTE). Platelet genetic polymorophisms in several proteins are linked to VTE occurrence, namely GPIa, GPVI and JAK2 (Montoro-García et al., 2016). Enhanced platelet aggregation and activation is also noted to be predictive of VTE risk, with soluble P-selectin, a marker of platelet activation, being included in a VTE risk prediction score (Ay et al., 2010; Montoro-García et al., 2016). Platelet count and MPV have also been associated with VTE (Montoro-García et al., 2016)

1.1.7 Platelets in Immunity & Inflammation

Beyond haemostasis, platelets are increasingly being appreciated as immune cells. For example, platelets can interact directly with microbes or recruit immune cells during infection (Deppermann & Kubes, 2018).

1.1.7.1 Interaction with Microbes

Sepsis, infection of the blood combined with organ dysfunction, is accompanied by thrombocytopenia and coagulopathy (Angus & van der Poll, 2013). Thrombocytopenia in septic patients is linked to increased mortality (De Stoppelaar et al., 2014). Bacteria may interact with platelets directly or indirectly via proteins such as VWF and fibrinogen (Deppermann & Kubes, 2018). GPIb, αIIbβ3 and toll-like receptors (TLR) have been reported

to interact directly with bacterial proteins and may induce platelet aggregation (Deppermann & Kubes, 2018). Interaction of bacteria with platelets may also stimulate interaction with immune cells, such as the interaction of platelets with neutrophils during S. *aureus* infection (Powers et al., 2015). Platelets may phagocytose bacterium but whether microbes are killed intracellularly or delivered to leucocytes is not known (Youssefian et al., 2002). Several antimicrobial compounds have been isolated from platelets, including thrombin-induced platelet microbicidal protein (tPMP-1) and thrombocidins (TCs) (Deppermann & Kubes, 2018). Platelets interact with Kuppfer cells in the liver via VWF to capture and form aggregates around bacteria, with subsequent platelet activation and leucocyte recruitment (Wong et al., 2013). Phagocytosis in platelets is mediated in part by FCγRIIα, which allows ingestion of immune complexes, including bacteria and viruses (Banerjee & Whiteheart, 2017). Platelets may also activate the complement system, which causes bacterial cell lysis (Deppermann & Kubes, 2018).

Platelets also play a role in viral infections, with thrombocytopenia being an indicator of various infections (Alonso & Cox, 2015; Jenne & Kubes, 2015). Viruses may activate platelets through TLR7 and also stimulate their interaction with neutrophils (Jenne & Kubes, 2015). Although they associated with platelets it is not known whether DNA viruses such as cytomegalovirus (CMV) are internalised (Koupenova et al., 2018). RNA viruses such as Human Immunodeficiency Virus (HIV) and influenza are smaller and can be internalised (Koupenova et al., 2018). Platelet-virus interaction can be beneficial or harmful. In CMV infection, virally activated platelets increasingly interact with leucocytes, promoting an immune response (Assinger et al., 2014). In Encephalomyocarditis Virus (EMCV), Dengue, Coxsackie B Virus (CBV), HIV and influenza infection, which are RNA viruses, platelet-leucocyte aggregates are increased, thrombocytopenia occurs and depletion of platelets prior to infection reduces survival in the case of EMCV and CVB (Koupenova et al., 2018, 2014; Onlamoon et al., 2010). In influenza infection, platelets are activated through FcγRIIA and thrombin generation and degranulation contributes to lung inflammation, reducing survival (Boilard et al., 2014; Lê et al., 2015). COVID-19, another RNA virus, has also been linked to platelet hyperactivation and increased thrombotic risk, evidence for a platelet-virus interaction is emerging (Zaid et al., 2020).

1.1.7.2 Interaction with the Endothelium in Inflammation

GPIb–V–IX, GPVI, and CLEC2 are involved in platelet adherence to the activated blood vessel wall (Kleinschnitz *et al.*, 2007; Ho-Tin-Noé *et al.,* 2018). VWF is secreted from Weibel-Palade bodies and deposited on endothelial cells and may trap platelets(Bierings & Voorberg, 2016). Platelets may also interact with the endothelium and leucocytes via P-selectin, E-selectin, VCAM and ICAM-1, which are expressed by the endothelium during inflammation or infection (Koupenova *et al.*, 2018; van der Meijden *et al.,* 2019). IL-1β is also involved in the platelet-endothelium reaction, as expression and release by platelets increases endothelial permeability and leucocyte recruitment Following adherence to the endothelium, platelets release chemokines and recruit leucocytes which initiate an inflammatory response at the site of vessel injury (Deppermann & Kubes, 2018). This may be pathological, such as in the case of acute lung injury, and has been treated with P-selectin blocking in mouse models (Zarbock *et al.,* 2006). In humans the development of a P Selectin inhibitor (Crizanlizumab) has been shown to decrease painful crises by reducing platelet endothelial crosstalk and microvascular thrombosis formation (Ataga et al., 2017). CCL5 (RANTES) and CXCL4 (PF4) are released by platelets and activate leucocytes, promoting adhesion to endothelial cells and degranulation (Deppermann & Kubes, 2018). In inflammatory states, the binding of GPVI and CLEC2 to collagen and podoplanin on macrophages and the release of platelet granules is important to maintain vascular integrity and prevent haemorrhage (Deppermann & Kubes, 2018). In stroke patients, endothelial cells in the brain contain few adhesion molecules but platelets bind and recruit leucocytes which contribute to the inflammatory state (Jenne & Kubes, 2015). Platelets or platelet-derived microparticles are involved in the pathogenesis of rheumatoid arthritis, by entering the synovial joint and interacting with leucocytes, creating a proinflammatory environment (Jenne & Kubes, 2015).

1.1.7.3 Platelets in Autoimmune Disorders

Platelets have been implicated in several auto-immune disease, reviewed by Łukasik et al. (Łukasik *et al.,* 2018) Rheumatoid arthritis (RA) is the most common connective tissue disease and is associated with mortality due to cardiovascular disease (Choy et al., 2014). Increased platelet turnover, platelet microparticles and platelet activation status are reported in RA patients. Systemic sclerosis is another autoimmune disease which presents with increased platelet activation). Systemic lupus erythematosus (SLE) is associated with thrombocytopenia, increased platelet activation and increased incidence of cardiovascular

disease, stroke and VTE. Anti-phospholipid syndrome (APS) is an autoimmune disorder associated with markedly increased thrombotic risk and the presence of anti-phospholipid antibodies (lupus anticoagulant, anticardiolipin antibodies, anti-β2 GPI), the main target of which are platelets. Anti-phospholipid antibodies may activate platelets directly or activate the endothelium which increases adhesion molecule expression. APS patients generally experience thrombocytopenia due to excessive platelet destruction (Baroni et al., 2017).

Patients with autoimmune diseases have an increased risk of cardiovascular events (Amaya-Amaya *et al.,* 2014). Platelet-neutrophil interaction stimulates NET (Neutrophil Extracellular Trap) formation, which activate platelets in a positive feedback loop and may cause tissue injury and a prothrombotic tendency (Sangaletti et al., 2012). Interaction with neutrophils allows platelets to move from the vasculature to tissues. Platelet activation facilitates tissue damage by production of cytokines and pro-inflammatory lipids, externalisation of epitopes which bind autoantibodies, activating complement, stimulating NET formation and activating endothelial cells. Immune complexes of autoantibodies can activate platelets via FcR signalling (Arman & Krauel, 2015). The platelet and microparticle association with dendritic cells via CD154 promotes autoantibody production by interaction with lymphocytes and also promotes interferon secretion.

However, platelets also have anti-inflammatory functions which have been employed in the treatment of autoimmune disease. Platelets secrete anti-inflammatory lipid mediators which help clear apoptotic cells and immune complexes, and study of the use of platelet rich plasma in the treatment of rheumatoid arthritis has led to some provocative data (Lippross *et al.*, 2011; Łukasik *et al.,* 2018). Platelets also interact with regulatory T-cells in brain injury and during atherosclerosis (Bergmann et al., 2016; N. Li, 2013). Production of the anti-inflammatory IL-10 by T-cells was enhanced by interaction with platelets and platelet-derived chemokines (Gerdes et al., 2011). The anti-inflammatory effect of platelets appears to depend on the stimulus, with pro-inflammatory responses occurring in response to low levels of stimulation, while severe sepsis triggers anti-inflammatory effects (Stocker et al., 2017).

1.1.7.4 Platelet-Leucocyte Interactions

Platelets recruit leucocytes to the site of injury or inflammation by anchoring to the endothelium or tissue and providing adhesive molecules which bind leucocytes or by secreting chemokines at the injury site (Zucoloto *et al.,* 2019). In the innate immune

response, platelets form aggregates with monocytes and neutrophils (Koupenova et al., 2018). Platelets also play a role in the adaptive immune response by trafficking lymphocytes to lymph nodes and liver sinusoids via P-selectin interaction with lymphocytes and expansion of lymphocytes during infection via CD40L interaction (Diacovo et al., 2016). The platelet interaction with leucocytes and microbes stimulates morphological changes in the platelets that are distinct from stimulants such a thrombin, which serve a haemostatic function, (Koupenova et al., 2018). However, platelet-leucocyte interaction and inflammation are also important for venous thrombus formation (Stevens & McFadyen, 2019). Platelet-leucocyte interaction is mediated by platelet GPIb, which binds to Mac-1 on leucocytes, platelet CD40, which binds to CD40 ligand on leucocytes and platelet P-selectin binding to leucocyte P-selectin glycoprotein ligand (PSGL) (van der Meijden *et al.,* 2019). Mac-1 may also bind to fibrinogen bound to activated platelets (Deppermann & Kubes, 2018).

Eosinophils

Eosinophils comprise approximately 2% of leucocytes and are involved in response to helminth parasite infection and allergic inflammation, causing asthma (Koupenova et al., 2018). Platelets interact with eosinophils via P-selectin / PSGL interaction and are reported to prolong eosinophil survival through GM-CSF secretion and to recruit eosinophils to the lungs during allergic inflammation, propagating tissue damage (Koupenova et al., 2018)

Monocytes

Platelet monocyte aggregates may be a sensitive method of assessing platelet activation (Michelson et al., 2001) and are reportedly elevated in myocardial infarction (Furman et al., 2001; Sarma et al., 2002) and associated with VTE (Shih et al., 2016). It is proposed that secretion of RANTES by activated platelets and human neutrophil peptide 1 (HNP1) by activated neutrophils form heterodimers which facilitate monocyte and macrophage adhesion and recruitment (Alard et al., 2015). CX3CR1 / CXC3L1 interaction also facilitates monocyte complexes with activated platelets (Postea et al., 2012). P-selectin and PSGL also facilitate this interaction and P-selectin binding has been shown to mediate accumulation in thrombi, fibrin formation and production of tissue factor by monocytes (Stevens & McFadyen, 2019).

Neutrophils

Platelets interact with neutrophils via P-selectin, GPIb and integrin αIIbβ3 (Zucoloto *et al.,* 2019). Activated platelets also release ICAM-2 which my bind to neutrophils via β2 integrins (Diacovo et al., 1994). Activated platelets also adhere to circulating neutrophils by released pro-inflammatory high-mobility box group 1 (HMBG1) , IL-1β and PDGF (Łukasik *et al.,* 2018). Activation of platelets via TLR7, TLR2 and TLR4 also increase interaction with neutrophils (Blair et al., 2009; Clark et al., 2007; Koupenova et al., 2014). Neutrophils may phagocytose activated platelets, mediated by PS exposure (Maugeri et al., 2009). P-selectin may stimulate neutrophils indirectly also via released soluble P-selectin (Zucoloto *et al.,* 2019). Interaction of P-selectin and PSGL induces integrin (LFA-1, Mac-1) activation in neutrophils (Rossaint *et al. ,* 2018).

Platelet interaction with neutrophils leads to increased neutrophil adhesion to the endothelium, reactive oxygen species (ROS) generation and the formation of NETs, which immobilise bacteria (Deppermann & Kubes, 2018; Stevens & McFadyen, 2019). NETs involve fusion of primary granules with the neutrophil nuclear membrane, causing destruction of nucleus content and release into the extracellular environment (Łukasik *et al.,* 2018). NETs are a feature of the innate immune system and are also involved in venous thrombus formation, termed NETosis (Stevens & McFadyen, 2019). TLR4 and P-selectin are key receptors in this interaction (Stevens & McFadyen, 2019). TLR-4 on platelets detect bacterial pathogen-associated molecular patterns (PAMPs) and activate platelets on binding, which then causes platelet-neutrophil interaction and NET production (Deppermann & Kubes, 2018). NETs may activate platelets, creating a positive feedback loop, and activate thrombin initiating coagulation (Stevens and McFadyen, 2019; Zucoloto *et al.,* 2019). NET formation and platelet-neutrophil microthrombi were identified as a feature of acute respiratory distress in COVID-19 (Middleton et al., 2020). They can also form in sterile inflammatory conditions, such as during acute lung injury (Deppermann & Kubes, 2018). Other than P-selectin-PSGL interaction, platelets may also stimulate NET formation via HMBG1, thromboxane A2 and β-defensin (Zucoloto *et al.,* 2019).

Lymphocytes

Platelets bind only to larger, activated lymphocytes (Li *et al.,* 2006). Although they do not aggregate with B-cells directly, platelet co-incubation with B-cells increases production of

IgG (Cognasse et al., 2007). Platelets aggregate with T-cells via platelet CD154 and lymphocyte CD11b (Li *et al.,* 2006). P-selectin, integrin αIIbβ3 and CD40 also facilitate interaction (Łukasik *et al.,* 2018). Platelet granule components including serotonin and CCL5 mediate T-cell activation and differentiation (Koupenova et al., 2018). Platelet interaction with T-cells facilitates recruitment of the cells to the site of injury or inflammation (Hu et al., 2010). They also interact with dendritic cells through CD40 and stimulate the cells to present antigens to T-cells (Semple *et al.,* 2011).

1.2 Platelets in an Inherited Bleeding Disorder : Actinin-1

Actinin is a widely expressed F-actin binding and cross-linking protein which has been identified in most eukaryotic organisms (Beggs et al., 1992; Blanchard et al., 1989). Actinin belongs to the actin-binding spectrin superfamily, in addition to spectrins and dystrophin (Blanchard et al., 1989; Virel & Backman, 2004). It was one of the first actin-crosslinking molecules reported in muscle cells (Ebashi et al., 1964; Maruyama & Ebashi, 1965) and was later also identified in non-muscle cells (Mimura & Asano, 1978). Actinin has wide ranging functions as it is a component of cell-cell and cell-matrix contacts, adhesion sites, cell protrusions, stress fibre dense regions and the Z disc in muscle cells (Foley & Young, 2014).

1.2.1 The Actin Cytoskeleton

The actin cytoskeleton has important functions in essentially all cell types. Its structure is well studied and is reviewed by Blanchoin et al. (Blanchoin et al., 2014). It has been particularly well studied in the context of migrating cells where actin filaments comprise key cellular structures including ventral stress fibres, which orientates in the direction of cell movement and transverse arcs which are parallel to the cell's leading edge and motile organelles such as lamellipodia (branched actin filaments) and filopodia (parallel actin filaments). Actin also forms the cell cortex, an actomyosin contractile shell beneath the cell membrane. The contractile properties of actin filaments in stress fibres, transverse arcs and the cell cortex are facilitated by myosin. Antiparallel actin filaments are linked by myosin and slide by the contraction of myosin in an ATP dependent reaction to allow cytokinesis and stress-fibre function.

Figure 1.2.1

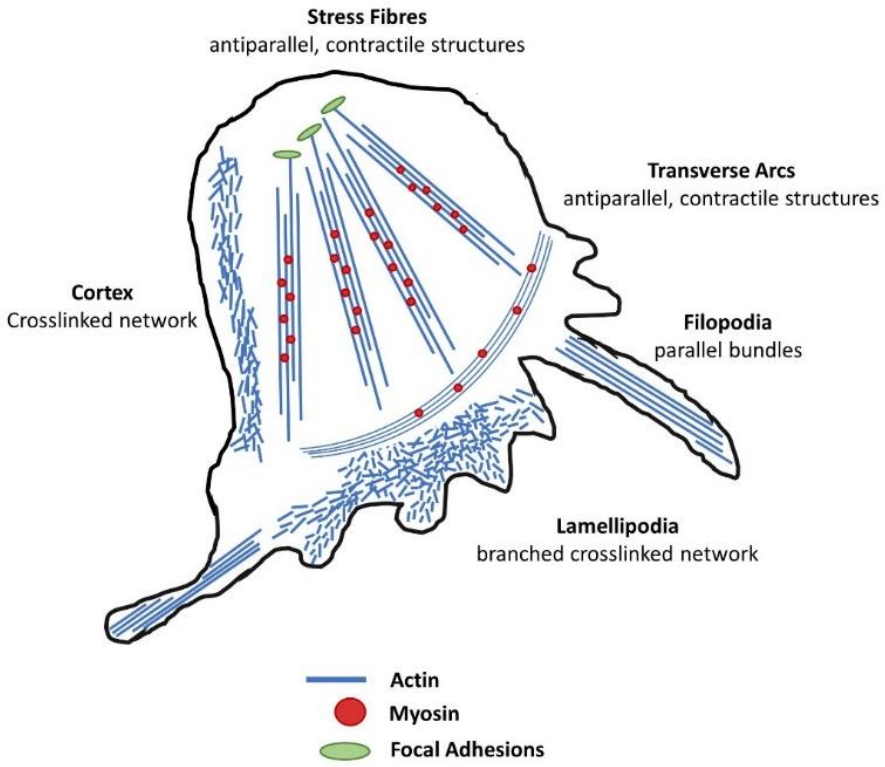

Figure 1.2.1 Illustration of actin structures in non-muscle cells. In non-muscle cells actin is arranged into key structural arrangements illustrated above. Lamellipodia and filopodia drive motility, while the cortex and contractile stress fibres and transverse arcs maintain the mechanical integrity and coordinated movement of the cell. *Figure is adapted from that published in Blanchoin et al., (2014).*

Actin filaments are assembled as 42 kDa actin monomers form trimers in a nucleation step which elongate and polymerise by the addition of monomers and hydrolysis of ATP bound to the actin units in the monomer. Filaments assemble with a right-handed helical twist and distinct barbed and pointed ends. The addition of actin monomers occurs more rapidly at the barbed end of the filament. Profilin regulates actin filament assembly at the barbed end by binding to monomers which can only be used for *de novo* assembly when catalysed by nucleation factors such as Arp 2/3, WASP, WAVE and formins (Blanchoin et al., 2014; Paavilainen et al., 2004). WASP activation of Arp2/3 occurs by stimulation via Rho GTPases (Pollard et al., 2000). Profilin also catalyses the recycling of actin monomers through nucleotide exchange (Pollard et al., 2000). Twinfilin also binds to actin-ADP and prevents nucleotide exchange and actin assembly (Paavilainen et al., 2004).

Arp 2/3 complexes participate in the generation of a branched actin network, along with capping proteins such as CapZ and gelsolin which block extension at the barbed ends (Cooper & Schafer, 2000). Branched actin networks are found at lamellipodia, phagocytic cups of haematopoietic cells and adherens junctions (Blanchoin et al., 2014; Rottner & Schaks, 2019; Rottner & Stradal, 2011). Cross-linked actin filaments are linked by cross-linking proteins, the size of which determines the distance between filaments. Actin filaments can also be assembled into bundles with barbed ends orientated in one direction at filopodia and microvilli, with filamin being involved in this assembly (Suarez & Kovar, 2016). Branched networks and bundles are involved in cellular force generation. Actin filament fragmentation and de-branching is induced by ADF/cofilin which binds to actin-ADP subunits at the filament away from the elongating barded end. Myosin induced fragmentation through contraction also disassembles the actin network. Actin assembly and disassembly occur simultaneously in a "treadmilling state", whereby actin monomers are removed at the pointed end and reincorporated at the barbed end (Manhart et al., 2019). The recycling of actin contributes to the availability of monomeric actin required for continued assembly (Suarez & Kovar, 2016).

1.2.2 Overview of Actinin Isoforms

Actinins are coded by the ACTN genes, with the four mammalian genes (ACTN1-4) arising from two gene duplication events (Dixson et al., 2003). Actinin-2 and actinin-3 are regarded as muscle isoforms and actinin-1 and actinin-4 are regarded as non-muscle (Foley & Young, 2013). Calcium sensitive and insensitive isoforms exist, arising due to alternative splicing of two variants (19a and 19b) of exon 19,which encode part of the first EF-hand of the CaM domain (Foley & Young, 2013). Actinin-1 and actinin-4 variants expressing 19a, which are calcium-sensitive, are similar in expression pattern and widely expressed (Foley & Young, 2013). However, calcium-insensitive variants expressing 19b differ, with calcium-insensitive actinin-4 being found only in the brain and spinal cord, while calcium-insensitive actinin-1 is also found in muscle and other tissues (Foley & Young, 2013). Also, an actinin-1 variant in the brain expresses exon 19a and 19b (Foley & Young, 2013). Actinin-2 and actinin-3 are calcium-insensitive and exclusively encode exon 19b (Foley & Young, 2014). Additionally, alternative splicing of exon 8 (8a and 8b), affecting the CH2 domain of the ABD, regulates actin binding, with brain-specific ACTN2 expressing alternate exon 8a (Lek et al., 2010). Actinin-4 also expresses exon 8a in most tissues but 8b in CNS and muscle (Foley

& Young, 2013). Table 1.2.2 and Figure 1.2.2 illustrate alternative splicing of exons 19 and 8 in actinin and expression patterns of actinin isoforms.

Figure 1.2.2

Figure 1.2.2 Schematic representation of alternative splicing patterns of exons 19 (A) and 8 (B). *The splicing and expression patterns of the various actinin isoforms are detailed in table 1.2.2 below. Figure is adapted from that in Foley & Young (2013).*

Table 1.2.2 : An overview of ctinin isoforms by alternative splicing of Exons 19 (A) and Exon 8 (B), calcium-sensitivity and tissue expression. The actinin isoforms details in this table are reviewed in Foley & Young (2014).

A.

Actinin Isoform	Exon		Calcium-sensitivity	Tissue Expression
	19a	19b		
Actinin-1			Sensitive	Widely expressed
Actinin-1			Insensitive	Muscle & CNS
Actinin-1			Sensitive	Brain
Actinin-4			Sensitive	Widely expressed
Actinin-4			Insensitive	Brain & CNS
Actinin-2			Insensitive	Cardiac & Skeletal Muscle, Brain
Actinin-3			Insensitive	Skeletal Muscle

B.

Actinin Isoform	Exon		Tissue Expression
	8a	8b	
Actinin-4			Most tissues
Actinin-4			CNS & Muscle
Actinin-2			Brain
Actinin-2			Muscle

Non-muscle actinin-1 and 4 isoforms are found at focal contacts and actin stress fibres, with actinin-1 being localised to stress fibres and at the perinuclear region more abundantly while actinin-4 is distributed to the curved ruffles and circular dorsal ruffles in

motile cells and is also found in the nucleus (Araki, Hatae, Yamada, & Hirohashi, 2000; Bolshakova et al., 2007). Actinin-4 is similar to actinin-1 in sequence (86% amino acid sequence homology) (Otey & Carpen, 2004). Actinin-4 is more abundant in highly motile cells (Otey & Carpen, 2004). Actinin-4 mutations are linked to kidney disease, namely Focal Segmental Glomerulosclerosis (FSGS) (Kaplan et al., 2000). Actinin-4 knockout in mice also causes abnormal podocyte morphology and kidney failure (Kos et al., 2003). Actinin-1 may compensate for actinin-4 in other tissues but does not rescue podocyte morphological changes in the kidneys in those with mutated actinin-4 (Kos et al., 2003). Actinin-4 can also regulate transcription and can translocate to the nucleus , with overexpression of the protein being reported in several cancers (Feng et al., 2015; Honda, 2015).

Actinin-2 and actinin-3 are found in skeletal and cardiac muscle and neuronal cells, with actinin-2 being found mainly in cardiac and oxidative skeletal muscle and actinin-3 in glycolytic skeletal muscle (Foley & Young, 2014). In muscle, they are found in the Z-disc and analogous dense bodies, where they form a lattice-like structure linking actin filaments from adjacent sarcomeres and stabilise the muscle contractile unit (Gautel & Djinović-Carugo, 2016). Actinin-2 and actinin-3 are 80% identical with overlapping functions (Mills et al., 2001). Although actinin-1 and -4 are also found in muscle, actinin-2 and actinin-3 are more strongly associated with the Z-line (Hsu et al., 2018). This is thought to arise due to calcium-sensitivity in the non-muscle isoforms, although a calcium insensitive actinin-1 isoform is also present in smooth muscle (Hsu et al., 2018).

The actinin isoforms are not thought to be redundant, as actinin-2 and actinin-3 were reported to shift muscle metabolic profiles in mice (Macarthur et al., 2008) and are not able to rescue isoform-specific defects (Gupta et al., 2012). Similarly, actinin-1 was not able to rescue actinin-4 related defects in some circumstances (Shao et al., 2010). Actinin isoforms can also form heterodimers (Chan et al., 1998; Foley & Young, 2013). Heterodimers are reportedly expressed in greater concentration in cancer cell lines, although the mechanisms and consequences of this have not been explored (Foley & Young, 2013).

1.2.2 Functions of Actinin

1.2.2.1 Adhesion Sites

At adhesion sites, such as focal adhesions, hemidesmosomes and adherent junctions, actinin links actin to transmembrane proteins (Sjöblom et al., 2008). These include integrins, ICAM-1 and vinculin (Sjöblom et al., 2008). The negatively charged actinin rod facilitates binding to positively charged cytoplasmic components of these proteins (Sjöblom et al., 2008). Actinin stabilises the adhesion site, contributes to cell shape, clusters adhesion molecules at the adhesion site and integrates signalling molecules to the adhesion site (Otey & Carpen, 2004).

In cell-cell junctions actinin binds to α-catenin in cadherin-catenin complexes and establishes a link to the actin cytoskeleton (Knudsen et al., 1995; Nieset et al., 1997). Actinin-4 also has a role in actin assembly at cadherin-enriched cell junctions (Tang & Brieher, 2012)

Focal adhesions are integrin-rich structures linking the extracellular matrix to the actin cytoskeleton (Burridge, 2017). They adhere to the extracellular matrix and transmit intracellular mechanical forces to the extracellular environment, termed the molecular clutch (Burridge, 2017; Case & Waterman, 2015). Actinin links the actin cytoskeleton to focal adhesions via interaction with the β-integrin cytoplasmic tail (Otey et al., 1990; Pavalko et al., 1991). Actinins also play a role in the assembly and disassembly of focal adhesions (Foley & Young, 2014). Actinin, talin and vinculin are involved in force transmission at focal adhesions (Case & Waterman, 2015; Roca-Cusachs et al., 2013; Ye et al., 2014). Actinins are also involved in maturation of nascent adhesions in migrating cells and regulate the orientation of elongating actin filaments with actinin-1 knockdown decreasing protrusion rates (Choi et al., 2008).

1.2.2.2 Cell Motility

Stress fibres in non-muscle cells are dynamic contractile structures of actin and myosin II which generate tension and allows cell migration through rear retraction (Hu et al., 2019). Dorsal stress fibres are connected to the extracellular matrix via focal adhesions at one end, while transverse arcs are not anchored to the substrate but are generated at the lamella through annealing of actin and myosin bundles (Hotulainen & Lappalainen, 2006).

Dorsal and transverse fibres can be converted to ventral fibres which are adhered to focal adhesion at both ends (Hotulainen & Lappalainen, 2006). Actinin-1 and actinin-4, and phosphorylation of actinins, are essential for the formation of dorsal and transverse arc stress fibres in migrating cells (Feng et al., 2013). Actinin-1 depletion results in loss of dorsal stress fibres, leading edge focal adhesion maturation and early cell spreading (Kovac et al., 2013). Actinin and tropomyosin compete for F-actin binding, which regulates actin crosslinking and myosin stack formation in stress fibre formation (Hu et al., 2019; Kempet al., 2018). Increased association of actinin to stress fibres in tropomyosin knockdown cells resulted in reduced actomyosin tension and traction forces (Hu et al., 2019).

Cell migration requires the formation of protrusions such as lamellipodia and filopodia, adhesion formation and retraction at the rear of the cell (Le Clainche & Carlier, 2008). Actinin-4 plays a role in the steering mechanism, cell speed and lamellipodial dynamics during keratinocyte cell migration (Hamill et al., 2015; Hamill et al., 2013). Actinin is important for the spatial regulation of the actin cytoskeleton in response to extracellular cues during migration (Senger et al., 2019).

1.2.2.3 Endocytosis & Exocytosis

Actinin also has a role in the cell processes of endocytosis and exocytosis (Foley & Young, 2014). Actinin-4 appears to have an important role, with distinct roles in GLUT4 trafficking in muscle cells (Talior-Volodarsky et al., 2008), transferrin receptor recycling (Yan et al., 2005) and distinct localisation with comparison to actinin-1 in phagocytic cups and phagosomes of macrophages (Araki et al., 2000). Actinin-4 also localised to lamellipodia and early macropinosomes (Araki et al., 2000), which involves plasma membrane ruffles or lamellipodia closing back onto the membrane to form vesicles with internalisation of extracellular solute and plasma membrane (Lim & Gleeson, 2011). In FcR and CR3 mediated phagocytosis, actinin is recruited, providing force generated by actin network to engulf the bound particle (May & Machesky, 2001). Actinin remains enriched in internalised phagosomes, possibly maintaining a link to the actin cytoskeleton (May & Machesky, 2001).

1.2.2.4 Cytokinesis

Cytokinesis, the process of cell division, involves remodelling of stress fibres, formation and constriction of a cleavage furrow and severing of the cell membrane (Liu & Robinson,

2018). Actinin localises to the cleavage furrow during cytokinesis (Fujiwara et al., 1978; Sanger et al., 1987). Protein complexes called nodes with emanating actin filament form in the centre of the cell during interphase and are condensed by the pulling of actin filaments by myosin II, forming a contractile ring (Foley & Young, 2014). Actinin is involved in node condensation (Wu et al., 2001) and in actinin null fission yeast cells, the formation of the contractile ring is delayed (Laporte et al., 2012). Additionally, actinin over-expression delays contractile ring formation due to stabilisation of actin filaments and inhibition of myosin dependent movements (Laporte et al., 2012). In mammalian cells actinin overexpression also impacted ingression of the cleavage furrow by slowing actin turnover and increasing actin concentration at the furrow (Jayadev et al., 2012; Low et al., 2010; Mukhina et al., 2007; Reichl & Robinson, 2007). Calcium sensitivity also aids accumulation of actinin at the cell centre during furrow formation (Jayadev et al., 2012).

1.2.2.5 Sarcomeric Z Disc

In muscle, actinin interacts with contractile, adaptor and signalling proteins involved in contracting cells (Sjöblom et al., 2008). This includes titin, nebulin, actin filament capping proteins (CapZ), Z-disc adaptor and associated proteins and actin-associated LIM protein (ALP) (Sjöblom et al., 2008). Actinin also interacts with metabolic enzymes required for energy generation in muscle cells including phosphorylase involved in glycogenolysis (Chowrashi et al., 2002), aldolase and fructose-1-6-biphosphatase (Rakus et al., 2003). Actinin binds these proteins to the sarcomere Z-disc where metabolites are available (Sjöblom et al., 2008).

In muscle, actin filaments are key components of the sarcomere, which is the contractile unit of the muscle fibre (myofibril) (Clark et al., 2002). The myofibril includes Z-lines connected by thin actin filaments and thick myosin filaments which coordinate to allow transmission of contractions to the costameres and muscle membrane (Berman & North, 2010). Actinin is found in the Z-line where they bind actin and other Z-line associated proteins (eg. ZASP, filamin, myopalladin) (Berman & North, 2010). Actinin also cross-links actin filaments and titin filaments from adjacent sarcomeres (Berman & North, 2010). Actinin interacts with titin via EF hands 3-4 of the CaM domain of actinin and the Z-links of titin and is regulated by PIP2 (Gautel & Djinović-Carugo, 2016). Actinin is also thought to contribute to the conformational change of the Z-line via its flexible neck region allowing movement of the bound actin (Gautel & Djinović-Carugo, 2016).

1.2.2.6 CNS Synapses

Actinin-1,2 and 4 are expressed in the brain, with both calcium sensitive and insensitive actinin-1 and 4 isoforms expressed (Foley & Young, 2014). In the CNS, actinin interacts with the NMDA and adenosine A2A receptors in synapses (Burgueño et al., 2003; Wyszynski et al., 1998). Actinin-4 also interacts with densin and CAMKII in CNS synapses, thought to stabilise the synapse and may contribute to neuronal functions including learning and memory (Otey & Carpen, 2004; Robison et al., 2005). Actinin is also involved in the structure and function of neuronal filopodia and neurite growth cones (Sobue & Kanda, 1989).

1.2.3 Actinin Structure

Actinin is a rod-shaped antiparallel dimer of monomers of 93 – 103 kDa (Blanchard et al., 1989; Imamura et al., 1988). It has significant elasticity and is curved axially and twisted, allowing it to resist mechanical forces and provide high affinity binding sites (Otey & Carpen, 2004). The structure of the actinin-2 dimer revealed that actinin is ~360 Å long and ~60 Å wide (Ribeiro et al., 2014). Actinin has three key structural domains, the actin-binding domain, rod domain and calmodulin-like domain, which are illustrated in Figure 1.2.3.1 and discussed further in this section.

Figure 1.2.3.1

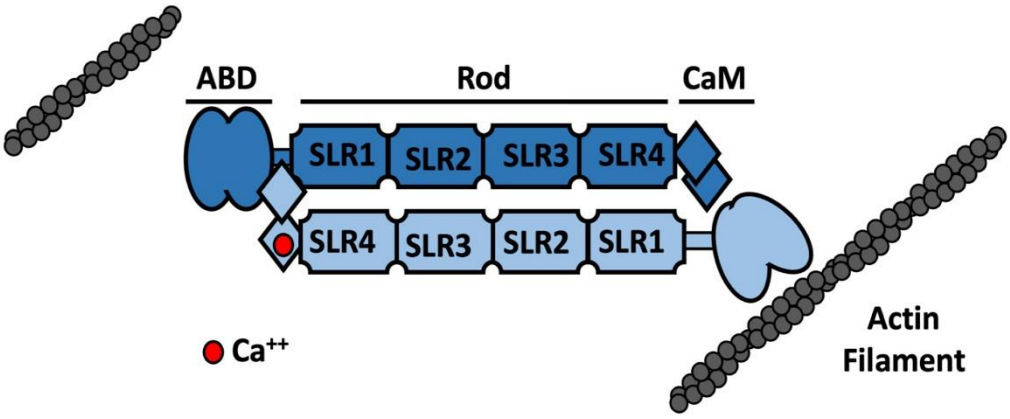

***Figure 1.2.3.1 Illustration of the actinin dimer**. Each monomer has three key domains. The actin binding domain (ABD) consists of two tandem calponin homology (CH) domains (CH1-CH2). The rod domain consists of four spectrin-like repeats (SR1-4).The Calmodulin-like Domain (CaM) is the calcium-binding domain and consists of four EF hands. Monomers*

assemble as an antiparallel dimer to bundle actin filaments (F-actin). The calcium-bound, inhibited state and calcium-free, F-actin-bound states are shown here on the left and right hand sides of a single actinin dimer for illustrative purposes only. Ca++ = calcium. This illustration was created by P Young and is published in (O'Sullivan et al., 2021).

1.2.3.1 Actin Binding Domain

In the actin monomer, the actin binding domain (ABD) is a 27 kDa domain is made up of two tandem N-terminal calponin homology (CH1-CH2) domains (Blanchard et al., 1989; Virel & Backman, 2004). The CH domains are made up of four helices (A, C, E, G) (Sjöblom et al., 2008). Helices A and G of CH1 interact with the CH2 with hydrophobic and polar contacts in a highly stable complex (Sjöblom et al., 2008). Using actinin-1 numbering, Trp128 (CH1) and Lys236 (CH2) are conserved residues of the ABD which interact to stabilise the domain (Bañuelos et al., 1998; Borrego-Diaz et al., 2006). Three actin binding sites (ABS1-3) are present on the ABD, two on CH1 and one on CH2 (Sjöblom et al., 2008). ABS2 and ABS3 form a contiguous region on the ABD surface while ABS1 is buried within the CH1-CH2 interdomain region when the ABD is in its closed conformation (Sjöblom et al., 2008). In the absence of actin, actinin is in the closed conformation (Ribeiro et al., 2014). When bound to actin, actinin is in a higher affinity state with rearranged domains (Borrego-Diaz et al., 2006). The ABD of smooth muscle actinin in its open conformation when bound to actin has been assessed by cryoelectron microscopy (McGough et al., 1994). The ABS and residues adjacent are conserved, in line with the conserved sequence of actin (Sjöblom et al., 2008). Linking the ABD to the first spectrin repeat is a 6-turn α-helical neck region (Ribeiro et al., 2014). The ABD can take various orientations due to flexibility of this region (Sjöblom et al., 2008; Taylor & Taylor, 1993; Winkler et al., 1997) Polar interactions between this neck region and EF3-4 of the CaM domain also stabilise the dimer (Ribeiro et al., 2014). The N-terminal region preceding CH1 may also play a role in localisation of actinin to various cellular actin structures (Harris et al., 2019).

1.2.3.2 Rod Domain

The actinin rod domain consists of four spectrin-like repeats (SR) of 122 amino acids in a coiled-coil conformation, with high sequence homology to those found in spectrin and dystrophin (Blanchard et al., 1989; Golji et al., 2009). The rod domain is highly conserved across species, highlighting its critical function in stabilising actinin structure and

involvement in binding other proteins (Blanchard et al., 1989). The rod domain facilitates the antiparallel dimerization of actinin by the binding of SR1 with SR4 of the opposing monomer, and interaction of SR2 with SR3 of the opposing monomer (Flood et al., 1995; Flood et al., 1997). SR2 and SR3 are stably bonded while SR1 and SR4 may dissociate and undergo mechanical unfolding and re-folding under force to confer elasticity to the actin cytoskeleton and expose buried binding sites, including that for vinculin in SR4 (Le et al., 2017). The rod also facilitates bending flexibility of actinin (Golji et al., 2009). In the homodimer, repeats consisting of triple-helix bundles are linked via a continuous α-helix of one repeat interacting with a continuous α-helix on the repeat of the other actinin molecule (Djinovic-Carugo et al., 1999). A 55° turn exists between SR 2 and 3 of the rod domain which facilitates complementary binding to the opposite actinin subunit (Djinovic-Carugo et al., 1999). The entire rod domain is axially twisted by 90°, stabilising the structure and orientating the ABDs 90° with respect to each other (Ylänne et al., 2001). There is an electrostatic polarity in the repeats, with SR 1 and 2 being positively charged, while SR 3 and 4 are negatively charged (Djinovic-Carugo et al., 1999). Negatively charged residues from SR 2 interact with positively charged residues from repeat 3 on the opposite actinin molecule (Djinovic-Carugo et al., 1999). In addition, hydrophobic and Van der Waal interactions and a hydrogen bond connect SR 2 and 3 (Djinovic-Carugo et al., 1999). Overall, extensive polar and non-polar contacts bury 11% of the monomer in the dimerization (Ylänne et al., 2001). Linker residues connect adjacent repeats and also function to stabilise the repeats (Djinovic-Carugo et al., 1999). The linker between SR 2 and 3 of one actinin subunit interacts hydrophobically with resides on adjacent SR 2 and 3 of the same actinin subunit (Djinovic-Carugo et al., 1999). In addition, interactions between loops of SR 2 and loops of repeat 3, and interaction of helix 2 of SR 2 and helix 1 of SR 3 stabilise repeats (Djinovic-Carugo et al., 1999). The rod domain determines the distance between actin filaments, with four repeats in human actinin but two repeats in some organisms, thought to have evolved by intragenic duplication (Virel & Backman, 2004). Unexpectedly, increases of the rod length by 15% was not critical to its function in the muscle Z-disc (Dubreuil & Wang, 2000). The rod domain surface is acidic and is the site of binding for various proteins other than actin (Djinovic-Carugo et al., 2002; Virel & Backman, 2004; Ylänne et al., 2001).

1.2.3.3 Calmodulin-Like Domain

The calcium binding calmodulin-like (CaM) domain comprises four C-terminal EF hands (Virel & Backman, 2004). Each EF hand is a helix-loop-helix motif (Sjöblom et al., 2008). The domain shifts from a closed to an open conformation, exposing hydrophobic residues, when bound to calcium (Ikura, 1996). A single calcium ion may bind to the CaM domain at the N terminal lobe (Prebil et al., 2016). Muscle actinins do not bind calcium, with variation in calcium binding residues which are thought to have evolved with the development of muscle tissue and allow constitutive actin binding independent of calcium concentration changes (Sjöblom et al., 2008). A lysine residue in these isoforms prevents calcium binding at the co-ordinating site (Blanchard et al., 1989). Both non-muscle and brain actinin-1 express exon 19a and bind calcium with a Kd of 45–55 µM (Backman, 2015). The CaM domain of muscle actinins also localises actinin to the Z-disc via titin binding (Young et al., 1998; Young & Gautel, 2000). In the actinin dimer, the CaM domain EF 3-4 interacts with the neck region between the ABD and first spectrin repeat of the other actinin subunit (Ribeiro et al., 2014; Young & Gautel, 2000). EF1-2 interacts with spectrin repeat 4 (Ribeiro et al., 2014). Electron microscopy of the full length actinin dimer suggested the CaM domain was not at this region, and potentially between the two CH domains of the ABD of the opposite actinin subunit (Liu et al., 2004; Tang et al., 2001). The NMR structure of the CaM domain showed that when not bound to calcium, the CaM domain is not associated or loosely associated with the neck region, while the EF3-4 region of the domain binds to the neck region in the presence of calcium (Prebil et al., 2016) A conformational change involving opening of EF hand 1-2 and structural stabilisation of the domain occurs when bound to calcium which also reduces the flexibility of the adjacent ABD and inhibits actin binding (Prebil et al., 2016).

1.2.4 Actinin Interaction with Actin

Actinin binds reversibly to F-actin but does not bind G-actin (Miyata et al., 1996). Increasing temperature increases actinin affinity for F-actin but diminishes the actin viscosity induced by actinin binding (Bennett et al., 1984). The actinin interaction with actin filaments occurs at angles clustered in five ranges (0,60,90,120,180 degrees) by a flexible neck region linking the ABD and rod domain (Hampton et al., 2007). Actin filaments can be crosslinked in a parallel orientation, at focal contacts and membrane attachments, and anti-parallel, at Z-

discs (Liu et al., 2004; J Ylänne et al., 2001). Actinin is stabilised by binding F-actin, with delayed digestion *in-vitro* (Jia & Kuroda, 2011).

Actin binds to the CH1 domain of the ABD (Way et al., 1992). CH2 is thought to be a negative regulator of actin binding and opening of the CH1-CH2 interface to remove the CH2 steric hindrance is required for actin binding (Galkin et al., 2010). In the actinin dimer, one ABD takes an open conformation, while the other is closed (Liu et al., 2004). The conformation of the ABD affects the binding of actinin to actin (Shams et al., 2016). Additionally, mutations in the CH1-CH2 interface of utrophin (which has tandem CH domains common to the ABD of actinin) which do not affect the open conformation can cause increases in actin affinity, suggesting other factors may influence affinity (Harris et al., 2019). In addition to the ABD, the CaM domain affects actinin affinity for F-actin by binding to the neck region and regulating the orientation and distance between actin and the ABD (Shams et al., 2016). Actin binding could also be regulated by triggering twisting and bending in the rod domain on the binding of actin to one ABD, affecting the orientation of the second ABD (Shams et al., 2016). Regulation of actin filament cross-linking by actinin is also modulated by other actin binding proteins such as cofilin and filamin (Bonet et al., 2010; Esue et al., 2009; Falzone et al., 2013). Two actinin ABDs may also bind to one actin filament, possibly with a role in protein anchoring (Hampton et al., 2007).

The two actin binding sites of actinin are separated by 30–40 nm and bind actinin monomers along the long-pitch helix (McGough et al., 1994). Actinin length may determine spacing of the protein along actin filaments (R. K. Meyer & Aebi, 1990). The range of lengths is suggested to confer linear elasticity in actin bundle formation (Hampton et al., 2007). The distribution of actin filament length is regulated by actin polymerisation and depolymerisation dynamics (Edelstein-Keshet & Ermentrout, 1998). Actinin regulates the distribution width of F-actin filament length (Biron & Moses, 2004). Actinin also regulates F-actin strain hardening under shear (Xu et al., 2000).

1.2.5 Actinin Regulation

1.2.5.1 Calcium

Non-muscle actinin isoforms bind actin in a calcium-sensitive manner (Blanchard et al., 1989). Calcium binding to actinin inhibits its ability to bundle actin into filaments at 50-100 µM but actin filaments are also affected (Pacaud & Harricane, 1993). 0.1 mM calcium reduces actin cross-linking activity in macrophages and platelets (Bennett et al., 1984; Landon et al., 1985). 10 µM calcium is sufficient to reduce actin binding by non-muscle actinin by 50% (Foley & Young, 2013). Magnesium and potassium ions also compete with calcium for actinin binding (Pacaud & Harricane, 1993). Actinin-1 isoforms include the calcium insensitive smooth muscle isoform, which encodes exon 19a, and the calcium sensitive non-muscle and brain isoforms which encode exon 19b and both 19a and 19b respectively (Foley & Young, 2013).The non-muscle and brain isoforms bind calcium with a Kd of 45-55 µM (Backman, 2015).

1.2.5.2 Proteases

Proteolysis is thought to contribute to actinin's role in detachment at focal adhesions at the rear of migrating cells (Dourdin et al., 2001). MEKK1 binds to actinin at these sites and modulates proteolytic cleavage of actinin by calpain (Christerson et al., 1999; Cuevas et al., 2003). Calpain inhibition also inhibited actinin co-localisation with zyxin, a focal adhesion protein linking actin to adhesion sites via actinin, and disassembly of the adhesion was inhibited, implying actinin cleavage is required for this process (Bhatt et al., 2002). Actinin-4 involvement in cell spreading, adhesion and migration is also sensitive to calpain cleavage, after Tyr13 and after Lys 283 (Shao et al., 2013). The final 11 amino acids of the C-terminal tail also act to prevent cleavage at Lys 283 in non-muscle actinin-1 and actinin-4 (Shao et al., 2013). Cleavage of actinin-4 at Tyr 13 is also regulated by phosphorylation at this site, with resistance to calpain cleavage in the phosphorylated actinin (Shao et al., 2018). Phosphoinositide binding also modulates sensitivity to calpain cleavage (Sprague et al., 2008).

1.2.5.3 Phosphatidylinositols

In calcium insensitive muscle actinins, actin binding is negatively regulated by phospholipid phosphatidylinositol 4,5-biphosphate (PIP2) binding (Burn et al., 1985; Fraley et al., 2003; Fukami et al., 1994; Fukami et al., 1996; Yin & Janmey, 2003). In skeletal muscle actinin, PIP2 binds to the loop between helix A and B of the CH2 domain, in proximity to the ABS3

(Franzot et al., 2005). PIP2 binding induces a conformational change which causes the release of the CaM domain from the neck region and allows the CaM domain to interact with other proteins including titin and PDZ and enhances actin binding (Sjöblom et al., 2008). PIP2 binds to CH2 of the ABD via its polar head, with it aliphatic chain extending to the neck region (Ribeiro et al., 2014). This activating event in muscle actinin triggers release of the CaM domain EF3-4 from the neck region, allowing it to interact with titin (Young & Gautel, 2000). Additionally, binding is reported to constrict CH2 and alter ABD orientation and to interfere with interaction of the N and C terminus in the actinin dimer, contributing to reduced affinity for F-actin and reduced bundling activity (Full et al., 2007). PtdIns (3,4,5,)-P3 (PIP3), produced by activated PI 3-kinase, reduces actinin affinity for β integrin and its ability to bundle F-actin, promoting cell detachment at focal adhesions in migrating cells (Fraley et al., 2005; Greenwood et al., 2000). PIP2 and PIP3 regulate proteolysis of actinin by calpain 1, with PIP2 decreasing cleavage and PIP3 increasing (Sprague et al., 2008). PIP3 increases cleavage by increasing the flexibility of the neck region connecting the ABD and SR1, while PIP2 stabilises this structure to reduce cleavage (Corgan et al., 2004). PIP2 and PIP3 are hence involved in regulating actinin turnover in the cell which controls remodelling of the actin cytoskeleton (Fraley et al., 2005).

1.2.5.4 Phosphorylation

Integrin-activated tyrosine kinase focal adhesion kinase ($pp125^{FAK}$) phosphorylates actinin-1 at Tyr12 of the ABD in non-muscle actinins, reducing actinin affinity for actin (Gonzalo Izaguirre et al., 2001a). This enhances cell motility (Gonzalo Izaguirre et al., 2001a). Tyrosine phosphorylation of actinin-4 at Tyr4 and Tyr31, stimulated through growth factor signalling, also inhibits actinin-4 binding to actin (Shao et al., 2010). Phosphorylation of Tyr4 and Tyr31 are shown to maintain the ABD in a closed conformation, inhibiting actin binding (Travers et al., 2013). Tyr4 phosphorylation acts as a switch which regulates phosphorylation of Tyr31, and is absent in calpain cleaved actinin (Travers et al., 2015). Actinin-1 and 4 phosphorylation is required for stress fibre maintenance and focal adhesion maturation (Feng et al., 2013) and regulate their incorporation into focal complexes (Von Wichert et al., 2003).

1.2.5.5 Mechanosensory Regulation

Actinin is also regulated by mechanical stresses from internal and external physical forces (Luo et al., 2013; Schiffhauer et al., 2016; Thomas & Robinson, 2017). Actinin-4 is capable of sensing extracellular matrix stiffness (Meacci et al., 2016) and a conformational change in the rod domain SR4 is induced which stabilises its interaction with vinculin in focal adhesions (Le et al., 2017; Shams et al., 2012). External mechanical pressure is increased in the tumour microenvironment and actinin-4 acts as a mechanotransducer which mediates increased cell proliferation by interaction with NF-κB (Downey et al., 2011). A FSGS linked actinin-4 mutant (Actinin-4 K225E) with higher affinity for actin was shown to be insensitive to mechanoregulation (Weins et al., 2007) and was predicted to have no catch-slip bond activity, where the binding lifetime of the bond increases with mechanical stress up to a threshold, and then ruptures beyond this threshold force (Hosseini et al., 2020; Schiffhauer et al., 2016).

1.2.6 Actinin Related Diseases

Mutations in all actinins have been linked to heritable diseases and traits (Murphy & Young, 2015). A number of thesis disorders are outlined below.

1.2.6.1 Focal Segmental Glomerulosclerosis (FSGS)

Focal Segmental Glomerulosclerosis (FSGS) is a kidney disorder characterised by proteinuria, declining renal function and kidney failure (Kaplan et al., 2000). Mutations in actinin-4 cause an autosomal dominant FSGS, with no apparent non-renal pathology in spite of widespread expression of actinin-4 (Kaplan et al., 2000). Actinin-4 mutations alter glomerular pores and impair filtration by reducing podocyte cytoskeletal flexibility and motility, cause podocyte effacement and reduced adherence, capillary collapse and the development of focal adhesions lacking actinin-4 (Dandapani et al., 2007; Ehrlicher et al., 2015; Michaud et al., 2006; Michaud et al., 2009; Weins et al., 2007). Familial actinin-4 related FSGS typically presented in early adulthood and progressed to end stage renal disease (Feng et al., 2015). Actinin-4 mutations which cause FSGS are reported only in the ABD of actinin-4 (Feng et al., 2015).

Actinin-4 has a kidney specific function, as actinin-4 null mice also develop FSGS in spite of actinin-1 expression (Kos et al., 2003). This is possibly due to podocyte sensitivity to

cytoskeletal disruption or an actinin involvement in protein-protein interaction (Kos et al., 2003) or the actinin-4 role in transcriptional activity (Khurana et al., 2012; Zhao et al., 2017). FSGS-causing mutations in actinin-4 cause increased F-actin binding affinity and insensitivity to calcium regulation (Weins et al., 2007). Although speculated to involve a conformational change with exposure of the actin binding site 1 in the ABD (Weins et al., 2007), the K225E mutation does not appear to affect ABD conformation (Lee et al., 2008). It is speculated that the mutations destabilise the CH1-CH2 interface, which causes an open high-affinity conformation (Galkin et al., 2010). Weakening of inter CH domain contacts is another proposed mechanism, although different mutations may have different molecular mechanisms facilitating increased F-actin association (Lee et al., 2008). Mutations also cause abnormal localisation of actinin-4, abnormal cytoskeletal architecture and cytoplasmic aggregates associated with the actin cytoskeleton (Weins et al., 2007). Additionally, dissociation of the K225E mutant actinin-4 from F-actin was slower (Ward et al., 2008) and degradation of the mutant actinin-4 was accelerated (Yao et al., 2004). Actinin-4 transcriptional regulating functions are also impacted, with inhibited localisation to the nucleus in mutant actinin-4 (Feng et al., 2015). Severity of disease varies with zygosity (Henderson et al., 2008).

In one study, phosphomimetic mutations in actinin-4, which have reduced actin binding, were able to rescue cell migration reduction in mutants and prevent actinin-actin aggregate formation (Shao et al., 2019). Continuous EGF signalling also causes this tyrosine phosphorylation of actinin-4 with subsequent reduction in actin binding, and may be explored to treat actinin-4 related FSGS (Shao et al., 2019).

1.2.6.2 Athletic Performance

Actinin-3 is expressed in fast glycolytic skeletal muscles which allow rapid and forceful contractions (Beggs et al., 1992; Mills et al., 2001). Actinin-3 is absent in those homozygous for the nonsense mutation p.Arg577X (R577X), due to degradation of the mutant (North et al., 1999), and this mutation affects approximately 16% of the population, with higher frequency in European and Asian populations (Lek et al., 2010). This null allele is thought to have arisen first in humans, as ACTN3 is conserved in other species and shows distinct localisation with comparison to ACTN2 during murine embryonic development (Mills et al., 2001). There is no apparent disease association in those lacking actinin-3, implying it may be compensated for in muscle fibres by actinin-2 (North et al., 1999). However, a high

frequency of the actinin-3 wild type allele is reported in sprint athletes and the null allele is found more commonly in endurance athletes compared with power athletes, implying actinin-3 is linked with athletic performance (Yang et al., 2003). Various studies of this phenomenon have been carried out and reviewed previously (Alfred et al., 2011; Eynon et al., 2013; Lee et al., 2016; Pickering & Kiely, 2017; Tharabenjasin et al., 2019). In a recent review of 44 studies, the association of the RR and RX genotype (expressing actinin-3), with faster sprint times, more fast-twitch muscle fibres and greater muscle size and strength versus those with the null genotype (XX) was reported (Tharabenjasin et al., 2019). However, the null genotype was not significantly associated with athletic performance, although reported in some studies (Tharabenjasin et al., 2019). In actinin-3 knockout mice, muscle mass and strength are reduced but within the normal range, while there is a shift to aerobic muscle metabolism, used typically by slow muscle fibres (Macarthur et al., 2008). Mitochondrial enzyme activity is also increased in actinin-3 knockout mice (Macarthur et al., 2008). Glycogen content is increased and glycogen phosphorylase activity is reduced in association with actinin-3 deficiency (Berman & North, 2010). This is in conjunction with an enhanced endurance, i.e. capable of greater running distances (MacArthur et al., 2007). Restoration of actinin-3 expression in null genotype mice unexpectedly did not enhance performance but impacted muscle metabolism (Garton et al., 2018). In addition to athletic performance, the R577X genotype has implications for patients with Duchenne muscular dystrophy, with the shift to oxidative metabolism in R577X patients conferring protection against progression of dystrophic pathology (Hogarth et al., 2017). Also, the genotype may impact other aspects of athletic performance such as training response, recovery following exercise and injury risk (Pickering & Kiely, 2017).

1.2.6.3 Myopathies

Actinin-2 is expressed in cardiac and skeletal muscle and in the brain (Beggs et al., 1992; Wyszynski et al., 1998). Actinin-2 is found in muscle as a major component of the Z-disc, cross-links actin filaments between sarcomeres, and may be involved in mechanosensing and signal transduction as it acts as a scaffold for interacting proteins in the Z-disc (Gautel & Djinović-Carugo, 2016). In the brain, in post-synaptic densities of excitatory synapses, actinin-2 binds to the NMDA receptor and is sensitive to calcium regulation both by inhibition of actinin-2 actin binding and by displacement of actinin-2 from the NMDA receptor (NR1) by calmodulin(Wyszynski et al., 1998). Mutations in actinin-2 are linked with heart defects including dilated cardiomyopathy (DCM) and hypertrophic cardiomyopathy

(HCM) (Chiu et al., 2010; Mohapatra et al., 2003). HCM is the most common genetic myocardial disease affecting 0.2% of the population (Maron et al., 1995). Sarcomere proteins and sarcomere related proteins are typically affected, with actinin-2 mutations thought to affect cell architecture, the Z-disc, signalling functions or localisation and function of ion channels (Good et al., 2020; Mohapatra et al., 2003). One study reported a non-significant reduction in F-actin binding affinity in mutated actinin-2 (Haywood et al., 2016) Mutations are reported in all regions of actinin-2, although heterogeneity in clinical presentation exists even in families with identical mutations, highlighting that environmental factors may also influence the disease course in these individuals (Chiu et al., 2010; Girolami et al., 2014; Kelly & Semsarian, 2009; Murphy & Young, 2015). An Ala119Thr mutation in the ABD of actinin-2 was linked to cardiac pathologies of varying clinical phenotype (Bagnall et al. , 2014).

In addition to cardiomyopathy, actinin-2 mutations are linked to congenital skeletal muscle disorders. Patients with actinin-2 mutations presented with early onset muscle weakness and respiratory involvement, with sarcomeric and Z-disk defects (Lornage et al., 2019). Another study identified actinin-2 mutations in patients with a late onset and progressive distal myopathy (Savarese et al., 2019)

1.2.6.4 Cancer

Actinin, particularly actinin-4, has been implicated in various cancers, reviewed in detail previously (Honda, 2015; Tentler et al., 2019). Various mechanisms for the actinin contribution to tumorigenesis have been reported. Actinin-4 can translocate to the nucleus and regulate transcription, including genes involved in epithelial-to-mesenchymal transition (EMT) and drug resistance (Feng et al., 2015; Honda, 2015; Tentler et al., 2019). Actinin also supports the structural changes facilitating cell metastasis and invasiveness as the actin cytoskeleton and associated proteins are involved in formation of invasive protrusions such as lamellipodia and invadopodia (Machesky, 2008; Tentler et al., 2019; Yamaguchi & Condeelis, 2007).

In breast cancer cells, actinin played a role in disassembling cell-cell junction, promoting metastasis (Guvakova et al., 2002). Although expression of actinin-1 and actinin-4 were increased in metastatic breast cancer cell lines, overexpression of actinin-4 only significantly promoted invadopodia formation, increasing metastatic potential (Yamaguchi et al., 2017). A similar observation of actinin-4 but not actinin-1 involvement in colorectal

cancer was reported, with actinin-4 causing immature focal adhesion formation and subsequent enhanced invasiveness (Fukumoto et al., 2015). Actinin-4 was also reported to an oncogenic regulator in melanoma (Zhang et al., 2018) and be involved in promoting an amoeboidal morphology promoting invasion, while actinin-1 was not involved (Shao et al., 2014). Actinin-4 knockdown was associated with reduced motility (Barbolina et al., 2008; Hayashida et al., 2005; Quick & Skalli, 2010), reduction in glioma cell speed (Sen et al., 2009) and reduced invasive potential in animal model of oral squamous cell carcinoma (Yamada et al., 2010). Of note, cytoplasmic actinin-4 is thought be involved in this process rather than nuclear actinin-4 (Honda et al., 1998; Jasalava et al., 2007)

Actinin is a prognostic indicator in some cancers. Actinin-4 was also associated with poorer prognosis in breast cancer and an infiltrative phenotype (Honda et al., 1998). A similar poor prognostic association was observed for ovarian cancer (Barbolina et al., 2008; Yamamoto et al., 2007, 2012), pancreatic cancer (Kikuchi et al., 2008; Welsch et al., 2009) and gliomas (Fukushima et al., 2014; Quick & Skalli, 2010). Interestingly, the actinin-4 isoform expressing exon 8b is reported to be an independent prognostic factor in neuroendocrine lung tumours (Miyanaga et al., 2013)..

In contrast, some studies report that actinin-4 has tumour suppressing functions (Menez et al., 2004; Nikolopoulos et al., 2000; Yoon et al., 2008). In human neuroblastoma cells, actinin-4 shows tumour suppressor activity and is downregulated in malignant cells (Nikolopoulos et al., 2000). Additionally, a recent study demonstrated that TFPI, a tumour suppressor in breast cancer, exerts its effect through interaction with cytoplasmic actinin-4 (Wang et al., 2018).

Actinin-1 was also shown to reduce motility in transformed fibroblasts (Glück & Ben-Ze'ev, 1994; Gluck et al., 1993). Increased expression of actinin-1 and actinin-3 were indicators of poor prognosis in acute myeloid leukaemia, with actinin-3 speculated to confer oncogenic metabolic changes (Yang et al., 2019).

1.2.6.5 Autoimmune Disease

Anti-actinin antibodies have been identified in patients with autoimmune diseases. Serum anti-actinin antibodies were increased in patients with systemic lupus erythematosus (SLE), rheumatoid arthritis and Sjøgren's syndrome (Becker-Merok et al., 2006). In systemic lupus erythematosus (SLE) anti dsDNA antibodies frequently cross-react with actinin (Deocharan

et al., 2002; Deocharan et al., 2007; Mostoslavsky et al., 2001; Renaudineau et al., 2007) and anti-actinin antibodies are present at a greater concentration in SLE patients versus those with other autoimmune diseases and healthy controls (Croquefer et al., 2005). These autoantibodies are implicated specifically in lupus nephritis, with deposition of autoantibodies to actinin in the glomeruli and an associated decrease in anti-actinin antibodies in the serum (Babaei et al., 2016; Zhang et al., 2010). Actinin-1 and actinin-4 were also overexpressed in mesangial cells of lupus-prone mice, possibly explaining the high actinin autoantibody titres in SLE patients (Zhao et al., 2006). However, longitudinal study did not report any significant clinical correlation with anti-actinin levels in SLE patients (Manson et al., 2009), while anti-actinin antibodies were associated with glomerulonephritis in another study (Renaudineau et al., 2007). Although the isoform of actinin implicated was not addressed in these studies, actinin-4 variants were associated with SLE previously (Ramos et al., 2011). Additionally, actinin is expressed on the membrane of parenchymal and ductal cells of the liver (Inada et al., 2008; Tsukada et al., 1995) and anti-actinin autoantibodies targeting the ABD have been reported in autoimmune hepatitis (Guéguen et al., 2006). Anti-actinin antibodies have prognostic potential in autoimmune hepatitis, as their presence was an independent predictor of response to treatment in one study (Zachou et al., 2012) and correlated with active disease, clinically and histologically (Renaudineau et al., 2008).

1.2.6.6 Congenital Macrothrombocytopenia (CMTP)

As discussed above, actinin-1 is widely expressed and has functions in adhesion, migration and cytokinesis by anchoring actin filaments to the cell membrane and cell junctions (Otey & Carpen, 2004). Heterozygous expression of an ACTN1 knockout allele in mice has been described (The International Mouse Phenotyping Consortium). Homozygous knockout allele mice were not used, likely as they were not viable, given the wide expression of actinin-1 (Murphy & Young, 2015). Interestingly, actinin-1 mutations appear to have a tissue specific consequence, causing the platelet disorder congenital macrothrombcytopenia (CMTP), characterised by a low platelet count and increased platelet size (Kunishima et al., 2013).

Inherited platelet disorders

More than 51 genes have been identified in inherited platelet disorders (Freson *et al.,* 2017). However, less than half of all those affected have a determined genetic cause (Freson *et al.,* 2017). The most severe platelet disorders include Glanzmann's thrombasthenia (GT), affecting αIIbβ3, and Bernard-Soulier Syndrome (BSS), affecting GPIb. Affected genes include those encoding platelet receptors, signalling proteins, cytoskeletal proteins, transcription factors (FL1, GATA1, NFE1, RUNX1, TAL1), and genes involved in granule synthesis (NBEAL2, GFI1B, HPS1 HPS3, HPS9) (van der Meijden *et al.,* 2019). Among the most widely known are mutations affecting alpha granules (grey platelet syndrome), dense granules (Hermansky-Pudlak syndrome) and all granules (platelet storage pool deficiencies) (van der Meijden *et al.,* 2019). α and dense granule disorders make up 3.7% and 9.3% of inherited platelet disorders (Bariana et al., 2017).

Several inherited platelet disorder (IPD) genes involve the cytoskeleton. Mutations in WAS cause Wiskott-Aldrich Syndrome, linking platelet dysfunction, eczema and immunodeficiency (Rand et al., 2018). The WAS protein (WASP) and its interacting protein (WIP) are involved in F-actin polymerisation and mutations cause microthrombocytopenia, microtubule and actin cytoskeleton disruption and reduced platelet spreading on fibrinogen and collagen (Nurden & Nurden, 2015). Myosin Heavy Chain IIA (MYH9), filamin A and tubulin β1 defects are also associated with macrothrombocytopenia and an altered cytoskeleton (Nurden & Nurden, 2015). Some mutations are gain of function (GP1bα, ORAI1) and lead to hyper-reactivity (Bunimov *et al.,* 2013; Nagy *et al.*, 2018).

Diagnosis of Inherited Platelet Disorders

Recent studies have aimed to standardise the investigation of inherited platelet disorders (Gresele et al., 2014). Beyond the assessment of bleeding history, platelet count and platelet morphological assessment, laboratory parameters including light transmission aggregometry (LTA), platelet-function analyser 100 (PFA-100) analysis, flow cytometry and bleeding time (now historic and largely replaced by the PFA-100 and flow cytometry), may be assessed (Gomez et al., 2021). A guideline by the British Society for Haematology has recently been published to guide the clinical diagnosis of inherited platelet disorders (Gomez et al., 2021). .

Genetic analysis is recommended for all patients suspected of having an inherited platelet disorder using a High-throughput sequencing (HTS) panel of causative genes (Gomez et al.,

2021). HTS has expanded the list of known genes associated with inherited platelet disorders (Freson et al., 2017). The ThromboGenomics consortium have compiled a HTS panel of 76 genes for the diagnosis of bleeding and platelet disorders (BPD) (Simeoni et al., 2016). Initial testing of the ability to detect previously identified variants yielded a sensitivity of 100% in 300 patients. When the variant was unknown, sensitivity was also high (>90%). However a diagnosis was not made in 90% of patients with a disorder of unknown genetic origin. In another study of 519 patients with platelet disorders, a known gene variant was identified in <10% of cases (Westbury et al., 2015).The UK-GAPP study compiled a panel of 329 potential BPD genes for analysis by whole-exome sequencing (WES) (Leo et al., 2015). Other groups have used a panel of 71 platelet-related genes (Lozano et al., 2016) and a panel of 87 genes for WES analysis in BPD diagnostics (Leinøe et al., 2017). A curated list of 91 genes for HTS were published more recently, highlighting the expanding profile of BPD linked genes (Megy et al., 2019)

For a variant to be named "pathogenic", it must be described in 3 unrelated families with a shared phenotype (Freson et al., 2017). Likely pathogenic variants involve a gene defect in a patient which is consistent with the phenotype reported and the variant is absent or present at a low frequency in a control database (Freson et al., 2017). Variants of Undetermined Significance (VUS) may be linked with the disease phenotype but the consequence of the variant is too uncertain (Freson et al., 2017). This classification relies on an adequate control database which includes variants from a wide array of ethnicities, while current databases have a European bias (Freson et al., 2017). The diagnoses of IPD may lead to knowledge of co-morbidities and potential future associated problems. Research is still evolving in this area but, for example, RUNX1 mutations are associated with acute myeloid leukaemia (AML) and SRC mutations are associated with myelofibrosis and bone defects (Freson et al., 2017).

1.2.7 Actinin In Platelets

As detailed above, actinins are a widely expressed group of proteins, with the actinin isoforms having tissue-specific expression patterns, mechanisms of regulation and disease associations. Actnin-1 is of particular interest in platelets, as mutations in actinin-1 cause the platelet disorder CMTP. A review of what is known about actinin expressed in platelets and megakaryocytes is provided in sections 3.1.3 and 3.1.6.

1.3 Acquired Platelet Dysfunction in Cancer : Multiple Myeloma

In addition to dysregulation of platelet count, functional defects in platelets can cause adverse consequences. Pathological disruption to the platelet activation status and aggregation ability is evident in various disease settings. Increasingly this is reported in cancer patients, and this phenomenon is assessed in this study in the context of Multiple Myeloma.

1.3.1 Features of Platelet Function

1.3.1.1 Activation

Platelets transition from a resting to an activated state in response to various stimuli, allowing them to adhere, aggregate and secrete granule contents. The ability of platelets to become activated is referred to as “responsiveness”. A number of features of the activation process are discussed here.

Platelet Agonists

Platelet agonists can stimulate the exposure of platelet surface receptors in the activation process and subsequently cause adhesion and aggregation (Baaten et al., 2017).

Collagen is one of the most potent platelet activators and stimulates activation physiologically when exposed to the circulation due to vascular injury or pathologically by the disintegration of atherosclerotic plaques(Shekhonin et al., 1985). There are approximately 3,700 copies of the collagen receptor, GPVI, on platelets (Gremmel *et al.,* 2016). This glycoprotein exists in a complex with FcR γ-chain in monomeric form in un-activated platelets with low affinity for collagen (Berlanga *et al.*, 2007; Gremmel *et al.*, 2016). Binding to the low affinity receptor causes inside-out activation of integrins and clustering of GPVI (Gremmel *et al.,* 2016). The dimeric form has high collagen affinity and also leads to intracellular signalling on binding collagen (Jung *et al.,* 2009; Gremmel *et al.*, 2016). Following binding, the GPVI receptor is shed from the cell surface (Gremmel *et al.,* 2016). The downstream effect of collagen stimulation has been reviewed by Van der Meijden et al. (van der Meijden *et al.,* 2019). Adhesion of platelets to collagen stimulates

SRC and SYK protein tyrosine kinase activation, stimulation of phospholipase C, elevation of intracellular calcium concentration and stimulation of protein kinase C. This causes activation of integrin αIIbβ3, granular secretion and, where calcium signalling is prolonged, exposure of phosphatidylserine.

Thrombin is a potent platelet activator and binds to the GPCR, protease-activated receptor (PAR)-1 and PAR-4, and GPIb-IX-V (Gremmel *et al.,* 2016). Thrombin is generated via tissue factor, present on smooth muscle cells, macrophages and inflamed endothelium (Swieringa et al., 2018). PAR-1 responds to low levels of agonist, while PAR-4 is involved at high concentrations and responds more slowly than PAR-1 (Gremmel *et al.,* 2016).

Thromboxane A2 and ADP, are a second messengers released by activated platelets (Bye et al., 2016). ADP activates platelets via purigenic GPCR, $P2Y_1$ and $P2Y_{12}$. $P2Y_1$ activation initiates platelet aggregation and shape change, and this is amplified and stabilised by P2Y12 activation (Hardy *et al.*, 2004; Gremmel et al., 2016). ADP is also secreted by red blood cells, the endothelium (Bye et al., 2016). Thromboxane is synthesised in activated platelets and is dependent on the enzyme cyclooxygenase-1 (COX-1), inhibited by aspirin (Karim et al., 1996).

The downstream effects of agonist stimulation are well-studied, as reviewed by Bye et al. (Bye et al., 2016). Briefly, platelet agonists stimulate key mediators of activation; phospholipase C (PLC), protein kinase C (PKC) and phosphatidylinositide-3-kinase (PI3K).This stimulates secretion of secondary activating mediators, cytoskeletal rearrangement, granule secretion and the activation of αIIbβ3. PLC activation catalyses PIP_2 cleavage and DAG generation, which activates PKC and IP_3. Activated IP_3 causes cytosoliccalcium levels increase through interaction with the dense tubular system. The pathways mediated by PLCγ2 are activated by GPVI, ITAM, collagen, fibrinogen and CLEC-2 stimulation. This pathway is particularly important in activation through interaction with matrix proteins during initial platelet adhesion (Nonne et al., 2005). PLCβ is activated through stimulation by GPCRs including PAR1, PAR4, thromboxane and ADP through $P2Y_1$and this isoform is important in amplifying platelet activation through response to secondary mediators(Nonne et al., 2005).

Platelet Subpopulations

Responsiveness can vary between platelets within an individual in terms of adhesion, spreading, granule secretion and pro-coagulant activity, creating a highly heterogeneous population, possibly due to the mechanism of platelet formation, involving random sorting of granules and organelles into mature platelets (van der Meijden *et al.,* 2019). It may also be a consequence of platelet ageing, with older platelets having reduced responsiveness (Karpatkin, 1969; Pleines et al., 2018). Platelets can also acquire RNA from the extracellular environment, altering protein content (Clancy et al., 2017).

Aggregating Platelets

Aggregatory platelets expose an activated integrin αIIbβ3, which has been stimulated to transition from a low-affinity state which prevents them binding to ligands fibrinogen and fibronectin and indirectly to other platelets (Sorrentino et al., 2016). On activation, talin and kindlin bind to the cytoplasmic tail of the integrin and induce a conformational shift to the high-affinity state (Sorrentino et al., 2016).

Secreting Platelets

When platelets are activated, the actin cytoskeleton constricts the circumferential microtubule coils forcing granules into the centre of the cell where they may merge and fuse with the open canalicular system or the plasma membrane, allowing release into the extracellular space (Stenberg *et al.*, 1984; Escolar *et al.,* 1986; Gremmel *et al.,* 2016). Fusion of membranes occurs via soluble-N-ethyl-malemide-sensitive (SNAREs) factor receptors, particularly vesicle-associated membrane proteins (VAMP-2, VAMP-3, VAMP-8) (Gremmel *et al.*, 2016; van der Meijden *et al.*, 2019). tSNAREs (syntaxin 8, syntaxin 11 and SNAP23), small GTPases, microtubules and kinesin 1 also contribute to granule secretion (van der Meijden *et al.,* 2019). Calcium mobilisation, both extracellular and from intracellular stores, also supports granule secretion (Lopez et al., 2015). The actin cytoskeleton differentially regulates release of granules, with disruption of the cytoskeleton in response to agonists facilitating release (Flaumenhaft et al., 2005). It has been demonstrated that granules are released individually at low levels of stimulation, while high agonist concentrations cause alpha granules to fuse prior to release (Eckly et al., 2016). P-selectin (CD62P) is a component of alpha granules which is exposed to the platelet surface following secretion

(Gremmel *et al.*, 2016). GPVI agonists stimulate high exposure of P-selectin and integrin activation but minimal CD63 expression (Baaten et al., 2017).

Procoagulant Platelets

Procoagulant platelets have several names in the literature including ballooned platelets, COAT-platelets (or coated platelet), sustained calcium-induced platelets and fibrinogen-capped platelets, owing to their larger surface area for coagulation factor binding (Agbani & Poole, 2017; Mattheij et al., 2016). Collagen is a key agonist in the formation of procoagulant platelets, while thrombin may also stimulate formation (Agbani & Poole, 2017). Intracellular oxidative stress increases the formation of procoagulant platelets in response to thrombin alone, implying priming of platelets for a procoagulant response (Agbani & Poole, 2017). Aspirin appears to have minimal effect on procoagulant platelet formation (Hua et al., 2015; Prodan, *et al.,* 2008). The procoagulant response resembles cell necrosis but is a gain of function process involving calcium dependence, formation of mitochondrial permeability transition pore (MPTP), cyclophilin D dependence, irreversible membrane ballooning, membrane permeabilization and calpain-dependent actin remodelling (Agbani & Poole, 2017). The procoagulant phosphatidylserine-exposing population of platelets are absent in patients with Scott syndrome, affecting the ANO6 gene, where protein phosphorylation and cleavage is affected, highlighting that post-translational modifications may also influence platelet responsiveness (Solari et al., 2016). Procoagulant platelets also undergo actin cytoskeleton remodelling during transformation to the procoagulant phenotype (Agbani et al., 2015).

Platelet Microparticles

Platelet microparticles (discussed in 1.1.5.3) are extracellular vesicles formed from the plasma membrane of platelets during activation (Varon & Shai, 2015). Microparticles can deliver ligands, such as P-selectin, to interacting cells and enhance their engraftment (Janowska-Wieczorek et al., 2001; Li & Cong, 2009). They have a procoagulant surface which stimulates thrombin generation *in-vitro* (Heemskerk et al., 2005). They are reportedly pro-inflammatory in the context of rheumatoid arthritis (Boilard et al., 2010) and are increased in cardiovascular disease, diabetes and inflammation (Nomura *et al.*, 2000; Koga *et al.*, 2006; Nomura *et al.,* 2008; Vasina *et al.*, 2010).

Downregulation of Platelet Activation by Receptor Shedding

Platelet receptors GPIbα of the GPIb-IX-V complex and GPVI are removed from the cell surface following ligand binding by proteolytic enzymes (shedases) ADAM17 (A Disintegrin and Metaloprotease 17) and ADAM10 (A Disintegrin and Metaloprotease 10) in a rapid and irreversible process (Andrews & Gardiner, 2016). GPVI shedding may also be stimulated by active thrombin (Gardiner et al., 2007; Ramakrishnan et al., 2001). Calmodulin regulates calcium-dependent ADAM-mediated receptor shedding (Andrews & Gardiner, 2016). Elevated shear stress or binding of immune complexes to FcγRIIa may also stimulate GPVI shedding (Andrews & Gardiner, 2016). Promotion and inhibition of receptor shedding is a novel therapeutic strategy for haematitic regulation which is being explored (Andrews & Gardiner, 2016). Plasma levels of shed GPVI are increased in stroke, coronary artery disease and disseminated intravascular coagulopathy (DIC) (Andrews & Gardiner, 2016).

Platelet Priming

Priming refers to a process in which exposure to a stimulus influences response to a second stimulus and has been reviewed by Baaten et al. (Baaten et al., 2017) and Van der Meijden et al. (van der Meijden *et al.,* 2019). The endothelium maintains platelets in a resting, non-activated state by productions of ectonucleotidases, thrombomodulin, prostaglandin A2 and nitric oxide. These negatively prime platelets by increasing cytosolic cAMP and cGMP levels which suppress platelet activity by activating protein kinase A (PKA) and protein kinase G (PKG) and reduce sensitivity to agonists (Bye et al., 2016; van der Meijden et al., 2019). In addition to suppression of activation by the endothelium, some factors can modulate platelet responsiveness and act to positively prime platelets. Ectonucleotidases degrade ATP, ADP and AMP in the circulation.

Epinephrine, thrombopoietin, insulin-like growth factor 1 (IGF1) TNFα and CD40L enhance platelet responses. Aspirin and $P2Y_{12}$ receptor agonist resistance is reported in platelets positively primed with TPO or IGF1 *in-vitro* (Blair et al., 2015). Adrenaline positively primes platelets by reducing cytosolic cAMP levels and lowering the threshold needed for activation by other agonists (Keularts et al., 2000). Other positive primers include insulin-like growth factor I and thrombopoietin, which enhance activation by the PI3K signalling pathway and increase collagen-dependent responses (Blair et al., 2014; Pasquet et al., 2000). Positive priming can act to override anti-platelet agents (Blair *et al.,* 2015). Chronic positive priming and activation can lead to exhausted platelets with reduced sensitivity to

agonists, evident in patients with malignancy, stroke, sepsis and myeloproliferative neoplasms.

Inherited mutations can impact platelet responsiveness to positively and negatively prime platelets. An acquired hypo-responsiveness in platelets is present in patients with haematological malignancy, which is likely a consequence of impaired thrombopoiesis (Fosset al., 2008; Leinoe et al., 2004). Patients with renal failure and uraemia also experience platelet hypo-responsiveness (Mannucci et al., 2012). Positive platelet priming is reported to occur in hypercholesterolaemia, myeloproliferative neoplasms and in diabetics (Baaten et al., 2017). Insulin can also increase platelet cAMP and cGMP levels and loss of this inhibitory process in diabetics may contribute to the platelet hyperactivation reported (Trovati et al., 1995)). Hypercholesterolaemia enhances platelet aggregation by influencing membrane structure(Icli et al., 2015). Chronic positive priming can co-exist with *in-vitro* hypo-responsiveness, reported as exhausted platelets. This has been reported in patients with solid tumours and co-exists with an increased risk of thrombosis (Boneu et al., 1984; J. Riedl et al., 2014; Riedl et al., 2017). The same phenomenon is reported in sepsis (Lundahl et al., 1998) and stroke patients (Jurk et al., 2004).

1.3.1.3 Aggregation

Aggregation is mainly mediated by integrin αIIbβ3 which enters its high-affinity state subsequent to inside-out signalling, enabling binding of fibrinogen and VWF (Gremmel *et al.,* 2016). On vascular injury, platelets are differentially exposed to agonists thrombin and collagen, creating an aggregate of highly activated, densely packed platelets at the core, surrounded by less activated, loosely adhered platelets at an outer shell (Stalker et al., 2014; Van Gestel et al., 2002). Platelets at the core are aggregatory, with activated integrin αIIbβ3 facilitating platelet-platelet interaction via fibrinogen, and secretory, expressing surface P-selectin (Munnix et al., 2007). There are 80-100,000 copies of integrin αIIbβ3 on platelet plasma membrane and also more molecules in the alpha granules, making it the most abundant receptor (Gremmel *et al.,* 2016). Platelets at the outer surface are pro-coagulant, with exposed PS, and may bind coagulation factors and fibrin (Munnix et al., 2007). The pro-coagulant outer platelets increase thrombin generation, amplifying the platelet response (Swieringa et al., 2018).

1.3.1.3 Adhesion

Platelet adhesion to the vascular endothelium is an important component of haemostasis and is facilitated mainly by platelet adherence to exposed VWF and collagen via the GPIb-IX-V complex. There are approximately 25,000 GPIb and GPIX and 12,500 GPV glycoproteins per cell making up the GPIb-IX-V Complex (Gremmel *et al.,* 2016). Clinical studies suggest elevated VWF levels increase the risk of venous thrombosis and blocking of the VWF-GPIb interaction prevent the development of deep vein thrombosis (DVT) in experimental models (Brill et al., 2011; Tsai et al., 2002). Platelets may also bind to thrombospondin and P-selectin on endothelial cells via this receptor (Romo *et al.*, 1999; Jurk *et al.*, 2003; Gremmel *et al.*, 2016). The GPIb-IX-V Complex also interacts with αMβ2 (Mac-1) on leucocytes (Simon et al., 2000). Integrin αIIbβ3 may also mediate adhesion by interaction with fibronectin, vitronectin and thrombospondin-1 (Gremmel *et al.,* 2016). GPVI, which adheres to collagen, and CLEC2 are also important for adhesion in arterial thrombus formation (Boulaftali et al., 2014).

1.3.2 Platelets in Cancer

Excessive blood clotting has long been linked with cancer (Haemmerle et al., 2018). Additionally, thromboembolism is the second leading cause of death in cancer patients, following disease progression (Khorana et al., 2007). Thrombocytosis was linked to malignancy in 40% of 140,000 patients in one early study (Levin & Conley, 1964), while the impact of platelet count alone on cancer progression remains inconclusive (Catani et al., 2020). Thrombocytosis is thought to arise due to increased TPO levels, released by the tumour itself or from factors released by the tumour stimulating hepatic TPO production, such as IL-6 (Catani et al., 2020). Thrombosis affects up to 20% of cancer patients (Khorana et al., 2007) with risk of venous thrombosis being increased 4 to 7.5 fold compared with controls (Blom et al., 2005).

1.3.2.1 Platelets in Tumour Growth & Progression

Activated platelets secrete mitogenic and angiogenic factors which promote tumour progression (Gay et al., 2011). Activation can be mediated by dying tumour cell release of HMGB1 which binds to platelet TLR4 (Xinyu Yang et al., 2015). Tumour cells may also activate platelets by released tissue factor, ADP and thrombin (Asghar et al. , 2019). Platelets secrete lysophosphatidic acid (LPA), which promotes cell proliferation and tumour

invasion and is upregulated in several cancers (Asghar et al. , 2019). LPA enhances endopeptidases which degrade and modulate the ECM allowing tumour cell to enter the blood stream (Asghar et al., 2019; Haemmerle et al., 2018).

Platelets are reported to enhance metastasis via various receptors and a reduction in count has a protective effect (Asghar et al., 2019; Haemmerle et al., 2018). GPVI inhibition has been demonstrated to reduced metastasis in mouse models (Jain et al., 2009). The absence of P2Y12 also reduced metastasis (Wang et al., 2013). PAR-4 deficiency reduced tumour thrombin induced platelet activation and protected from experimentally induced metastasis (Camerer et al., 2004). Platelet integrin αIIbβ3 also interacts with tumour cell αvβ3 and disruption of this interaction reduces metastasis in melanoma (Lonsdorf et al., 2012). P-selectin deficiency reduced tumour metastasis in mice (Coupland et al., 2012; Kim et al., 1998). In addition to facilitating aggregates with tumours, P-selectin promotes tissue factor exposure in monocytes and triggers thrombin generation (Catani et al., 2020). GPIb-IX-V inhibition has been linked with both reduced and enhanced metastasis exposing mechanistic uncertainty (Asghar et al., 2019).

Platelets are thought to regulate tumour cell interaction with the endothelium during metastasis (Asghar et al. , 2019). Circulating tumour cells have properties of cells undergoing Epithelial–Mesenchymal Transition (EMT) (Armstrong et al., 2011). Platelets help maintain tumour cells in this state (Labelle et al., 2011). This process also involves interaction with leucocytes and induction of CCL5 (RANTES) receptors (Läubli et al., 2009). Other factors including LPA and PGE2 also aid to disrupt the endothelium aiding metastasis (Asghar et al. , 2019). Platelet granule contents such as TGF-β, PDGF and ADP also support tumour EMT and metastasis (Asghar et al. , 2019). VEGF promotes angiogenesis and is released into the tumour micro-environment by activated platelets (Möhle et al., 1997). Other factors like PDGF and cytokines also promote angiogenesis (Haemmerle et al., 2018)

1.3.2.2 Tumour Protection by Platelets

Platelets can aggregate with tumours via activated integrin αIIbβ3 and fibrin to form a heteroaggregate in the blood (Gay & Felding-Habermann, 2011). Tumours coated with platelets in mouse models are protected from NK cell destruction (Nieswandt et al., 1999) and tumour necrosis factor α (TNF- α) (Philippe et al., 1993). The tumour-platelet interaction is reported to involve fibrinogen (Palumbo et al., 2005). Platelet activation and degranulation is increased by tumour cell interaction, downregulating NK cell NKG2DL and

IFNγ production via TGFβ release (Kopp *et al.,* 2009). Activated platelets may also transfer the MHC to tumour cells which allows evasion of immune surveillance (Placke et al., 2012). Tumour cells may also express platelet receptors to escape immune destruction (Tímár et al., 2005). Platelets can also promote tumour cell survival in the circulation by protecting from shear forces and allowing adhesion to the vessel wall (Asghar et al. , 2019).

1.3.2.3 Tumour-Educated Platelets

Platelets can endocytose components from the plasma and other cells, including tumour cells (Best et al., 2015). The relationship is bi-directional, with platelets also transferring RNA to tumour cells (Michael et al., 2017). These platelets contain a different RNA profile and are termed tumour-educated platelets and research has aimed to utilise this diagnostically (Best et al., 2015). Using 5000 differentially expressed RNAs, cancer patients were distinguished from healthy controls with 96% accuracy (Best et al., 2015). In addition, the tumour type and oncogenic status of certain tumours (eg. HER2 positivity, KRAS mutations) was also identified (Best et al., 2015). Besides RNA, proteome components, such as platelet VEGF which is 6.5-28.2 fold higher in cancer patients, may be quantified and used diagnostically (Haemmerle et al., 2018). Morphological changes in platelets of cancer patients have also been reported (Wang et al., 2015). Compared with other targets of "liquid biopsies", such as cell-free DNA and circulating tumour cells, platelets have the advantage of being abundant and easy to isolate (Haemmerle et al., 2018). Challenges in the use of platelet-based liquid biopsies include the need to limit platelet activation *in-vitro*, complete removal of leucocytes and red blood cells and the stability of RNA (Haemmerle et al., 2018).

1.3.2.4 Cancer & Thrombosis

Tumour-cell induced platelet aggregation (TCIPA) described the ability of tumour cells and tumour-derived factors to activate and aggregate platelets (Haemmerle et al., 2018). Increased platelet activation has been reported in several cancers and correlates with metastatic potential (Honn et al., 1992). Platelet activation is induced by GPVI and CLEC-2 stimulation or by soluble factors including TXA2, thrombin and ADP (Asghar et al. , 2019). Integrin αIIbβ3 stimulation also causes TCIPA and secretion of pro-angiogenic factors (Engebraaten et al., 2009). Platelet surface P-selectin also facilitate interaction with tumour cells and the endothelium (McCarty et al., 2000). Increased circulating platelet

microparticles also correlated with increased thrombotic risk and poorer prognosis, possibly related to their pro-angiogenic factors, transfer of platelet surface receptors or delivery of RNA to cancer cells (Haemmerle et al., 2018).

1.3.3 Treatment of Platelet Dysfunction

1.3.3.1 Anti-Platelet Therapies

Thrombosis may be pathological in the context of platelets adhering to sites of atherosclerotic plaque rupture and the formation of arterial thrombi, which may cause acute myocardial infarction and stroke (Stevens & McFadyen, 2019). Antiplatelet drugs are a first-line therapy for cardiovascular disease and atherothrombosis prevention (Mackman, 2008).

Aspirin and NSAIDs are widely used and inhibit COX1, blocking thromboxane A_2 synthesis (van der Meijden *et al.,* 2019). Aspirin irreversibly inhibits COX1 and is associated with bleeding risk (Halvorsen et al., 2014; Patrono et al., 2017). NSAIDs reversibly inhibit COX1 and also cause adverse bleeding (van der Meijden *et al.,* 2019). COX-2 specific inhibitors, which are involved in prostaglandin production, were associated with increased thrombotic risk due to disrupted thromboxane / prostaglandin balance (Funk & FitzGerald, 2007). Aspirin use for the prevention of venous thrombosis is an area of ongoing research. The Aspirin for the Prevention of Recurrent Venous Thromboembolism (WAR-FASA) trial demonstrated a reduction in VTE incidence in patients treated with aspirin and warfarin versus warfarin alone (Becattini et al., 2012). The Low-Dose Aspirin for Preventing Recurrent Venous Thromboembolism (ASPIRE) study showed a non-significant but reduced incidence of VTE in aspirin users (Brighton et al., 2012). Aspirin use has also been shown to reduce VTE incidence in post-operative patients, but direct-acting oral anticoagulants are more widely used (Anderson et al., 2018).

The P2Y12 receptor is another common target of anti-platelet agents (Cattaneo, 2009; Cattaneo, 2006), while no antagonists for P2Y1 are available. Antiplatelet agents are reviewed by Van der Meijden et al. (van der Meijden *et al.,* 2019). P2Y12 targeting agents include reversible (clopidogrel, prasugrel) and irreversible (tricagrelor, cangrelor) inhibition (van der Meijden *et al.,* 2019). Dual anti-platelet therapy with aspirin and a P2Y12 inhibitor block signalling by secondary mediators, thromboxane and ADP, and also serve to prevent

platelet aggregation. Antibodies or molecules blocking active sites on αIIbβ3 are highly effective and, not unsurprisingly, associated with a high bleeding risk

Dual anti-platelet therapy is commonly prescribed in patients with stents (reduce stent blockage) or acute coronary syndrome (Olie *et al.,* 2018).Inhibitors of integrin αIIbβ3 (abciximab, eptifibatide, tirofiban) have been approved for clinical use in patients undergoing coronary procedures (Lischke *et al.*, 2011; Gremmel *et al.,* 2016). A novel agent has recently been described which combines an anti-integrin αIIbβ3 antibody with a Xa inhibitor and is reported to inhibit DVT without increasing bleeding time (Hanjaya-Putra et al., 2018).

A PAR-1 antagonist (vorapaxar) was approved in 2014 for clinical use in peripheral arterial disease and in prophylaxis for patients with a history of myocardial infarction (Morrow et al., 2012; Tricoci et al., 2012), but is also associated with elevated bleeding risk (van der Meijden *et al.,* 2019).

Novel agents aim to target other platelet processes including adhesion, secretion, procoagulant activity (van der Meijden *et al.,* 2019). Examples include GPIb-V–IX inhibitors to prevent binding to VWF and GPVI and CLEC2 inhibitors, blocking ITAM-like signalling (McFadyen *et al.,* 2018). Specific blocking of GPIb-Mac-1 interactions has been shown to reduce incidence of arterial thrombosis (Yunmei Wang et al., 2017). PI3Kβ inhibitors and tyrosine kinase inhibitors are other non-specific agents with antiplatelet properties, inhibiting aggregation and ITAM signalling respectively (van der Meijden *et al.,* 2019). Anti-secretion agents targeting surface P-selectin or secreted ADP are also being investigated (Moeckel et al., 2014; Tardif et al., 2013). Also, polyphosphate (polyP) inhibitors, targeting secreted polyphosphate, have been trialled and shown effective in reducing incidence of thrombosis (Labberton et al., 2016). As current platelet-function tests assess aggregation (LTA, PFA-100), alternative function tests may be required to monitor efficacy of novel agents which target other platelet processes (van der Meijden *et al.,* 2019). Blocking of platelet aquaporins may inhibit membrane ballooning seen in procoagulant platelets and have been shown efficacious in mice (Agbani et al., 2018). Carbonic anhydrase enzymes may also inhibit procoagulant platelets by inhibiting chloride ion entry (Agbani et al., 2020).

Antiplatelet therapies are also being explored for their application in inflammatory and infectious disease. Aspirin and clopidogrel were effective in delaying hepatocellular carcinoma in mouse models of chronic hepatitis B infection, where platelets are involved in

homing effector CD8+ T cells to the liver, causing tissue damage through chronic stimulation (Aiolfi *et al.,* 2015).

Anti-platelet agents targeting various receptors including P-selectin, PAR-1 and P2Y12, have been assessed therapeutically in cancer patients (Haemmerle et al., 2018). P-selectin inhibitors have been shown to prevent homing of malignant plasma cells in the bone marrow of myeloma patients (Azab et al., 2012). P2Y12 antagonists, including clopidogrel, prasugrel and ticagrelor, used to treat patients with acute coronary syndromes were linked to increased cancer incidence (Haemmerle et al., 2018). Similarly, PAR1 inhibitors were linked with solid cancer incidence in one trial (Haemmerle et al., 2018). This highlights a yet to be determined potentially protective effect of the cancer-platelet interaction.

1.3.3.2 Prohaemostatic Therapies

Few therapeutic options exist to prevent platelet-related bleeding. Thrombopoietin mimetics are used to increase platelet count, particularly in ITP and liver disease (van der Meijden *et al.,* 2019). Tranexamic acid, a fibrinolytic inhibitor, is also widely and safely used in thrombocytopenic patients to promote a stable clot and reduce bleeding associated with thrombocytopenia (Cornelissen et al., 2021). 1-deamino-8-D-arginine vasopressin (DDAVP) is a prohaemostatic therapy which has been reportedly used in patients with platelet function disorders (Colucci et al., 2014) It is used to increase VWF levels and Factor VIII activity but has also been shown to enhance the production of procoagulant platelets and platelet-dependent thrombin formation (Colucci et al., 2014). Recombinant factor VIIa has also shown efficacy in thrombocytopenic patients, and those with inherited platelet disorders, as it promotes platelet surface thrombin generation (Roberts et al., 2004) Alternatively, platelet transfusions can increase platelet count (van der Meijden *et al.,* 2019). Platelet transfusions are associated with various challenges, such as donor variation, in terms of platelet recovery and survival, and transfusion reactions (Smethurst & Cardigan, 2021). Additionally transfusions are complicated in scenarios such as the inherited platelet disorder, Glanzmann's Thrombasthenia, by the risk of allo-antibody production (Solh et al., 2015). As mentioned, platelet haemostatic potential is largely independent of platelet count, with significant reductions tolerated without clinical consequence (Morowski et al., 2013; Neunert et al., 2008).

1.4 Thesis Overview

As discussed, platelets are classically considered clot-forming cells but are increasingly being recognised as players in a variety of physiological processes and disease states. The maintenance of platelet count and normal platelet function are vital. Dysregulation of platelet count is assessed in this study in terms of the congenital platelet disorder, CMTP. In chapters 2 and 3, I assess actinin-1 related CMTP mutations in terms of their molecular impact on actinin-1 function and consider the role actinin-1 plays in platelet formation and platelet function. Dysregulation of platelet function is considered in the context of the acquired prothrombotic state in multiple myeloma. In chapters 4 and 5, dysregulation of platelet function in these multiple myeloma patients was assessed.

2.0 Investigation of Calmodulin-Like and Rod Domain Mutations Suggests Common Molecular Mechanism for α-Actinin-1-Linked Congenital Macrothrombocytopenia

Chapter 2 details work which is published in *O'Sullivan LR, Ajaykumar AP, Dembicka KM, Murphy A, Grennan EP, Young PW. Investigation of calmodulin-like and rod domain mutations suggests common molecular mechanism for α-actinin-1-linked congenital macrothrombocytopenia. FEBS Lett. 2020 Jan;594(1):161-174. doi: 10.1002/1873-3468.13562. Epub 2019 Aug 9. PMID: 31365757*. I generated constructs for R320Q, L547P, T737S, T737N actinin-1 mutants by site-directed mutagenesis and cloned these into suitable plasmids. Other plasmids used in this chapter were cloned by co-authors A. Murphy, E. Grennan, A. P. Ajaykumar and A. Murphy (Murphy et al., 2016) . Actin co-sedimentation assays for R320Q, L547P, T737S, T737N actinin-1 mutants were carried out by me and co-author K. Dembicka. My supervisor P. Young and I co-wrote the published manuscript. In figure 2.3.6 D, I imaged transfected and untransfected cells and actin fibre diameter was measured blindly by P. Young in images taken. I reviewed results and carried out statistical analysis of this data. P. Young generated Figure 2.4.1 and made observations of the potential structural impact of CMTP mutants on actinin-1. A note on this was included in the figure legend. I carried out all other experiments and statistical analysis presented in the chapter.

2.1 Introduction

The platelet disorder congenital macrothrombocytopenia (CMTP) is characterised by a low platelet count (<150 x10^9 cells / L) and large platelet size resulting in a heightened bleeding risk of varying severity (Kunishima & Saito, 2006). Recently described mutations in actinin-1 are thought to contribute to 5% of CMTP cases, making it the fourth most common cause of this disease (Faleschini et al., 2018). CMTP-associated mutations in the actinin-1 ABD have been demonstrated to increase its affinity for F-actin, a molecular mechanism common to the inherited kidney disorder, focal and segmented glomerulosclerosis (FSGS) that is caused by actinin-4 mutations (Feng et al., 2018; Murphy et al., 2016). In this chapter, CMTP-causing mutations in the rod and CaM-like domain of actinin-1 are assessed in terms of their impact on actinin's interaction with actin and regulation by calcium.

As detailed extensively in the introduction, α-actinins (actinins) are actin-binding proteins which exist as antiparallel dimers consisting of an actin-binding domain (ABD), a carboxyl-terminal, calcium-binding calmodulin-like (CaM-like) domain and a central rod region (Fig. 2.1). The rod is comprised of four spectrin-like repeats (SR1-SR4) which connect the two functional domains (Blanchard et al., 1989). Actinin cross-links actin filaments, with major functions in cytokinesis, cell motility and adhesion (K. S. Foley & Young, 2014; Kao et al., 2015). The CaM-like domain comprises two pairs of EF hand motifs (EF1-2 and EF3-4) and in the non-muscle isoform of actinin-1 calcium binding to the EF1 inhibits binding and cross-linking of actin filaments. The recently described structure of the actinin-1 CaM-like domain suggests that the binding of a single calcium ion to EF1 facilitates a restructuring of the EF3-4 region to a more open conformation, stabilising its binding to the "neck" region adjacent to the ABD of the opposing subunit and thereby regulating actinin's interaction with F-actin (Prebil et al., 2016).

Figure 2.1

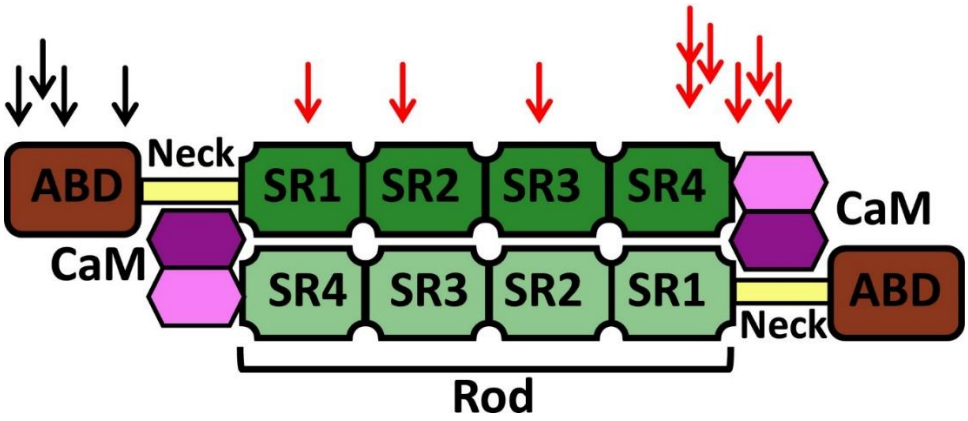

Figure 2.1 Location of amino acids that are mutated in CMTP within the actinin protein structure. *Domain organisation of the actinin-1 dimer showing the interaction of the CaM-like domain with the neck region of the opposing subunit that is thought to regulate actin binding (Prebil et al., 2016; Ribeiro et al., 2014; Young & Gautel, 2000). The approximate positions of selected CMTP-linked mutations are indicated by arrows. Red arrows indicate the mutations in the rod and CaM-like (CaM) domains examined in this study, while black arrows represent mutations in the ABD that were previously shown to increase actinin-1 association with F-actin (Murphy et al., 2016).*

Genetic linkage studies in Japanese and French families led to the identification in 2013 of the first mutations in actinin-1 that cause CMTP (Guéguen et al., 2013; Kunishima et al., 2013). Subsequently these and additional novel mutations were identified in other patient cohorts. A review in 2017 catalogued 20 mutations (Westbury, Shoemark, & Mumford,

2017) and more recent studies have brought the total number of different CMTP-causing actinin-1 mutations identified to approximately 40 (Andres et al., 2018; Faleschini et al., 2018; Kanhai et al., 2018; Luo et al., 2021; Vincenot, 2019). With one exception (Luo et al., 2021) these are all missense mutations that change a single amino acid within the actinin-1 protein, and all appear to be inherited in a dominant fashion. Mutations affecting all the functional domains of the protein (ABD, rod and CaM-like domain) have now been described (Westbury et al., 2017). Thrombocytopenia caused by actinin-1 mutations is mild, with platelet counts of typically 50–130 × 10^9/L and the presence of enlarged platelets with a platelet diameter that has been reported to be 30% greater than controls (Kunishima et al., 2013; Westbury et al., 2017). Bleeding risk is generally low, platelet mass may be only slightly reduced and no abnormalities beyond platelet count and size have been noted. More recently it has been noted that some actinin-1 mutations, while causing macrocytosis are not always associated with thrombocytopenia (Faleschini et al., 2018). The residues mutated in actinin-1 linked CMTP are conserved in other actinin isoforms (actinin-2, -3 and -4) and hence likely have importance for all actinin isoforms (Murphy & Young, 2015).

Although actinin-1 is widely expressed and has a broad range of cellular functions, it appears that actinin-1 mutations have consequences only in platelets (Faleschini et al., 2018), implying a tissue-specific role. Actinin-1 was first identified in platelets as being a prominent component of the platelet cytoskeleton (Landon & Olomucki, 1983; Rosenberg et al., 1981). Genome wide association studies (GWAS) have implicated actinin-1 in platelet parameters including platelet size and platelet count indicating they play a role in platelet formation (Astle et al., 2016; Gieger et al., 2011; Schick et al., 2016). Actinin-1 has an important role in cytokinesis, and has been implicated in endomitosis in megakaryocytes, the process whereby a failure of cytokinesis creates polyploid cells (Dessen et al., 2006; Elagib et al., 2013a). At later stages of platelet production, megakaryocytes display extension of cytoplasmic processes with platelet-sized buds, termed proplatelet tips, which are released into the vasculature (Machlus et al., 2014). Mutant actinin-1 proteins were shown to diminish the number of proplatelet tips and increase their size in an *in-vitro* study (Kunishima et al., 2013). However, analysis of megakaryocytes from affected individuals suggested proplatelet production was active but cells displayed large granules and the cytoplasm showed disorganisation (Guéguen et al., 2013). Actinin-1 also plays important roles during platelet activation and can associate with other platelet activation components including Von Willebrand Factor (VWF) binding GpIb-IX-V complex, integrin β2 and signalling intermediates PI3K and PKN (Feng et al., 2002; Izaguirre et al., 1999; Otey et al.,

1993; Reséndiz et al., 2004). However, platelets isolated from individuals affected with actinin-1 related CMTP are functionally normal in terms of platelet activation (Bottega et al., 2014; Kunishima et al., 2013). Hence the molecular mechanisms underlying actinin-1 related CMTP have yet to be fully defined.

In this chapter, we tested the hypothesis that CMTP-causing mutations in the CaM-like domain might affect calcium binding and thus the regulation of actinin-1's association with F-actin. However, we find that calcium binding is not consistently compromised and rather that actin bundling ability *in-vitro* and association with F-actin in cells is enhanced for three CaM-like domain mutations examined. In addition, we show that mutations in the rod domain also enhance actin bundling ability *in-vitro*. This gain of function phenotype is very similar to that seen for mutations affecting the ABD (Murphy et al., 2016). Hence a common molecular mechanism likely exists for all actinin-1 mutations implicated in CMTP, regardless of the affected protein domain.

2.2 Methods

2.2.1 Actinin-1 cDNA Constructs

The calcium-sensitive (non-muscle, exon 19a-containing) splice variant of human actinin-1 was used in all experiments (Accession no. NM_001102). Wild type and mutant actinin-1 constructs for both bacterial and mammalian expression were prepared previously (Murphy et al., 2016) or were introduced to WT actinin-1 using the Quikchange site directed mutagenesis kit (Agilent Technologies). Constructs to produce the isolated WT and mutant CaM-like domain encoded amino acids 740-892 of actinin-1 with an additional three amino acids (Gly-Ser-Ser) at the amino terminus. For actin co-sedimentation and isothermal calorimetry (ITC) assays, constructs were cloned into the pET24-HGT plasmid, containing an N-terminal His-tag, glutathione-S-transferase sequence, and a Tobacco Etch Virus (TEV) protease cleavage site, as used previously (Murphy et al., 2016). For cytoskeletal purification experiments, constructs were subcloned into the pCMV-NFLAG plasmid, encoding an N-terminal FLAG sequence.

2.2.2 Protein Expression & Purification

Constructs in pET24-HGT plasmids were transformed into E. coli BL21 and grown selectively on 30 µg/mL Kanamycin agar. Cells expressing plasmids were cultured in LB media containing 30 µg/mL Kanamycin at 37℃ and protein expression was induced at log phase of growth using 0.2mM isopropyl-D-thiogalactopyransoside (IPTG) and grown for a further 4 hours. Cells were pelleted at 4500 x g for 20 minutes at 4℃. Cells were resuspended in ice cold 0.2% Triton, 5mM β-mercaptoethanol (βME), 1 phenylmethylsulfonyl fluoride (PMSF) in PBS and lysed using 0.1 mg/mL Lysozyme and 1 mg/mL DNAse for 20 minutes on ice, followed by sonication. Lysates were isolated by centrifugation 12,500 x g for 20 minutes at 4℃. GST/His tagged protein was purified from lysates initially using Glutathione Sepharose (GST) affinity resin (GE Healthcare). Unbound protein was washed from the column using wash buffer (0.2% Triton, 5mM βME, PBS) and bound protein was eluted using fresh elution buffer (10 mM Glutathione , 50 mM Tris-HCL pH8). The N-Terminal His/GST tag was cleaved from purified proteins using His-tagged TEV Protease (produced in-house) at 20℃ for 12 hours followed by 24-48 hours at 4℃ to maximise cleavage. Cleavage efficiency was assessed by SDS-PAGE before final purification steps. Purified protein was isolated from His/GST tag following cleavage using Nickel affinity resin . Nickel columns were washed thoroughly using dH_2O and equilibrated with wash solution (0.5M NaCl, 50 mM KPO 4 pH8, 20mM βME, 5 mM Imidazole pH7, 0.1% Triton) prior to loading sample and collecting flow-through. Flow-through was purified using Fast Protein Liquid Chromatography (FPLC) on the AKTA Purifier 10 (GE Amersham) on a Superdex 75 10/300 GL column (GE Healthcare) for CAM-Domain proteins (15kDa) and Superdex 200 10/300 GL column (GE Healthcare) for full length actinin proteins (100 kDa). For CaM domain proteins, proteins were eluted in filtered and degassed 100mM NaCl, 20 mM HEPES pH 7.5 in MilliQ water. For full length actinin proteins, proteins were eluted in filtered and degassed 10 mM Tris pH7.5, 100mM NaCl, 0.1 mM DTT in MilliQ water. Purity of proteins was assessed finally by SDS-PAGE analysis with Coomassie staining and concentrations were obtained using Nanodrop TM ND1000 (Mason Technology) readings of absorbance at 280nm. For ITC and Thermal Shift Analysis, proteins were treated with Chelex-100 calcium binding resin (Sigma-Aldrich) for 2 - 16 hours at 4℃ prior to analysis.

2.2.3 Thermal Shift Assays

Purified actinin-1 CaM-like domain proteins were mixed with Sypro Orange dye (Sigma-Aldrich, S5692) used at a 1:250 dilution in either the presence or absence of 1 mM $CaCl_2$.

Samples were heated across a temperature range from 25 to 95 ℃ with a rate of change in temperature of 1℃ / min in a StepOne Plus Real Time PCR System (Applied Biosystems) while recording fluorescence at 1 min intervals using ROX Dye filter setting (Em 610nm). Fluorescence emission signal was plotted against temperature using Microsoft Excel and an average plot was deduced for each protein. The melting temperature (Tm) of each protein in the presence and absence of $CaCl_2$ was then deduced from a plot of the first derivative of fluorescence emission with respect to temperature, with the lowest point on this curve representing the Tm.

2.2.4 Isothermal Calorimetry

Calcium binding efficiency was assessed with the Microcal PEAQ-ITC Isothermal Calorimeter (Malvern Panalytical) using purified actinin-1 CaM-like domains. 160-200µM CaM-like domain protein in reaction buffer (100 mM NaCl, 20 mM HEPES pH 7.5) was loaded into the reaction chamber. $CaCl_2$ was added to reaction chamber in 19 sequential 2 µL injections with an initial small injection of 0.4 µL (4 seconds per injection) at 150 second intervals, and an initial delay of 60s, from a reservoir of 8 mM $CaCl_2$ in identical reaction buffer. The reference cell contained reaction buffer. Heat change was monitored from a baseline of 25 ℃ relative to increase in calcium:protein molar ratio. Sample results were analysed following subtraction of heat of dilution, which was obtained by measuring heat change when calcium chloride was added to reaction buffer without protein, using the same protocol as for protein analysis. Dissociation constant (Kd), molar ratio of ligand to target (N), heat change (ΔH) and free energy change (ΔG) were calculated by Microcal PEAQ-ITC Analysis software (Malvern Panalytical).

Raw data were normalized per mole of injectant and integrated with respect to time, and then reference data were subtracted. Data were fitted by least squares minimization using the Origin software package (Microcal, USA) to optimize the fitting parameters stoichiometry (n), enthalpy (DH) and association constant (Kb). A single binding site model was used to fit the data in all cases and gave the best r2 values.

2.2.5 Actin Co-Sedimentation Assays

For actin co-sedimentation assays, 2 µM of polymerized rabbit skeletal muscle actin (Cytoskeleton Inc., AKL99) was mixed with 1 µM purified full-length actinin in F-actin buffer

(10 mM Tris-HCl pH 7.5, 100 mM NaCl, 10 mM NaN3, 10 mM MgCl2, 1 mM ATP, and 1mM DTT) in the presence of 0.2 mM ethylene glycol tetra-acetic acid (EGTA) for analysis of actinin in the calcium-unbound state or 0.1 mM $CaCl_2$ for analysis of actinin in the calcium-bound state. For all wild type and mutant actinin proteins, a control actin-free reaction was carried out to account for artefactual sedimentation of actinin. An actin-only control was also carried out per experimental replicate. Reactions, in a total volume of 100 µL, were incubated for 30 min at 30℃ and bundled actin was then pelleted by centrifugation at 10,000 x g at 30 ℃. Pellets and supernatants were analysed on SDS-polyacrylamide gels stained using GelCodeTM BlueSafe Protein Stain (Thermo Scientific). Gels were imaged and bands were quantified using Odyssey Image Studio Software (LI-COR Biosciences). Sedimented actin in actinin-free control reaction and sedimented actinin in actin-free control reactions were subtracted from experimental reactions. Actin bundling as well as the actin-binding ability of wild type and mutant actinins in the presence and absence of calcium was determined by quantifying the percentage of actin or actinin sedimented in pellets of $CaCl_2$ and EGTA containing reactions respectively.

2.2.6 Cytoskeletal Purification Assays

Purification of cytoskeletal fraction from HeLa cells was carried out as previously described (Choi, 2014, Murphy 2016). HeLa cells (0.4 x 106 cells per plate) were plated on 6cm dishes and grown for 24 hours at 37℃ in DMEM, 10% FBS, 1%Penicillin/Streptomycin media. At 24 hours, cells were 40 - 50% confluent and media was replaced with 1.7mL antibiotic-free DMEM, 10% FBS media per plate. Cells were transfected with 2 µg Actinin-NFlag plasmid DNA and 0.5 µg pEGFP plasmid DNA as a transfection and fractionation control. DNA was suspended in 300 µL OptiMEM media and 2 µL Lipofectamine and added to 1.7 mL media per plate. Media was changed 16 hours post transfection to DMEM, 10% FBS, 1% Penicillin/Streptomycin media and cytoskeletal purification was carried out 36 hours post-transfection.

Media was removed from plates and plates were placed on ice. Plates were washed twice in 800µL PBS and washes were discarded. 200µL Lysis Buffer (50 mM PIPES pH 6.9, 50mM NaCl, 5% Glycerol, 0.1% NP-40, 0.1% Triton X-100, 0.1% Tween 20) was added to the plates on ice and the plates were rocked for 1.5 minutes before removing and retaining lysate. 800µL wash buffer (Tris-HCl pH 7.5) was used to rinse plates on ice following lysis and this wash was discarded. The plates were removed from ice and 100µL nuclease buffer (10 mM

MgCl2, 2mM $CaCl_2$, 10 U/mL Benzoase, 50 mM Tris-HCl pH7.5) was added to the centre of each plate and allowed to flow to edges of plate. The nuclease buffer was allowed to incubate at room temperature for 10 minutes and was pipetted off and returned to the centre of plates at 2.5 minute intervals. The nuclease buffer was removed following incubation and retained. Without rinsing plates, the plates were returned to ice and lysis buffer was added back onto plates and rocked to cover plates for 0.5 minutes. The lysis buffer was then removed and added to the nuclease buffer and retained as the "cytosolic / nuclear fraction". The plates were then rinsed with 800µL Lysis buffer on ice and this rinse was discarded. The plates were washed with 800µL wash buffer three times on ice. The plates were then removed from ice and 100µL 1% SDS was added to the plates and the "cytoskeletal fraction" was collected. All fractions contained protease (Roche protease inhibitor cocktail) and phosphatase inhibitors (5mM sodium fluoride and 2mM sodium orthovanadate).

The cytosolic / nuclear fraction and cytoskeletal fraction were assessed by SDS-PAGE and western blotting. Fractionation efficiency was assessed by detection of GAPDH and GFP, where transfected, in the cytosolic / nuclear fraction and actin was used as a loading control. Stability of actin-actinin association was assessed by detection and quantification of actinin-N-FLAG in both fractions. Detection was by Odyssey infrared imaging system for β-actin and x-ray films with Enhanced chemiluminescence (ECL) detection for N-FLAG, GAPDH and GFP. Actin and FLAG epitope tag detected was quantified using ImageJ National Institute of Health (NIH) and Image Studio (LI-COR Biosciences) Software. FLAG signal was normalised to actin for all samples and all samples were expressed as a normalised ratio with respect to the wild-type sample of that run.

2.2.7 Immunofluorescence Studies

Sterile glass cover slips were air-dried in 6-well plates and coated with poly-L-lysine by incubation at room temperature for 1 hour, followed by rinsing with sterile PBS. HeLa cells (0.2 x 106 cells per well) were plated onto sterile cover slips and grown at 37 ℃ until 60% confluent. Transfection was carried out as described for cytoskeletal purification assays, using 2 µg Actinin-1-GFP plasmid. 36 hours post transfection, cover slips were rinsed twice in PBS and fixed in 4% paraformaldehyde (PFA) on ice for 10 minutes. Coverslips were then rinsed again with PBS and blocked for 30 minutes at room temperature with blocking solution (5% normal goat serum, 2% BSA, 0.2% Triton). Following blocking and rinsing again

in PBS, coverslips were stained with rhodamine phalloidin (1:3000) and DAPI (1:10,000) in blocking buffer without Triton for 1 hour at room temperature and then rinsed again with PBS. Coverslips were mounted on glass slides using Fluoromount (Sigma) and edges of coverslips were sealed with varnish. Images were acquired on a Leica DM6000 upright fluorescence microscope. MEG-01 (DSMZ, ACC 364) cells were grown in RPMI-1640, 10% FBS, 1% Penicillin, Streptomycin media for 12 days with differentiation using phorbol 12-myristate 13-acetate (PMA) at 1 ng/mL on days 1-3 and 10 ng/mL on days 3-12, with a complete media change every 2-3 days. On day 10, media was changed to RPMI-1640, 10% FBS and 0.5 x 106 cells were plated on glass-bottomed dishes. Transfection was carried out using 1 µg Actinin-1-GFP plasmid with 1 µL Lipofectamine2000 in 100 µL OptiMEM per dish in 1 mL of culture. On day 11, dishes were supplemented with an additional 1 mL of media. On day 12, media was removed and adhered cells were fixed and stained as described for HeLa cells. Glass component of dishes were removed and mounted on coverslips as described for HeLa cells.

Analysis of the width of bundled actin fibres was performed by a researcher who was blinded to the identity of the transfected actinin proteins. Measurements of 2-4 phalloidin stained actin fibres in 5-7 cells per mutant protein were made using ImageJ software (Rasband). Local thresholding was performed for each fibre and a fibre segment 2-10 µm long was defined using the “analyse particles” function. Measurements of the area and length (taken as the Feret diameter) were made and the area divided by the length was used to calculate the average fibre width.

2.2.8 Statistical Analysis

Analysis was carried out using SPSS (IBM) data analysis software.

2.3 Results

2.3.1 Expression & Purification of CaM-domain and Full Length Actinin-1 Proteins

The CaM-domain of actinin-1 was expressed and purified to assess the calcium binding ability of mutant proteins. Figure 2.3.1 demonstrates purification of 15 kDa WT and mutant CaM proteins. The full-length actinin protein was expressed and purified for actin-bundling analysis and is demonstrated in Figure 2.3.2.

Figure 2.3.1

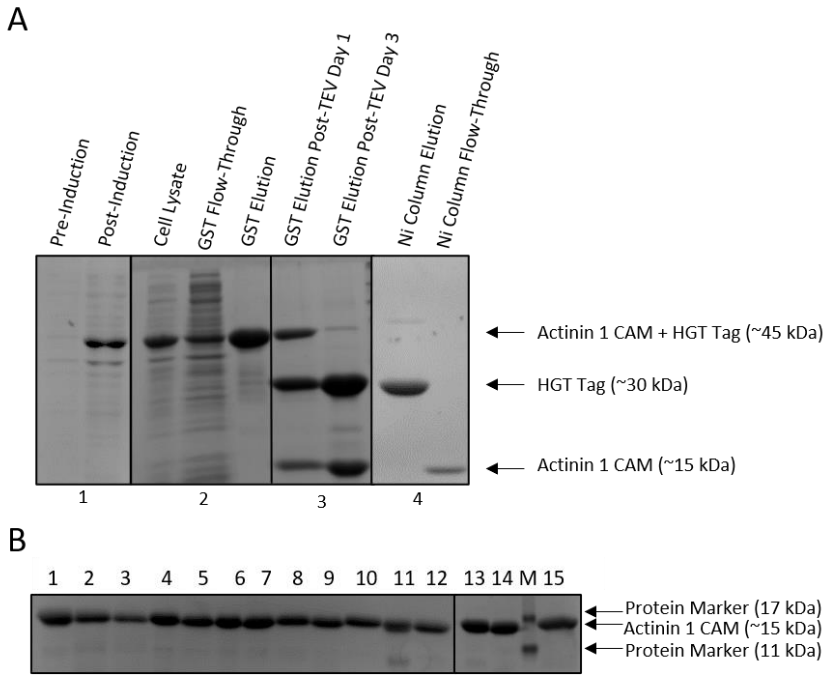

Figure 2.3.1 Representative Coomassie-stained SDS-PAGE gel images of the expression & purification of CaM-domain actinin-1 proteins. (A) Representative gel images of the *protein expression and purification process demonstrated on 15% SDS-PAGE gel with Coomassie staining as: (1) Induction with 0.2 mM IPTG at 37°C, (2) GST column purification, (3) TEV Cleavage, (4) Ni Column purification**. (B)** Purified α-actinin-1 CAM domain proteins used for ITC analysis shown on 15% SDS-PAGE gel with Coomassie staining. Protein concentration range was 150µM - 210µM. Sample in lane 3 (WT 116µM) was not used for analysis. Samples as follows : 1-3 = WT, 4-7 & 15 = E769K, 8-10 = G764S, 11-14 = R752Q, M = Protein Marker.*

Figure 2.3.2

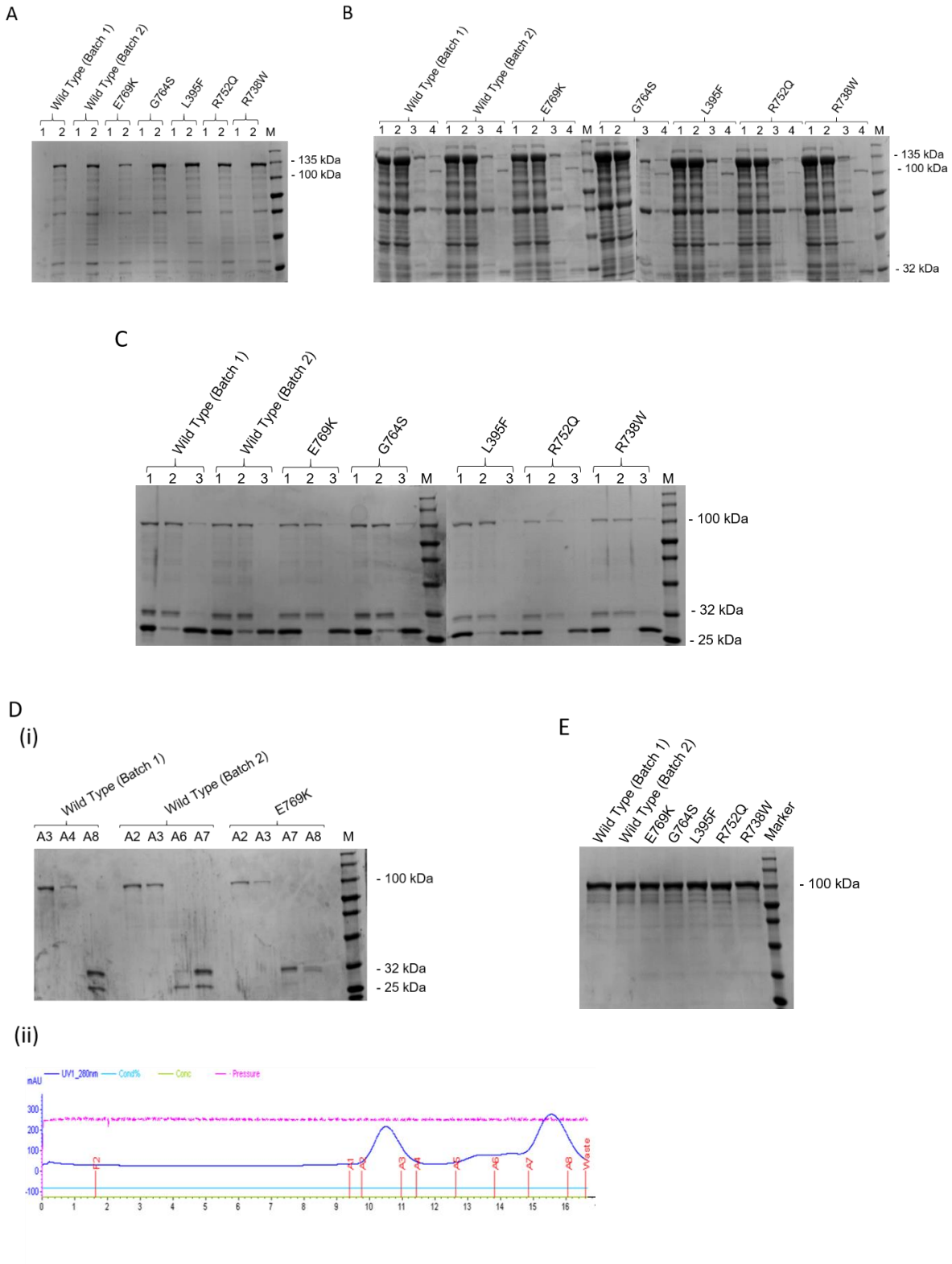

Figure 2.3.2 Representative Coomassie-stained SDS-PAGE gel images of the expression & purification of full-length actinin-1 proteins. *(A) Expression of full length actinin-1 in pet24-HGT vector in BL21 cells using 0.2 mM IPTG. 1 = Pre-Induction, 2= Post-Induction. (B) GST*

column purification of full length actinin-1 and cleavage of eluate with TEV protease. 1 = Cell Lysate, 2 = GST Column FT, 3 = GST Column Elution, 4 = GST Elution post overnight TEV Cleavage. (C) Nickel column purification of TEV-Cleaved full length actinin-1. 1 = GST Column Elution post 48 hours of cleavage with TEV protease, 2 = Ni Column FT, 3 = Ni Column Elution. (D) (i) Analysis of FPLC purification elutions. ~ 1 mL concentrated sample was purified for each actinin protein. UV plot for E769K sample is shown in (ii). (E) Purified actinin-1 proteins. 3 µL of 2 µM protein in 2X SDS loading buffer loaded per sample. Bands indicate the following: actinin with HGT tag (~130 kDa), actinin without tag (~100 kDa), HGT tag (~30 kDa).

2.3.2 Actinin-1 CaM-Like Domains with CMTP-Causing Mutations Have Decreased Thermal Stability But Maintain Calcium Binding Ability.

Three CMTP-linked mutations (R752Q, G764S and E769K) which are located within the calcium-binding EF1 region of the CaM-like domain of actinin-1 were assessed in this chapter. R752Q is positioned in the middle of the first helix away from the calcium-binding site whereas both G764S and E769K are adjacent to residues directly involved in coordination of calcium. As a first step in the functional characterization of these mutations we examined the thermal stability of the isolated CaM-like domain using a thermal shift assay in which increased fluorescence of Sypro Orange dye gives a readout of protein unfolding. In this assay both the WT and mutant proteins exhibited an unexpectedly high initial fluorescence signal that trended downwards as the temperature increased from 25 to approximately 55 ℃ (Figure 2.3.3 A). This is possibly due to loose association between the dye and hydrophobic regions of the CaM-like domain. Nevertheless, as the temperature climbed above 60 ℃, a clear peak in fluorescence is observed that we interpret as corresponding to unfolding of the CaM-like domain, with increased Sypro Orange binding initially and its subsequent dissociation as the protein aggregates (Figure 2.3.3 B). This interpretation is supported by the observation that this peak is shifted to the right in the presence of calcium, which would be expected to stabilize the CaM-like domain. Melting temperatures (Tm) for WT and mutant CaM-like domains in the presence and absence of calcium were determined from a plot of the first derivative of fluorescence emission with respect to temperature (Figure 2.3.3 C). The Tm values of the mutant proteins were somewhat lower than the WT, both in the absence and presence of calcium (Figure 2.3.3 D). These differences were statistically significant for the G764S and E769K

mutants, implying that these mutants are less thermally stable than the WT protein. Examining each individual protein in the presence and absence of calcium we found that Tm was significantly increased for all proteins in the presence of calcium, but while the extent of this increase was 8-10 ℃ for the WT, R752Q, G764S proteins it was only 4 ℃ for the E769K mutant. Thus, while some small differences in their thermal stability was observed, all the mutant proteins are capable of binding calcium.

Figure 2.3.3

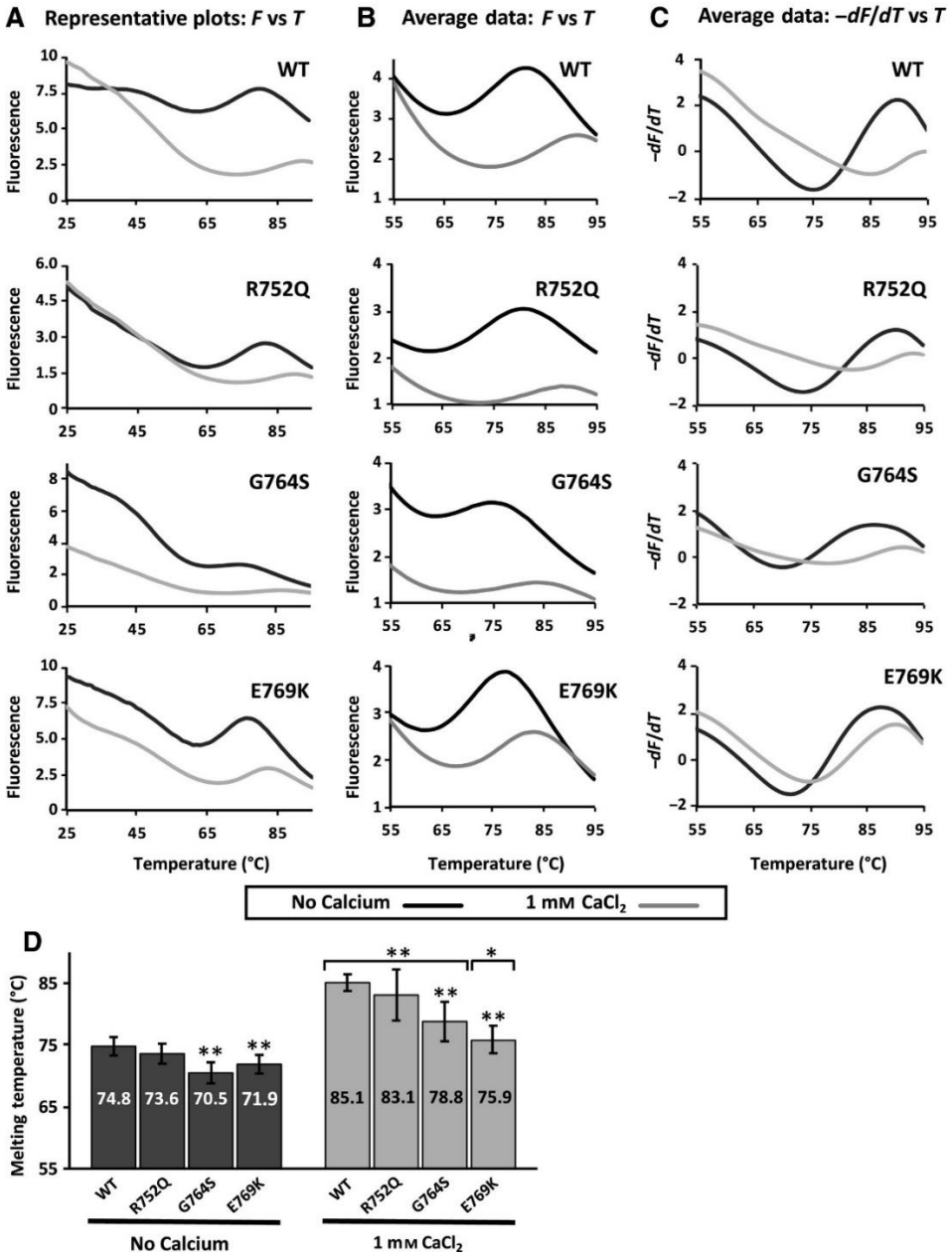

Figure 2.3.3 Analysis of thermal stability and calcium binding in CaM-like domain mutants by thermal shift assay. *(A) Representative plots of fluorescence verses temperature for WT*

*and mutant CaM-like domain proteins in the absence (dark grey) and presence of 1 mM$CaCl_2$ (light grey). High initial fluorescence was seen for all proteins, with typical melting profiles seen as the temperature rose above 60°C. (B) Average plots of melting profiles for all proteins (n= 7). (C)Derivative plots of average data where the lowest points on the curve correspond to melting temperature. (D) Analysis of melting temperatures in the absence and presence of calcium. All proteins exhibited increased thermal stability in the presence of calcium (significance level indicated above the brackets), while two mutants(G764S and E769K) had significantly lower melting temperatures than the WT protein under both conditions (significance level indicated above the error bars; n= 7; error bars represent SEM). Statistical analysis by One-Way ANOVA and post-hoc analysis by Dunnett's test was used to compare WT and mutant protein melting temperatures. The paired sample T-test was used to compare melting temperatures for each protein in the presence and absence of calcium.**P<0.01, *P<0.05*

2.3.3 Calcium Binding Affinity of Actinin-1 CaM-like Domains is Not Dramatically Affected by the G764S and R752Q CMTP-Causing Mutations.

While thermal shift assays indicated that CaM-like domains with the R752Q, G764S and E769K mutations retained their ability to bind calcium it is possible that they differ quantitatively from the WT protein in their calcium binding affinity. Therefore, isothermal calorimetry was used to quantitatively assess calcium binding of WT and mutant actinin-1 CaM-like domain proteins. The thermogram for the WT CaM-like domain protein shows a single endothermic event (Figure 2.3.4 A). The binding stoichiometry (N) of 0.96 ± 0.15 for the WT protein implies a single binding event per CaM-like domain molecule, and the calculated Kd of 114.94 ± 15.20 µM (Table 2.3.1) is in line with a previous report (Prebil et al., 2016). Melting profiles for G764S and R752Q proteins appeared similar to the WT and the calculated Kd and N values are also comparable, although variability between experimental replicates was somewhat greater than for the wildtype protein (Figure 2.3.4 B and C, Table 2.3.1). Hence calcium binding efficiency appears largely unaffected in the G764S and R752Q mutants. Thermograms for the E769K mutant differed substantially however, exhibiting DP and ΔH values that are approximately 10-fold lower than for the other proteins (Figure 2.3.4 D). Results from replicate experiments with different batches of E769K protein was highly variable which precluded the accurate calculation of binding parameters for this mutant.

Figure 2.3.4

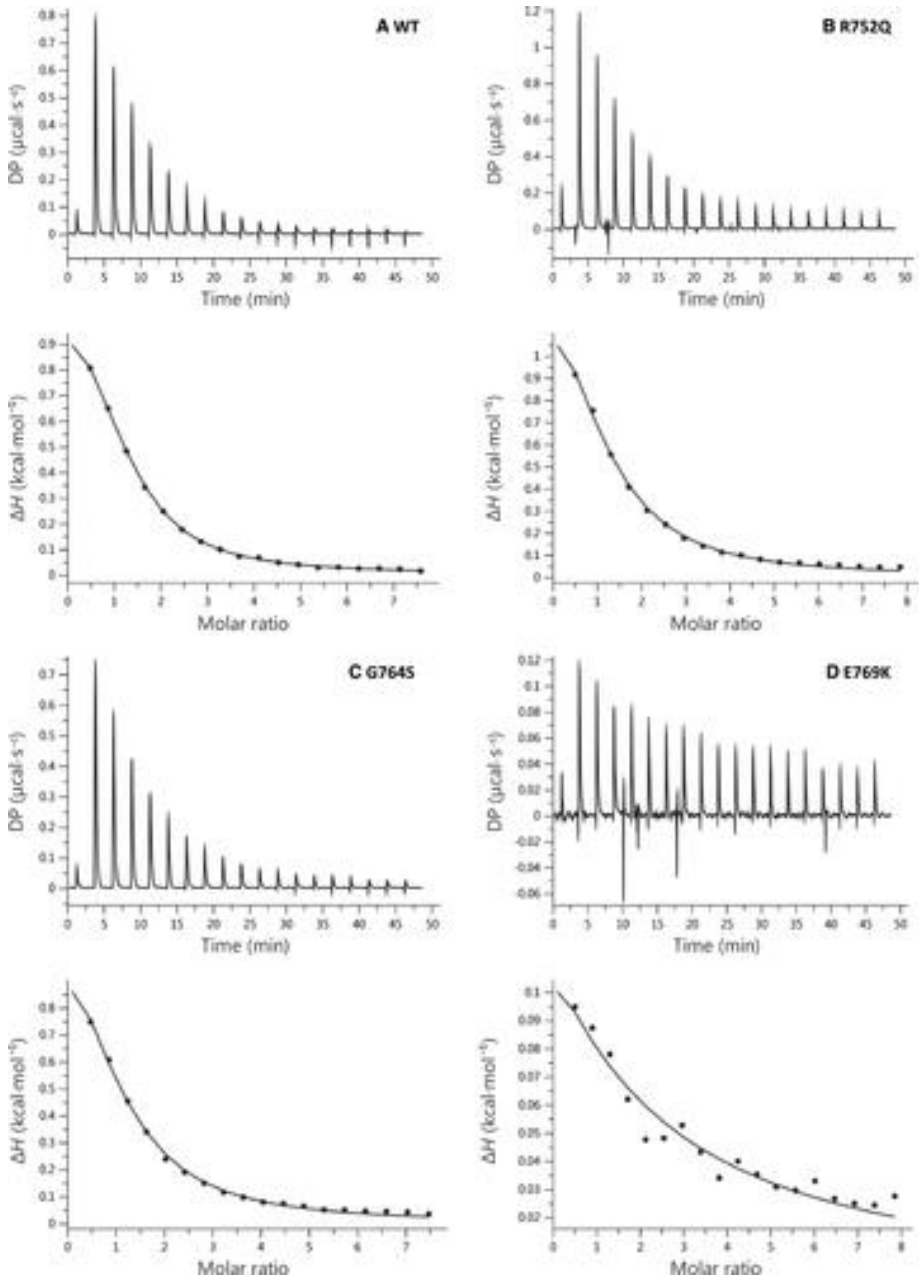

Figure 2.3.4 Calcium binding affinity of WT and mutant actinin-1 CaM-like domains assessed by isothermal calorimetry. *Calcium chloride was titrated against WT or the indicated mutant CaM-like domain proteins by injections of equal volume at regular time intervals. The top graph in each case shows the raw data as a function of time; the heat of the binding reaction is monitored as the differential power (DP) (µcal/s) required to maintain the experimental cell at the same temperature (25°C) as the reference cell. The lower graph shows the processed data after normalization per mol of injectant, integration*

with respect to time and subtraction of reference data. The solid line is the calculated best fitting curve to this data obtained by optimization of the fitting parameters stoichiometry (n), enthalpy (∆H) and dissociation constant (Kd) using the Microcal-PEAQ ITC software (Malvern Panalytical). Graphs shown are representative runs while the average values of these parameters obtained for each protein are shown in Table 2.3.1.

Table 2.3.1 : Thermodynamic parameters obtained in the analysis of calcium binding efficiency in WT and CaM domain mutant actinin-1 proteins by ITC.

Sample	n	Kd (µM)	N	ΔH	ΔG	TΔS
WT	3	114.94 ± 15.20	0.96 ± 0.15	1.97 ± 0.56	-5.38 ± 0.83	7.34 ± 0.48
R752Q	4	119.7 ± 80.29	0.81 ± 0.61	21.13 ± 39.25	-5.52 ± 0.56	26.64 ± 39.27
G764S	4	102.24 ± 67.64	1.53 ± 1.14	14.15 ± 26.17	-5.60 ± 0.53	6.8 ± 0.45
E769K	4	1420.00 ± 307.21	1.67 ± 2.88	66.9 ± 22.69	-3.91 ± 0.14	70.80 ± 22.55

2.3.4 CMTP-Causing Mutations in the Rod and CaM-like Domain Enhance the F-actin Bundling Ability of Actinin-1.

We next assessed the ability of full-length actinin-1 proteins with mutations in the CaM-like domain to bundle actin filaments in co-sedimentation assays. We also examined proteins with the R738W mutation at the very end of SR4 (Figure 2.1) and the L395Q mutation within SR2 of the rod domain (Figure 2.1). Analysing levels of actin and actinin-1 in the supernatants and pellets from these assays (Figure 2.3.5 A) it is apparent that the WT and all mutant actinin-1 proteins are able to bind to (Figure 2.3.5 B), and bundle (Figure 2.3.5 C) actin filaments in the absence of calcium. These abilities are significantly decreased in the presence of calcium for all proteins implying that calcium sensitivity is maintained in full-length actinin-1 proteins harbouring CMTP-causing mutations. Examining actin bundling in the absence of calcium it was found that all the mutant proteins assessed had a greater ability to bundle actin than WT actinin-1 (Figure 2.3.5 C). This was statistically significant for

one rod (L395Q), and two CaM-like domain (R752Q and E769K) mutations. By comparison while the levels of bound actinin were generally higher for the mutants compared to the WT this was not statistically significant for any of the mutant proteins (Figure 2.3.5 B).

The observation that mutations in the CaM-like and rod domains affect actin binding/bundling in a similar manner to ABD mutations is somewhat surprising, especially for the L395Q mutation given its location in the middle of the central rod domain. This suggests that enhanced actin binding/bundling might be common to all CMTP-linked actinin-1 mutations and that actin bundling might be a functional assay that could distinguish pathogenic mutations from those of uncertain significance. Therefore actin bundling was assessed for another four rod domain mutations. These included R320Q and L547P, located in SR1 and SR3 respectively, which are classified as likely pathogenic (Westbury et al., 2015). We also assessed two mutations of the same residue, one of which (T737N) is likely pathogenic (Bottega et al., 2015; Westbury et al., 2015) , and the other (T737S) that was deemed to be a variant of unknown significance (Faleschini et al., 2018). The R320Q, T737N and T737S mutant proteins all show a highly significant increase in actin bundling activity whereas a much smaller and not statistically significant increase was seen for L547P (Figure 2.3.5 D-F). These findings indicate that mutations throughout the rod domain can affect actin binding properties, albeit to varying extents, and that relatively conservative amino acid substitutions such as T737S can nevertheless have functional consequences.

Figure 2.3.5

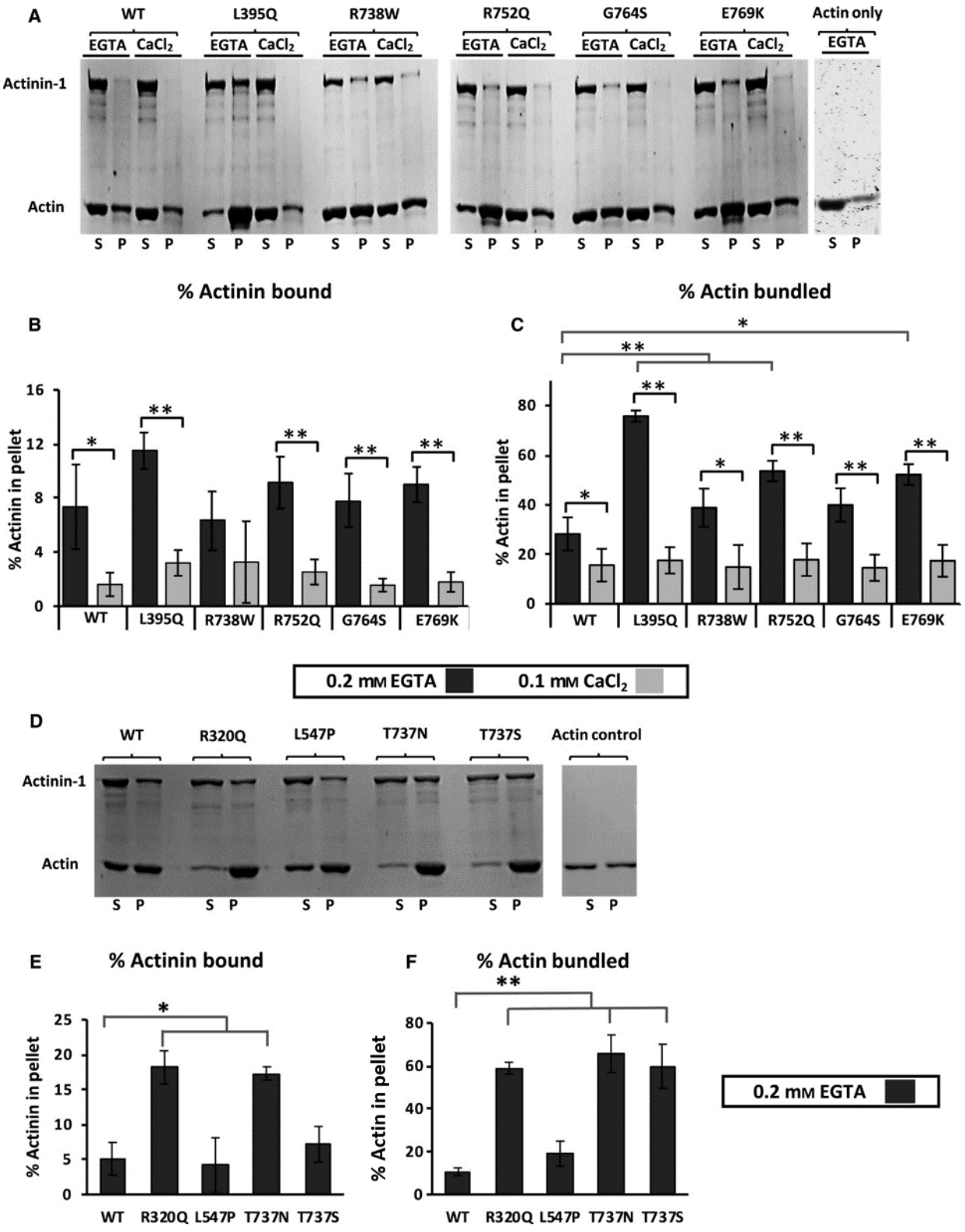

Figure 2.3.5 Comparison of the actin bundling efficiency of WT and mutant actinin-1 proteins. *Comparison of the actin bundling efficiency of WT and mutant actinin-1 proteins.*

*(A) Representative gels showing actin present in supernatant (S) and pellet (P) following bundling reaction in the presence of 0.2 mM EGTA or 0.1 mM$CaCl_2$for WT and mutant actinin-1proteins. WT (n= 13) L395Q (n= 9), R738W (n= 7), R752Q (n= 10), G764S (n= 11) and E769K (n= 8). (B) Percentage actinin bound to actin in pellets in presence of 0.2 mM EGTA and 0.1 mM$CaCl_2$ for WT and mutant actinin-1 proteins. Bundling efficiency is reduced in presence of $CaCl_2$. (C) Percentage actin bundled in bundling reactions shown in (A). (D) Representative gels showing actin present in supernatant (S) and pellet (P) following bundling reaction in the presence of 0.2 mM EGTA for additional rod domain mutants. (n= 3 for all samples). (E) Percentage actinin bound to actin in pellets in the presence of 0.2 mM EGTA for additional rod domain mutants. (F) Percentage actin bundled in the reactions shown in (D). Quantification of results is presented as the mean ± SEM. Actin bundling and actinin binding by mutants was compared to WT using One-Way ANOVA and post-hoc analysis using Dunnett's test. Actin bundling and actinin binding for EGTA and $CaCl_2$ reactions were compared for all samples using a paired T-test for related samples. *P<0.05, **P<0.01*

2.3.4 CMTP-causing mutations in the CaM-like domain of actinin-1 increase the stability of its association with the actin cytoskeleton in cells.

To assess if the increased actin-bundling of the CaM-like domain and rod domain mutants was evident *in-cellula*, the association of FLAG-tagged actinin-1 with F-actin in cytoskeletal fractions purified from cultured HeLa cells was examined for the L395Q, G764S and E769K mutations. Significantly increased actinin-1 in cytoskeletal fractions was observed for the two CaM-like domain mutations (G764S and E769K) compared to the WT protein (Figure 2.3.6 A & B), whereas an increase for rod domain mutation L395Q was very slight and not statistically significant.

It has been reported that actinin-1 proteins with CMTP-linked mutations can disrupt the actin cytoskeleton and have an altered distribution in the cytosol of cultured megakaryocytes, human fibroblasts and CHO cells (Bottega et al., 2015; Faleschini et al., 2018; Guéguen et al., 2013; Kunishima et al., 2013; Vincenot, 2019; Yasutomi et al., 2015) whereas we did not find this to be the case in HeLa cells for FLAG-tagged proteins with mutations in the ABD for example (Murphy et al., 2016). To further examine this issue we transiently expressed WT GFP-tagged actinin-1 as well as two mutants affecting the ABD (V105I and E225K), two affecting the rod domain (L395Q and R738W) and three affecting

the CaM-like domain (R752Q, G764S and E769K) in HeLa cells (Figure 2.3.6 C). We then examined the localization of actinin-GFP in relation to the F-actin cytoskeleton. The majority of transfected HeLa cells could not be distinguished from untransfected cells in terms of F-actin organization and consistent co-localization of both WT and all mutant actinin-1-GFP proteins with F-actin was observed in HeLa cells (Figure 2.3.6 C). Quantification of the diameters of bundled actin fibres in HeLa cells did not reveal significant differences between cells expressing WT and mutant actinin-1 proteins (Figure 2.3.6 D), in contrast to a recent report using CHO cells for different CMTP-linked actinin-1 mutations (Vincenot, 2019). Our findings suggest that, at least in HeLa cells, the mutant actinin-1 proteins examined here retain their association with F-actin and do not dramatically affect cytoskeletal organization. Mutant GFP-tagged actinin-1 was also transiently expressed in differentiating MEG-01 megakaryoblast cells to ascertain if some megakaryocyte-specific cytoskeletal disruption occurred (Figure 2.3.7). Although no clear disruption to the cytoskeleton was noted, the morphology of these cells varied widely, limiting comparison of WT and mutant cells.

Figure 2.3.6

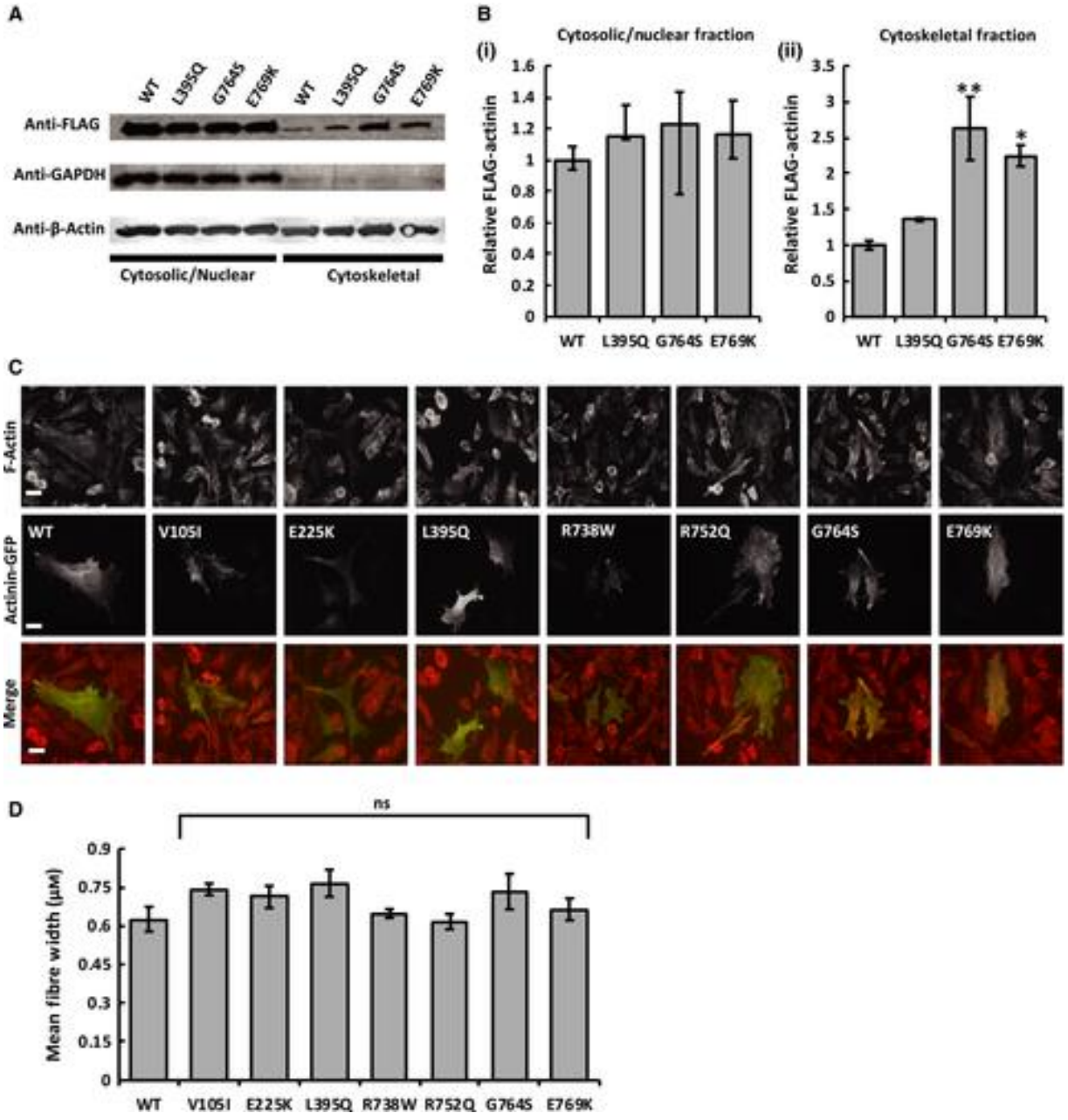

Figure 2.3.6 Cytoskeletal association of actinin-1 proteins with CMTP-associated mutations in-cellula and actin cytoskeletal organisation in HeLa cells expressing GFP-tagged actinin-1 proteins with CMTP-associated mutations. *(A, B) Cytosolic/nuclear and cytoskeletal fractions were prepared from HeLa cells transfected with FLAG-tagged WT or mutant actinin expression constructs. (A) Western blot analysis showing the levels of FLAG-actinin in each fraction as well as demonstrating successful fractionation as indicated by the detection of GAPDH primarily int he cytosolic/nuclear fraction. (B) Quantification of the amount of mutant FLAG-actinin relative to the WT protein in each fraction (normalized to*

*actin levels). Proteins with the CaM-like domain mutations G764S and E769K are present in the cytoskeletal fraction at significantly greater higher levels as assessed by One-Way ANOVA and post-hoc Dunnett's test. (**P<0.01, *P<0.05;n= 3). (C) Expression of WT and mutant actinin-GFP proteins in HeLa cells. F-actin is stained with rhodamine phalloidin and actinin-1 proteins are detected through GFP fluorescence (red and green in merged images). The actin cytoskeleton does not appear disorganised in HeLa cells expressing mutantactinin-1 proteins, compared with cells expressing WT actinin-1 or neighbouring untransfected cells. GFP-tagged actinin-1 co-localises to a great extent with actin for both WT and mutant actinins. Scalebar represents 20 µm. (D) Quantitative analysis of the width of actin fibres in HeLa cells transfected with WT or mutant actinin-GFP as indicated in (C). Statistical analysis of mean actin fibre width by One-Way ANOVA and post-hoc Dunnett's test showed that variation between samples was non-significant.*

Figure 2.3.7

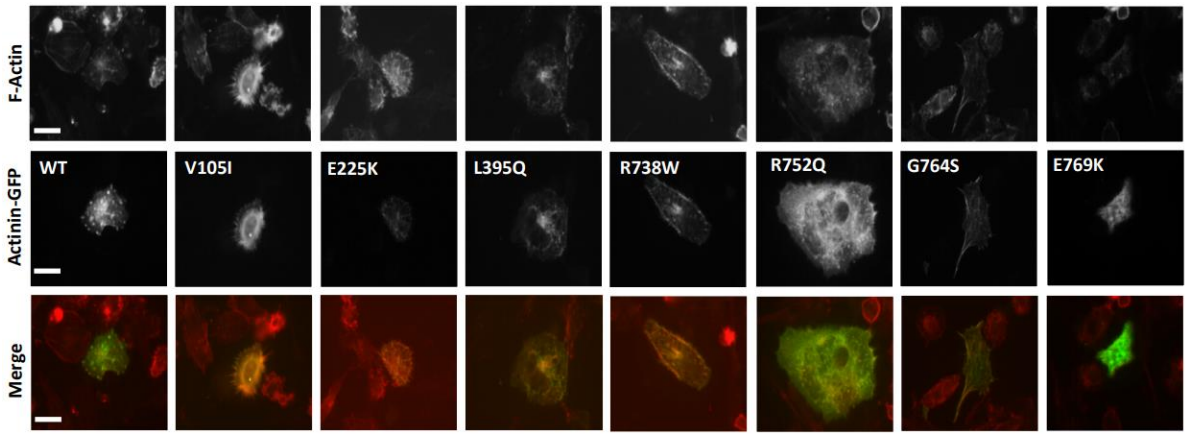

Figure 2.3.7 Expression of actinin-1 proteins with CMTP-associated mutations in MEG-01 cells. *Expression of WT and mutant actinin-GFP proteins in HeLa cells. F-actin is stained with rhodamine phalloidin and actinin-1 proteins are detected through GFP fluorescence (red and green in merged images). Scalebar represents 20 µm.*

2.4 Discussion

As detailed, to date over 40 mutations in actinin-1 have been reported in association with CMTP. It was previously demonstrated that CMTP-linked mutations in actinin-1 that occur in the ABD (black arrows, Figure 4.2.1 A) increase the protein's affinity for and cross-linking of actin filaments (Murphy et al., 2016). Here this analysis has been extended by focusing on mutations in the CaM-like and rod domains (red arrows, Figure 4.2.1 A) to ascertain whether they have similar effects on actin binding properties.

Figure 2.4.1

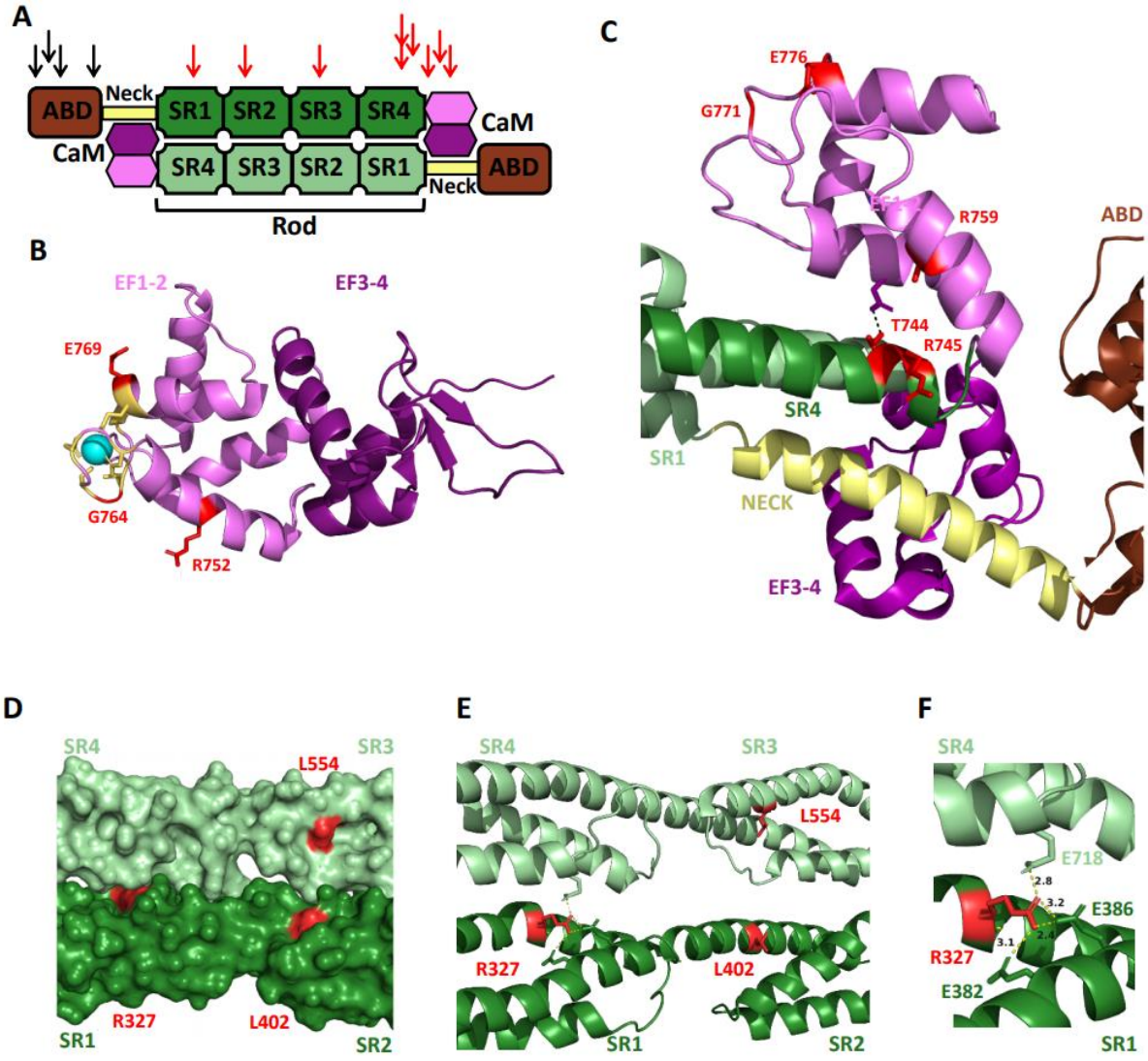

Figure 2.4.1 Location of amino acids that are mutated in CMTP within the actinin protein structure.

(A) *Domain organisation of the actinin-1 dimer showing the interaction of the CaM-like domain with the neck region of the opposing subunit that is thought to regulate actin binding* (Prebil et al., 2016; Young & Gautel, 2000)*. The approximate positions of selected CMTP-linked mutations are indicated by arrows. Red arrows indicate the mutations in the rod and CaM-like (CaM) domains examined in this study, while black arrows represent mutations in the ABD that were previously shown to increase actinin-1 association with F-actin* (Murphy et al., 2016)*.*

(B) *An NMR structure of the CaM-like domain of actinin-1 with Ca^{++} bound (PDB ID: 2N8Y)* (Prebil et al., 2016)*). Residues that are mutated in actinin-1-linked CMTP are highlighted in red, while those that co-ordinate the calcium ion (blue sphere) are coloured yellow (with side chains shown).*

(C) *The crystal structure of the full-length actinin-2 (PDB ID: 4D1E;* (Ribeiro et al., 2014)*), highlighting the end of spectrin-like repeat 4 (SR4) of the rod domain and CaM-like domain from one monomer and the ABD and neck region of the opposing monomer in the anti-parallel dimer. The residues within actinin-2 that are equivalent to the CMTP-linked mutations in actinin-1 are coloured red with side chains shown (R738 = R745, R752 = R759, G764 =G771, E769 = E776, T737=T744).*

(D-E) *The crystal structure of the full-length actinin-2 (PDB ID: 4D1E; (Ribeiro et al., 2014), highlighting a region of the rod domain that includes SR2 and a portion of SR3 from the opposing monomer. The L395Q (L402 in actinin-2) mutation maps to the first helix of SR2 in the middle of rod domain. L547P (L554) maps to SR3. The R320Q (R327) mutation maps to helix 2 of SR1.*

(F) *The sidechain of the R327 residue in actinin-2 makes polar contacts with three glutamate residues, one located in SR4 of the other actinin subunit and two located in helix 3 of SR1.*

(Note) This figure and associated observations relating to the structural impact of actinin-1 mutations detailed were made by supervisor and co-author P. Young. The figure was included in the thesis for clarity as it visually illustrates several points made in the discussion.

2.4.1 CaM-like Domain Mutations

Three amino acids mutated in actinin-1-linked CMTP map to EF-1 of the CaM-like domain, the only EF hand motif in actinin-1 that is functional in terms of calcium binding. R752Q or R752P mutations have been reported in four families (Bottega et al., 2015; Faleschini et al., 2018; Kunishima et al., 2013; Westbury et al., 2015) while the G764S and E769K mutations have each been reported in a single family to date (Bottega et al., 2014). Calcium binding to EF-1 is thought to cause structural stabilisation of the CaM-like domain of actinin-1 with a more open conformation of EF3-4 promoting its interaction with the neck region adjacent to the ABD of the opposing subunit in the actinin dimer and consequently impairing actinin's ability to cross link F-actin, due to increased rigidity in the neck region (Prebil et al., 2016).

Thermal shift assays allowed the examination of the effects of CMTP-linked mutations on both the stability and calcium binding ability of the isolated CaM-like domain. The high levels of fluorescence at room temperature that was observed for both the WT and mutant CaM-like domain (Figure 2.3.3) may be due the lack of a compact globular shape or the positioning of hydrophobic regions of a protein and has been reported to occur in 15-25% recombinant proteins (Crowther et al., 2010; Huynh & Partch, 2015). Nevertheless, a peak in fluorescence that was observed for the WT protein as the temperature rose above 60 °C could be interpreted as corresponding to the thermal denaturation of the CaM-like domain on the basis that (1) it was shifted to the right in the presence of calcium (but not magnesium; data not shown) and (2) the observed Tm values of 74.8 and 85.1 °C in the absence and presence of calcium are in line with the high melting temperatures that have been reported for calmodulin and related EF-hand-containing proteins (Brzeska et al., 1983; Wendt et al., 1988). The Tm values for CaM-like domains with the G764S and E769K mutations were significantly lower than the WT protein both in the absence and presence of calcium. This indicates that these mutations do affect the stability of the CaM-like domain although, given the high thermal stability of this domain, the importance of this destabilization at physiological temperatures are not clear. Similar to the WT CaM-like domain, a statistically significant increase in Tm was seen for all three mutant proteins (R752Q, G764S and E769K) in the presence of calcium, indicating that they are able to bind and be stabilised by calcium ions. For the R752Q mutant the magnitude of this shift was similar to the WT at approximately 10°C, whereas for the G764S and E769K mutants it was somewhat less at 8 and 4°C respectively. This comparatively smaller shift is suggestive of less structural stabilisation due to sub-optimal calcium binding and would fit with the

location of the G764S and E769K mutations immediately adjacent to the calcium coordinating residues in the EF-1 hand domain (Figure 2.4.1 B).

Assessing calcium binding more quantitatively by isothermal calorimetry, it was found that the WT CaM-like domain demonstrated a single binding event and a dissociation constant (114.94 ± 15.20 μM) in line with a previous report (Prebil et al., 2016). Similar average Kd values were calculated for the R752Q and G764S, albeit with greater variance in the data obtained for these mutants. By contrast, binding efficiency appeared to be compromised in the E769K mutant for which DP and ΔH values were 10-fold lower than WT or other mutants. This precluded the accurate calculation of a Kd value but suggests a significant deficiency in calcium binding for this mutant. However, the high protein concentrations required for calorimetry experiments must be borne in mind as they may exacerbate changes in protein stability that might not be so significant under conditions of more physiological protein concentrations. Additionally, the experiment was carried out at 25℃, and it was shown in the thermal shift assay that the E769K mutant was the least thermally stable of the proteins assessed, although maintained a relatively high melting temperature of 75.9℃ in the presence of calcium. Potentially its reduced stability impacted binding in *in-vitro* analysis.

In actin bundling assays full-length actinin-1 proteins harbouring these mutations all bundled actin more efficiently than the WT protein and this bundling was reduced in the presence of calcium, indicating that all the CaM-like domain mutant proteins retain their calcium-sensitivity in this context. Cytoskeletal association of the G764S and E769K mutants in HeLa cells was also significantly enhanced, and all three mutants co-localized with actin filaments in both HeLa and differentiating MEG-01 megakaryoblast cells. Overall our data on the CaM-like domain mutations indicates that the E769K mutation has the greatest impact on protein stability and affects, but does not abolish, calcium binding, whereas R752Q and G764S mutant proteins appear to be minimally affected in this regard. In addition, enhanced bundling of and/or association with actin filaments is seen for all the three mutant proteins.

Calcium-sensitive regulation of actin by actinin-1 and other proteins is relevant to key aspects of platelet function including platelet activation when intracellular calcium concentration doubles (Oliver et al., 1999) and plays a role in driving dramatic changes in cell shape (Gupta et al., 2016). Given the mild phenotype and normal platelet activation reported for patients with actinin-1 associated CMTP, it is perhaps unsurprising that

calcium-binding efficiency is not dramatically affected by the reported CaM-like domain mutations, as the loss of calcium regulation of actinin-1 would likely have severe consequences for platelet function and for other actinin-1 expressing cells (Bottega et al., 2015; Kunishima et al., 2013).

2.4.2 Rod Domain Mutations

A cluster of CMTP-linked mutations map to amino acids 737 and 738 that lie at the end of the last alpha helix of the 4th SR of the rod domain. Four families with either T737N or T737S mutations and eight families with R738W or R738Q mutations have been reported (Bottega et al., 2015; Boutroux et al., 2017; Faleschini et al., 2018; Kunishima et al., 2013; Westbury et al., 2015). Interestingly the T737S mutation was classified as a variant of uncertain significance presumably due to, (1) its occurrence in a single family, (2) it being a relatively conservative substitution with low scores for its disruptive potential according to predictive bioinformatics algorithms and, (3) the lack of observed disruption of the actin cytoskeleton in cells transfected with actinin-1 harbouring this mutation (Faleschini et al., 2018) .

In the crystal structure of actinin-2 EF1-2 lies on top of and is in close contact with SR4 and the residues equivalent to T737 and R738 are close to this interface (Figure 2.4.1 C) (Ribeiro et al., 2014). Mutations of these residues in actinin-1 may thus affect the interaction of SR4 with the CaM-like domain and alter its regulation of actin binding. However, in the actinin-2 structure, while the equivalent threonine residue in forms two hydrogen bonds with residues from EF-2, the arginine side chain projects away from EF-2, not making close contact with the CaM-like domain.

It was found that both the T737N and T737S mutations increased actinin-1's ability to bundle actin filaments *in-vitro*, while the actinin-1 R738W protein has only a very slightly increased ability to bundle actin filaments that is not statistically significant. This was in agreement with our previous findings that showed a slight but not significant increase in cytoskeletal association for this mutant (Murphy et al., 2016). These findings indicate that the T737S mutation has functional consequences, supporting the case for it being classified as a likely pathogenic mutation and also suggesting that bundling assays may be a useful quantitative method to assess the functional implications of actinin-1 mutations.

In contrast to this cluster of mutations at the end of SR4, the R320Q, L395Q and L547P rod domain mutations that we examined are located some distance from the ABD and CaM-like domains (Figure 2.4.1 D-E). Based on the actinin-2 structure, R320 lies close to the dimer interface whereas L395 and L547 do not. Nevertheless, all three mutant proteins elute as dimers from a gel filtration column (data not shown), and can bundle actin filaments, indicating that dimerization of the rod domain is not disrupted. The R320Q and L395Q mutant proteins have dramatically increased actin bundling ability *in-vitro* whereas actin bundling for L547P was not significantly increased.

The L395Q mutation maps to the first helix of SR2 in the middle of rod domain and in the actinin-2 structure the equivalent leucine residue is facing away from the dimer interface with its sidechain projecting towards helix 2 of SR2. The R320Q mutation maps to helix 2 of SR1. The sidechain of the equivalent arginine residue in actinin-2 makes polar contacts with three glutamate residues, one located in SR4 of the other actinin subunit and two located in helix 3 of SR1 (Figure 2.4.1 F). Our current understanding of actin filament cross linking by actinin indicates that the 90 degree twist present within the rod domain would favour the crosslinking of actin filaments in a perpendicular orientation (Prebil et al., 2016; Ribeiro et al., 2014; Ylänne et al., 2001) is not compatible with the bundling of actin filaments in a parallel or anti-parallel orientation. Such bundling of filaments into tight fibres may require dissociation of EF3-4 from the neck region to give this region the conformational flexibility required to re-orient the ABD appropriately. It is conceivable then that mutations in the rod domain may influence the bundling of actin filaments either by altering the twist of the rod domain or by long range structural effects that influence the “clamping” of the neck region by EF3-4. A structure of the full-length actinin-1 dimer would greatly aid our understanding in this regard.

Yasutomi et al. (Yasutomi et al., 2015) reported that CHO cells expressing actinin-1 L395Q exhibited disorganization of the actin cytoskeleton with shorter and thicker actin fibres and similar effects have previously been reported for other CMTP-linked actinin-1 mutations (Bottega et al., 2014; Faleschini et al., 2018; Guéguen et al., 2013; Kunishima et al., 2013) and for eleven newly identified mutations (including nine in the rod domain) (Vincenot, 2019). We found that actinin-1 L395Q association with the cytoskeleton in cultured HeLa cells appears similar to that of WT actinin-1 in contrast to the CaM-like domain mutations G764S and E769K. In addition, we did not observe notable cytoskeletal disruption, nor increased actin fibre diameter in HeLa cells for L395Q or the other mutations that we examined. Thus it appears that the relationship between actin bundling properties *in-vitro*

and actin association or organisation *in-cellula* is not straightforward and is likely to be cell line-specific. We attempted to use differentiating MEG-01 megakaryoblast cells as a more relevant cellular model (Figure 2.3.7), but a high degree of intrinsic morphological heterogeneity in these cells complicated any analysis of the effects of transfected actinin-1 proteins. Primary cultures of rodent megakaryocytes are likely to be a better model to examine the mechanisms by which actinin-1 mutations affect platelet production. Defining features such as the number of proplatelet, proplatelet length and proplatelet tip size could be assessed in these cells.

In summary, all CaM-like and rod domain actinin-1 mutants assessed here show varying degrees of increased association with F-actin *in-vitro* and/or *in-vivo*. This phenotype was demonstrated previously for several CMTP-causing mutations in the actinin-1 ABD (Murphy et al., 2016). A common mechanism thus appears to exist in the pathogenesis of actinin-1 related CMTP, regardless of the functional domain of actinin-1 affected. We hypothesise that increased F-actin affinity could impact platelet production during events such as the extension of proplatelet shafts in megakaryocytes, along which platelets are released or the fission of large pre-platelets into mature platelets in the vasculature (Schwertz et al., 2010; Thon et al., 2010). An interesting development in actinin-1 CMTP research comes with the recent identification of a novel frameshift mutant generating N-terminally truncated actinin-1 and 49% less actinin-1 expression in heterozygous carriers (F.-M. Luo et al., 2021). Although patients also exhibited macrothrombocytopenia, this was suggested to be a loss-of-function mutation, in contrast to the gain-of-function, in terms of actin binding, mutants assessed in this chapter. Hence there may an alternate role actinin has in platelet production, beyond its interaction with actin. Potentially, other protein-protein interactions could be disrupted by CMTP linked mutations which are essential for platelet formation, given the many proteins which interact with actinin-1 (Djinovic-Carugo et al., 2002).

3.0 Assessment of Actinin in Platelet Production

3.1 Introduction

3.1.1 Overview of Platelet Formation

Platelet formation can be considered in a number of sequential steps. Firstly, MK mature by undergoing endomitosis to increase ploidy (Poulter & Thomas, 2015) , illustrated in Figure 3.1.1 (A&B). This process is thought be important to generate large quantities of RNA and granule contents for platelets (Machlus et al., 2014). This occurs through a failure of cytokinesis and involves, F-actin, myosin-IIA and RhoA (Poulter & Thomas, 2015). For RhoA, knockdown caused increased MK ploidy, aberrant proplatelet release and macrothrombocytopenia (Poulter & Thomas, 2015). Rac1, CDC42 and cofilin also have roles in MK maturation in formation of the demarcation membrane system (DMS), granule trafficking and maintaining structural integrity in terms of actin and microtubule coordination (Poulter & Thomas, 2015). DMS structure heavily relies on actin dynamics, regulated by Cdc42 and Pak 1/2/3 (Antkowiak et al., 2016). Additionally, down regulation of MYH10 by RUNX1 regulates the failure of cytokinesis during endomitosis through a defect in the actin-myosin II contractile ring (Poulter & Thomas, 2015). The protein tyrosine phosphatases Shp1 and Shp2 are also important for MK maturation (Machlus et al., 2014)

MK move from the haematopoietic niche to the vascular niche within the bone marrow and, at the vascular niche, extend cytoplasmic protrusions called proplatelets (Figure 3.1.1 C) through the vessel endothelium into the bloodstream (Poulter & Thomas, 2015). Type I collagen was shown to suppress proplatelet production, while type IV collagen, fibrinogen and fibronectin stimulate production (Semeniak et al., 2016). They are also suppressed by sphingosine 1-phosphate in the haematopoietic niche (Niazi et al., 2019) and MK are sensitive to extracellular matrix rigidity, producing proplatelets on softer matrices (Abbonante et al., 2017). Proteasome function is another regulator of proplatelet production (Shi et al., 2014). Platelets are then released from the proplatelet in the bloodstream and shear-induced release of platelets involves MYH10 (Poulter & Thomas, 2015).

Microtubules are the major component of proplatelets (Machlus & Italiano, 2013). They extend from the cell centre to the cortex in immature megakaryocytes and form

pseudopods in the early stages of proplatelet production (Machlus & Italiano, 2013). Proplatelets are formed through the extension of these pseudopods, with microtubules lining the proplatelet shaft (Machlus & Italiano, 2013). Microtubule sliding, driven by the motor protein dynein, makes a major contribution to this proplatelet extension process (Bender, Thon, et al., 2015). The microtubules loop back into the shaft at the end of each process, forming a platelet-sized tip (Machlus & Italiano, 2013). Microtubule sliding and the motor protein kinesin also facilitate the delivery of granules and organelles to the platelets, at proplatelet tips (Poulter & Thomas, 2015). MYH9 defects cause increased contractility, in terms of stress fibres, and reduced proplatelet formation, possibly implying that increased contractility inhibits proplatelet formation (Poulter & Thomas, 2015).

Figure 3.1.1

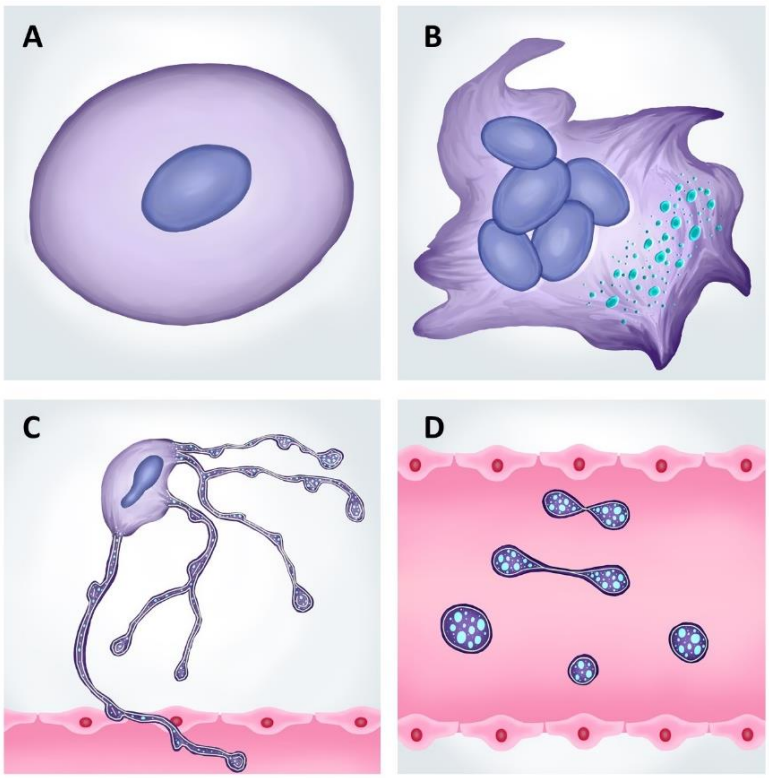

Figure 3.1.1 Illustration of the steps involved in MK maturation, platelet production and platelet release. *(A) Immature megakaryocyte. (B) Megakaryocyte maturation involving polyploidisation and cell enlargement. (C) Extension of proplatelets with platelet-sized tips from the bone marrow into the vasculature. (D) Fission of large pre-platelets into mature platelets with intermediate bar-bell shaped platelet formed during the process. (Illustration by Lara O'Sullivan)*

The actomyosin network is also important for proplatelet formation. Platelets are formed only at the ends of proplatelets, and actin promotes branching of the proplatelets, yielding a greater number of tips (Italiano et al., 1999). Although actin has a role in increasing tip number on the proplatelets, actin disruption accelerates proplatelet extension (Poulter & Thomas, 2015). Regulators of actin polymerisation also play a role in platelet formation, with RhoA, Pak2 and mDia1 affecting proplatelet formation (Poulter & Thomas, 2015). Myosin IIA mutations also decrease the number of proplatelets formed (Poulter & Thomas, 2015). Actin and WASp-rich podosomes are also necessary to degrade the ECM and allow proplatelets to enter the blood stream (Schachtner et al., 2013). WASp and profilin knockdown reduce proplatelet formation and cause premature release of platelets in the marrow, with associated microthrombocytopenia (Poulter & Thomas, 2015).

When the proplatelet tips are released into the blood, they may take the form of premature platelets including preplatelets (2-10 µm) (Figure 3.1.1 D) or bar-bell shaped platelets (two 2 µm platelets which are connected via a microtubule coil) (Poulter & Thomas, 2015). These mature into discoid 2 µm platelets, driven by shear forces during blood flow (Poulter & Thomas, 2015) or at sites such as the lung microvasculature (Machlus et al., 2014).

Evidence also exists for a proplatelet-independent form of platelet production which occurs when platelet count increases are required acutely, such as during thrombocytopenia and inflammation (Kowata et al., 2014). More recent microscopy techniques have shown that megakaryocytes densely populate the marrow and typically reside at capillary sinusoidal vessels (Stegner et al., 2017). Another theory suggests that platelet production is a consequence of megakaryocyte apoptosis, however apoptotic pathways were shown to be dispensable for thrombopoiesis (Josefsson et al., 2014). Another alternative to the proplatelet model is the production of large protrusions into the sinusoidal space, without microtubule bundles, through mass inner and plasma membrane fusion (Brown et al., 2018). Additionally, 50% of platelet production is reported to occur in the lung, implying that MK or large MK fragments must enter the bloodstream (Lefrançais et al., 2017).

3.1.2 Megakaryocyte Podosomes and Their Role in Platelet Formation

Podosomes are 0.7-1 µm actin rich structures associated with cell motility, adhesion and ECM degradation, found in cells specialised in crossing basement membranes and cellular boundaries (Cox et al., 2012; Van Den Dries et al., 2013). This includes myeloid and

dendritic cells (van den Dries et al., 2013). Podosomes have been assessed in various cell types including a monocytic cell line, THP-1 (Cox et al., 2012), murine megakaryocytes (Becker et al., 2020) and dendritic cells (van den Dries et al., 2013). They have been studied on various substrates including uncoated glass coverslips or coverslips with fibronectin, collagen type I, or laminin (van den Dries et al., 2013).

They were first observed in Rous sarcoma virus transformed fibroblasts (Tarone et al., 1985). They can arrange into clusters, belts or ring-shapes called rosettes and are located at the cell – ECM boundary (Alonso et al., 2019; Van Den Dries et al., 2013). They are transient structures which form and dissociate over a period of 5-10 minutes (Cox et al., 2012). Podosomes are similar to invadopodia in cancer cells, with functions in cell migration (Seano & Primo, 2015).

Podosomes are speculated to be important in various processes, including cell motility, dendritic cell antigen presentation and angiogenesis (F. Alonso et al., 2019). Early studies of MK spreading in response to ADP note that actinin, filamin and actin form punctate (0.8-1.1 µm) structures throughout the cytoplasm, possibly indicating podosome formation (Leven & Nachmias, 1982). It was speculated that the formation of these structures in response to ADP was an aggregation of proteins involved in platelet maturation (Leven & Nachmias, 1982). Podosomes are now implicated in platelet formation, whereby podosome clusters connected by the actomyosin network enable the passage of proplatelets through the endothelial barrier during thrombopoiesis (Eckly et al., 2020). They use matrix metalloproteases to degrade the basement membrane and release platelets into the bloodstream (Schachtner et al., 2013). They also function in mechanosensing, responding differently on stiff and soft substrates (Linder & Wiesner, 2016; van den Dries et al., 2019). Megakaryocytes are reported to regulate proplatelet formation and platelet release through signalling stimulated by mechanosensitive ion-channels, which respond to matrix stiffness (Abbonante et al., 2017). Haematopoietic stem cells also use podosomes to cross the bone marrow endothelium in a transcellular process (Rademakers et al., 2020).

Podosome structure is comprised of an actin core, associated with protrusion, and an outer ring made up of proteins including vinculin and talin, associated with adhesion (Cox et al., 2012; van den Dries et al., 2013). The core and ring are connected via an actomyosin network and cores on adjacent podosomes are connected via radial actin filaments (Van Den Dries et al., 2013). Tensions generated by the F-actin core and radiating actin network regulate the protrusive and adhesive activity of the podosome clusters (van den Dries et al.,

2013). These radial filaments include ventral actin filaments bound by vinculin which connect to the cell membrane, and dorsal interpodosomal filaments, crosslinked by MHCIIA (Van Den Dries et al., 2019).

The core consists of actin and actin binding proteins, WASP, Arp 2/3, cortactin (predominantly associated with branched actin filaments, at the core centre) and actinin (associated with linear actin filaments at the core periphery) (Van Den Dries et al., 2019). At the periphery of the core, vinculin is also bound, with close association to integrins (Van Den Dries et al., 2019).

Figure 3.1.2

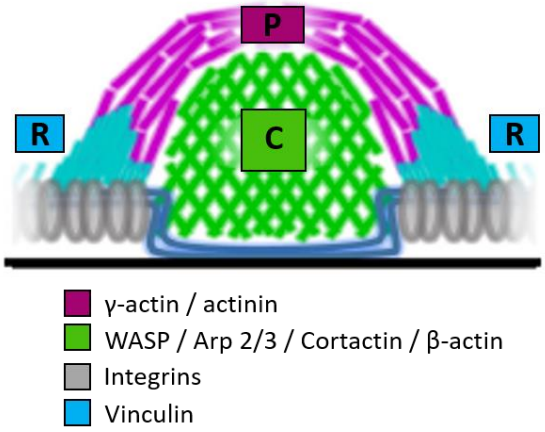

Figure 3.1.2 Illustration of podosome structure. *Proteins present in various regions of the structure are indicated. C = centre of core, P= periphery of the core, R=outer ring. Illustration is modified from that published in Van Den Dries et al., 2019.*

Talin and integrin are localised throughout the podosome cluster, but excluded from the actin core (van den Dries et al., 2013). Their co-localisation is suggested to cause constitutively activated integrins, which are primed for adhesion to the ECM (van den Dries et al., 2013). Vinculin is located in proximity to the actin core and near the radial actin filaments connecting cores (van den Dries et al., 2013). Arp 2/3 transiently associated with vinculin at sites of integrin clustering in response to signals that trigger membrane protrusion (DeMali et al., 2002). Actinin has previously been reported to interact with vinculin at focal adhesions and adherens junctions (Bois et al., 2005). Mechanical stimuli may regulate exposure of the actinin vinculin-binding site, which is thought to reinforce the actinin-actin interaction (Shams et al., 2012).

Loss of Arp2/3 impaired the formation of transendothelial pores and the production of cytoplasmic processes in the megakaryocytes of Arp 2/3 knockout (in the MK lineage) mice (Eckly et al., 2020). In a MHCIIA knockout mouse model, loss of MHCIIA affected podosome size, distribution, number and caused scattered transendothelial pores (Eckly et al., 2020). Deficiencies in actin regulatory proteins twinfilin and cofilin in mice are associated with macrothrombocytopenia and increased MK numbers in the bone marrow and spleen, and are associated with increased F-actin and enhanced microtubule stability (Becker et al., 2020). These mutations also cause reduced podosome formation (Becker et al., 2020). Wiskott Aldrich Syndrome (WAS), involving a congenital mutation in the WAS protein (WASP), a regulator of actin polymerisation, is also associated with premature platelet release into the bone marrow and microthrombocytopenia (Sabri et al., 2006). Another regulator of actin dynamics, phospholipase D is required for podosome formation, but does not impact platelet count in mice (Stritt et al., 2014). Regulators of WASp and ARP 2/3, cortactin and HS1 were shown not to be required for MK podosome formation and did not impact platelet count or function in knockout mouse models (S. G. Thomas et al., 2017).

3.1.3 Actinin in Megakaryocytes

In this study, the role of actinin in platelet formation was explored. Actinin could play a role in various steps of megakaryocyte maturation and function during thrombopoiesis.

In the earlier stages of megakaryocyte maturation, actinin is known to regulate cytokinesis and overexpression causes a failure in cytokinesis and thus polyploidization (Mukhina et al., 2007). Actinin-1 knockdown in megakaryocytes caused filamin A levels to be diminished and cell polyploidisation and enlargement were prevented (Elagib et al., 2013b). A genome-wide association study of platelet count found that an ACTN1 SNP in the intron 1 enhancer region was predictive of platelet count and MPV, also suggesting actinin has a regulatory role in platelet production (Schick et al., 2016). It is possible that actinin mutations could impact this process.

Additionally, actinin is reportedly present in important morphological features of megakaryocytes. When megakaryocytes spread over an adherent surface, membrane ruffling with a redistribution of contractile proteins occurs (Leven & Nachmias, 1982). When adhering to the surface, they extended short filopodia which are ~5 µm long (Leven & Nachmias, 1982). They rapidly undergo membrane ruffling and extend longer 10 µm filopodia (Leven & Nachmias, 1982). Fully spread cells are large (100 µm) with thin

cytoplasm (Leven & Nachmias, 1982). Prior to spreading, cytoskeletal proteins myosin, actinin, filamin, actin are diffusely spread throughout the cytoplasm (Leven & Nachmias, 1982). Myosin staining increased at the ruffling region of cells during spreading (Leven & Nachmias, 1982) and filamentous structures, arranged circumferentially or like chords extend from the cell centre (Leven & Nachmias, 1982). Actinin and filamin were noted to form punctate (0.8-1.1 µm) structures throughout the cytoplasm, with a strongly staining band behind the ruffle (Leven & Nachmias, 1982). Actinin and filamin were also found in circumferential filaments and radial filaments in some spread cells (Leven & Nachmias, 1982).

Other actin rich structures, podosomes and proplatelets, likely also rely on normal actinin function and may be impacted by actinin-1 mutations. These structures are examined in this study.

3.1.4 Megakaryocytic Cell Models

In this study, two megakaryocytic cell lines were used to assess actinin in megakaryocytes; MEG-01 and CMK.

CMK was established from a megakaryoblastic leukaemia patient with Down's Syndrome (Sato et al., 1989). CMK cells express integrin αIIbβ3 (Komatsu et al., 1989; Sato et al., 1989). They can be differentiated into mature polyploid megakaryocytes using phorbol 12-myristate 13-acetate (PMA), with most mature cells expressing Integrin αIIbβ3 (Komatsu et al., 1989). A subset of the differentiated cells also displayed cytoplasmic segmentation, which resembled platelet formation (Sato et al., 1989). Platelet integrin activation has been assessed in CMK cells, although it was noted that optimal activation required higher agonist concentrations, and activation levels were lower than in platelets (S. Tadokoro et al., 2011). PMA treated CMK cells previously been used as models of megakaryocytic differentiation (Zhan et al., 1997).

MEG-01 are reported to extend cytoplasmic processes similar to proplatelets following treatment with aphidicolin (DNA polymerase inhibitor) (Takeuchi et al., 1998) or nitric oxide (Battinelli et al., 2001). They also are reported to release platelet-sized particles which can undergo a shape change, release P-selectin and aggregate in response to thrombin, although the numbers produced are low (Schweinfurth et al., 2010; Takeuchi et al., 1998). Differentiation of MEG-01s (a subline of MEG-01) with PMA caused cells to become adherent, polyploid, express granules and display cytoplasmic blebbing (Ogura et

al., 1988). Various proteins including integrin αIIbβ3 and VWF were increased with PMA treatment (Ogura et al., 1988). Various methods of DNA delivery to MEG-01 cells have been described, with nucleofection reportedly having the highest efficiency (Yoshimasa Isakari et al., 2007).

3.1.5 The Cytoskeleton in Platelet Function

Several cytoskeletal proteins have been implicated in platelet function including MYH9 (Balduini et al. , 2011), Filamin A (Rosa et al., 2019) and WASP (Poulter et al., 2015). Actin is the most abundant protein in platelets, with 70% of actin being in the filamentous form in activated platelets (Sorrentino et al., 2015). In resting platelets, the actin cytoskeleton resembles spokes of a wheel, with F-actin radiating from the membrane to cell centre and a dense spectrin rich shell encases the actin core (Sorrentino et al., 2015). A microtubule circumferential coil maintains platelets in a discoid shape in the resting state (Cuenca-Zamora *et al.,* 2019). A cortex of tightly packed actin filaments make up the cell cytoskeleton (Sorrentino et al., 2016). This coil is maintained by dynein and kinesin activity in resting cells (Figure 3.1.4) (Cuenca-Zamora *et al.,* 2019). When intracellular calcium levels increase during activation, dynein activity is enhanced, while kinesin activity is suppressed, causing the microtubule coil to expand and coil (Cuenca-Zamora *et al.,* 2019). Cells transition from a discoid to a spherical shape, as the microtubules expand and coil into the centre of the cell (Cuenca-Zamora *et al.,* 2019). Actin filaments are severed in this process and then polymerised to form filopodia (Sorrentino et al., 2016). Filopodia consist of actin filaments that push the membrane forward (Sorrentino et al., 2016). Lamellipodia consist of a mesh of densely packed actin filaments (Sorrentino et al., 2016). Granules are centralised in the platelet during this process (Cuenca-Zamora *et al.,* 2019). This process results in spread adherent platelets taking a “fried egg” shape with lamellipodia and a network of depolymerised microtubules (Figure 3.1.4) (Sorrentino *et al.*, 2016; Cuenca-Zamora *et al.,* 2019).

Figure 3.1.3

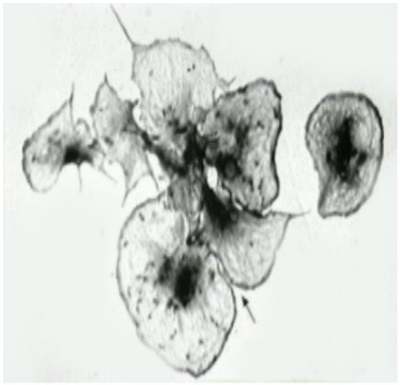

***Figure 3.1.3 Electron micrograph of spread platelets**. Platelets from a patient with coronary artery disease were spread on Formvar and imaged using the Hitachi H500 transmission electron microscope. Platelets were imaged at 9000X magnification. Arrow shows "fried egg" appearance of spread cells. Image taken and kindly provided by Prof M Cahill* (Cahill, 1995).

Figure 3.1.4

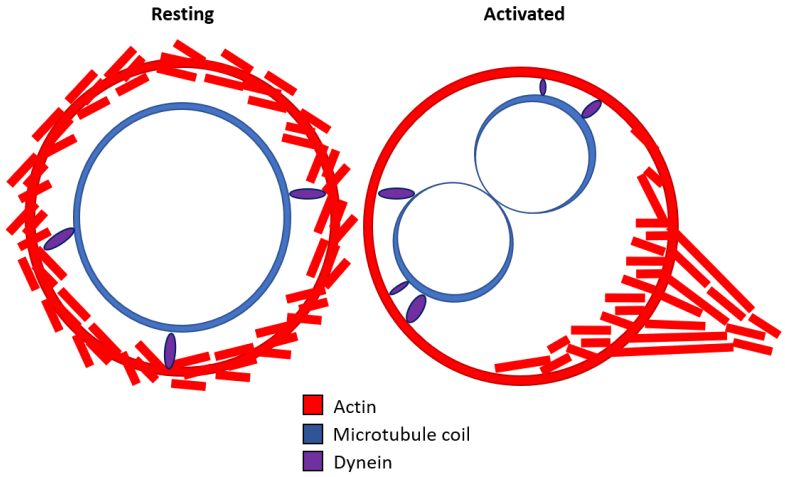

***Figure 3.1.4 Illustration of the platelet actin cytoskeleton and microtubule coil during the resting and activated stated.** Actin filaments are short and densely packed forming a cell cortex in the resting state. Activation causes actin severing and polymerisation to form long parallel filaments in filopodia. The microtubule band expands and coils during activation by dynein activity (Sorrentino et al., 2016). Figure is a modified version of that published in (Sorrentino et al., 2016).*

3.1.5.2 Platelet Actin Nodules

Platelets contain actin structures, called actin nodules, which form during early adhesion and spreading (Calaminus et al., 2008; Poulter et al., 2015). Platelet actin nodules are similar to podosomes and enhance platelet aggregate stability under flow (Poulter et al., 2015). Actin nodules in platelets consist of 1-4 dense F-actin loci which are interconnected by actin fibres (Poulter et al., 2015). They are smaller than podosomes, with average diameter being 0.50 ± 0.12 µm, and have a median lifespan of 22.1s (Poulter et al., 2015). WASp and Arp 2/3 are necessary for their formation (Poulter et al., 2015).

3.1.6 Actinin in Platelets

Early analysis of the platelet cytoskeleton reported the presence of actin, actin binding protein (filamin) and a 105 kD protein, which was purified and reported to be similar to muscle actinin (Rosenberg et al., 1981). Actinin was once thought to be identical to Glycoprotein III, to reside at the platelet surface membrane and to facilitate platelet aggregation (Gerrard et al., 1979). Actinin was later shown to be distinct from Glycoprotein III (Gogstad et al., 1981; Langer et al., 1982; Langer et al., 1984; Sixma et al., 1982). Actinin isolated from platelets was reported to gelate actin solutions (Schollmeyer et al., 1978). It was noted in later studies that platelet actinin differed to muscle actinin, being calcium-sensitive and slightly larger in molecular weight (100-102 kDa versus 96 kDa) (Landon & Olomucki, 1983; Rosenberg et al., 1981). Sequencing of platelet actinin cDNA confirmed that the actinin isoform expressed in platelets is identical to that in non-muscle cells (Izaguirre et al., 2001).

3.1.6.1 Actinin Isoforms in Platelets

Early studies refer to multiple actinin isoforms in platelets, with the nomenclature a, b, c based on molecular mass (Landon et al., 1985). Two isoforms, dimers aa (2 x 97 kD) and cc (2 x 94 kD) were described as being calcium-sensitive actin-binding and cross-linking proteins, although aa was shown to be more strongly inhibited than cc (Landon et al., 1985). Additionally, the actin cross-linking efficiency was higher in cc than aa (Landon et al., 1985). Cross linking efficiency of aa was substantially reduced compared to cc at 20˚C (Landon et al., 1985). It is now known that actinin-4 and actinin-1 are calcium sensitive actinin isoforms in platelets and potentially this early study represents their presence.

Recent work suggests the actin binding affinity and calcium sensitivity are similar in each isoform (Foley & Young, 2013).

3.1.6.2 Actinin Localisation in the Platelet

A proportion of actinin resides at the platelet membrane, but is not a transmembrane protein and is not accessible at the cell surface (Sixma et al., 1982). Actinin links the cytoskeleton to the cell membrane (Burn et al., 1985) and it is thought actinin at the membrane has a role in spatial arrangement of the actin filaments (Sixma et al., 1982). In resting platelets, the cytoskeleton is made up mostly of actin, actinin and filamin (Dubernard et al., 1997). Platelets also contain a matrix of 10 µm filaments, consisting of tightly packed 10 nm filaments, containing various proteins including spectrin, myosin, actin, actinin and tropomyosin (Harsfalvi et al., 1991). Additionally, a proportion of actinin is also localised in the cytoplasm and the alpha granules (Dubernard et al., 1995; 1997).

On activation with thrombin, actinin forms complexes with fatty acids and diacylglycerol (Burn et al., 1985). It is detected on the cell surface of thrombin activated platelets in complexes with TSP-1, particularly at the pseudopods (Dubernard et al., 1997). After thrombin activation, filamin association with the cytoskeleton increases and myosin is incorporated to the cytoskeleton (Dubernard et al., 1997). Actinin association with the actin cytoskeleton during thrombin activation did not increase, and was estimated to comprise 70% of the actinin pool (Dubernard et al., 1997). Actinin in the alpha granules which redistributes to the plasma membrane during thrombin activation was not associated with actin (Dubernard et al., 1997). Other studies have shown that thrombin stimulation causes redistribution of actinin to the cytoskeleton (Hoyt & Lerea, 1995).

In surface-activated spread platelets, actinin was localised at punctuate structures and co-localised with actin filaments, in the cytoplasm, at the filopodia edges, on the cell membrane and around the granulomere (Takubo et al., 1999). Following spreading on fibrinogen, it is reported to be localised in actin bundles and more abundantly at adhesion sites (Lickert et al., 2018). Myosin is also present in a speckled pattern along the actin filaments (Takubo et al., 1999). Actinin localised with myosin at the cell membrane, in the cytoplasm and near the granulomere (Takubo et al., 1999). Vinculin was also concentrated at punctate structures near the plasma membrane, possibly associated with actinin at sites of adhesion (Takubo et al., 1998). Actinin has also been implicated in pseudopod formation as it is important for lateral actin filament associations and the formation of parallel actin

bundles in association with actin-binding protein (Schollmeyer et al., 1978). Hence actinin may have a role in adhesion and filopodia formation during platelet spreading.

3.1.6.3 Regulation of Actinin in Platelets

The regulation of actin-actinin interaction is essential in platelets, which undergo rapid cytoskeletal re-organisation during activation. The affinity of actinin for actin greatly affects the properties of the actin-actinin gels formed *in-vitro*, ranging from a dynamic fluid to solid state, depending on the association of actinin (Wachsstock et al., 1993). Actinin is regulated through various mechanisms in platelets.

It was noted that calcium-activated proteases cleaved actinin in platelets *in-vitro* (Gache et al., 1984). This study reports the proteolysis of an actinin aa isoform but an actinin cc isoform is insensitive to this protease (Gache et al., 1984).

Actinin cross-linking and binding of actin was diminished in the presence of platelet tropomyosin, speculated to be due to steric blockage of binding sites on the actin filaments (Pruliere et al., 1986). Filamin was also reported to compete with actinin for actin binding (Rosenberg et al., 1981).

It was shown that the phosphorylation of actinin was not unique to haematopoietic cells and occurs by FAK, but this phosphorylation is speculated to be more robust in activated platelets due to tight regulation by phosphatases in other adherent cell types (Izaguirre et al., 2001). The phosphatase inhibitor calyculin A reduced the platelet aggregation response to thrombin, and the redistribution of actinin and other proteins to the cytoskeleton, possibly due to altered PI metabolism and activation of protein kinase C (Hoyt & Lerea, 1995).

In platelets, actinin is dephosphorylated by SHP-1 in resting and thrombin stimulated platelets (Lin et al., 2004). SHP-1 is predominantly expressed in haematopoietic cells (Zhang et al., 2000). Mice lacking SHP-1 experience thrombocytopenia (Jean Max Pasquet et al., 2000). However, in fibrinogen adherent platelets, SHP-1 fails to dephosphorylate actinin, thought to be due to an inactivation of SHP-1 (Lin et al., 2004). In thrombin stimulated platelets, the dephosphorylation of actinin may strengthen its association with integrins and the cytoskeleton, aiding aggregates to resist shear forces (Lin et al., 2004). In contrast, fibrinogen activation causes sustained actinin phosphorylation and reduced association with actin, promoting a dynamic network that favours cell movement and reorganisation of

actin filaments (Lin et al., 2004). Additionally, compartmentalisation of SHP-1 and phosphorylated or dephosphorylated actinin may regulate actin dynamics at different regions of the cell (Lin et al., 2004).

Increases in platelet cytosolic calcium during oxidative stress cause a dissociation of actinin from the cytoskeleton and the formation of high molecular weight aggregates containing actin, actinin and filamin (Mirabelli et al., 1989).

Nitric oxide (NO) may also regulate platelets by a transient tyrosine nitration of actinin, thought to prevent its phosphorylation (Marcondes et al., 2005). NO functions in the circulation to maintain elevated cGMP levels which inhibits platelet adhesion (Marcondes et al., 2005).

3.1.6.4 Actinin Interaction With Platelet Signalling Molecules

Integrin αIIbβ3

Integrins link actin filaments to the plasma membrane at focal contacts, where adhesions to the extracellular matrix occur (Otey et al., 1990). Various proteins are present at these sites including actin binding protein, vinculin, talin and actinin (Otey et al., 1990). Several studies note the transient associations between actinin and the fibrinogen receptor, integrin αIIbβ3.

At integrin aggregates, FAK was reported to be recruited, followed by actinin , talin and vinculin (Miyamoto et al., 1995). Actinin was reported to bind specifically to αIIbβ3 in phospholipid vesicles into which the integrin was incorporated (Otey et al., 1990). It was shown that RGDS binding (a synthetic peptide which binds to and inhibits fibrinogen binding to the RGD motif of αIIbβ3) stimulated the release of actinin and vinculin from adhesion plaques in live 3T3 cells (Stickel & Wang, 1988). Shear also causes dissociation of actinin from β3 (Feng et al., 2002). These authors speculate on a similar finding in rat fibroblasts, whereby actinin dissociates from β3 of αvβ3 when stimulated by PDGF, directed by PI3K generated PIP3, and causes the restructuring of focal adhesions and the dissolution of actin fibres which allows for cell motility (Feng et al., 2002).

More recently, it has been shown that actinin-1 associates with β3 in the resting state in platelets but becomes phosphorylated and dissociates in response to inside-out signalling from protease activated receptors, with long-lasting activation of αIIbβ3 in response to

PAR4 stimulation (Tadokoro et al., 2011). αIIbβ3 was reported to stimulate Protein Kinase C dependent phosphorylation of actinin in PMA activated platelets (Izaguirre et al., 1999). Focal adhesion kinase (FAK) was determined to phosphorylate actinin-1 at tyrosine 12 (Izaguirre et al., 2001). Phosphorylation also reduced actinin association with F-actin (Izaguirre et al., 2001). The P2Y12 ADP receptor also appears to regulate this signalling process as the dissociation of actinin was impaired in P2Y12 deficient platelets (Tadokoro et al., 2011).

The binding of actinin to β3 was later shown not to activate the integrin but triggers adhesion maturation (Roca-Cusachs et al., 2013). The expression of the integrin binding domain only in actinin depleted cells reduced force generation on fibronectin, highlighting that actinin also elicits its effect independent of actin interaction (Roca-Cusachs et al., 2013). The mechanisms behind this have assessed using molecular dynamics simulations recently (Shams & Mofrad, 2017). The binding of actinin to β3 was shown to cause a proline-induced kink in the transmembrane domain, which impairs integrin signalling (Shams & Mofrad, 2017). It also impairs talin binding to β3, possibly by interacting with both proteins simultaneously (Shams & Mofrad, 2017). Hence actinin is thought to have a role in setting αIIbβ3 to a low-affinity state (S. Tadokoro et al., 2011).

Constitutively activated αIIbβ3, as reported for Glanzmann's thrombasthenia patients, was shown to inhibit actin turnover and cytoskeletal reorganisation, and to cause macrothrombocytopenia, proplatelets with reduced tip numbers and a reduction in bar-bell shaped platelets (Bury et al., 2016; Kashiwagi et al., 2004). In patients with Glanzmann's thrombasthenia, platelet concentrations of actinin were found to be normal or increased (Langer et al., 1984). A role for integrin regulation in platelet production and macrothrombocytopenia has also been considered in the context of filamin A mutations and was found to be mediated by increased RhoA activity, a defective actomyosin contractility and defective proplatelet production (Donada et al., 2019).

CLP36

CLP36, or PDLIM1 (characterised by their PDZ and LIM domains), is a cytoskeletal protein of the actinin-associated LIM protein (ALP) family ,with roles in neuronal synapse formation and cytoskeletal regulation (Zhou et al., 2021). It interacts with actinin in protein complexes in a variety of cells, including with actinin-2 in myocardium and actinin-1 and actinin-4 in colonic epithelial cells (Zhou et al., 2021). CLP36 associates with actin filaments in activated

platelets via actinin-1 (Bauer et al., 2000). CLP36 binds to actinin-1 via SR2 and SR3 of the rod domain in both the resting and activated state in platelets (Bauer et al., 2000). The complexed proteins are not localised to focal adhesions, speculated to be due to a regulatory role of CLP36 (Bauer et al., 2000). This was thought to involve the promotion of actinin-actin interactions at stress fibres through the inhibition of actinin-integrin interactions at focal adhesions, mediated by CLP36 binding (Bauer et al., 2000). Actinin, non-filamentous actin, CLP36 and plasma membrane Calcium ATPase (PMCA) are found in a complex in resting and activated platelets (Bozulic et al., 2007). This demonstrates a potential role of actinin in localising proteins to platelet structures such as filopodia in activated platelets (Bozulic et al., 2007).

GPIb-IX

The VWF - GPIb-IX interaction is a stimulus of platelet aggregation and eventual activation of integrin αIIbβ3 (Julio C. Reséndiz, Feng, Ji, & Kroll, 2004). Actinin and GPIb-IX Complex were co-immunoprecipitated in response to exposure to shear, and this was dependent on VWF binding to GPIbα and actinin becoming phosphorylated (S. Feng et al., 2002). Shear stress and the subsequent phosphorylation also enhanced PKN binding to actinin, speculated to indicate a role for actinin in the formation of a signalling complex with GPIb-IX in response to shear and VWF (S. Feng et al., 2002). In resting platelets, non-phosphorylated actinin associates with phosphatidylinositol 3-kinase (PI 3-KIA), protein kinase N (PKN) and PIP_2 (S. Feng et al., 2002; Julio C. Reséndiz et al., 2004). Shear stress induced the dissociation of actinin and PIP_2 from PI 3-KIA and the production of PIP_3 (Julio C. Reséndiz et al., 2004). This complex reassembles at integrin GPIb, with actinin linking the receptor to the cytoskeleton and a second phase of PIP_3 production occurs speculated to maintain integrin GPIb in an activated state and stabilise the nascent thrombus (Julio C. Reséndiz et al., 2004).

B1 integrin

The β1 subunit of integrin is found in various receptors including the fibronectin, laminin and collagen receptors (Otey et al., 1990). β1 integrin interacts directly with actinin via its cytoplasmic domain (Otey et al., 1990). Actinin restricts the motion of the β1 cytoplasmic tail, supporting talin association (Shams & Mofrad, 2017). This regulation of integrins could

modify mechanical signal transmission in the processes of adhesion and cell spreading (Shams & Mofrad, 2017).

3.1.6.5 Actinin in Platelet Activation

Platelet activation causes actinin to become phosphorylated, binding affinity for actin is reduced and the detergent insoluble fraction of actinin increases (Izaguirre et al., 1999; 2001). Platelet activation stimulated by PMA, thrombin, or fibrinogen triggers two waves of signalling events. The first involves the tyrosine phosphorylation of pp72syk, RFTK/PYK, Vav and MAP kinase family members (Izaguirre et al., 1999). The second is dependent on fibrinogen binding to αIIbβ3 and involves phosphorylation of various proteins including calpain and phosphatase SHIP, and cytoskeletal reorganisation (Izaguirre et al., 1999). The tyrosine phosphorylation of actinin stimulated by fibrinogen binding is protein kinase C, PI3 kinase and phospholipase A2 dependent , but phosphorylation by IgG binding to FcγRIIa is protein kinase C dependent but not PI3 kinase or phospholipase A2 dependent (Izaguirre et al., 1999).

ADP or fibrinogen stimulation of platelets increased integration of actinin and actin into the cytoskeleton and aggregation (May et al., 1996). This process is reversed during disaggregation, stimulated by $MgCl_2$, αIIbβ3 antagonists or cAMP (J. A. May et al., 1996). In PMA activated platelets, the tyrosine phosphorylated faction of actinin (estimated to be 15-20% of total actinin) was recovered from the soluble platelet fraction (Izaguirre et al., 1999). Tyrosine phosphorylation of actinin also coincides with the formation of large protein aggregates, suggesting actinin may play a role as a protein scaffold (Izaguirre et al., 1999). In thrombin activated platelets, phosphorylated actinin has been reported to immunoprecipitate with transient receptor membrane channels (TRPC), possibly indicating a role in store operated calcium entry (SOCE), which the authors note is similar to a reported role for muscle actinin in calcium channel regulation in cardiac myocytes (Redondo et al., 2007).

3.2 Methods

3.2.1 Culture of MEG-01, CMK and HEK293FT Cells

MEG-01 (DSMZ, ACC 364) was cultured in RPMI-1640 (Sigma, R8758), 1% Penicillin/Streptomycin, 10% Fetal Bovine Serum. CMK (DSMZ, ACC 392) was cultured in RPMI-1640 (Sigma, R8758), 1% Penicillin/Streptomycin, 20% Fetal Bovine Serum. HEK293FT (Invitrogen, P/N 51-0035) cells were cultured in DMEM (Sigma, D6429), 1% L-Glutamine, 1% Penicillin/Streptomycin, 1% Non-essential Amino Acids (NEAA), 1% Sodium Pyruvate, 10% Fetal Bovine Serum. Cells were cultured at 37°C in 5% CO_2. Cells were counted using Trypan Blue method by diluting cells in dye 1:1. Suspension cells (MEG-01 and CMK) were split by centrifuging cells at 200 RCF for 4 minutes, discarding supernatant, resuspending cells in fresh media and seeding 0.3 x 10^6 cells/mL into flask or plate as needed. Adherent cells (HEK293FT) were split as needed when 90% confluent. For some experiments, cells were treated with PMA (Fisher Bioreagents BP685-1, dissolved in DMSO). 0.625 ng/mL PMA was used for days 0-3 of incubation. Concentration of PMA was then increased to 10 ng/mL and cells were treated for up to 14 days, as described previously (Zou et al., 2017). Media was refreshed every 2-3 days by pelleting cells and replacing media with media containing the appropriate PMA concentration, and cells were re-plated without splitting.

3.2.2 Culture and Differentiation of Primary Murine Megakaryocytes

Murine megakaryocytes were cultured from fetal liver-derived haematopoietic stem cells as previously described (Vijey et al., 2018). Briefly, pregnant female mice (gestation day 13.5) were euthanised according to ethical guidelines and fetal livers were harvested. Livers were homogenised and passed through a 40 µm cell strainer, before being pelleted and resuspended in 2-4 mL DMEM 10% FBS 1% P/S with 70 ng/µL TPO (Peprotech). Cells were incubated in 1-2 wells of a 6-well plate (depending on number of livers harvested, <6 were plated in 1 well). Cells were incubated at 37℃ for 4 days. Megakaryocytes were isolated at day 4 using a BSA density gradient. First, cells were removed from the 6-well dish and transferred to a 15 mL tube. The plate was washed with media twice and the washed off cells were added to the 15 mL tube. Cells were pelleted at 200 x g for 5 minutes. The gradient was set up (in ascending order in a 15 mL tube) as 1 mL 3% BSA/PBS, 1 mL 1.5% BSA/PBS and 1 mL cells in DMEM 10% FBS 1% P/S (no TPO). The cells were incubated (with the tube in an upright position in incubator) on the density gradient for 30 minutes at 37℃.

Following the density gradient step, media and BSA were removed from the top of the tube and cells which had sedimented to the bottom of the tube were resuspended in DMEM 10% FBS 1% P/S (no TPO). Cells were then plated in a new dish or onto coated coverslips. Cells were analysed at 3 – 24 hours after plating.

3.2.3 Staining of Suspension Cells

Glass coverslips were coated with fibronectin (Sigma – F2006) (100 µg/mL), Poly-D-Lysine (0.1 mg/mL) (Sigma) or Type I collagen (Sigma - C8919) (100 µg/mL), for 1 hour at room temperature, allowed to air dry and then rinsed with PBS. Cells were plated onto coverslips and allowed to adhere for 4 to 48 hours.

Cell media was removed, cells were washed twice in PBS and then were fixed in 4% PFA / PBS for 10 minutes at room temperature. Cells were rinsed again in PBS three times and then blocked in blocking buffer (5% Normal Goat Serum, 2% BSA, 0.2% Triton) for 30 minutes at room temperature. Cells were then rinsed in PBS three times and stained, by dilution of antibodies in blocking buffer without Triton. Following staining, coverslips were rinsed in PBS and mounted onto glass slides, using Fluoromount (Sigma – F4680), and the edges were sealed with nail varnish. Slides were allowed to dry and washed with water and dried before being analysed. Fluorescent imaging was carried out using the Leica DMI 3000 microscope. Details of the antibodies used for staining can be found in Appendix Table 6.1.

3.2.4 Transfection of CMK & MEG-01 Cells

3.2.4.1 Optimisation of Nucleofection using MEG-01 Cells

10^6 MEG-01 cells were suspended in 100 µL of various buffers with 5 µg of pEGFP in 2 mm cuvettes and programmes T-01 and X-05 were trialled, as these were previously reported to be efficient for MEG-01 cells (Y Isakari et al., 2007). SA-A buffer (15 mM $MgCl_2$, 40 mM HEPES, 300 mM HPO_4 buffer pH 7.1) (home-made nucleofection buffer developed by Prof Seamus Martin, Trinity College Dublin), HEPES Buffer (10 mM HEPES pH 7.5, 250 mM Sucrose, 1 mM $MgCl_2$) or RPMI were trialled for nucleofection. Cells were then plated in 2 mL RPMI 20% FBS. Cells were counted using trypan blue staining at 24 hours post nucleofection. GFP positivity was quantified by flow cytometry using the Accuri C6 flow cytometer (BD).

3.2.4.2 Nucleofection of CMK Cells

10^6 cells were suspended in 100 µL RPMI with 5 µg pEGFP plasmid in 2 mm cuvettes. Nucleofection programmes T-01 and X-05 were trialled. Following nucleofection, cells were suspended in 2 mL media (RPMI, 20% FBS, no antibiotic). Cells were analysed after 24 hours.

3.2.4.3 Trial of Various Electroporation Buffers

10^6 MEG-01 cells were suspended in 300 µL of various buffers. PBS, SA-A buffer, RPMI 10% FBS or HEPES Buffer (10 mM HEPES, 250 mM Sucrose, 1 mM $MgCl_2$) were trialled. A protocol of 10 µs pulse length, 3 pulses and 3.75 kV/cm was used to electroporate cells in 4mm cuvettes. Efficiency was assessed in terms of delivery of propidium iodide (40 µM) (Biolegend – 421302) to cells and assessment of cell viability, which was measured by flow cytometry using the Accuri C6 flow cytometer (BD) 24 hours after electroporation as previously described (Ruzgys et al., 2019).

3.2.4.4 Optimisation of Electroporation using MEG-01 Cells

SA-A buffer was chosen as a suitable buffer to carry out electroporation of MEG-01 cells. 10 µg of pEGFP plasmid was added to 10^6 MEG-01 cells in 300 µL buffer in 4 mm cuvettes. The number of pulses was kept at 8 for the trial, and various voltages and pulse lengths were assessed. Cells were then plated in 2 mL RPMI 20% FBS. Cells were counted using trypan blue staining at 24 hours post electroporation. GFP positivity was quantified by flow cytometry using the Accuri C6 flow cytometer (BD).

3.2.4.5 Transfection of CMK & MEG-01 Cells.

Transfections were carried out using pEGFP N1 or pEGFP N1 with actinin-1 or actinin-4 sequences cloned into it. The non-muscle, exon 19a-containing, calcium-sensitive splice variant of human actinin-1 sequence was used (Accession no. NM_001102). The non-muscle, calcium-sensitive human actinin-4 sequence was used (Accession no. NM_004924).

The calcium phosphate method and Lipofectamine-2000 and Trans-IT transfection reagents were trialled to transfect the megakaryocytic cell lines. Each protocol is described for the

transfection of 0.8 x 10^6 cells in one well of a 6-well plate in media without antibiotics. Cells were analysed for GFP expression by immunofluorescent microscopy at 48 hours post-transfection. Cells were imaged using the Leica DMIL microscope.

For the calcium phosphate method, 2.5 µg pEGFP and 250 mM $CaCl_2$ were mixed with 2X HEPES-buffered saline (HBS) (274 mM NaCl, 1.4 mM Na_2HPO_4, 27 mM HEPES, H_2O pH7.2) to create a 100 µL solution. This was incubated at room temperature for 1 minute and added to cells in 1 mL of media. The media was changed after 4 hours to antibiotic-containing media.

For Lipofectamine-2000, 2 µg pEGFP and 5 µL Lipofectamine were prepared in 100 µL OptiMEM and incubated at room temperature for 20 minutes. The solution was added to cells in 1 mL of media. The media was changed after 16-24 hours to antibiotic-containing media.

For Trans-IT, 2.5 µg pEGFP and 7.5 µL Tran-IT were prepared in 250 µL OptiMEM incubated at room temperature for 20 minutes. The solution was added to cells in 2 mL of media. The media was changed after 16-24 hours to antibiotic-containing media.

Another Lipofectamine-2000 transfection protocol was trialled but showed similar efficacy. For this protocol, 5µg pEGFP and 7 µL Lipofectamine-2000 in 100 µL OptiMEM media were added to 10^6 cells in 1 mL media (RPMI, 10% FBS, without antibiotics).

3.2.5 Transfection of Primary Cells

3.2.5.1 Transfection of Primary Cells with Lipofectamine-2000

Cells were cultured as previously described and concentrated using a BSA gradient. Immediately post BSA gradient, cells were resuspended in 2 mL DMEM 10% FBS (no antibiotics). Various protocols were trialled on one batch of primary cells:

A. 1 µg pEGFP and 2 µL Lipofectamine-2000 in 40 µL OptiMEM added to cells in 400 µL media.
B. 1 µg pEGFP and 1 µL Lipofectamine-2000 in 40 µL OptiMEM added to cells in 400 µL media.
C. 1 µg Actinin-1 WT-GFP and 1 µL Lipofectamine-2000 in 40 µL OptiMEM added to cells in 400 µL media.

D. 0.5 µg Actinin-1 WT GFP and 0.5 µL Lipofectamine-2000 in 40 µL OptiMEM added to cells in 400 µL media.

Cells were imaged at 24 and 48 hours post transfection.

3.2.5.2 Electroporation of Primary Cells

Cells were cultured as previously described and concentrated using a BSA gradient. Immediately post BSA gradient, cells were counted using trypan blue staining. 1.2 x 10^6 cells were suspended in 300 µL SA-A buffer and electroporated using protocol : 2000V – 8 pulses – 60 µs. Cells were analysed at 24 hours post electroporation.

3.2.5.3 Nucleofection of Primary Cells

Nucleofection was carried out immediately before or immediately after the BSA gradient purification step on two separate batches of primary cells. Cells were resuspended in 100 µL SA-A buffer and 5 µg pEGFP. Protocol X-05 was used for nucleofection. Cells were then plated in 2 mL DMEM 10% FBS (no antibiotic). Cells were analysed at 24 hours post nucleofection.

3.2.6 Lentiviral Infection of Primary Murine Megakaryocytes

3.2.6.1 Lentivirus Constructs

Plasmids FUGW, CMVΔ8.9 and VSVg were used to construct lentiviruses. This was a second generation lentiviral system involving a packaging plasmid (CMVΔ8.9 with CMV promoter and Gag, Pol, Rev, and Tat genes), a transfer plasmid (FUGW, with long terminal repeat (LTR) sequence for genome integration, hUbC promoter and EGFP sequence) and an envelope plasmid (VSV-G, encoding Vesicular stomatitis virus G glycoprotein which allows wide infectivity). Plasmid maps are available as appendix figure 6.3. Actinin-1 GFP (WT, R461, L395Q, R752Q) and Lifeact mCherry constructs were cloned into FUGW. Biosafety approval was granted from the Environmental Protection Agency (EPA) for the generation and use of lentiviral particles to infect cells.

3.2.6.2 Optimisation of Transfection of HEK293FT Cells

The following protocols were assessed and applied to HEK293FT cells at approximately 70% confluency, in one well of a 6-well plate in 1.28 mL media. Cells were transfected with FUGW plasmid and GFP positivity was assessed 24 hours post transfection.

Figure 3.2.1

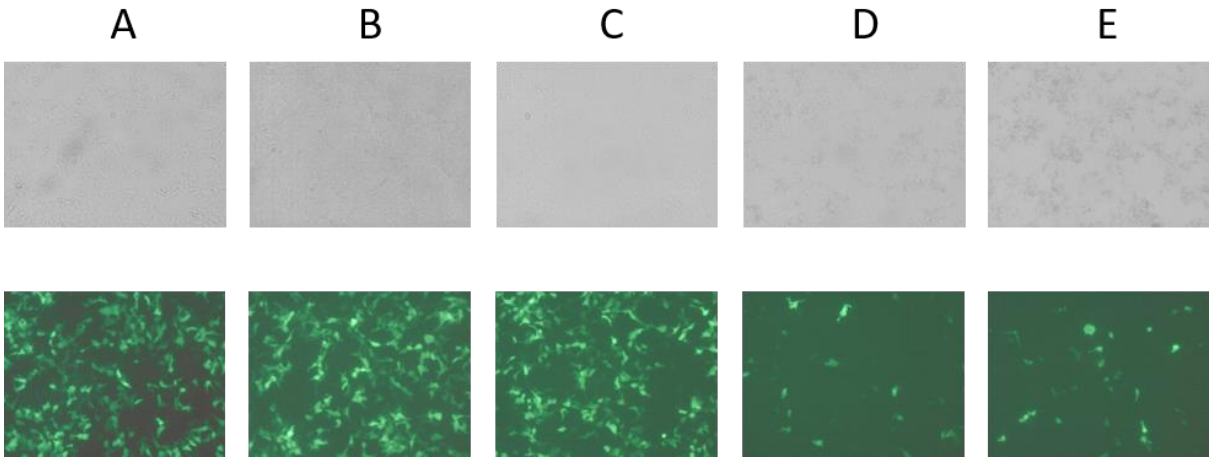

Figure 3.2.1 Results of transfection protocols trialled to optimiseHEK293FT cell transfection efficiency for virus production. *Top panels show brightfield images of the HEK293FT cells 24 hours post transfection. Bottom panels show GFP expression in transfected cells at 24 hours post transfection, in the same fields as brightfield images shown in corresponding top panels. The protocols trialled are shown:*

A. *2.3 µg DNA + 3.8 µL lipofectamine-2000 in 128 µL OptiMEM, media changed after 16 hours*
B. *2.3 µg DNA on 6 well + 2 µL lipofectamine-2000 in 128 µL OptiMEM, media changed after 16 hours*
C. *4.2 µg DNA on 6 well + 3.8 µL lipofectamine-2000 in 128 µL OptiMEM, media changed after 16 hours*
D. *2.3 ug DNA, 16.7 µL $CaCl_2$ in 128 µL H2O and 128 µL 2X HBSS, media changed after 16 hours*
E. *1.5 ug DNA 16.7 µL $CaCl_2$ in 128 µL H2O and 128 µL 2X HBSS, media changed after 16 hours*

3.2.6.3 Optimisation of lentiviral plasmid concentration ratios for virus production.

Trial 1 (Table 4.2.1) was carried out by transfecting HEK293FT cells using the calcium phosphate method with 9 µg total DNA on a T-75 dish. Media was changed after four hours and the virus was harvested at 48 hours post-transfection. Unconcentrated and undiluted virus-containing media was used to infect HEK293FT cells on a 24-well plate in 500 mL total media and 5 µg/mL polybrene (Sigma - TR-1003-G). Cells were split onto 6-well plates 24 hours post-infection. GFP positivity was assessed at 36-48 hours post-infection.

Table 3.2.1: Trial of varying lentiviral plasmid concentration ratios to optimise virus production.

Trial 1	**FUGW (µg)**	**Δ8.9 (µg)**	**VSVg (µg)**	**Total (µg)**	**Dish Used**
A	4	3	2	9	T-75
B	4	4	1	9	T75
C	4	2.5	2.5	9	T-75
Trial 2	**FUGW (µg)**	**Δ8.9 (µg)**	**VSVg (µg)**	**Total (µg)**	**Dish Used**
A	4.26	1.06	1.06	6.4	T-25
B	2.84	1.78	1.78	6.4	T-25

Figure 3.2.2

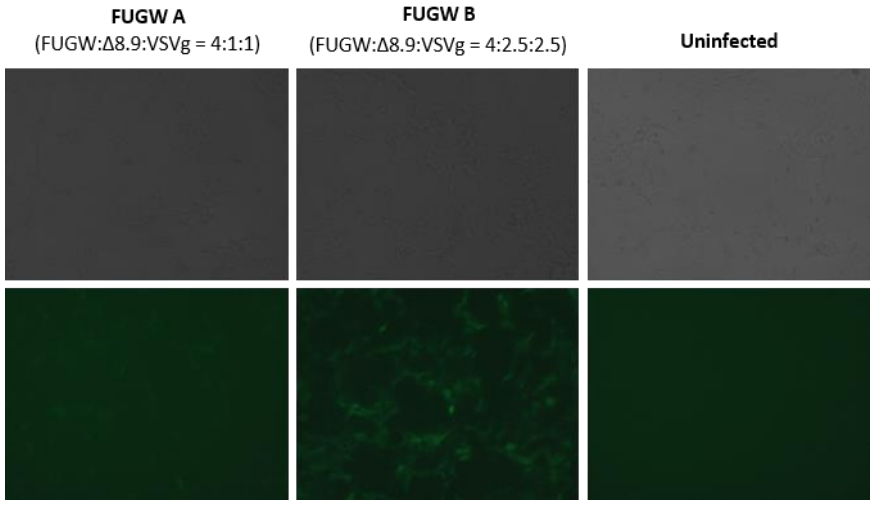

Figure 3.2.2 HEK293 cells infected with two batches of lentivirus, produced by alternate transfection methods. *Top panels show brightfield images of the HEK293FT cells 24 hours post transfection. Bottom panels show GFP expression in transfected cells at 24 hours post*

transfection, in the same fields as brightfield images shown in corresponding top panels. An uninfected control well with HEK293 cells is also shown for comparison.

As the lipofectamine-2000 transfection efficiency was higher, subsequent transfections were carried out using this method. The ratio of plasmids was optimised using the lipofectamine-2000 transfection protocol. 6.4 µg total DNA and 5.56 µL Lipofectamine-2000 in 356 µL OptiMEM were added to 3.56 mL media in a T-25 flask, containing HEK293FT cells at approximately 70% confluency. The ratios outlined in Trial 2 (Table 4.2.1) were assessed. Unconcentrated and undiluted virus-containing media was used to infect HEK293FT cells on a 24-well plate in 300 mL total media and 10 µg/mL Polybrene. Cells were split onto 6-well plates 24 hours post-infection. GFP positivity was assessed at 48-36 hours post-infection.

3.2.6.4 Optimisation of Lentivirus Production

Batch 1 : Calcium Phosphate Transfection

On 6 x T75 flasks, HEK293FT cells were grown to >70% confluency, by splitting 1:4 two days prior to transfection. Media was changed prior to transfection to DMEM 5% FBS (no antibiotics). 9 µg DNA per flask containing FUW : Δ8.9 : VSVg plasmids in the ratio 4:3:2 was added to 0.25 M $CaCl_2$ in 1 mL H_2O and then mixed with 1mL 2X HBSS. 2 mL of the DNA mix was added to 10 mL media per plate. 4 hours post-transfection, media was changed to DMEM, 5% FBS, 1% P/S. At 48 hours post-transfection, the flask media was replaced. Media that was harvested was stored at 4˚C until concentration. At 72 hours post transfection, media was harvested again and pooled with the stored media. The flasks were autoclaved and discarded after media was collected.

Batch 2: Lipofectamine-2000 Transfection

On 2 x T75 flasks, HEK293FT cells were grown to >70% confluency, by splitting 1:4 two days prior to transfection. Media was changed prior to transfection to DMEM 5% FBS (no antibiotics). 18 µg DNA per flask containing FUW : Δ8.9 : VSVg plasmids in the ratio 4:2.5:2.5 was added to 15 µL Lipofectamine-2000 in 1 mL OptiMEM. 1 mL of the DNA mix was added to 10 mL media per plate. 16 hours post-transfection, media was changed to DMEM, 5% FBS, 1% P/S. At 48 hours post-transfection, the flask media was replaced. Media that was harvested was stored at 4˚C until concentration. At 72 hours post transfection,

media was harvested again and pooled with the stored media. The flasks were autoclaved and discarded after media was collected.

3.2.6.5 Concentration of the Lentivirus

Lentivirus-containing media was spun at 200 x g for 5 minutes to pellet any cells in media. Supernatant was then filtered through 0.45 µm filters (Sarstedt – 83.1826) to remove any final contaminating cells. The virus was then concentrated using a sterilised Vivaspin-20 100 kDa (Sartorius) by spinning cells at 4200 RPM, discarding flow through and re-filling the concentrator until the desired volume was reached. For Batch 1, 132 mL media was concentrated to 13 x 100 µL aliquots (100X). For Batch 2, 48 mL media was concentrated to 5 x 100 µL aliquots (100 X). Concentrated virus aliquots were stored at -80℃ until use.

3.2.6.6 Assessment of Lentiviruses by Infection of HEK293FT cells

Infections were carried out using concentrated or unconcentrated virus as detailed in Table 4.2.1. Cells were 50-70% confluent at the time of infection and were split 24 hours post-infection onto 6-well plates (for trials 2-4). For trial 1, media was changed after 24 hours but cells were not split. HEK293FT cells were grown in DMEM 5% FBS 1% P/S for the infection protocol. GFP positivity was assessed at 48-36 hours post-infection.

Table 3.2.2: Trial of various infection protocols to infect HEK293FT cells

Protocol	Plate	Media Volume	Polybrene Concentration	Virus Used	Virus Concentrations
1	6-well	1 mL	2.5 µg/mL	Batch 1 FUGW & WT Actinin-1 GFP	2X – 1:20
2	24-well	0.5 mL	5 µg/mL	Batch 1 Lifeact mCherry & R46Q Actinin-1 GFP	33X – 1:65
3	24-well	0.25 mL	5 µg/mL	Batch 1 R752Q Actinin-1 GFP & L395Q Actinin-1 GFP	100X – 1X
4	24-well	0.3 mL	5 µg/mL	Batch 2 FUGW	1X

Figure 3.2.3

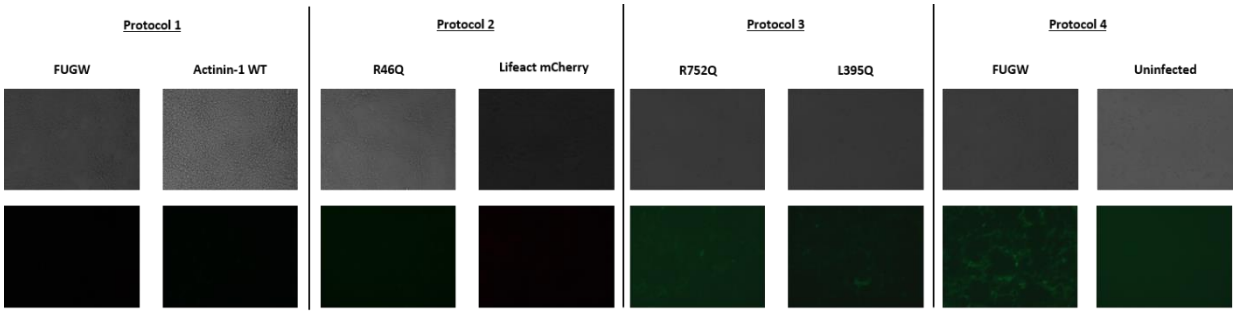

Figure 3.2.3 The results of infections of HEK293FT cells by lentiviruses using varying infection protocols are shown. *Top panels show brightfield images of the HEK293FT cells 24 hours post transfection. Bottom panels show GFP expression in transfected cells at 24 hours post transfection, in the same fields as brightfield images shown in corresponding top panels. Protocols 1-4 for lentivirus infection are detailed in Table 4.2.2.*

3.2.7 Infection of Primary Murine Megakaryocytes

Cells were grown in filter-sterilised DMEM, 10% FBS, 1% P/S. TPO (70 ng/µL) was used to differentiate cells on days 0-4 post-harvesting. Five experimental runs were performed as described below. Batch 2 viruses at 100X concentration were used for the runs 1-4 and freshly produced viruses (produced and concentrated using the same protocol as Batch 2) were used for runs 5-6. All viruses for runs 1-4 had been stored at -80℃ and were thawed at4℃ immediately prior to use. Polybrene concentration was constant at 8 µg/mL.

Run 1: Cells were harvested from 1 pregnant mouse as previously described. Cells were plated on 3 wells of a 24-well plate in 500 µL media with 70 ng/µL TPO. Cells were incubated for 24 hours prior to infection. Suspension cells were then removed, pelleted, and resuspended in 0.25 mL media with 90 µL, 10 µL or 0 µL of 100X virus. Viral suspensions were added to 0.25 mL media containing 2X TPO and 2X Polybrene and plated onto the adherent cells. The cells were incubated until day 4 and the BSA gradient was carried out as described. Cells were then plated onto Fibronectin (100 µg/mL) coated wells of a 24-well plate. Cells were imaged 24 hours after plating.

Run 2: Cells were harvested from 1 pregnant mouse as previously described. Cells were plated on 2 wells of a 12-well plate in 0.25 mL media with 2X TPO and 2X Polybrene. 0.25 mL media with 100 µL or 0 µL of 100X virus and added to the wells. 24 hours post infection, cells were washed from the wells, pelleted, and resuspended in media with TPO. The cells were incubated until day 4 and the BSA gradient was carried out as described. Cells were then plated onto Fibronectin (100 µg/mL) coated glass coverslips of a 24-well plate. 24 hours after plating, the coverslips were washed, fixed, blocked and stained as previously described Phalloidin Rhodamine, DAPI and GFP Booster. Coverslips were mounted onto glass slides and sealed.

Run 3: Cells were harvested from 1 pregnant mouse as previously described. Cells were plated on 1 well of a 12-well plate in 0.25 mL media with 2X TPO and 2X Polybrene. 0.25 mL media with 100 µL of 100X virus and added to the wells. 24 hours post infection, suspension cells were removed, pelleted, and resuspended in media with TPO and returned to a new well of the 24-well plate in 1 mL media. The adherent cells were undisturbed and media was replaced with 1 mL media with TPO. The cells were incubated until day 4 and the BSA gradient was carried out as described. Cells were then plated onto Fibronectin (100 µg/mL) coated glass coverslips of a 24-well plate. 24 hours after plating, the coverslips were

washed, fixed, blocked and stained as previously described Phalloidin Rhodamine, DAPI and GFP Booster. Coverslips were mounted onto glass slides and sealed.

Run 4: Cells were harvested from 2 pregnant mice as previously described. Cells were plated on 3 wells of a 12-well plate in 0.25 mL media with 2X TPO and 2X Polybrene. 0.25 mL media with 0 µL virus or 100 µL of 100X virus (FUGW and Actinin-1 WT GFP) and added to the wells. 24 hours post infection, suspension cells were removed, pelleted, and resuspended in media with TPO and returned to a new well of the 24-well plate in 1 mL media. The adherent cells were undisturbed and media was replaced with 1 mL media with TPO. The cells were incubated until day 4 and the BSA gradient was carried out as described. Cells were then plated onto Fibronectin (100 µg/mL) coated glass coverslips of a 24-well plate. 24 hours after plating, the coverslips were washed, fixed, blocked and stained as previously described Phalloidin Rhodamine, DAPI. Coverslips were mounted onto glass slides and sealed.

Run 5: Cells were harvested from one pregnant mouse as previously described. Cells were plated on 2 wells of a 24-well plate in 0.120 mL media with 2X TPO and 2X Polybrene. 120 µL of 100X virus (Lifeact mCherry or Actinin-1 WT GFP) was added to the wells. 24 hours post infection, suspension cells were removed, pelleted, and resuspended in media with TPO and returned to a new well of the 6-well plate in 2 mL media. The adherent cells were undisturbed and media was replaced with 0.5 mL media with TPO. The cells were incubated until day 4 and the BSA gradient was carried out as described. Cells were then plated onto Fibronectin (100 µg/mL) coated glass coverslips of a 24-well plate. 24 hours after plating, the coverslips were washed, fixed, blocked and stained as previously described Phalloidin Rhodamine, DAPI. Coverslips were mounted onto glass slides and sealed.

Run 6: Cells were harvested from one pregnant mouse as previously described. Cells were plated on 2 wells of a 24-well plate in 0.100 mL media with 2X TPO and 2X Polybrene. 100 µL of 100X virus (Actinin-1 L395Q-GFP or Actinin-1 R46Q-GFP) was added to the wells. 24 hours post infection, suspension cells were removed, pelleted, and resuspended in 0.1 mL media with 2X TPO and 2X Polybrene, and then replated on new wells of the 24-well plate. 0.1 mL of 100X virus was added to each well to reinfect cells. 24 hours post infection 2, suspension cells were removed, pelleted, and resuspended in 2 mL media with 1X TPO each and returned to new wells of a 6-well plate. When removing cells from the 24-well plate after each infection, the adherent cells were undisturbed and media was replaced with 0.5 mL media with TPO. The cells were incubated until day 4 and the BSA gradient was carried

out as described. Cells were then plated onto Fibronectin (100 µg/mL) coated glass coverslips in a 24-well plate. 24 hours after plating, the coverslips were washed, fixed, blocked and stained as previously described Phalloidin Rhodamine, DAPI. Coverslips were mounted onto glass slides and sealed.

Table 3.2.3: Summary of Infection Protocols Trialled For Primary Megakaryocyte Infection

Run	Plate	No. of wells	Total Volume per well	Virus Volume Used	Virus Storage	Note
1	24-well	3	500 µL	90 µL, 10 µL or 0 µL of 100X virus	Frozen	Infection carried out on Day 1
2	12-well	2	500 µL	100 µL or 0 µL of 100X virus	Frozen	
3	12-well	1	500 µL	100 µL of 100X virus	Frozen	
4	12-well	3	500 µL	100 µL or 0 µL of 100X virus	Frozen	2 mice used
5	24-well	2	120 µL	100 µL of 100X virus	Fresh	
6	24-well	2	100 µL	100 µL of 100X virus	Fresh	Cells infected twice (day 0 and day 1)

3.2.8 Analysis of Actinin-1 and Actinin-4 in Platelets and Megakaryocytic Cell lines.

3.2.8.1 Protein Expression and Purification

BL21 cells expressing the plasmid of interest were grown in a 50 mL overnight culture of cells and diluted the following day to 100 mL in LB with the appropriate antibiotic. After 1 hour incubation at 37℃, protein expression was induced by the addition of 0.5% Arabinose for pBAD expressing cells and 0.2 mM IPTG for pRSF expressing cells. Cells were incubated for 4 hours at 37℃ after induction. Cells were pelleted at 4500 RPM for 20 minutes and the

supernatant was discarded. The cells were lysed in buffer (PBS 0.2% Triton, 20 mM β-mercaptoethanol, 1 Mm PMSF) with lysozyme and DNAse for 25 minutes on ice. The cells were then sonicated for 3 x 30 seconds with incubation on ice between runs. The lysate was then collected by centrifuging samples at 12,000 x g for 20 minutes at 4˚C. His-tagged actinin-1 was purified using the Nickel Column as described in section 3.2.9.2. MBP-tagged actinin-4 was purified using the amylose column as described in section 3.2.9.3. Eluted proteins were then dialysed for 3 overnight incubations at 4˚C with 300 µL TEV protease (homemade), added as 3 x 100 µL aliquots every 24 hours. Dialysis was carried out in dialysis buffer (20 mM Tris-HCl pH 7.5, 100 mM NaCl, 5 mM βME). The proteins were then purified by the nickel column (actinin-1) or by amylose column (actinin-4). The flow-through from these columns were then purified by FPLC on the Superdex 200 column in running buffer (20 mM HEPES, 100 mM NaCl, 0.5 mM DTT). Purified elutions were concentrated to 200 µL using the 10K Amicon filter and frozen in liquid nitrogen before storing at - 80˚C in 10 µL aliquots. The relative concentration of the samples was confirmed by analysing the samples on an SDS-PAGE gel and Coomassie staining.

3.2.8.2 Quantification of Actinin-1 and Actinin-4 by Western Blot

HEK293 cell were transfected with pEGFP-Actinin-1-or pEGFP-Actinin-4 plasmids using the calcium phosphate method of transfection. Media was changed to antibiotic-free media and incubated at 37˚C for 1 hour prior to transfection. To transfect 1 well, a solution of 1-2 µg plasmid DNA and 250 mM $CaCl_2$ in 150 µL sterile dH2O was first prepared. A second 150 µL solution of 2X pH 7.2 HEPES Buffered Saline (HBS) (274 mM NaCl, 2.8 mM Na2PO4, 54.5 mM HEPES) was prepared. The DNA / $CaCl_2$ solution was added to the HBS solution in a dropwise manner and allowed to stand for 1 - 2 minutes. The solution was then added to the well and the cells were incubated for 48 hours at 37˚C before lysing. 10^6 untransfected MEG-01 and CMK cells were also lysed. Cells were lysed in RIPA buffer (150 mM NaCl, 1% NP40, 0.5% deoxycholate, 0.1% SDS, 50 mM Tris-Cl pH 8.0, 1 protease inhibitor cocktail tablet per 10mL (Roche)) when analysing antibody specificity. To analyse relative actinin-1 and actinin-4 concentrations in human platelets, CMK, MEG-01 and THP-1 cells, cells were lysed in lysis buffer (20 mM Tris, pH 7.4, 150 mM NaCl, 10 mM EDTA, 1% Triton X-100, protease inhibitor (Roche)). Cells were lysed for 30 minutes at 4˚C and the suspension was centrifuged at 12,000 x g for 10 minutes at 4˚C. Supernatants were mixed with SDS gel loading buffer (50 mM Tris pH 6.8, 5% β-ME, 2% SDS, 0.1% Bromophenol Blue, 10% Glycerol) and boiled for 10 minutes before running on an 8% SDS-PAGE gel. The gel was

then transferred to PVDF membrane at 100V for 60 minutes and blocked in 4% Milk/TBST for 1 hour at room temperature. The blot was probed with anti-actinin-1 (Santacruz H2) at 1:500 dilution or anti-actinin-4 (Immunoglobe) at 1:1000 dilution. Secondary antibodies (anti-mouse IR700 and anti-rabbit IR800) were used at 1:10,000 dilution. Densitometry analysis was performed using Odyssey Image Studio Software (LI-COR Biosciences, Cambridge, UK).

Actinin-1 and actinin-4 protein controls were also prepared by expression of pBAD-Actinin-4 (MBP) or pRSF-Actinin-1 (His) plasmids in BL21 cells and purification, as described in section 3.2.8.1.

3.2.8.3 Pull-down of Actinin-1 and Actinin-4 from CMK cells

5 x 10^6 CMK cells were used for each sample. Cells were washed twice with PBS and pelleted at 250 x g for 5 minutes. Cell pellets were resuspended in 100 µL PBS and 100 µL 2X lysis buffer (15 mM HEPES pH 8, 150 mM NaCl, 2% Triton X-100, 10 mM EGTA, 1 mM Na_3VO_4, protease inhibitor (Roche)) was added. Cells were incubated on ice for 30 minutes and pipetted periodically. Lysates were centrifuged at 13,000 x g for 4 minutes at 4˚C. A 10 µL sample of lysate was removed for analysis. The remaining lysate was incubated with rotation for 1 hour at 4˚C with 20 µL Protein A/G (Thermo Fisher Scientific – 11511931) beads alone to clear non-specific binding. 100 µL of the lysate was used for the pull-down experiment and 0.5µL of antibody was added. 100 µL of the lysate was used as a negative control and no antibody was added. Samples were incubated with rotation overnight at 4˚ C. After 16-24 hours incubation, 40 µL Protein A/G beads was added to the samples. Samples were incubated with rotation for 1.5 hours at 4˚C. Beads were then pelleted and washed three times in 500 µL lysis buffer. 25 µL 2X SDS-GLB was added to the pelleted beads after washing and the beads were boiled for 7 minutes. The beads were pelleted and the eluted proteins were removed for analysis.

3.2.8.4 Immunofluorescent Imaging of Actinin-1 and Actinin-4

Assessment of specificity of actinin antibodies for Immunofluorescent staining

HEK293 cells were grown on poly-D lysine (0.1 mg/mL) (Sigma) coated coverslips. HEK293 cell were transfected with Actinin-1-pEGFP or Actinin-4-pEGFP plasmids using the calcium

phosphate method of transfection as described. 48 hours post-transfection, cells were washed with PBS and fixed in 4% PFA/PBS for 10 minutes at room temperature. Cells were blocked in blocking buffer (5% NGS, 2% BSA, 0.2% Triton, PBS) for 30 minutes at room temperature. Cells were stained with primary antibodies as outlined in Table 4.2.4, diluted in buffer (5% NGS, 2% BSA, PBS). Coverslips were washed and mounted onto glass slides for analysis. Cells were imaged using a Leica DM6000 upright fluorescence microscope.

Table 3.2.4: Details of actinin antibodies used for immunofluorescent staining of HEK293 cells

Antibody	**Source / Clone**	**Species**	**Dilution**
Anti-actinin-1	Santacruz-H2	Mouse IgG	1:250
Anti-actinin-1/4	Sigma BM 75.2	Mouse IgM	1:500
Anti-actinin-4	Honda	Rabbit	1:400
Anti-actinin-4	Immunoglobe 3	Rabbit	1:250
Anti-actinin-1/2/3/4	Santacruz-H300	Rabbit	1:250

3.2.8.5 Assessment of Ploidy in Actinin-1 Transfected MEG-01 Cells

MEG-01 cells were treated with PMA for 12 days, as described in section 3.2.1. Cells were distributed into poly-d-lysine coated (0.1 mg/mL) glass bottom dishes in 1 mL media with 0.5 x 10^6 cells per dish. Cells were then transfected on day 10 using 1 µg Actinin-GFP and 1 µL Lipofectamine-2000 in 100 µL OptiMEM as described in section 3.2.4.5. 48 hours post-transfection, supernatant and non-adherent cells were removed and the cells were washed with PBS. Cells were fixed with 1% PFA/PBS for 10 minutes. Cells were blocked in blocking buffer (5% NGS, 2% BSA, 0.2% Triton, PBS) for 30 minutes at room temperature. Cells were then stained with rhodamine-labelled phalloidin (1:3000) and DAPI (1:10,000) for 1 hour at room temperature, washed and then mounted with fluoromount onto glass slides by pushing out the glass bottom from the dish. Ploidy was assessed in these cells by visualising the slide from the top left in a zig-zig format across the slide. The transfected cells were assessed in each field until 100 cells were counted on the slide or all transfected cells were assessed where <100 transfected cells were seen on the slide. Imaging was carried out using the Leica DMI 3000 microscope.

The assessment of ploidy in PMA treated cells by flow cytometry was initially trialled with propidium iodide staining of untransfected cells. Cells were treated with 10^{-7} M PMA for 0-6 days. Cells were then harvested, washed in PBS, and fixed in 70% ethanol for 2 hours at 4℃. Cells were then washed in PBS and stained with propidium iodide (Propidium Iodide (Biolegend) 0.02 mg/mL, Triton X 0.1%, RNAse A 0.2 mg/mL) for 15 minutes at 37℃. Propidium iodide positivity was quantified using the FL-2 channel of the Accuri C6 (BD).

Ploidy of MEG-01 cells was also assessed by flow cytometry with staining of nuclear material with DRAQ5 (Biostatus – DR50200). Cells were treated with PMA for 12 days , as described in section 3.2.1 Cells were then transfected on day 10 using 1 µg Actinin-pEGFP as described in section 3.2.4.5. 48 hours post-transfection, supernatant and cells were removed and the cells were washed with PBS. Cells were stained with 1 µL DRAQ5 in 500 µL of cells in PBS. Cells were then incubated for 20 minutes at room temperature. Cells were assessed using an Accuri C6 flow cytometer (BD). GFP positivity was assessed using the FL-1 channel, with untransfected cells used to establish the negative gate. Ploidy was assessed by DRAQ5 staining, detected in the FL-3 channel of the Accuri C6 (BD).

3.2.9 Analysis of Actinin-1 and Actinin-4 Heterodimers

3.2.9.1 Expression & Purification of Actinin-1 and Actinin-4 proteins

BL21 cells were transformed with the following plasmids:

- pBAD-Actinin-4 (MBP)
- pRSF-Actinin-1 (His)
- pRSF-Actinin-1 & pBad-Actinin-4 (MBP & His)

Protein was expressed as described in section 3.2.8.1. After 1 hour incubation at 37℃, protein expression was induced by the addition of 0.5% Arabinose for pBAD expressing cells and 0.2 mM IPTG for pRSF expressing cells. For cells expressing both plasmids, equal expression of actinin-1 and actinin-4 was achieved by trialling varying concentrations of arabinose (0.0001%, 0.0002%, 0.001%, 0.01%, 0.05%, 0.1%, 0.2% and 0.5%) and IPTG concentration (0.2 mM and 1 mM). Cells were incubated for 4 hours at 37℃ after induction. Induction was also trialled at 20℃ for 7 hours or overnight.

His-tagged actinin-1 was purified using the Nickel Column as described in section 3.2.9,2. MBP-tagged actinin-4 was purified using the amylose column as described in section 3.2.9.3. The lysate containing co-expressed His-tagged actinin-1 and MBP-tagged actinin-4 was first purified using the nickel column, then dialysed overnight in 1 L amylose column wash buffer at 4℃. The dialysed elution was then purified using the amylose column. When purifying using the amylose column, the first flow through was re-loaded onto the column to maximise binding of the protein. Washes and elutions were collected and analysed. Elutions were concentrated using a centrifugal filter (Amicon Ultra-4 10K).

3.2.9.2 Nickel Column Purification

A gravity flow column containing 2 ml of Nickel-NTA agarose (Merck-Millipore 70666) was equilibrated with wash solution (0.5M NaCl, 50 mM KPO4 pH 8, 20 mM β-mercaptoethanol, 5 mM imidazole pH 7, 0.1% Triton). The lysate was added to the column and the flow through was collected for analysis. The column was washed using 40 mL wash solution. The bound protein was eluted using elution solution B (20mM imidazole pH 7, 20mM β-mercaptoethanol) or solution C (200mM imidazole pH 7, 20mM β-mercaptoethanol).

3.2.9.3 Amylose Column Purification

The amylose resin (New England Biolabs) was equilibrated with wash solution (20 mM Tris-HCl pH 7.5, 150 mM NaCl, 1 mM DTT). The lysate was added to the column and the flow through was collected for analysis. The column was washed using 40 mL wash solution. The bound protein was eluted in elution buffer (10 mM Maltose, 20 mM Tris-HCl pH 7.5, 150 mM NaCl, 1 mM DTT).

3.2.9.4 Analysis of Heterodimers expressed in BL21 E. *coli* by Native PAGE

Purified MBP or Ni tagged actinin proteins were analysed on a native PAGE gel. Elutions from the amylose or nickel columns (described in sections 3.2.3.2 and 3.2.9.3) were analysed on a 5% native PAGE gel, run at 80V for 4.5 hours. For native PAGE, acrylamide gel and running buffer were prepared without SDS and gel loading buffer was prepared without beta mercaptoethanol. The gel was stained with Coomassie stain and destained overnight. Native gels were also analysed by western blotting, by transferring to PVDF

membrane, blocking in 4% Milk/TBST and probing with anti-actinin antibodies (anti-actinin 1 Santacruz H2, anti-actinin-4 Immunoglobe).

3.2.9.5 Expression of Actinin-2 Rod Heterodimers in HEK293 Cells

The following plasmids were transfected in HEK293 cells using the calcium phosphate method.

- pBud-Actinin-2 Rod – double mCherry (EFI multiple cloning site (MCS))
- pBud-Actinin-2 Rod – GFP (EFI MCS)
- pBud-Actinin-2 Rod – double mCherry (EFI MCS) -Actinin-2 Rod – GFP (CMV MCS)

Cells were grown on a 10 cm dish to approximately 50% confluency prior to transfection. 6 µg DNA and 250 mM $CaCl_2$ were mixed with 2X HBSS to create a 1 mL solution. This was incubated at room temperature for 1 minute and added to cells in 11 mL of media on one 10 cm dish per construct. The media was changed after 6 hours to antibiotic-containing media. Cells were lysed 24 hours post transfection in 167 µL TAPTag buffer (150 mM NaCl, 50 mM Tris-HCl pH 7.5, 1% NP-40, 10% Glycerol, protease inhibitor (Roche) on ice for 30 minutes. Samples were them spun at 10,000 RPM for 10 minutes at 4℃.

Three samples were set up for heating and cooling experiments:

- 10 µL GFP sample + 10 µL TAPTag buffer
- 10 µL mCherry sample + 10 µL TAPTag buffer
- 10 µL mCherry sample + 10 µL GFP Sample.

For all conditions assessed, samples were analysed in duplicate. The following conditions were trialled:

- 4℃ for 1 hour
- 37℃ for 1 hour
- 42℃ for 1 hour
- 45℃ for 1 hour
- 55℃ for 1 hour
- 4℃ for 10 minutes, 30 minutes, 1 hour, 2 hours or 4 hours.
- 37℃ for 10 minutes, 30 minutes, 1 hour, 2 hours or 4 hours.

Samples were assessed for heterodimer formation by analysing on an 8% Native-PAGE gel at 120V for 80 minutes. An alternative lysis protocol without detergent was also trialled using Tris Buffer (10 mM Tris Ph 7.5, 100 mM NaCl, 0.1 mM DTT, protease inhibitor (Roche)). Physical lysis methods were used in tandem to the Tris buffer, with lysis by repeated needle aspiration and injection and sonication trialled. To assess the impact of detergent on the formation of heterodimers, 1% NP-40 was added to samples of the detergent-free lysates for comparison.

3.3 Results

3.3.1 Transfection of MEG-01 and CMK cells

As discussed, MEG-01 and CMK cells are megakaryocytic cell lines which have been used previously to assess megakaryocytic differentiation, proplatelet production and platelet-like particle release (Komatsu et al., 1989; Takeuchi et al., 1998). In order to assess the role of actinin-1 and CMTP-causing mutations in actinin-1, I aimed to express fluorescently tagged actinin-1 and mutated actinin-1 in these cells. A range of protocols were trialled to optimise this.

Three different transfection protocols (Calcium Phosphate, Lipofectamine-2000, Trans-IT) were trialled initially to transfect MEG-01 and CMK cells. No transfected cells were observed following the calcium phosphate protocol. The Lipofectamine-2000 and Trans-IT transfection reagents showed similar efficacy, but this was relatively poor as approximately 5% of cells were transfected. Alternative methods to deliver DNA to the cells were then considered and electroporation and nucleofection were tried next.

The suitability of various electroporation buffers was first assessed by quantifying by flow cytometry the uptake of propidium iodide into MEG-01 cells during electroporation using the BTX Square Wave Electroporation System. Table 3.3.1 and Figure 3.3.1 shows the % cells in mid and high fluorescent regions, as quantified by flow cytometry. This indicates live cells containing PI (mid fluorescence) and dead cells (high fluorescence) (Ruzgys et al., 2019). The efficiency of each buffer was assessed by the equation (% positive cells x % viable cells / 100). As we favoured a protocol that did not impact viability substantially, the SA-A buffer was used in subsequent protocols.

Electroporation parameters were next optimised with the settings trialled outlined in Table 4.3.2. A protocol of 2000V, 8 pulses, 60 µs pulse length was found to be the most efficient and resulted in GFP expression in 12% MEG-01 cells and 54% viability at 24 hours post electroporation.

Nucleofection using the Amaxa Nucleofector II was then optimised by trialling delivery of pEGFP to MEG-01 cells in various buffers and using various settings, outlined in Table 4.3.3. The X-05 protocol was the most efficient, with similar efficacy in HEPES buffer and RPMI.

Efficiency using nucleofection was lower than that achieved with electroporation. However, the highest % GFP positivity achieved was using nucleofection. Nucleofection and Lipofectamine-2000 were also trialled using CMK cells. It was found that nucleofection protocol T-01 was the most efficient for these cells, with the results of protocols assessed reported in Table 4.3.4.

Figure 3.3.1

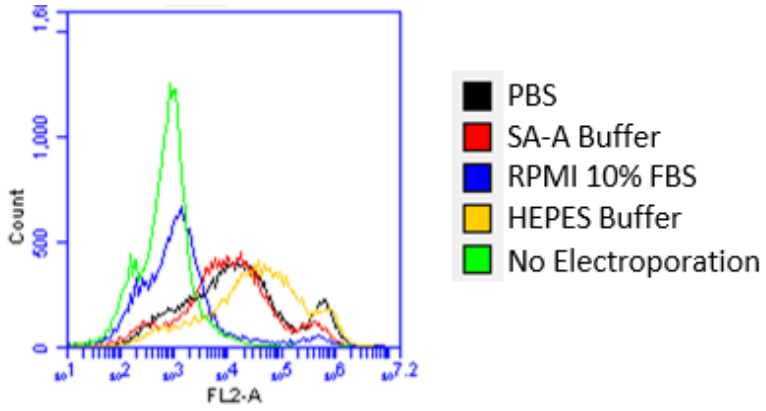

Figure 3.3.1 Optimisation of Electroporation Buffer: *MEG-01 cells were electroporated in buffer containing Propidium Iodide (PI) and analysed by flow cytometry for fluorescence intensity in the FL-2 channel of the Accuri C6 Flow Cytometer (BD). Post-electroporation cells in various buffers are indicated in black, red, blue, and yellow colours. A non-electroporated cell sample is shown in green. Three peaks indicate PI-=negative cells (dim fluorescence), PI-positive live cells (mid fluorescence) and non-viable cells (high fluorescence). Results are quantified in Table 4.3.1.*

Table 3.3.1: Trial of Various Electroporation Buffers

Buffer	% mid fluorescence (PI Positive Cells)	% high fluorescence (Dead Cells)	Efficiency (Mid x (100-High) / 100)
PBS - No electroporation	0.49	0.01	0
PBS	27.99	14.20	24.01
SA-A	27.16	8.20	24.93
RPMI 10% FBS	3.12	3.37	3.01
HEPES Buffer	43.90	18.50	35.78

Table 3.3.2: Trial of Electroporation Protocols using MEG-01Cells

Voltage (V)	Pulses	Pulse Length (µs)	% Viability	% Positivity	Efficiency
1000	8	20	99	1.8	1.78
500	8	100	99	0.7	0.69
2000	8	60	54	12.8	6.91
2000	8	40	43	8.3	3.57

Table 3.3.3: Trial of Nucleofection Protocols using MEG-01 Cells

Programme	Buffer	% Viability	% Positivity	Efficiency
T-01	SA-A	100	2.05	2.05
T-01	HEPES	68	2.74	1.8632
T-01	RPMI	44	4.67	2.0548
X-05	SA-A	30	8.86	2.658
X-05	HEPES	22	13.13	2.8886
X-05	RPMI	16	16.56	2.6496

Table 3.3.4: Trial of Lipofectamine-2000 Transfection and Nucleofection of CMK Cells

Method		Positivity (Estimated % cells expressing GFP)	% Viability	Efficiency
i	Lipofectamine-2000	<5	100	<5
ii	Nucleofection (T-01)	35	60	21
iii	Nucleofection (X-05)	30	25	7.5

3.3.2 CMTP Mutations Do Not Affect MEG-01 Cell Ploidy

To assess the impact of CMTP-causing mutations in actinin-1, a suitable cell model of platelet production which could be transfected was sought. MEG-01 cells were first assessed. To assess the potential for platelet like-particle production by megakaryocytic cell lines, MEG-01 cells were differentiated with PMA. After 6 days of PMA treatment, an

increase in ploidy was noted in cells when stained with propidium iodide and analysed by flow cytometry (Figure 3.3.2.1 A & B). Additionally, average cell size, assessed by forward scatter, increased with PMA treatment (Figure 3.3.2.1 C). It was then assessed whether platelet-like particles were produced by the differentiated cells. β-tubulin staining of the differentiated cells did not show any platelet-sized (~2μm) cells with a distinctive tubulin-ring at the cell periphery (Figure 3.3.2.1 Di). Washed platelets from a healthy adult donor were analysed by the same staining protocol, confirming the presence of cells with tubulin ring staining (Figure 3.3.2.1 Dii). Although transfection efficiency was improved to allow microscopic analysis of actinin-GFP expressing cells, transfected cells did not produce proplatelets. The analysis of actinin-GFP transfected cells over 12 days of PMA treatment did not reveal the production of proplatelets. Although some process-like structures were imaged, the characteristic long processes with platelet-sized tips at the end of the processes were not seen in the differentiated cells (Figure 3.3.2.1 E). Hence, PMA differentiated MEG-01 cells increased in ploidy but transfected cells did not produce proplatelets or platelet-like particles using the protocols assessed.

Figure 3.3.2.1

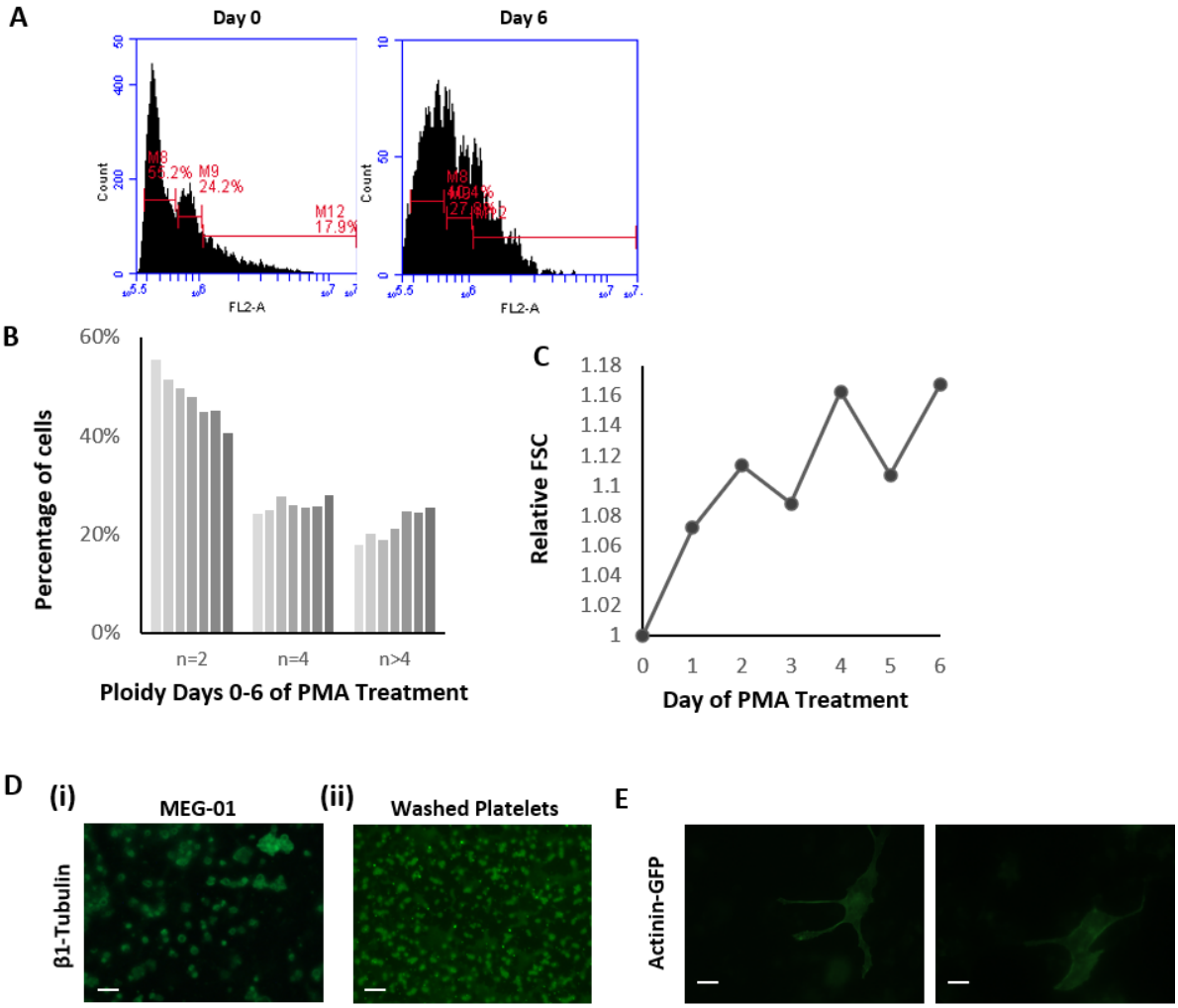

Figure 3.3.2.1 Optimisation of Electroporation Buffer: *(A) MEG-01 cells pre and post 6 days of treatment with 10^{-7} M PMA were stained with propidium iodide. Cell ploidy was assessed by a shift in fluorescence on FL-2 channel of Accuri C6 Flow Cytometer (BD). Peaks denote 2n, 4n and >4n. The percentage of cells in each peak are shown in (B). (C) The mean FSC of cells assessed over 6 days of PMA treatment was compared relative to cells at Day 0 of PMA treatment. (D) β-Tubulin staining of (i) PMA differentiated MEG-01 cells and (ii) washed human platelets on Poly-D-Lysine coated coverslips. (E) MEG-01 cells expressing actinin-1 GFP cells were imaged after 12 days of PMA treatment. Cells were transfected with pEGFP-actinin-1 48 hours prior to imaging .625 ng/mL PMA was used for days 0-3 of incubation. Concentration of PMA was then increased to 10 ng/mL and cells were treated for 12 days, as described previously (Zou et al., 2017). Scale bars = 20 µm.*

These cells were therefore a suitable model to assess the impact of actinin-1 mutations on cell ploidy. MEG-01 cells differentiated with PMA over 12 days and transfected on day 10. Ploidy was assessed microscopically and by flow cytometry. Microscopic analysis involved the assessment of the initial 100 transfected cells per coverslip and classification of the cells are 2n, 4n or ≥8n (Figure 3.3.2.2 A). Flow cytometric analysis of ploidy by DRAQ 5 staining was also verified before analysis by assessment of ploidy increase over 12 days of PMA treatment (Figure 3.3.2.2 B). The analysis of ploidy by microscopy and flow cytometry did not show any difference between WT and mutant actinin-1 expressing cells (Figure 3.3.2.2 C). Microscopic analysis did not show any significant difference between WT and mutant actinin expressing cells in terms of ploidy >2n ($p=0.347$) or >4n ($p=0.118$). Ploidy was also assessed by flow cytometry in terms of the percentage of cells with a ploidy of >2n or >4n and normalised to the results of the WT actinin-1 transfected cells in the same run. This analysis showed no significant difference in terms of the percentage of cells >2n ($p=0.423$) and >4n ($p=0.603$). As it is known that actinin-1 over-expression causes a cytokinesis failure (Mukhina et al., 2007) and increase in cell ploidy, variation between wells was controlled for by comparison of the change ploidy between transfected cells and untransfected cells. There was an increase in ploidy present for all cells transfected with actinin-1 (Figure 3.3.2.2 C (i)). The percentage increase in ploidy between untransfected and transfected cells was normalised to the result of the WT actinin-1 transfected cells from the same run. The increase in the percentage of cells >2n was not significantly different between WT and mutants ($p=0.989$) the increase in the percentage of cells >4n was also not significantly different ($p=0.897$). Comparison was carried out by one-way ANOVA.

Figure 3.3.2.2

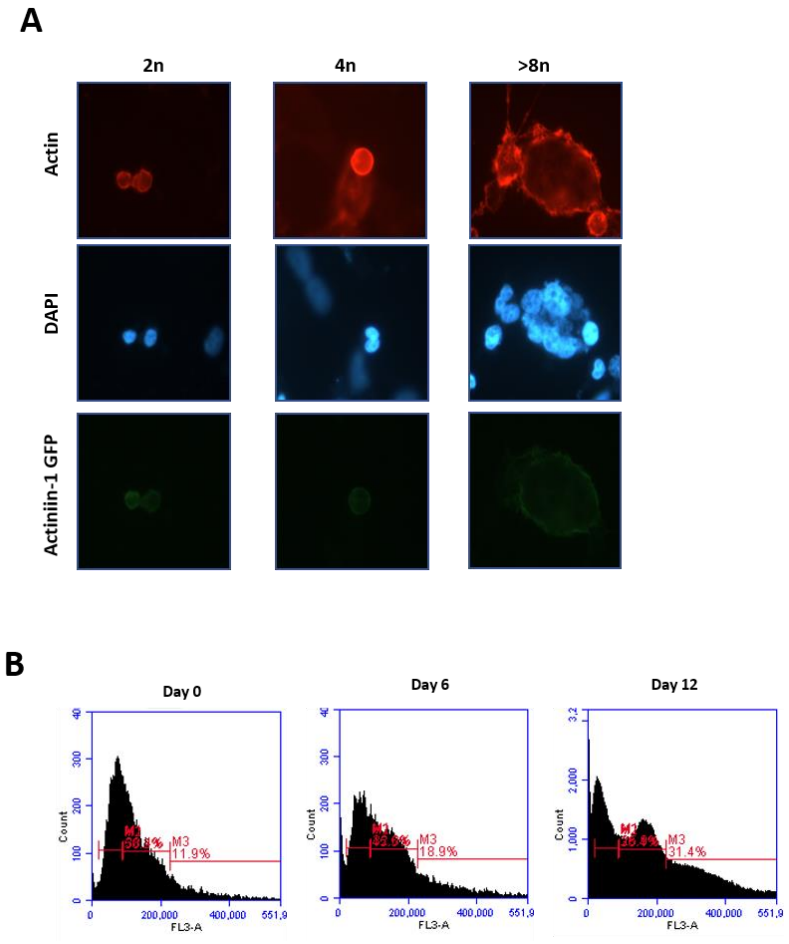
A
2n
4n
>8n
Actin
DAPI
Actiniin-1 GFP
B
Day 0
Day 6
Day 12
Count
FL3-A
M3
11.9%
18.9%
31.4%

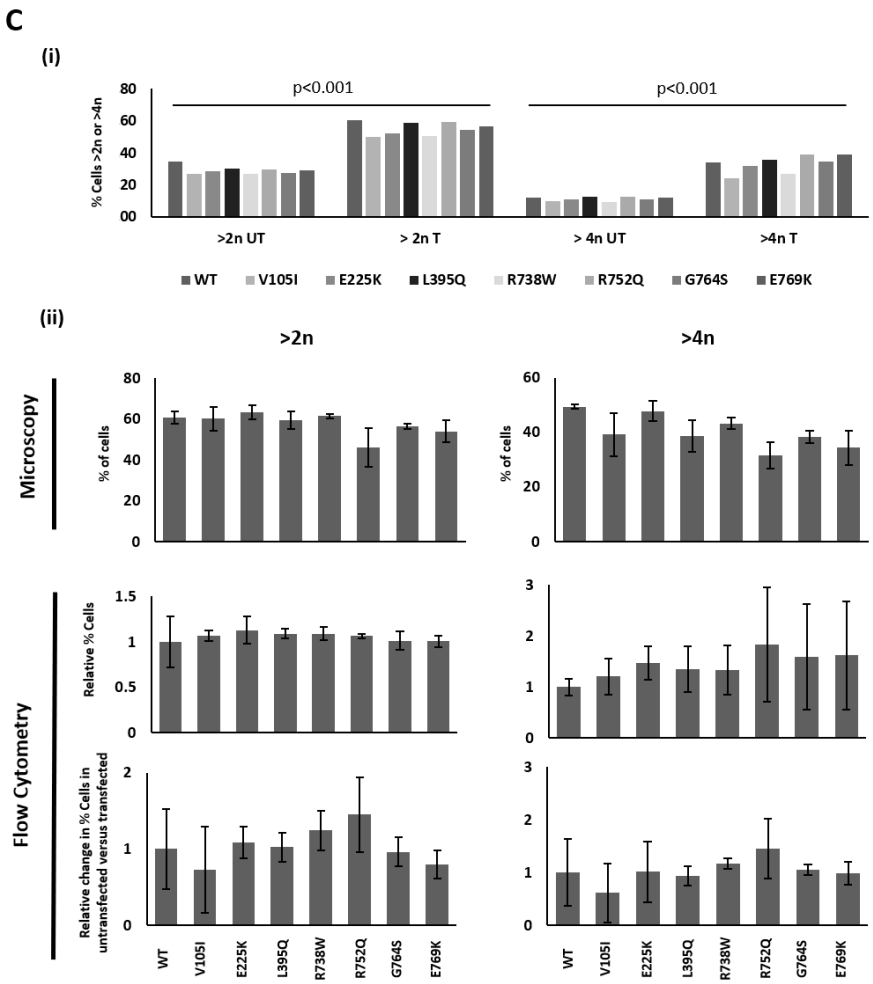

Figure 3.3.2.2 Assessment of the impact of mutant actinin-1 on cell ploidy in differentiating MEG-01 cells: *(A) Sample images of MEG-01 cells after 12 days of PMA treatment and transfection with pEGFP actinin-1. Cells were classed as 2n , 4n or >4n based on DAPI staining as shown. Rhodamine phalloidin demonstrates actin staining. (B) Representative images of analysis of MEG-01 cell ploidy over 12 days of PMA treatment using DRAQ5 staining. Ploidy was assessed using the FL-3 channel of Accuri C6 Flow Cytometer (BD). Three peaks representing 2n, 4n and >4n are noted. (C) (i) Comparison of cell ploidy in untransfected cells and cells expressing WT or mutant Actinin-1 GFP by DRAQ5 staining and quantification by flow cytometry. UT = Untransfected, T=Transfected. Statistical analysis was by paired sample T-Test. (ii) Quantification of the percentage of actinin-1-GFP WT or mutant expressing MEG-01 cells with ploidy >2n and >4n assessed by microscopy and flow cytometry. For flow cytometry, the percentage of cells in each ploidy group is expressed relative to the WT Actinin-1 of the same experimental run (middle charts). Results of flow cytometric analysis are also expressed in terms of percentage change in ploidy between untransfected and transfected cells in the same well, normalised to results of the WT actinin-1 for each run. For both*

experiments n=3. Bar charts show average ± SD. For flow cytometric data, WT average and SD was calculated based on WT results of 3 runs and normalised to the average of WT results. For mutants, results were normalised to the WT result from the same run and average and SD were calculated from normalised results from 3 runs. For both experiments, cells were treated with PMA for 12 days. 0.625 ng/mL PMA was used for days 0-3 of incubation. Concentration of PMA was then increased to 10 ng/mL and cells were treated for 12 days, as described previously (Zou et al., 2017). WT = Wild Type.

3.3.3 Actinin-1 and Actinin-4 Are Present in MEG-01, CMK and Human Platelets at Varying Concentrations.

As a key aim of the study is to determine the actinin-1 specific functions of actinin in platelets and megakaryocytes, it was important to distinguish this isoform from other actinin isoforms present. The western blot shown in Figure 3.3.3 A shows that actinin-1 and actinin-4 are present in the megakaryocytic cell lines, CMK and MEG-01. Additionally, to confirm the specificity of the actinin-1 (Santacruz-H2) and actinin-4 (Immunoglobe) antibodies used to quantify actinin-1 and actinin-4 in platelets and cell lines, HEK cells expressing actinin-1 GFP or actinin-4 GFP were assessed by western blotting using the antibodies. There was no cross reaction of antibodies with the alternate actinin isoform.

To quantify the relative amounts of the actinin isoforms present in cell lines and platelets, recombinant actinin-1 and actinin-4 protein were expressed and purified and their relative concentrations were confirmed by Coomassie staining of proteins on SDS-PAGE gels (Figure 3.3.3. B(i)). Faint lower molecular weight bands showing degraded or contaminating proteins were also seen, and so densitometric analysis of the full-length actinin band was favourable to other protein quantification assays. Densitometric analysis revealed that actinin-1 protein was 2.275 times more concentrated than the actinin-4 protein control (Figure 3.3.3 B (ii & iii)). This was adjusted for in subsequent analysis.

Relative actinin-1 and actinin-4 concentrations were quantified by western blotting of platelet lysates from three healthy adult donors using a standard curve generated by the recombinant actinin-1 and actinin-4 protein standards. Figure 3.3.3 C (i) and (ii) show samples and the use of the standard curve to generate an equation to quantify relative concentrations of actinin-1 and actinin-4 in samples. All sample concentrations were within

the range of the standard curve. It was found that platelet lysates contained 14.25 ± 3.76 (Average ± SD) times more actinin-1 than actinin-4. The relative concentrations of the actinin isoforms were then assessed in megakaryocytic cell lines (CMK, MEG-01) and a monocytic cell line (THP-1) and it was found that the actinin-1 to actinin-4 concentration ratio was lower than for platelets in these cells with 6.5 times more actinin-1 in CMK cells and 7.2 times more actinin-1 in THP-1 cells (Figure 3.3.3 D). MEG-01 cells contained more actinin-4 than actinin-1, with the actinin-1 to actinin-4 concentration ratio being 0.75 (Figure 3.3.3 D).

Figure 3.3.3

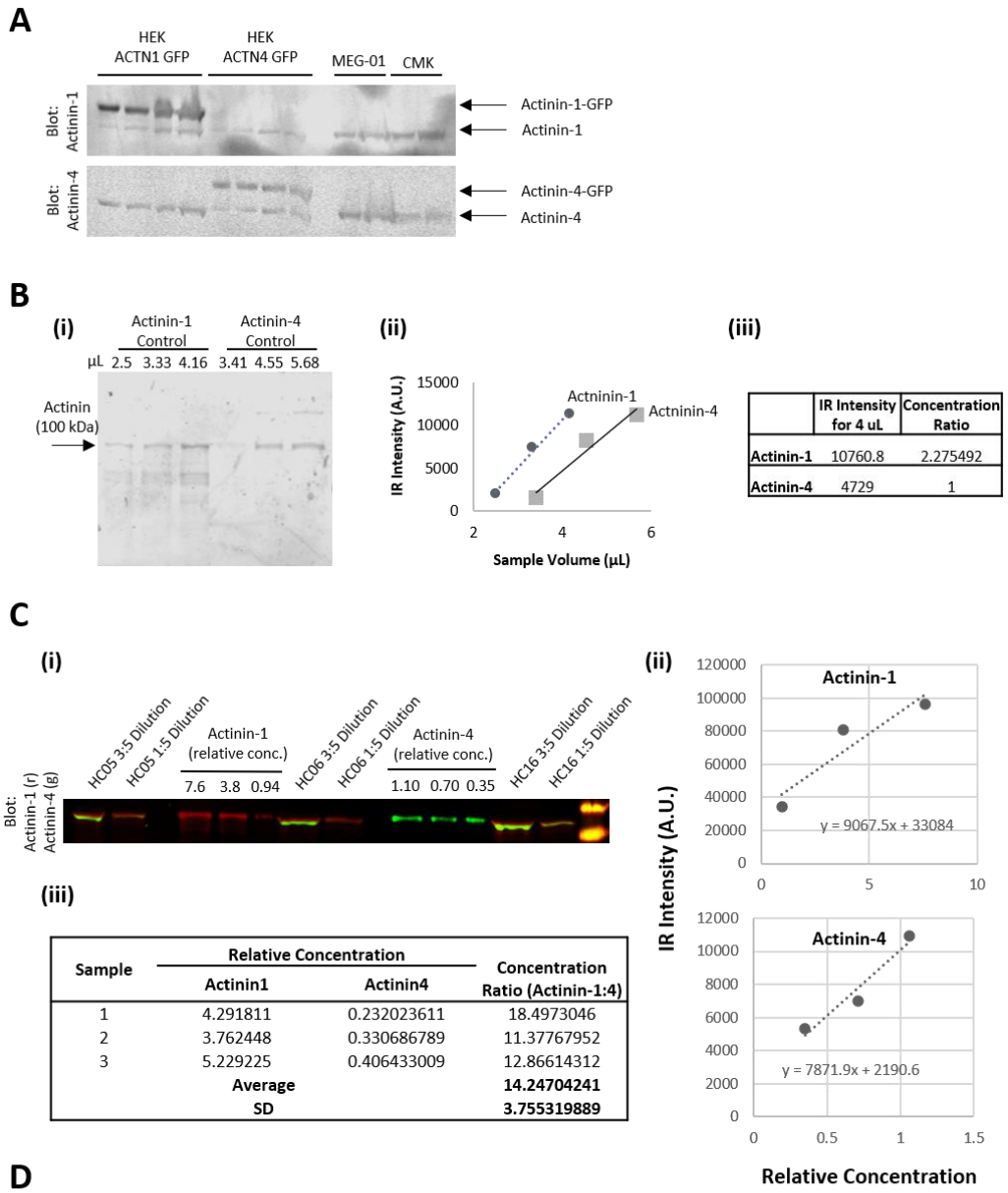
A
HEK ACTN1 GFP
HEK ACTN4 GFP
MEG-01
CMK
Blot: Actinin-1
Actinin-1-GFP
Actinin-1
Blot: Actinin-4
Actinin-4-GFP
Actinin-4
B
(i)
Actinin-1 Control
Actinin-4 Control
µL 2.5 3.33 4.16 3.41 4.55 5.68
Actinin (100 kDa)
(ii)
IR Intensity (A.U.)
Actninin-1
Actninin-4
Sample Volume (µL)
(iii)
IR Intensity for 4 uL
Concentration Ratio
Actinin-1 10760.8 2.275492
Actinin-4 4729 1
C
(i)
HC05 3:5 Dilution
HC05 1:5 Dilution
Actinin-1 (relative conc.)
7.6 3.8 0.94
HC06 3:5 Dilution
HC06 1:5 Dilution
Actinin-4 (relative conc.)
1.10 0.70 0.35
HC16 3:5 Dilution
HC16 1:5 Dilution
Blot: Actinin-1 (r) Actinin-4 (g)
(ii)
Actinin-1
y = 9067.5x + 33084
Actinin-4
y = 7871.9x + 2190.6
IR Intensity (A.U.)
Relative Concentration
(iii)
Sample
Relative Concentration
Actinin1
Actinin4
Concentration Ratio (Actinin-1:4)
1 4.291811 0.232023611 18.4973046
2 3.762448 0.330686789 11.37767952
3 5.229225 0.406433009 12.86614312
Average 14.24704241
SD 3.755319889
D
(i)
HC05 1:5 Dilution
HC05 3:5 Dilution
CMK (2 µL)
CMK (3 µL)
Actinin-1 (relative conc.)
0.91 3.8 7.6
MEG-01 (1.5 µL)
MEG-01 (10 µL)
THP-1 (1 µL)
THP-1 (2 µL)
Actinin-4 (relative conc.)
0.3 0.7 1.1
Blot: Actinin-1 (r) Actinin-4 (g)
(ii)
Sample
Relative Concentration
Actinin1
Actinin4
Concentration Ratio (Actinin-1:4)
Platelets 6.596 0.382 17.26702
CMK 1.297 0.199 6.517588
MEG-01 0.673 0.895 0.751955
THP-1 3.872 0.539 7.183673

Figure 3.3.3 Analysis of actinin isoforms in platelets and megakaryocytic cell lines: *(A) The specificity of actinin-1 and actinin-4 antibodies was confirmed by the staining of lysates from HEK293 cells expressing actinin-1-GFP or actinin-4-GFP. MEG-01 and CMK cell lysates were analysed in tandem and confirmed to express both actinin isoforms. (Bi) The relative concentration of purified Actinin-1 and Actinin-4 protein controls was assessed by Coomassie staining of samples run on an SDS-PAGE gel. (Bii) Densitometric analysis of samples run on an SDS-PAGE gel allowed comparison of sample concentrations, with results plotted on the graph shown. (Biii) The equations of each volume versus IR intensity line, shown in (Bii) were used to determine the IR intensity per unit volume, at an arbitrary volume within the range of the lines (4 µL). The concentration ratio was then calculated. (Ci) The lysates from washed platelets from three healthy adult donors were analysed by western blotting in tandem with actinin-1 and actinin-4 protein controls to compare relative concentrations of the lysates. Actinin-1 is shown in the IR700 channel (red) and actinin-4 is shown in the IR800 channel (green). (Cii) Demonstration of standard curves generated by densitometric analysis of actinin-1 and actinin-4 protein standards. Equations of the lines were used to quantify the concentrations of proteins present in the platelet lysates. The concentration of protein in the lysates was within the range of the standards. (Ciii) Results of the quantification of relative actinin-1 and actinin-4 concentration in platelet lysates. (Di) The lysates from washed platelets, CMK, MEG-01 and THP-1 cells were analysed in tandem with actinin-1 and actinin-4 protein controls to compare relative concentrations of the lysates. Actinin-1 is shown in the IR700 channel (red) and actinin-4 is shown in the IR800 channel (green). A representative blot from two experiments are shown. (Dii) Results of the quantification of relative actinin-1 and actinin-4 concentration in the lysates. For all blots, actinin-1 was detected with anti-actinin-1 (Santacruz H2) antibody at 1:500 dilution and actinin-4 was detected with anti-actinin-4 (Immunoglobe 3) antibody at 1:1000 dilution. Densitometry analysis was performed using Odyssey Image Studio Software (LI-COR Biosciences, Cambridge, UK).*

3.3.4 Actinin-1 / Actinin-4 Interacting Proteins

Various actinin antibodies were trialled for their ability to immunoprecipitated actinin from CMK cell lysates (Figure 3.3.4). The actinin Sigma BM75.2 antibody was efficient for the immunoprecipitation of actinin-1, although also precipitated a smaller quantity of actinin-4. The actinin Honda antibody (generously provided by Kaufumi Honda (Honda et al., 1998)) was most efficient for actinin-4 immunoprecipitation but also precipitated a smaller

quantity of actinin-1. The presence of actinin isoforms non-specific to the antibody used may be indicative of the immunoprecipitation of actinin 1/4 heterodimers.

To probe whether known interactors of actinin in platelets may be actinin-1 or actinin-4 specific, the actinin antibody immunoprecipitated proteins were probed with an anti-CD61 antibody to detect integrin β3, which has been reported to interact with actinin-1 previously (Shams & Mofrad, 2017; Tadokoro et al., 2011). In two independent experiments, the actinin Honda antibody was shown to immunoprecipitate actinin-4, actinin-1 and CD61. Non-specific signal was reduced by the use of the Trueblot HRP antibody which recognises the non-denatured primary antibody in the western blot but not the denatured antibody used for immunoprecipitation.

Figure 3.3.4

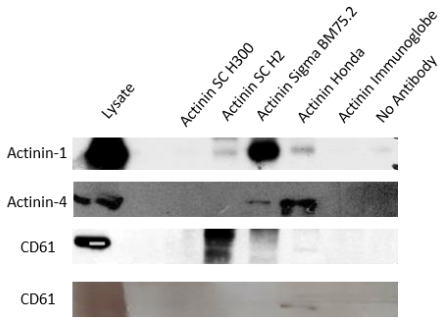

Figure 3.3.4 Results of the immunoprecipitation of actinin-1 and actinin-4 from CMK cell lysates using various actinin antibodies. *Western blotting of elutions from the immunoprecipitation experiment was carried out with Actinin-1 (Santacruz H2) and actinin-4 (Immunoglobe* 0042-05*) antibodies. HRP or Trueblot HRP secondary antibodies and detection by ECL were used. Elutions from the immunoprecipitation experiments were also probed with anti-CD61 (Biolegend) in two separate experiments.*

3.3.5 Actinin is Present in Proplatelets and Podosomes in Primary Megakaryocytes

Although the megakaryocytic cell lines were useful in the study of megakaryocytic differentiation and the study of protein-protein interactions, these cells did not form detectable platelet-like particles or proplatelets under the conditions assessed. As this process was hypothesised to be impacted by ACTN1 mutations, the culture of primary murine megakaryocytes was next established with the intention of assessing the role of

actinin and CMTP-causing mutations in proplatelet formation. The culture of primary megakaryocytes for the assessment of proplatelet production is well established and as the cytoplasmic processes extended from these cells closely resemble those described *in-vivo*, this was a more physiologically relevant model of this process. However, the delivery of DNA and expression of recombinant proteins in these cells is known to be technically difficult, and hence various methods of DNA delivery were trialled. I also describe immunofluorescent staining of the primary megakaryocytes, with a focus on two morphological features; proplatelets and podosomes.

3.3.5.1 Optimisation of Antibodies for Immunofluorescent Staining

A number of actinin antibodies were available in the lab and had been assessed in terms of their suitability for western blotting (Foley, 2013). However, it was important to assess the suitability and specificity of these actinin antibodies when used for immunofluorescence staining (Appendix Figure 6.2). Optimisation of the anti-actinin antibodies for immunofluorescent staining showed that the anti-actinin-4 Immunoglobe antibody was specific for actinin-4, as actinin-4 -GFP expressing HEK293 cells were stained more intensely than untransfected cells. The actinin-4 Immunoglobe antibody stained actinin-1-GFP expressing cells and untransfected cells with similar intensity. The anti-actinin Sigma antibody stained actinin-1-GFP and actinin-4-GFP expressing cells more intensely than untransfected cells, suggesting that the antibody stains both actinin-1 and actinin-4. The actinin Santacruz H2 antibody did not stain actinin-1-GFP expressing cells or untransfected cells and was not suitable for immunofluorescent staining under the conditions assessed. The actinin Santacruz H300 antibody did not stain the actinin-1-GFP expressing cells with increased intensity versus untransfected cells, consistent with its binding to all actinin isoforms. The Honda antibody stained actinin-4 -GFP expressing HEK293 cells more intensely than untransfected cells, hence this antibody was suitable for immunofluorescent staining specifically for actinin-4.

3.3.5.2 Actinin is Present in Proplatelets and Podosomes in Primary Megakaryocytes

As the megakaryocytic cell lines were not a suitable model to assess proplatelet formation, primary murine megakaryocytes were cultured for this purpose. Megakaryocytes were cultured from murine fetal liver tissue by differentiating fetal liver cells with TPO for 4 days and isolating megakaryocytes using a BSA density gradient, as described previously (Vijey et

al., 2018). Megakaryocytes were identified as large polyploid cells with long processes (proplatelets) with platelet sized tips at the end of these processes (Figure 3.3.5.1). In vinculin, actin and actinin stained cells, punctate staining was noted. These structures were thought to be podosomes. Further staining confirmed the co-localisation of WASP, characteristic of podosomes, with actin and actinin in these structures (Figure 3.3.5.2). As the actinin Sigma antibody stains actinin-1 and actinin-4, the specific isoform stained cannot be determined. The actinin-4 immunoglobe antibody specifically stains actinin-4, hence actinin-4 was confirmed to be present in these structures. MHCIIA also co-localised to these structures generally, although MHCIIA was noted in some cases to show punctate staining distinct from the actin punctate staining. The primary megakaryocytes formed podosomes when plated onto fibronectin (Figure 3.3.5.2 A and B) and onto collagen (Figure 3.3.5.3). It was also determined that podosomes were evident in cells at 3 hours post plating and remained present at 16 hours after plating onto fibronectin or collagen (Figure 3.3.5.4). Proplatelets were also formed on fibronectin or collagen (3.3.5.5 & 3.3.5.6). Proplatelets were shown to be stained with antibodies against actinin, MHCIIA, vinculin, actin, and WASP (Figure 3.3.5.6). Tubulin staining showed the characteristic ring structure at the proplatelet tips (Figure 3.3.5.6). The proplatelet tips, platelet size swellings along the proplatelets and branching points in the proplatelets were areas which stained brightly with all antibodies used. Positive staining was verified by comparison with negative controls, stained with secondary antibodies only (Figure 3.3.5.7).

Figure 3.3.5.1

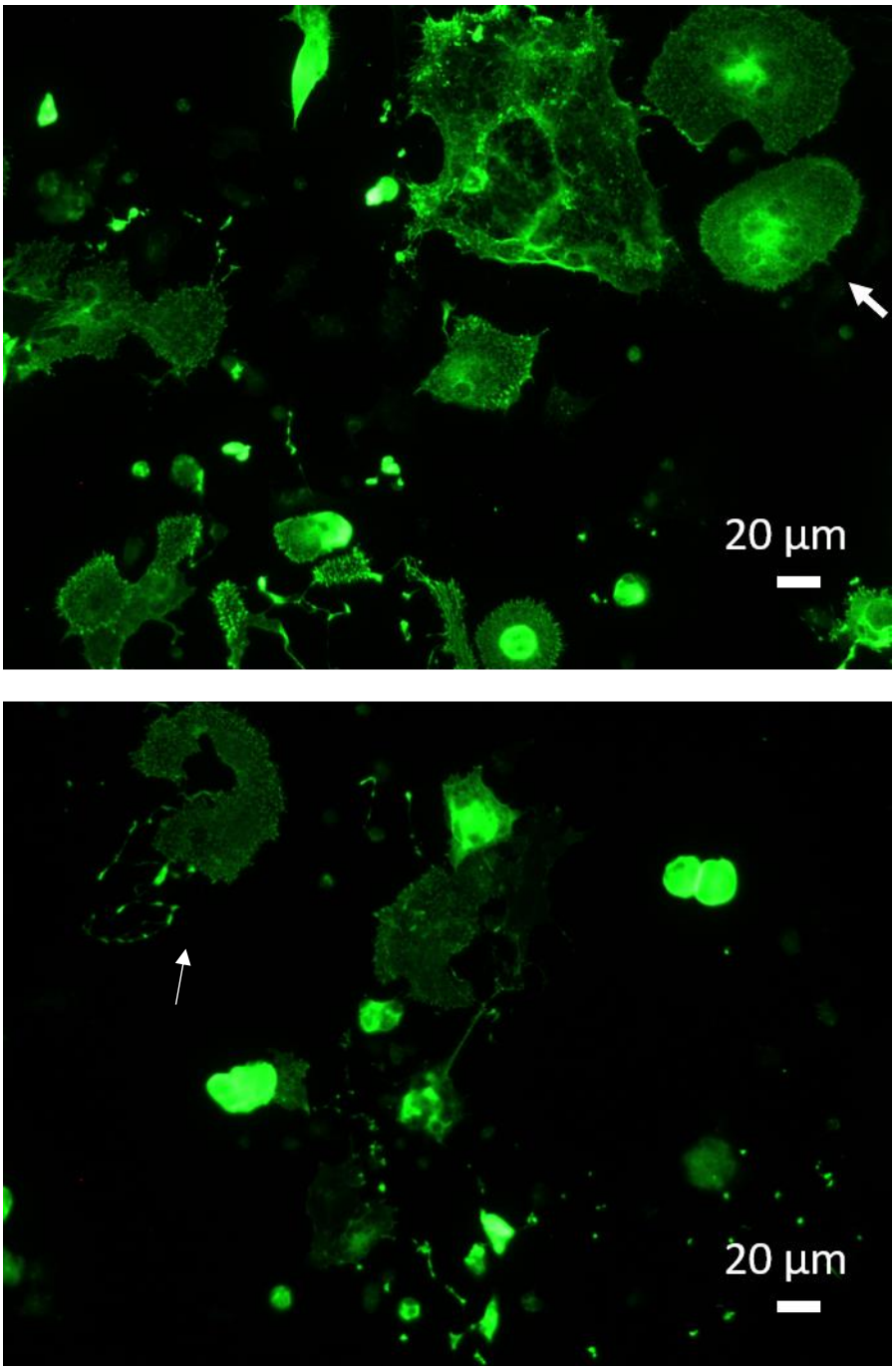

Figure 3.3.5.1 Representative images of primary megakaryocytes cultured from murine fetal liver tissue. *Cells were plated onto fibronectin (100 µg/mL) coated glass coverslips and were stained with anti-vinculin antibody (Sigma – V9131). Thick arrow shows presence of cells with punctate staining, thought to be podosomes. Thin arrow shows proplatelets with platelet-like particles budding along the proplatelet process.*

Figure 3.3.5.2 A

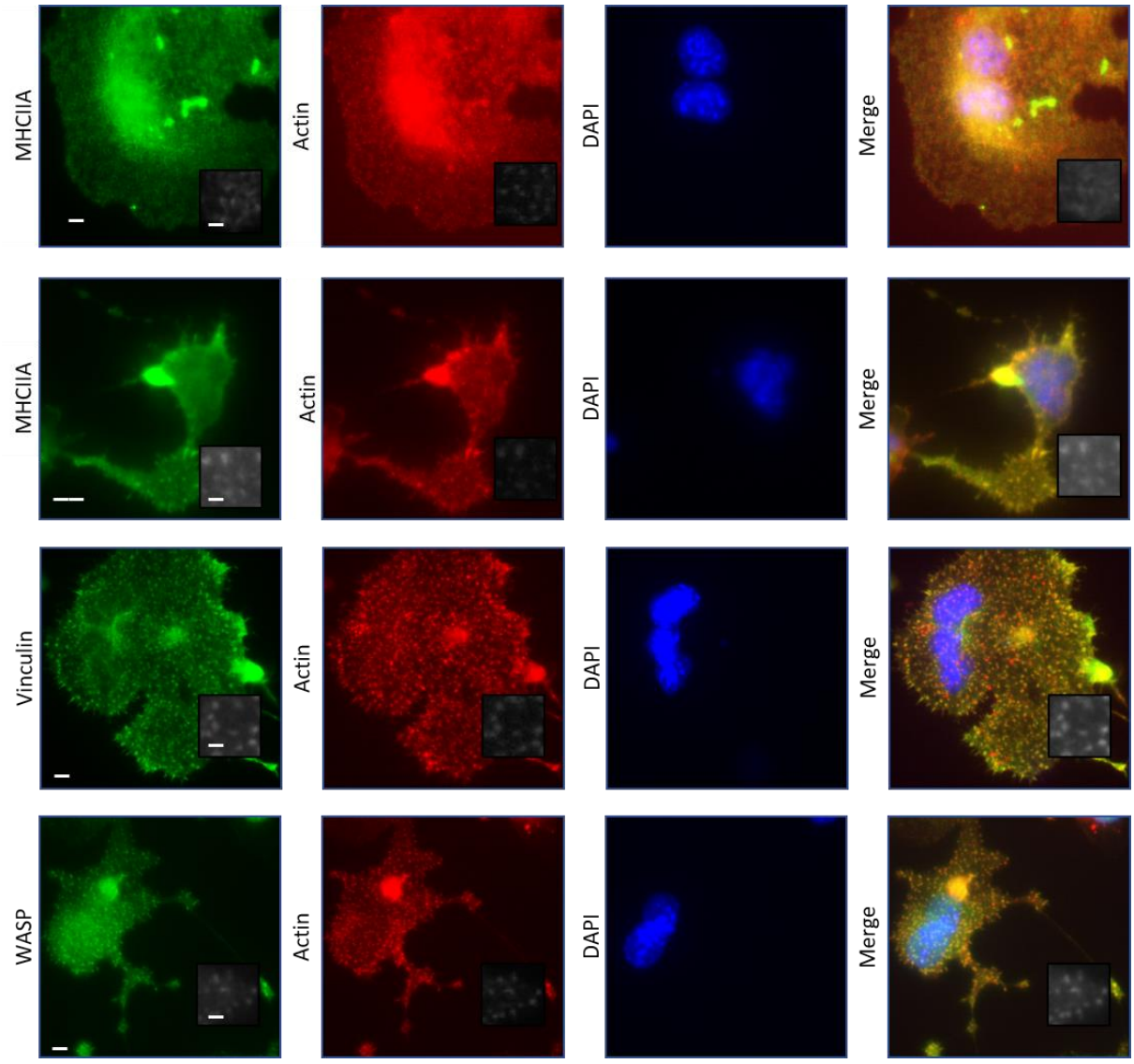

Figure 3.3.5.2 A Podosomes imaged in primary murine megakaryocytes. *Images show staining of podosomes in primary murine megakaryocytes plated on fibronectin (100 µg/mL) coated glass coverslips. Cells were identified as megakaryocytes based on characteristic polyploidy or the presence of proplatelets. Podosomes are shown as punctate structures, highlighted in the figure inserts. Scale bar = 10 µm. Inserts show magnification of the podosomes, scale bar = 2 µm.*

Figure 3.3.5.2 B

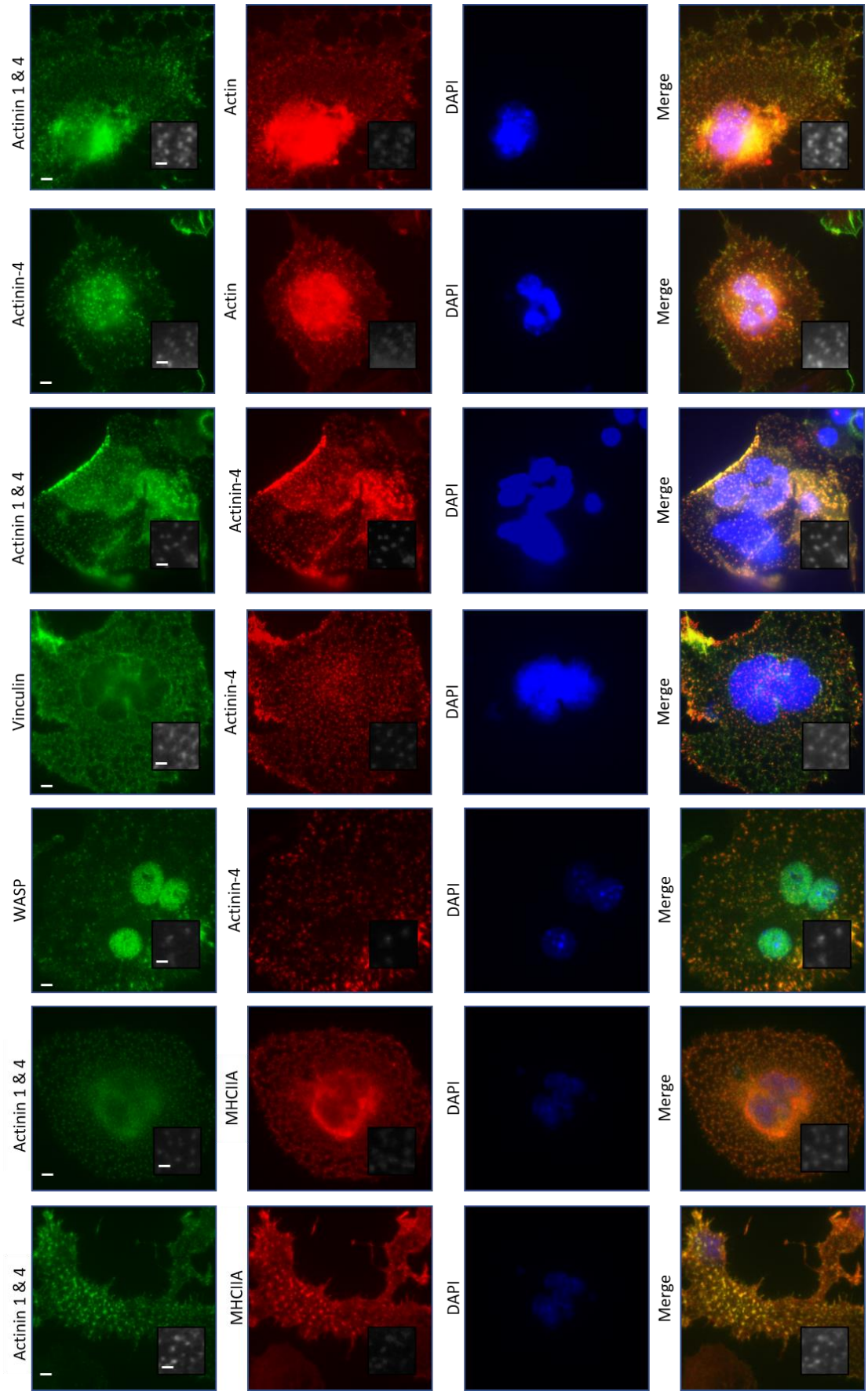

Figure 3.3.5.2 B Actinin-1 and actinin-4 imaged in podosomes in primary murine megakaryocytes adhered to fibronectin. *Images show staining of podosomes in primary murine megakaryocytes plated on fibronectin (100 µg/mL) coated glass coverslips. Cells were identified as megakaryocytes based on characteristic polyploidy or the presence of proplatelets. Cells were stained with podosome-specific markers (WASP, Vinculin, Actin) and show co-localisation of actinin-1, actinin-4 and MHCIIA to these structures. Scale bar = 10 µm. Inserts show magnification of the podosomes, scale bar = 2 µm.*

Figure 3.3.5.3

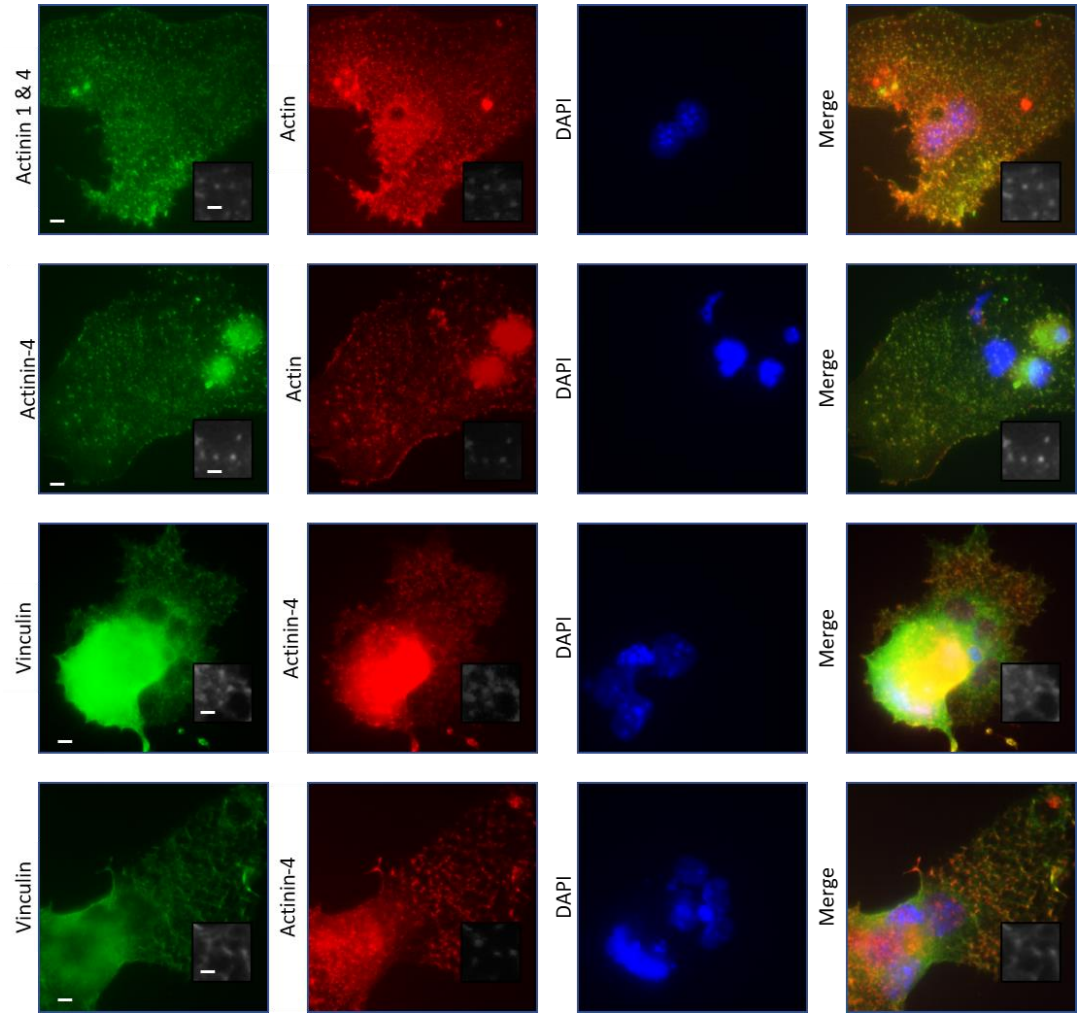

Figure 3.3.5.3 Actinin-1 and actinin-4 imaged in podosomes in primary murine megakaryocytes adhered to collagen. *Images show staining of podosomes in primary murine megakaryocytes plated on collagen (100 µg/mL) coated coverslips. Cells were identified as megakaryocytes based on characteristic polyploidy or the presence of proplatelets. Podosomes are highlighted as punctate structures in the inserts. Staining shows*

co-localisation of podosome-specific markers with actinin-1 and actinin-4. Scale bar = 10 µm. Inserts show magnification of the podosomes, scale bar = 2 µm.

Figure 3.3.5.4

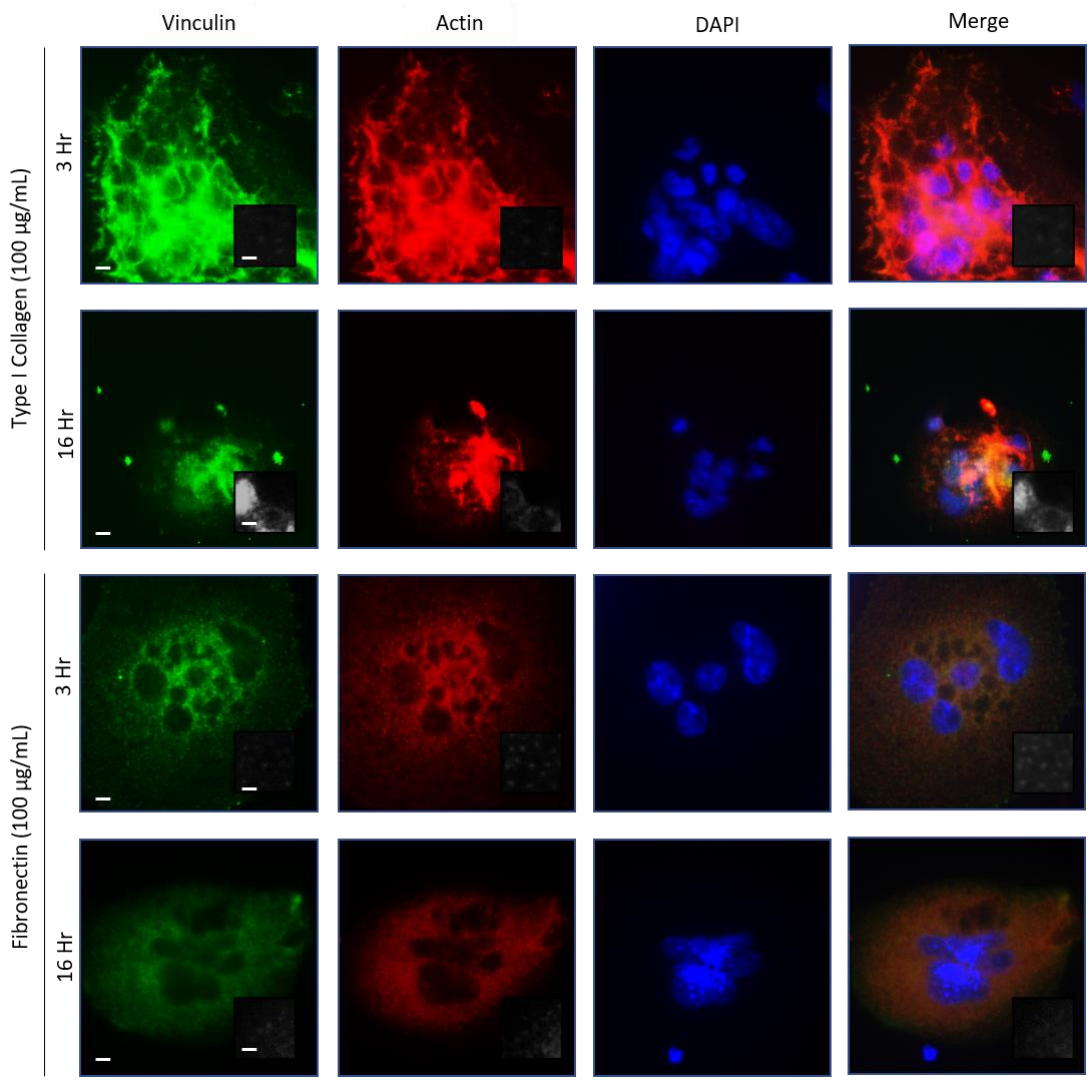

Figure 3.3.5.4 Assessment of podosome formation at 3 hours or 16 hours post plating onto collagen or fibronectin coated glass coverslips. *Cells were identified as megakaryocytes based on characteristic polyploidy or the presence of proplatelets. Scale bar = 10 µm. Inserts show magnification of the podosomes, scale bar = 2 µm.*

Figure 3.3.5.5

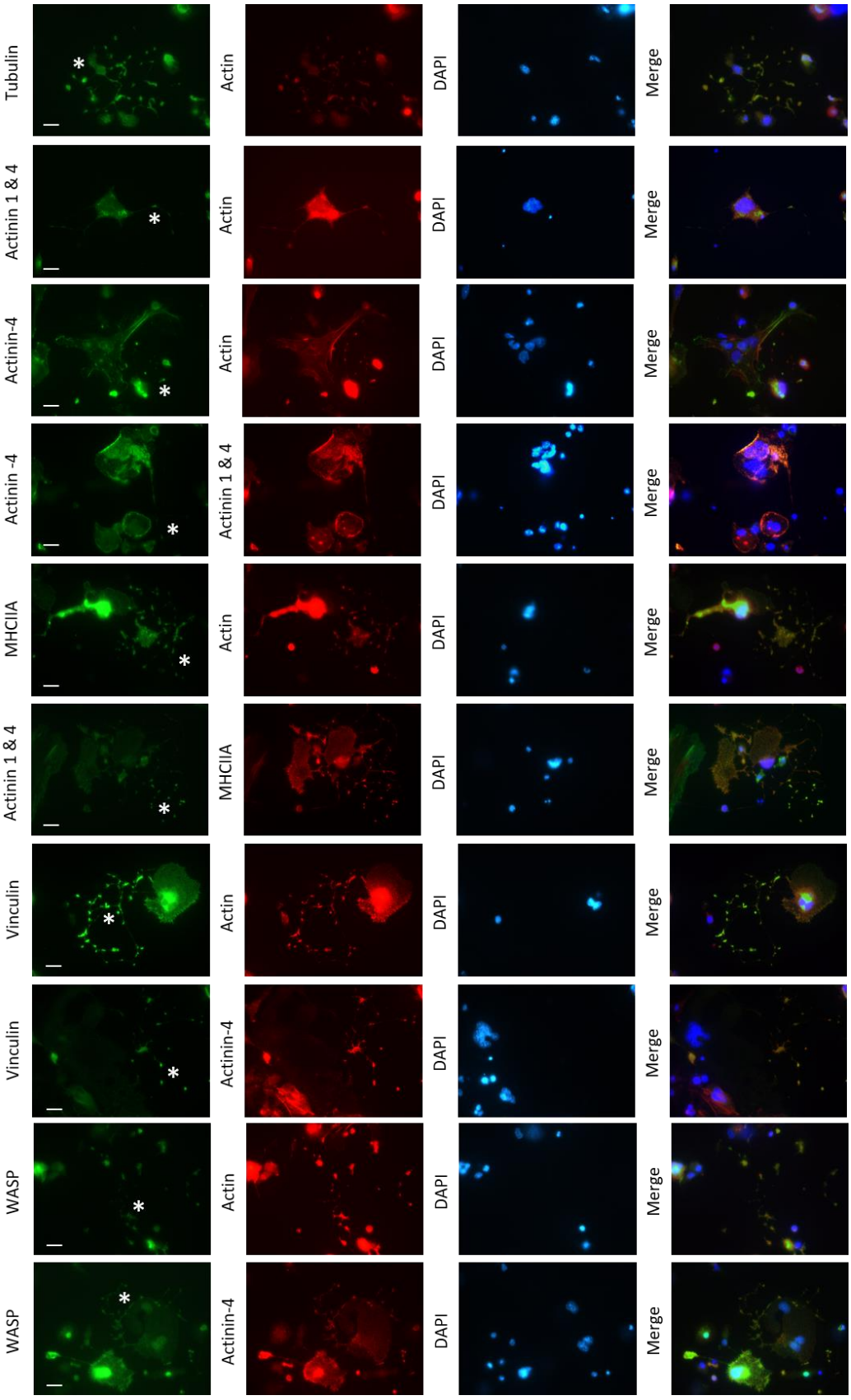
Tubulin
Actin
DAPI
Merge
Actinin 1 & 4
Actin
DAPI
Merge
Actinin-4
Actin
DAPI
Merge
Actinin -4
Actinin 1 & 4
DAPI
Merge
MHCIIA
Actin
DAPI
Merge
Actinin 1 & 4
MHCIIA
DAPI
Merge
Vinculin
Actin
DAPI
Merge
Vinculin
Actinin-4
DAPI
Merge
WASP
Actin
DAPI
Merge
WASP
Actinin-4
DAPI
Merge

Figure 3.3.5.5 Immunofluorescent imaging of actinin-1 and actinin-4 in proplatelets of primary murine megakaryocytes adhered to fibronectin. *Cells were plated onto fibronectin (100 µg/mL) coated glass coverslips. Asterisks show proplatelets and proplatelet tips. Scale bars show 20 µm.*

Figure 3.3.5.6

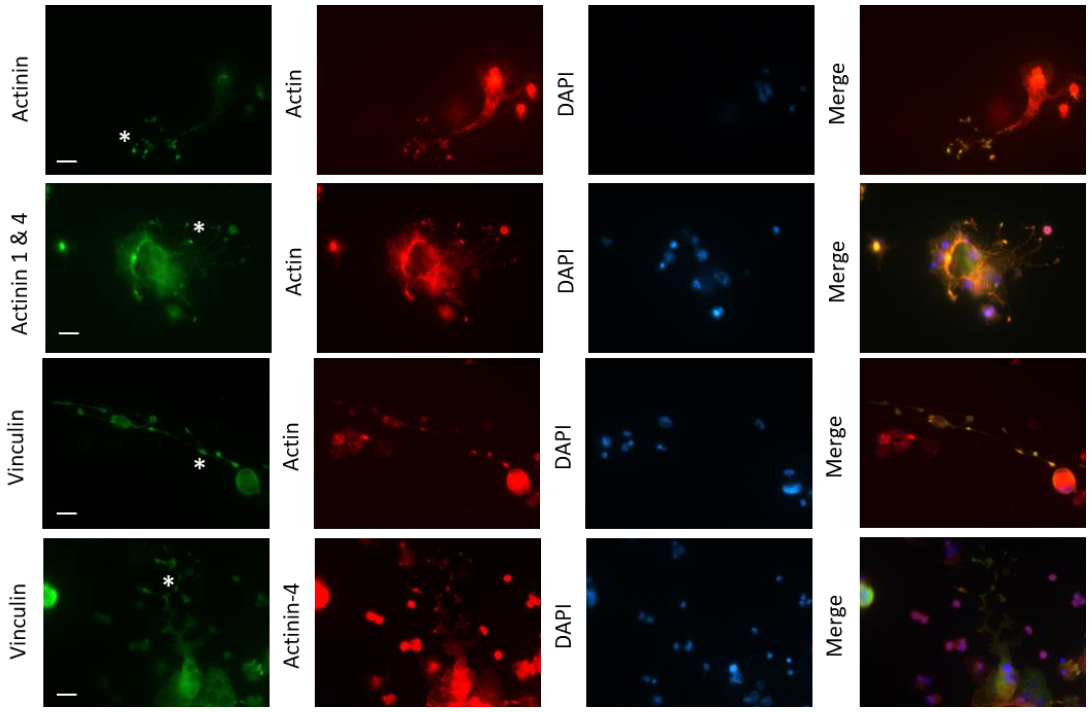

Figure 3.3.5.5 Immunofluorescent imaging of ctinin-1 and actinin-4 in proplatelets of primary murine megakaryocytes adhered to collagen. *Cells were plated onto Type I collagen (100 µg/mL) coated glass coverslips. Asterisks show proplatelets and proplatelet tips. Scale bars show 20 µm.*

Figure 3.3.5.7

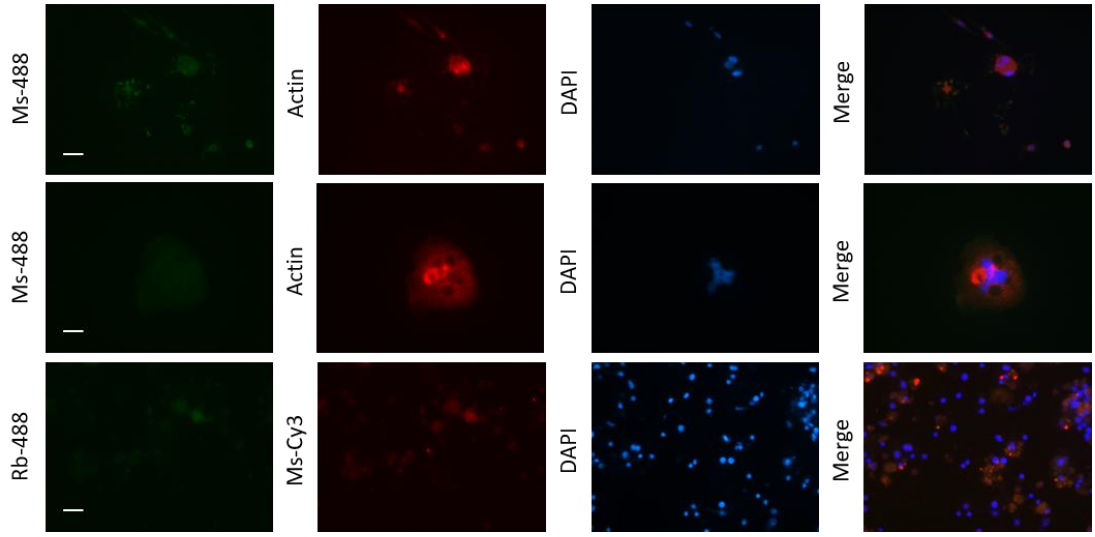

Figure 3.3.5.7 Immunofluorescent staining negative controls. *Staining of primary murine megakaryocytes with secondary antibodies only. Cells were plated onto fibronectin (100 µg/mL) coated glass coverslips. Scale bars show 20 µm.*

3.3.6 Transfection of Primary Murine megakaryocytes.

Using the conditions optimised with MEG-01 and CMK cells, lipofectamine-2000, electroporation and nucleofection were trialled on primary murine megakaryocytes. All methods trialled were inefficient, and results are summarised in Table 4.3.5. Lipofectamine-2000 did not result in efficient GFP expression but cell morphology appeared non-significantly impacted, with cells extending proplatelets seen (Figure 3.3.6 A i). Electroporation appeared to impact cell viability significantly, as morphology was abnormal after incubation (Figure 3.3.6 ii). Trypan blue staining revealed no viable cells remained. Nucleofection did not appear to impact cell viability as significantly, with cells extending proplatelet observed after incubation (Figure 3.3.6 iii-iv). All nucleofection methods were similarly poor in delivering pEGFP to cells, with the majority of cells not expressing GFP. Most GFP positive cells did not have megakaryocyte-defining features, such as proplatelets. One GFP positive cell with proplatelets was seen (Figure 3.3.6 iv b). As the methods trialled gave poor results and involved the expression of EGFP, which we knew to be expressed more robustly than the actinin-1-GFP constructs that we ultimately aimed to use, it was decided that these methods were too inefficient for use in the analysis of mutant actinin-1 expression. Consequently, delivery of actinin-1 plasmids to primary megakaryocytes was next attempted using lentivirus infection.

Table 3.3.5: Summary of Results of Primary Megakaryocyte Transfection

Method		Positivity (Estimated % cells expressing GFP)	Cell Morphology / Viability
i	Lipofectamine-2000	<1	All methods trialled were similarly poor efficiency but cell morphology was normal. Cells with proplatelets seen.
ii	Electroporation (2000V – 8 pulses – 60 µs)	<1	No live cells by trypan blue staining
iii	Nucleofection X-05 (pre BSA)	<1	Few Cells Some cells with proplatelets seen
iv	Nucleofection X-05 (post BSA)	<1	Some cells with proplatelets seen One GFP-expressing cell with proplatelets

Figure 3.3.6

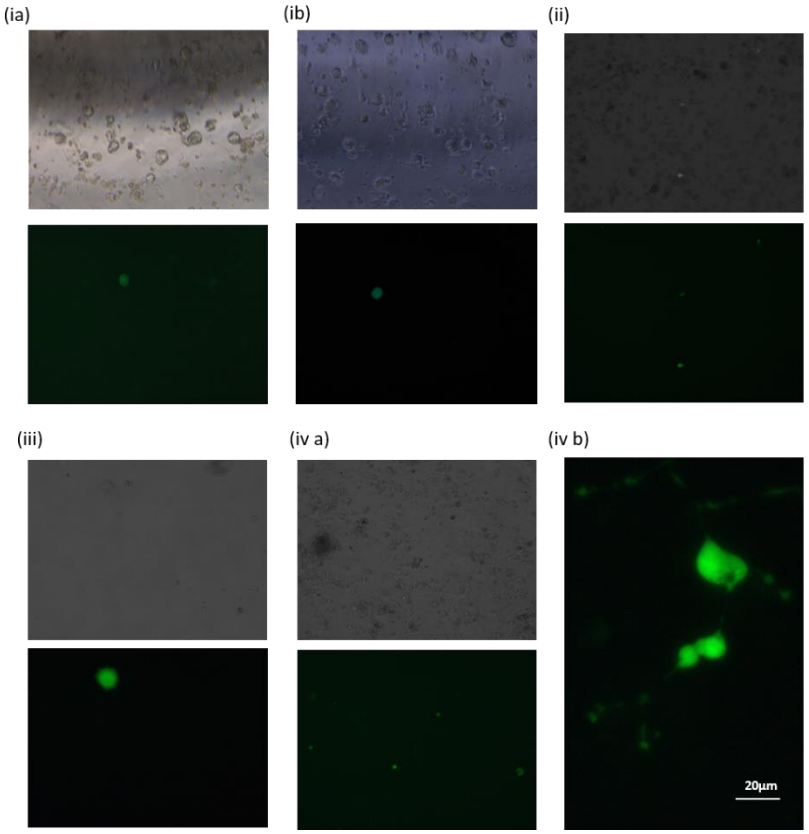

Figure 3.3.6 Results of trials of various methods used to deliver pEGFP to primary murine megakaryocytes. *(i) Lipofectamine-2000, (ii) Electroporation, (iii) Nucleofection pre concentration of megakaryocytes by BSA gradient, (iv a) Nucleofection post concentration of megakaryocytes by BSA gradient. (iv b) GFP expressing primary murine megakaryocyte post Nucleofection. Upper panel shows brightfield image and lower panels show GFP fluorescence in same field. Results are further detailed in Table 4.3.5.*

3.3.7 Lentiviral Infection of Primary Murine Megakaryocytes.

A second generation lentiviral infection system was used in this study, involving three plasmids; the envelope plasmid (VSVg), the packaging plasmid (CMVΔ8.9) and the transfer plasmid (FUGW), which was cloned with actinin-GFP or Lifeact-mCherry constructs. Initially the virus production and concentration protocol was optimised. The virus was propagated in HEK293FT cells by the transfection of cells with the three viral plasmids. The first batch of lentiviruses, produced by the calcium phosphate method of transfection, did not appear to infect HEK293FT cells with high efficiency in titration experiments. Although >50% of cells showed some fluorescence, the fluorescence was dim and unclear. Hence, to improve efficiency, the transfection method used to produce the viruses in HEK293FT cells was optimised. The second batch of lentiviruses were produced using an optimised Lipofectamine-2000 based protocol (2.3 µg DNA per 6 well + 2 µL lipofectamine-2000 in 128 µL OptiMEM). Sample images of infection of HEK293FT cells by viruses produced in Batch 2 are shown in Figure 3.3.7.1. Infection of HEK293FT cells with this batch of virus was significantly improved, with the majority of cells expressing GFP. Fluorescence intensity was also increased. This batch of lentiviruses was used to infect primary megakaryocytes.

Various infection protocols were trialled on primary megakaryocytes but efficiency was consistently poor. Sample images from each trial are shown in Figure 3.3.7.2. Although some green fluorescence was seen in cells infected with GFP plasmids, and some cells with actin staining seen in Lifeact mCherry infected cells, this was rarely bright or was often not in cells with podosomes or proplatelets. A high background green fluorescence in the uninfected cells also hindered the reliable detection of infected cells. Hence the infection methods trialled were not efficient enough to allow analysis of mutant actinin-1 expression.

Figure 3.3.7.1

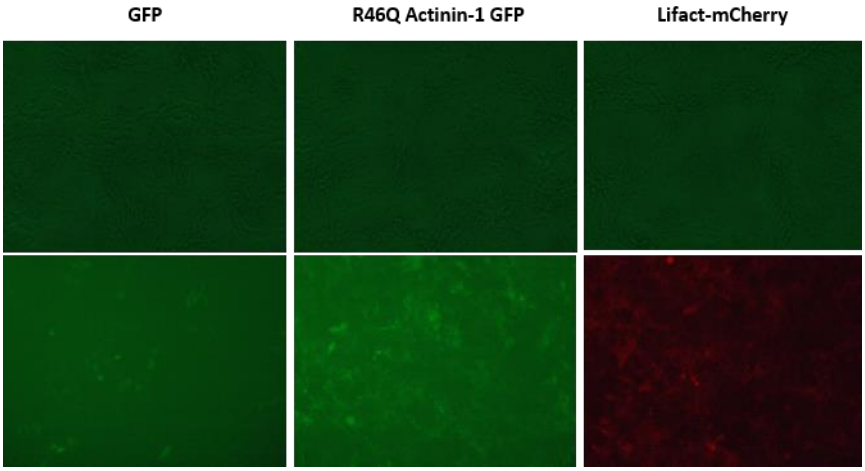

Figure 3.3.7.1 Infection of HEK293FT cells with lentiviruses produced in Batch 2. *Upper panels show brightfield images captured through a GFP filter cube. Lower panels show GFP or mCherry fluorescence images of the same field.*

Figure 3.3.7.2

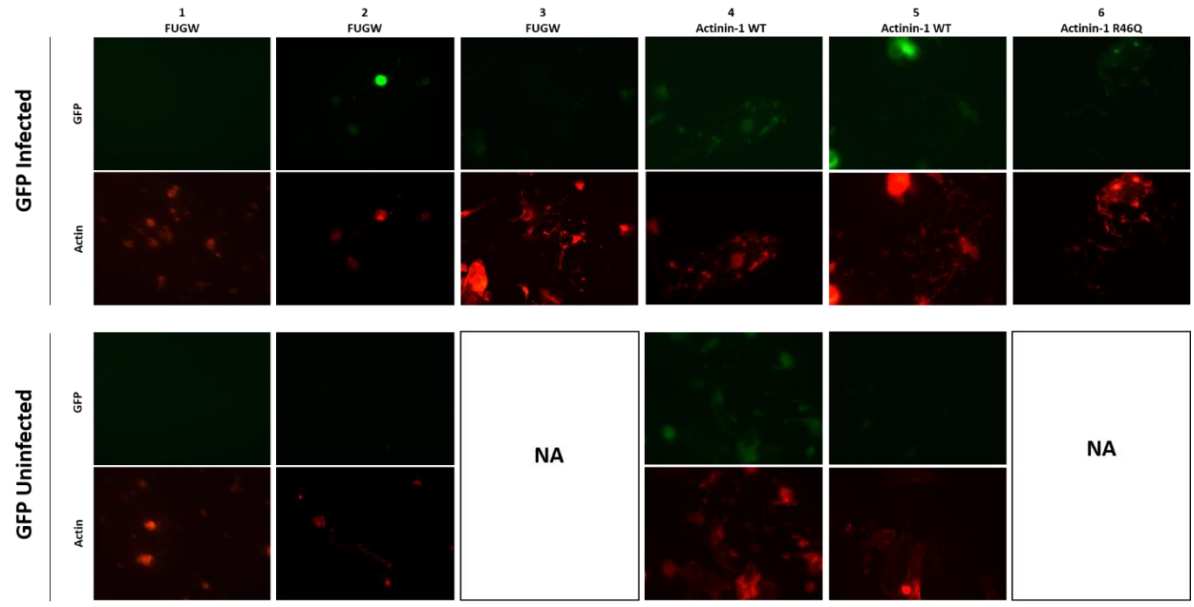

Figure 3.3.7.2 Representative images from attempt 1-6 of the infection of primary murine megakaryocytes with GFP, Actinin-GFP or Lifeact mCherry lentiviruses. *Numbers 1-6 denote the experiment number, with details of the protocols used for each run summarised in Table 3.2.2. GFP or Actinin-GFP infected cells are shown on top, and cells which were uninfected or infected with Lifeact mCherry lentivirus (Run 5) are shown on bottom. Upper panels show GFP*

fluorescence and lower panels show actin staining by phalloidin rhodamine or lifeact mCherry expression (Run 5). NA = not analysed as all cells cultured were used for the infection attempt.

3.3.8 Production of Actinin-1 and Actinin-4 Heterodimers.

As actinin-1 and actinin-4 were shown to be present in platelets and MK cell lines in varying amounts, be present in key morphological structures (podosomes and proplatelets) and possibly have varying protein interactors in these cells, the question of the role of actinin-1/4 heterodimers was raised. CMTP causing actinin-1 mutations could also impact the formations of actinin dimers and possibly impact any function heterodimers have in these cells. Hence the expression of recombinant heterodimers in mammalian cells and the purification of heterodimers for *in-vitro* study was of interest. A method to achieve this was explored in this study.

Initially, expression and purification of heterodimers was trialled in BL21 E. *coli*. Equimolar expression of pBAD actinin-1 and pRSF actinin-4 plasmids was achieved by the induction of BL21 with 0.0001% Arabinose and 1 mM IPTG (Figure 3.3.8.1 A). The actinin proteins were purified by nickel and amylose affinity purification as appropriate (Figure 3.3.8.1 B). It was noted that the amylose column had poor binding efficiency to the actinin-4 MBP protein. An MBP control was expressed to verify the efficiency of the column and showed good binding efficiency (data not shown). This hindered the efficient purification of heterodimers. Only actinin-4 MBP was seen after tandem nickel and amylose purification, including after concentration, implying that no heterodimers were not formed or were produced at too low a concentration to detect (Figure 3.3.8.1 C). The purified actinin-1, actinin-4 and actinin-1 / actinin-4 proteins were then run on a Native PAGE gel and analysed by Coomassie staining and western blotting. No clear heterodimer formation was noted (Figure 3.3.8.1 D & E).

Figure 3.3.8.1

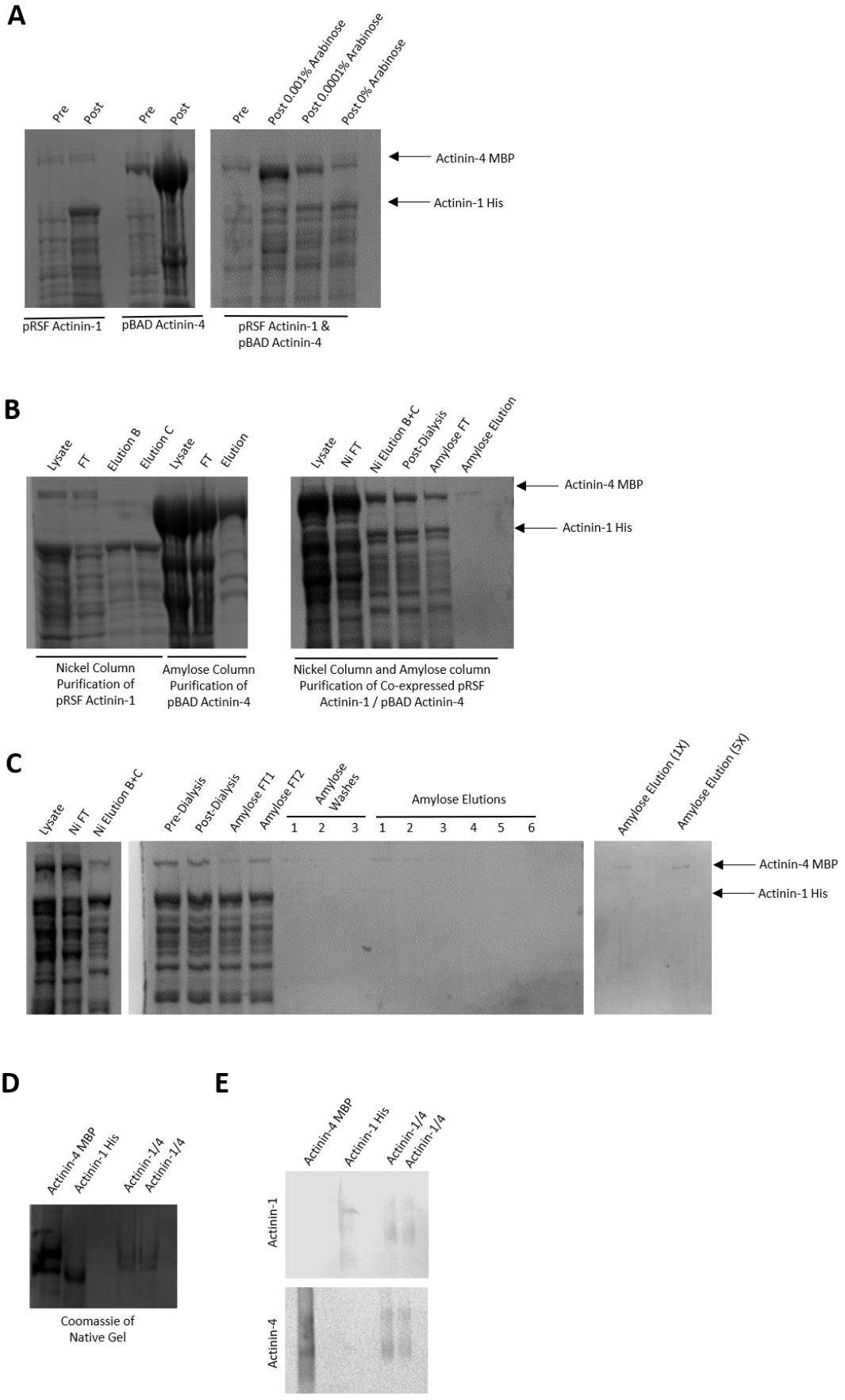
A
Pre
Post
Pre
Post
Pre
Post 0.001% Arabinose
Post 0.0001% Arabinose
Post 0% Arabinose
Actinin-4 MBP
Actinin-1 His
pRSF Actinin-1
pBAD Actinin-4
pRSF Actinin-1 &
pBAD Actinin-4
B
Lysate
FT
Elution B
Elution C
Lysate
FT
Elution
Lysate
Ni FT
Ni Elution B+C
Post-Dialysis
Amylose FT
Amylose Elution
Actinin-4 MBP
Actinin-1 His
Nickel Column
Purification of
pRSF Actinin-1
Amylose Column
Purification of
pBAD Actinin-4
Nickel Column and Amylose column
Purification of Co-expressed pRSF
Actinin-1 / pBAD Actinin-4
C
Lysate
Ni FT
Ni Elution B+C
Pre-Dialysis
Post-Dialysis
Amylose FT1
Amylose FT2
Amylose
Washes
1 2 3
Amylose Elutions
1 2 3 4 5 6
Amylose Elution (1X)
Amylose Elution (5X)
Actinin-4 MBP
Actinin-1 His
D
Actinin-4 MBP
Actinin-1 His
Actinin-1/4
Actinin-1/4
Coomassie of
Native Gel
E
Actinin-4 MBP
Actinin-1 His
Actinin-1/4
Actinin-1/4
Actinin-1
Actinin-4

Figure 3.3.8.1 Expression and purification of actinin-1 / actinin-4 heterodimers. *(A) optimisation of the expression protocol to produce equimolar concentrations of actinin-1 and actinin-4 in BL21 E. coli co-transformed with the pBAD Actinin-1 and pRSF Actinin-4 plasmids. Pre= pre-induction, Post = post induction with 0.2 mM IPTG for pRSF , 0.5% arabinose for pBAD or 1 mM IPTG and the indicated arabinose concentration for co-expression of pBAD and pRSF. (B) Purification of pRSF and pBAD plasmids by nickel column and / or amylose column purification. FT = Flow through or proteins from the lysate unbound to the column. Elution B and C contained 20 mM and 200 mM imidazole respectively. Ni = nickel column. (C) Extended analysis of the purification process of the co-expressed actinin-1 and actinin-4 proteins. 1X and 5X indicate concentration of the eluted proteins. (D) Purified singly and co-expressed actinin-1 and actinin-4 proteins were run on a Native PAGE gel and analysed by Coomassie staining or (E) western blotting using anti-actinin-1 (Santacruz H2) or anti-actinin-4 (Immunoglobe antibodies, with detection using IR700 and IR800 antibodies (Li-Cor Biosciences).*

Analysis of heterodimer formation using transfected HEK293 lysates was then carried out. When the actinin-2 rod domain GFP and actinin-2 rod domain mCherry constructs were expressed on the same plasmid in cells, heterodimers were formed, evident as a band running between the mCherry and GFP tagged proteins on a Native PAGE gel and having a yellow colour on the Typhoon fluorescence imager (Figure 3.3.8.2 A). It was next assessed if the lysates containing actinin-2 mCherry or actinin-2 GFP could form heterodimers *in-vitro* by mixing, heating and cooling. Heterodimers were formed by mixing lysates at 4˚C or at 37˚ C for 1 hour, although a greater quantity of heterodimers were formed at 37˚C.

Heterodimer formation was also assessed at 55˚C, however proteins aggregated and did not enter the gel (Figure 3.3.8.2 B). The formation of heterodimers over several time points at 4˚C and 37˚C was then assessed. Heterodimers were first observed after 2 hours when mixed at 4˚C. At 37˚C, heterodimer formation was observed after just 10 minutes (Figure 3.3.8.2 C). It was noted that assessing the dimer stability in a buffer without detergent may be more physiologically relevant and hence lysis of the cells expressing the actinin-2 rod proteins was carried out by alternative lysis protocols, with their efficiency demonstrated in Figure 3.3.8.2 D. A repeat of the mixing and heating of samples with and without detergent revealed that no heterodimers were observed in the absence of detergent after 1 hour but were present in samples with detergent after 10 minutes (Figure 3.3.8.2 E). As the dimer is reported to be relatively stable at 37˚C, the formation of heterodimers in buffer without

detergent was assessed at higher temperatures (Figure 3.3.8.2 F). Heterodimer formation was unclear at 45℃ and 42℃ in the buffer used.

Figure 3.3.8.2

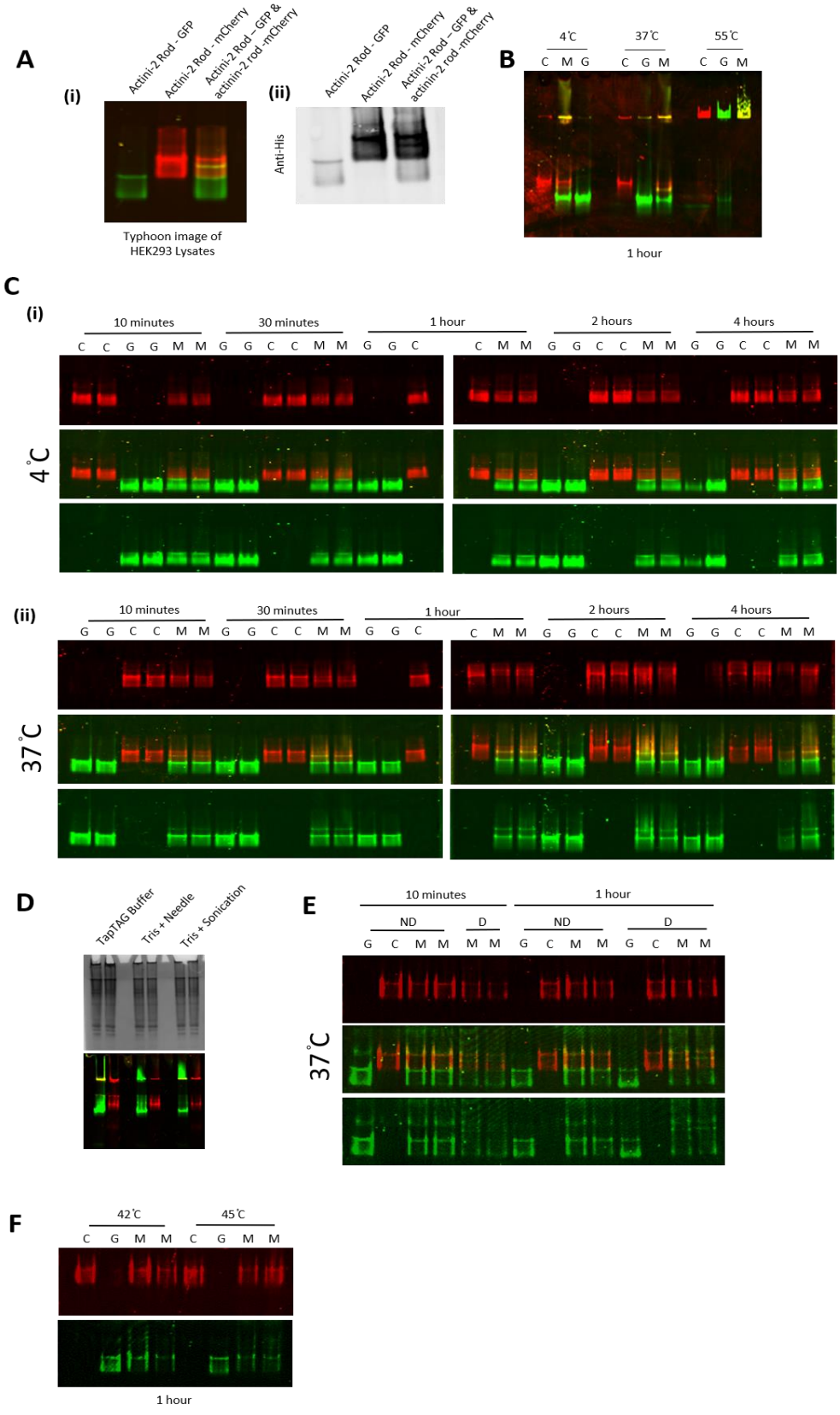
A
(i)
Actinin-2 Rod - GFP
Actinin-2 Rod - mCherry
Actinin-2 Rod – GFP & actinin-2 rod -mCherry
Typhoon image of HEK293 Lysates
(ii)
Anti-His
B
4˚C
37˚C
55˚C
C M G C G M C G M
1 hour
C
(i)
10 minutes
30 minutes
1 hour
2 hours
4 hours
4˚C
(ii)
37˚C
D
TapTAG Buffer
Tris + Needle
Tris + Sonication
E
ND
D
37˚C
F
42˚C
45˚C
C G M M C G M M
1 hour

Figure 3.3.8.2 Analysis of heterodimer formation using lysates from HEK293 cells expressing actinin-2 rod -GFP and / or actinin-2 rod mCherry. *(A) Lysates from cells expressing actinin-2 rod -GFP and / or actinin-2 rod mCherry run on a Native PAGE gel and imaged using the Typhoon fluorescence imager (i) or (ii) by western blotting and detection by anti-His antibody (Genscript). (B) In-vitro formation of heterodimers by mixing of actinin-2 rod GFP and actinin-2 rod mCherry at the indicated temperatures for 1 hour and analysis on Native-PAGE and imaging using the fluorescent imager. (C) In-vitro formation of heterodimers by mixing of actinin-2 rod GFP and actinin-2 rod mCherry 4˚C or at 37˚C for the indicated time periods and analysis on Native-PAGE and imaging using the fluorescent imager. (D) Trial of detergent-free lysis methods. Tris = (10 mM Tris pH 7.5, 100 mM NaCl, 0.1 mM DTT, protease inhibitor (Roche)). Needle = repeated aspiration and release of lysate through needle. (E) In-vitro formation of heterodimers by mixing of actinin-2 rod GFP and actinin-2 rod mCherry at 37˚C for the indicated time periods and analysis on Native-PAGE and imaging using the fluorescent imager. D = detergent added (1% NP-40), ND= no detergent. (F) In-vitro formation of heterodimers without detergent by mixing of actinin-2 rod GFP and actinin-2 rod mCherry at 42˚C or 45˚C for 1 hour and analysis on Native-PAGE and imaging using the fluorescent imager. For all experiments, whole cell lysates from HEK293 cells expressing tagged actinin-2 rod proteins were used. C = actinin-2 rod mCherry, G = actinin-2 rod GFP, M = mixed lysates containing actinin-2 rod mCherry & actinin-2 rod GFP.*

3.4 Discussion

In this chapter I aimed to establish a model of thrombopoiesis and assess the impact of CMTP causing mutations in actinin-1 on this process. I initially assessed two megakaryocytic cell lines, MEG-01 and CMK, for their suitability as experimental models of thrombopoiesis and platelet function. The MEG-01 cell line has been reported to produce platelet-like particles *in-vitro* (Isakari et al., 2007) and so was a potential model for thrombopoiesis. The CMK cells line has been used as a model of platelet function previously (Tadokoro et al., 2011), and could be used to assess actinin-1 specific interactions in MK and platelets.

MEG-01 cells were assessed for their ability to produce proplatelets and platelet-like particles. PMA treatment of MEG-01 cells caused cells to become adherent, larger, polyploid and some cells extended processes. It was also explored whether platelet like particles were produced by the differentiated MEG-01 cells but these were not detected by microscopy. This was consistent with the absence of cell processes with bead-like features and platelet-sized tips at the end of the processes, which are reported in literature. Although MEG-01 cells reportedly produce platelet-like particles spontaneously, and the process is accelerated by PMA treatment (Isakari et al., 2007), no detectable platelet-like particles were evident under the conditions assessed in this study. This would prevent the analysis of recombinant platelets, expressing mutant actinin-1. However, the impact of mutant actinin on cell ploidy could be assessed in these cells.

A method to deliver CMTP-related mutant actinin-1 constructs to MEG-01 and CMK cells was then explored. The efficiency of DNA delivery to CMK and MEG-01 cells was poor using all methods trialled. Nucleofection, using protocol T-01 to deliver pEGFP, was most efficient for CMK cells, with an efficiency of 21%. Nucleofection also proved most efficient for MEG-01 cells but was poor, with an efficiency of 2.5-2.9% in various buffers using protocol X-05. Nucleofection also reduced cell viability substantially for both MEG-01 and CMK cells. However, assessment of cells by flow cytometry was possible as it allowed gating of live, GFP-expressing cells. Lipofectamine-2000 transfected very few cells (<5%) but did not impact cell viability. Hence, it remained a useful tool to examine cells by microscopy

Actinin-1 has a role in cytokinesis by regulating the actin cortical network during cleavage furrow formation and over expression of actinin-1 causes an increase in cell ploidy through a failure of cytokinesis (Mukhina et al., 2007). Although cytokinesis is a ubiquitous cell

process, differentiating megakaryocytes undergo a process called endomitosis, which involves a failure of cytokinesis and generation of polyploid cells (Mazzi et al., 2018). Hence it was of interest to explore whether actinin-1 mutations could impact platelet count through an effect on the actin network and the process of endomitosis. CMTP causing mutations in actinin-1 cause an increased association with actin (Murphy et al., 2016; O'Sullivan et al., 2019), but the effect of mutant actinin-1 on actin cytoskeletal organisation in MK remains unclear. CMTP-causing actinin-1 mutants were reported to disrupt the actin cytoskeleton in transduced murine megakaryocytes (Kunishima et al., 2013). The assessment of megakaryocytes from a single ACTN1 CMTP patient was carried out and revealed a disorganised cytoplasm by electron microscopy, while culture of the patients haematopoietic stem cells resulted in a normal rate of MK colony formation (Guéguen et al., 2013). However, in our assessment of the actin cytoskeleton in actinin-1 mutant expressing HeLa or MEG-01 cells, no disruption to the actin cytoskeleton was noted (O'Sullivan et al., 2019). In this study, an increase in the proportion of polyploid cells was noted in cells over-expressing WT or mutant actinin-1 but there was no significant difference in ploidy between WT and mutant expressing cells. . Similar to the lack of disruption to the actin cytoskeleton previously reported, an effect on cytokinesis by mutants would impact cells other than MK, which is not the case in CMTP patients, and so the lack of variation is reasonable. It is noted that transfection was carried out 48 hours prior to analysis, during a 12 day differentiation process. Although the transient over-expression of actinin in these cells appeared to affect ploidy at day 12, it is possible that stable expression of the tagged actinin over the entire differentiation period may have revealed a difference in ploidy between mutants and WT. The influence of endogenous actinin-1 also cannot be excluded here, and the study of MK endomitosis in actinin-1 knockdown cells could be of interest to further assess this.

As the production of proplatelets could not be assessed in the MK cell lines, a murine fetal liver derived MK cell model was established. Following a BSA gradient enrichment, a significant proportion of the isolated MK produced proplatelets. Additionally, adherent MK formed podosomes, which are thought to degrade the extracellular matrix during proplatelet extension into the bloodstream (Schachtner et al., 2013). It was first shown in this study that actinin is present in both proplatelets and podosomes of primary MKs by immunofluorescent staining of fixed cells. The actin cytoskeleton functions in proplatelets to increase branching and subsequently the number of proplatelet tips from which platelets are released (Italiano et al., 1999). It has previously been reported that expression

of actinin-1 with CMTP mutations causes a reduced number of proplatelets and proplatelet tips in murine megakaryocytes (Kunishima et al., 2013). As CMTP mutations in actinin-1 cause an increased association of actinin with actin, it is possible that mutations impact actin function in these structures. Vinculin, WASP and MHCIIa also showed staining at the podosomes and appeared co-localised with actin and actinin (total actinin and actinin-4). The proteins assessed showed brightest staining at the proplatelet tips, platelet sized swellings along the proplatelets and at branch points along the proplatelets. Localisation along the proplatelet shaft and at the branching or swelling structures was not possible at the resolution of images obtained during this study but would be of interest to assess in future study. WASP deficiencies cause premature proplatelet release (Sabri et al., 2006). Myosin IIA mutations also decrease the number of proplatelets formed (Poulter & Thomas, 2015).

A study of dendritic cells showed that actin is present in several components of podosomes; the protrusive core, connecting the core to the outer vinculin / talin ring, and connecting cores of adjacent podosomes (Van Den Dries et al., 2013). Actin has a mechanosensing and protrusive role in podosomes (van den Dries et al., 2019, 2013). The finding of actinin in these structures in primary MKs is hence unsurprising, given the importance of actin in the structures and the finding from other cells types. In dendritic cell podosomes, actinin is localised to the peripheral actin module of the podosome core, cross links actin filaments here, partially colocalises with vinculin at the ventral side and is closely associated with the integrins (van den Dries et al., 2019). In podosomes, talin and integrins co-localise at the outer ring, thought to cause constitutively activated integrins for adhesion (Van Den Dries et al., 2013). It is interesting to note that actinin is reported to regulate integrin activation through competition with talin (Shams & Mofrad, 2017). Additionally, mechanical stimuli may regulate exposure of the actinin vinculin-binding site, which is also present at the podosome outer ring (Shams et al., 2012). Hence beyond a structural role in actin crosslinking, actinin may have other regulatory roles in podosomes. The importance of podosomes in platelet formation is a topic of current research and the finding of actinin, associated with CMTP, may support a role for these structures in some aspect of thrombopoiesis. Macrothrombocytopenia associated with MHCIIA mutations (Eckly et al., 2020) and deficiencies in the actin regulatory proteins twinfilin and cofilin (Becker et al., 2020) also impacted podosome numbers, supporting their role in the disease. It would be of interest to elucidate the precise role of actinin in podosomes and the impact of CMTP mutations on podosomes.

Following the identification of actinin in proplatelets and podosomes in primary MKs, it was of interest to assess if these structures were affected by the expression of CMTP related mutant actinin-1. To assess this, I aimed to express GFP tagged mutant actinin-1 in primary murine megakaryocytes. Various methods were trialled, namely Lipofectamine-2000, electroporation, nucleofection and lentiviral transduction, but no method resulted in expression levels adequate to carry out experiments.

In assessing the role of actinin-1 in thrombopoiesis and platelets, it was important to consider the presence of other actinin isoforms in these cells and the roles actinin-1 might play which cannot be compensated for by other actinin isoforms. Of particular interest is the calcium-sensitive non-muscle actinin-4. As previously discussed, actinin-4 mutations cause the kidney disorder FSGS but no apparent non-renal pathology, suggesting an isoform specific function in the kidney podocytes (Kaplan et al., 2000). A similar phenomenon may exist for actinin-1 in MK and platelets. In this study, the relative amounts of actinin-1 and actinin-4 were quantified in platelets and it was found that there is on average 14.25 ± 3.76 times more actinin-1 than actinin-4 in platelets. A previous platelet proteomic study reported an approximate 2:1 ratio of actinin-1 to actinin-4 in a pooled platelet sample from 4 donors (Burkhart et al., 2012). Protein isolation methods may have given rise to variation, but authors also note the limitation of the proteomic method used to discriminate protein isoforms with nonunique peptides reliably (Burkhart et al., 2012). In the CMK and THP-1 cell lines, this was lower at 7.2 times more actinin-1, while MEG-01 cells had slightly more actinin-4 than actinin-1. This was in contrast to the finding of approximately equal amounts of the isoforms in non-megakaryocytic cell lines (Foley & Young, 2013). It is possible that actinin-4 was over-expressed in the MK cell lines, as actinin-4 over-expression is widely reported in cancers (Honda, 2015). The relative abundance of these isoforms in healthy human megakaryocytes could be explored in future study. The apparent higher expression of actinin-1 in this lineage may contribute to the tissue-specific nature of ACTN1 related CMTP.

Another consideration in this analysis is the formation of actinin1/4 heterodimers. It was previously reported that in various cell lines expressing approximately equal amounts of actinin-1 and actinin-4, heterodimers comprise 50% of actinin, making them the predominant isoform (Foley & Young, 2013). The higher expression of actinin-1 in platelets and MK likely skews the relative abundance of the homo and heterodimers. It is

conceivable that more actinin-1 homodimers and less actinin-4 homodimers or actinin1/4 heterodimers are present in these cells and this could explain the lack of compensation by actinin-4 in platelets and megakaryocytes of CMTP patients. This could be assessed in future study.

Actinin isomers are also known to vary in their interactions with other cellular components (Foley & Young, 2013). It was of interest to optimise a method of assessing the actinin isoform-specific interactions in MK and platelets and consider the impact CMTP mutations may have on these interactions. Although two antibodies efficiently immunoprecipitated actinin-1 and actinin-4 (Sigma BM 75.2 and Honda, respectively), both also immunoprecipitated a lesser amount of the alternate isoform, likely indicating the presence of actinin 1/4 heterodimers, or cross reactivity of the Sigma BM 75.2 antibody with ACTN4 (Foley, 2013). To assess a known interactor of actinin, the immunoprecipitated samples were probed for CD61 (β3 integrin), which is an interactor of actinin of particular interest in platelet and MK biology (Tadokoro et al., 2011). Actinin has a role in maintaining integrin αIIbβ3 in a low-affinity state (Tadokoro et al., 2011) and loss of integrin activation regulation has been implicated in macrothrombocytopenia related to Glanzmann's Thrombasthenia and Filamin A mutations (Bury et al., 2016; Donada et al., 2019), making it an interesting interaction to explore in the context of actinin-1 related CMTP. Previous IP experiments demonstrating the CD61-actinin interaction have probed CD61 pull-down samples with the purportedly actinin-1 specific Sigma antibody BM 75.2 (Feng et al., 2002; Tadokoro et al., 2011) or an antibody that reacts with actinin-1 and actinin-4 (Roca-Cusachs et al., 2013) in CMK cells (Tadokoro et al., 2011), platelets (Feng et al., 2002; Tadokoro et al., 2011) and fibroblasts (Roca-Cusachs et al., 2013). The Sigma BM 75.2 was found to cross-react with actinin-4 by western blot in previous work (Foley, 2013). Hence it has not been distinguished whether actinin-1 alone or actinin-4 and actinin 1/4 heterodimers are also involved in the interaction. In this study, the Sigma BM 75.2 antibody did not pull down CD61, despite efficient actinin-1 pull-down. It is possible that immunoprecipitation of CD61 would have enriched CD61-actinin complexes more efficiently. However, the Honda antibody, specific for actinin-4, pulled down CD61 and actinin-1, possibly as actinin 1/4 heterodimers. As there is less actinin-4 than actinin-1 in CMK cells, possibly the actinin-CD61 complexes were more efficiently enriched by this approach. Hence it appears that actinin-4 and/or actinin 1/4 heterodimers also interact with CD61. Optimisation of the pull down of actinin-1/ CD61 complexes is needed to further explore whether CMTP mutations in actinin-1 affect this interaction.

To further study actinin-1/4 heterodimers in the context of formation of heterodimers in the presence of CMTP mutations and to study actinin-1 / actinin-4 specific interactions, a method to express and purify these proteins *in-vitro* was trialled. Initially, intracellular formation of heterodimers in E. coli BL21 was trialled by the co-expression of actinin-1-His and actinin-4-MBP. This method did not result in clear heterodimer formation, or heterodimers were produced at a low concentration and could not be detected. The presence of non-specific or degraded proteins in the Nickel column elution is noted, possibly indicating poor purification efficiency. Additionally, purification of actinin-4 was poor as the column failed to concentrate the protein, despite the column efficiently purifying MBP alone. As heterodimers were known to be formed in mammalian cells (Foley, 2013), expression of tagged actinin-2 rod proteins was carried out in HEK293 cells. The expression of fluorescently tagged proteins allowed analysis of the heterodimers formed without purification. This system worked well, as heterodimers formed in cells co-expressing the GFP and mCherry tagged constructs. The analysis of heterodimers by native PAGE and Typhoon imaging was also more sensitive than analysis by SDS-PAGE and Coomassie staining. Using this imaging method, it was trialled whether heterodimers could be formed *in-vitro* by heating, mixing, and cooling the tagged proteins. It was found that heterodimers could be formed *in-vitro* in this way, and the efficiency of this was increased in the presence of detergent. In future experiments, this could be an alternative method to obtain purified heterodimers or to assess the efficiency of heterodimer formation.

In conclusion, the MEG-01 cell line was a suitable model to assess MK differentiation and the CMK cell line was suitable to explore actinin-1 specific interactions in MK. However, no method of DNA delivery trialled was efficient for these cell lines and this technical challenge hinders their suitability to assess CMTP causing actinin-1 mutations. These cell lines were not an optimal model of proplatelet and platelet production, under the conditions assessed in this study. However, the impacts of CMTP mutations on cell ploidy could be assessed and did not appear to affect this process. Primary murine megakaryocytes were a good model of this thrombopoiesis but delivery of DNA to these cells is technically challenging and was not achieved in this study. Alternative viral-based methods or micro-injection could be assessed in future study. Despite the challenges in assessing CMTP-causing mutations in actinin-1 in these cell models, the specific role of WT actinin-1 in MK and platelets could be assessed in these cells and potential areas of interest are highlighted in this chapter. Future work could involve the establishment of a mouse

model of actinin-1 related CMTP to assess the role of actinin on megakaryocytes and thrombopoiesis.

Actinin-1 and another actinin isoform, actinin-4, are localised to proplatelets and podosomes in MK, and potentially play a role in platelet formation at these structures. Although an interaction between CD61 and actinin-1 was not demonstrated in this study, an interaction between CD61 and actinin-4 and/or actinin-1/4 heterodimers was shown, and the specificity of this actinin-CD61 interaction may be of interest to explore further. It was also shown that actinin-1 is more abundant in both CMK cell lines and platelets than actinin-4, possibly explaining in part the tissue-specific nature of actinin-1 related CMTP. The ability of CMTP mutated actinin-1 to form heterodimers, and the role of actinin heterodimers in MK and platelets are questions of interest further to the specific role actinin-1 plays in these cells. I have also trialled the expression and purifications of actinin heterodimers which could be a useful experimental tool for this purpose. Overall, much is yet to learn about the role of actinin-1 in MK and platelets and this study may guide future work in the technical aspects of exploring this.

4.0 Platelet Hyperactivation in Multiple Myeloma is also Evident in Patients with Premalignant Monoclonal Gammopathy of Undetermined Significance

Chapter 4 details work published in O'Sullivan, L.R., Meade-Murphy, G., Gilligan, O.M., Mykytiv, V., Young, P.W. and Cahill, M.R. (2021), Platelet hyperactivation in multiple myeloma is also evident in patients with premalignant monoclonal gammopathy of undetermined significance. Br J Haematol, 192: 322 332. In the presented work, I designed the study and wrote the published manuscript with co-authors G. Meade-Murphy, P. Young and M.R. Cahill. V. Mykytiv, O. Gilligan and M.R. Cahill recruited and obtained informed consent from patients and healthy controls. G Meade-Murphy performed the experiment presented in Supplementary Table 4.6. I performed all other experiments and data analysis.

4.1 Introduction

Multiple myeloma (MM) is a haematological malignancy affecting bone marrow plasma cells characterised by the clonal production of non-functioning immunoglobulins, termed paraproteins. Where paraproteins are detected in the absence of uncontrolled proliferation of plasma cells (<10% bone marrow cells) or associated symptoms, the diagnosis of monoclonal gammopathy of undetermined significance (MGUS) is made (Rajkumar et al., 2014). MGUS is very common and has a reported prevalence of 2-4% in the over 60's with a higher prevalence in Afro-Caribbean ethnic groups (Landgren et al., 2017). The transition from MGUS to MM occurs at a rate of approximately 1% per annum (Rajkumar et al., 2014). Smouldering Myeloma (SM) are an intermediate group, with higher risk of progression. As with various cancers, MM is associated with an increased thrombotic risk and population-based study has determined a hazard ratio of 7.5 for MM and 3.4 for MGUS for venous thromboembolism (VTE) in the year following diagnosis (S. Y. Kristinsson et al., 2010). In addition, immunomodulatory drugs, including lenalidomide and thalidomide, dexamethasone and anthracyclines contribute to clotting risk (Fotiou et al., 2019), necessitating VTE prophylaxis with aspirin or low molecular weight heparin (LMWH) in MM patients undergoing treatment with these drugs (NICE, 2018). There is increasing evidence of VTE risk in MGUS patients (Gregersen et al., 2011; S. Y. Kristinsson et al., 2008, 2010; Muslimani et al., 2009; Sallah, Husain, Wan, Vos, & Nguyen, 2004; Srkalovic et al., 2004), particularly in patients with paraprotein levels > 16 g/L (Sallah et al., 2004). Despite

this increased risk for MGUS, there is little research on this question and no agreed preventive imperative or paradigm. The identification of criteria that better stratify newly diagnosed MGUS, SM and MM patients in terms of their thrombotic risk could yield significant clinical benefits at this time.

Current understanding of the role of platelet dysregulation in the prothrombotic state in MGUS, SM and MM is incomplete. Platelet hyperactivation, as reflected by increased platelet surface P-selectin levels, has been reported in untreated, newly diagnosed MM patients (Robak et al., 2012; Takagi et al., 2018), as well as in MGUS patients (Takagi et al., 2018). Soluble P-selectin levels have also been reported as elevated in newly diagnosed MM patients (Lemancewicz et al., 2014). Another indicator of platelet activation, cell-surface exposure of phosphatidylserine (PS) was also shown to be elevated in MM (Guo et al., 2018). Hence, preliminary evidence suggests that platelet hyperactivation co-exists with the pro-thrombotic state in MGUS and MM. Various aspects of platelet responsiveness have also been assessed in MGUS and MM. For example, Cieslar *et al.* (2002) reported diminished platelet aggregation responses to collagen, ADP and thrombin receptor-activating peptides (TRAPs) in MM patients at various disease and treatment stages. Some of these changes may be therapy related. Closure times from a PFA100 analysis measured in the presence of collagen/ADP and collagen/epinephrine were found to be increased in MM patients at diagnosis compared to healthy controls (Robak et al., 2012). Decreased platelet aggregation as well as reduced platelet surface P-selectin exposure were reported in MM compared to MGUS patients in response to *in-vitro* activation in another study (Egan et al., 2014). Platelet hyperactivation at baseline in MM and MGUS combined with these observations of decreased responsiveness could be indicative of a phenomenon termed platelet exhaustion, that has been described in Myeloproliferative Neoplasm and other malignancies (Boneu et al., 1984; Mannucci et al., 1989), where 'resting platelets' have been shown to have increased baseline expression of platelet activation markers (Cahill *et al.*, 1996). However, this is a hypothesis that requires further investigation.

Here we examined platelet activation in newly diagnosed MGUS, SM and MM patients by flow cytometry using the most comprehensive panel of platelet activation markers employed to date (integrin αIIbβ3 activation assessed by PAC-1 binding, platelet surface exposure of P-selectin and CD63, phosphatidylserine (PS) exposure detected by Annexin V binding, and platelet-leucocyte aggregate formation). These parameters were measured both at baseline and following stimulation with ADP and TRAP6 in order to assess platelet responsiveness to agonists *in-vitro*. Reticulated (RNA positive) platelet levels and Platelet-

Associated Immunoglobulins (PAIg) were also assessed. This work thus extends previous studies of platelet function in MM and addresses the under-representation of premalignant MGUS patients in the published literature. We find that while baseline cell surface markers of platelet activation were generally elevated in MGUS and SM/MM patients, this surprisingly, was more pronounced and only statistically significant for MGUS patients compared to healthy controls. Interestingly, for a subset of MGUS and SM/MM patients, multiple markers of platelet activation were elevated. Some evidence of platelet hyporesponsiveness was also revealed, but this was only significant for certain markers and stimuli in MGUS patients. PAIg were also elevated in a subset of patients. Overall, our findings paint a fuller picture of the platelet activation status across the spectrum of disease progression in myeloma and reveal a previously unappreciated degree of platelet dysregulation in premalignant individuals with MGUS, a condition which is common in the over 60's. This finding in itself merits further investigation and if substantiated with further data may impact on future therapeutic consideration.

4.2 Methods

4.2.1 Patient Recruitment

19 MGUS, 12 MM and 4 SM patients were recruited for this study between February 2018 and October 2019 with informed consent following ethical approval from the local Clinical Research Ethics Committee (CREC) and in accordance with the Declaration of Helsinki. Patients were recruited according to the following criteria:

***Patient** Selection*

Exclusion Criteria for Participation

1. Anti-myeloma therapy use (prior to start of participation in the study)
2. Current malignancy other than myeloma
3. Known bleeding or thrombotic disorder
4. Abnormal liver or renal function
5. Recent (<1 month prior to collection) surgery or blood transfusion
6. Recent (<2 weeks prior to collection)antithrombotic, antibiotic, antiviral or steroid-based therapy use.

Inclusion Criteria for Participation

1. MM patients: diagnosis based on International Myeloma Working Group diagnostic criteria (Rajkumar et al., 2014).

Healthy Control Selection

Exclusion Criteria for Participation

1. Current or previous malignancy
2. Known bleeding or thrombotic disorder
3. Thrombocytopenia
4. Previous clot (DVT/PE/VTE)
5. Abnormal liver or renal function
6. Recent (<1 month prior to collection) surgery or blood transfusion
7. Recent (<2 weeks prior to collection) antithrombotic, antibiotic, antiviral or steroid-based therapy use.

Inclusion Criteria for Participation

1. Age 45 years or older

MGUS and SM patients were recruited at outpatient clinic appointments and consecutive newly diagnosed MM patients who met criteria for study were recruited. SM and MM patients were grouped for analysis as these patients had similar paraprotein levels, and as clinically relevant renal or liver dysfunction was an exclusion criterion, these patients were clinically similar in this regard. Healthy controls were recruited based on described exclusion criteria and similar age range to patients. 20 healthy controls were recruited but 4 of these (over 50) were excluded from the study following a positive paraprotein screen, resulting in a median age lower than the patient groups, as shown in Table 4.2.1. This disparity was considered in subsequent analysis. Platelet-related parameters of the participants are also outlined in Table 4.2.1, and show a lower platelet count in MM, although non-significant, including when stratified by age and sex (Supplementary Table 4.1).

Table 4.2.1: Characteristics of study participants. Median and IQR are shown and analysis by Kruskall–Wallis one-way ANOVA was used to calculate P value reported.

Parameter	Parameter Median (IQR)			P-Value
	HC	MGUS	SM / MM	
n	16	19	16	NA
Age (Years)	48 (38 - 61)	69 (62 – 71)*	64 (56 – 74)*	0.003
Age Range (Years)	35 - 75	50 - 83	36 - 92	
Sex (n) [%]				
Male	7 [40]	8 [42]	13 [81]*	0.036
Female	9 [60]	11 [58]	3 [19]*	
Paraprotein (g/L)	0	13 (6.6 – 17.1)*+	27.9 (18.4 – 38.6)*+	<0.001
Antibody Class (n) [%]				
IgG	NA	15 [79]	13 [81.25]	NA
IgA	NA	2 [10.5]	2 [12.5]	NA
IgG & IgA	NA	2 [10.5]	1 [6.25]	NA
Platelet Count x 10^9 / L	278 (268 – 326)	256 (182 – 326)	204.5 (182 – 282)	0.051
Mean Platelet Volume (fl)	10.9 (10.1 – 11.2)	10.4 (9.7– 11.3)	10.1 (9.8 – 10.75)	0.314
% RNA – positive Platelets	2.11 (1.8 – 8.2)	1.88 (0.65 – 10.2)	2.2 (0.60 – 3.66)	0.700
Leucocyte Count x 10^9 / L	5.8 (4.9 – 7.2)	6.8 (5.7 – 7.5)	4.9 (3.9 – 7.2)	0.065

HC, healthy control; MGUS, monoclonal gammopathy of undetermined significance; MM, multiple myeloma; SM, smouldering myeloma. For %RNA-positive analysis, a smaller sample size was assessed: HC (n = 7), MGUS (n = 8), SM/MM (n = 9). NA, not applicable. Asterisks (*) indicate significant difference between patient group and HC group (P < 0·05), and (†) indicates significant difference between patient groups (P < 0·05), when pairwise comparison was carried out.

4.2.2 Assessment of Platelet Activation Status and Reactivity by Flow cytometry

Whole blood was collected into 3.2% sodium citrate vacutainers (BD) and stained for flow cytometry within 30 minutes of venepuncture (Pearson et al., 2009). For staining, whole blood was diluted 1:15 in 1% BSA / PBS and stained with anti CD61- PerCP (BioLegend product no. 336410) or IgG- PerCP isotype control (product no. 400148) and appropriate activation marker. Antibodies used were from Biolegend and as follows : anti-CD41/CD61 (PAC-1)-FITC (product no. 362804), anti-CD63-APC (product no.353008), anti-P-selectin-PE (product no. 304906), anti-Annexin V-FITC (product no. 640906), anti-CD45-FITC (product no. 304006), anti-CD66-APC (product no. 305118), anti-CD14-APC (product no. 367118) or appropriate isotype controls. Staining was carried out for 15 minutes at room temperature. Where platelet reactivity was assessed, whole blood was diluted as described with addition of ADP to final concentration of 10 µM or TRAP-6 (Bachem H7764) to final concentration of 100 µM. *In-vitro* activation was carried out for 15 minutes at room temperature. Following activation and immunolabelling, samples were fixed in sterile filtered 1% paraformaldehyde (PFA)/PBS and analysed using the BD Accuri C6 flow cytometer 30 minutes to 3 hours after fixation.

To analyse platelet activation marker levels, platelets were selected for based on FSC / SSC and CD61-PerCP staining, with the threshold set on FL-3. The selected population was then assessed in terms of activation marker status. The negative gate for each marker was established using platelets from the same individual stained with isotype controls for each marker. ADP (10 µM) was included in the staining reaction with isotype controls to ensure an accurate negative gate was selected.

To analyse platelet-leucocyte aggregates, leucocytes were selected for based on FSC / SSC and CD45-FITC staining, with the threshold set on FL-1. Granulocytes, monocytes, and lymphocytes were gated for based on characteristic FSC / SSC profile and staining for CD66 (granulocytes) and CD14 (monocytes). Each gated population was then assessed in terms of CD61-PerCP positivity, with a negative gate established by staining with a PerCP isotype control.

4.2.3 Washed Platelet Preparation

Washed platelets were prepared from whole blood in 3.2% sodium citrate. Whole blood was diluted 1:1 in wash buffer (36 mM Citric acid, 5 mM Glucose, 5 mM KCl, 2 mM CaCl2, 1 mM MgCl2, 103 mM NaCl pH 6.5) supplemented with Prostaglandin E1 (0.2 µM) (Sigma P5515) at room temperature. Samples were centrifuged at 200 x *g* for 12 minutes without brake. Platelet rich plasma (PRP) was removed from top of the tube, added to a new tube, and centrifuged under the same conditions to remove contaminating cells. PRP was removed and diluted 1:1 in wash buffer supplemented with apyrase (0.3 U/mL) (Sigma A6132) and centrifuged at 1500 x *g* for 12 minutes with low brake to pellet platelets. Cells were resuspended in resuspension buffer (10 mM HEPES, 5 mM Glucose, 3 mM KCl, 42 µM $NaHCO_3$, 0.5 mM $MgCl_3$, 140 mM NaCl) for use.

4.2.4 Reticulated Platelet Quantification

Washed platelets (~150 x 10^6 cells per sample) were fixed for 15 minutes in 1% PFA at room temperature. Following fixation, cells were stained with Thiazole Orange (TO) (Sigma – 390062) to quantify reticulated platelets, as described previously (Dale et al., 1995; Kienast & Schmitz, 1990). Cells were pelleted and resuspended in 1 mL TO solution (0.2 µg/mL TO, 2 mM EDTA, PBS) and incubated for 30 minutes in the dark at 37 °C. FL1 staining was assessed using the BD Accuri C6 flow cytometer. Platelets were initially gated for using FSC / SSC. A TO stained and unstained control for each sample was analysed in tandem. Including preliminary analysis, 7 HC samples, with normal platelet count and no known disorder that could affect platelet production, were analysed in total. The gate was adjusted such that the unstained control was at 0% positive events and HC samples fell within the range 0.5-10.8%. In this data, median (95% range) of %RP was 2.11% (1-10.41%). A gate at <10% for HC is in line with previous data on HC samples (Fujii et al., 2000; Kienast & Schmitz, 1990; Salvagno et al., 2006) and is a gating strategy that practically allowed comparison of samples analysed on different dates. Preliminary analysis demonstrated a reduction in TO signal following treatment with RNAse (data not shown). As an additional verification, a sample from an ITP patient was assessed as described and %RP was 31.95%, in line with previous study (Bonan et al., 1993; Fujii et al., 2000).

4.2.5 Analysis of Platelet-Associated Immunoglobulin (PAIg)

Washed platelets were prepared as described in 4.3.2 and analysed using the Thrombocytest flow cytometry kit as per manufacturer's instructions (Becton Dickinson, BD - 659178). Briefly, washed platelets were stained with anti-CD42a and with anti-immunoglobulin antibodies of each class. An anti-rabbit immunoglobulin antibody acted as a negative control. Normal ranges were established using samples from four HC and the assay was validated using positive controls from two Immune Thrombocytopenia patients (Supplementary Figure 4.2A).

4.2.6 Quantification of FcγRIIa in Washed Platelets

Washed platelets were prepared as described in 4.3.2 and stored at -80℃ until use. FcγRIIa analysis was based on a protocol previously published (Nazi et al., 2013, 2011). Platelet pellets were lysed in lysis buffer (20 mM Tris, pH 7.4, 150 mM NaCl, 10 mM EDTA, 1% Triton X-100) at 4℃ for 20 minutes and then centrifuged at 1200 x g for 10 minutes. A sample of lysates was used for total protein quantification by the Pierce™ BCA Protein Assay (ThermoFisher Scientific), as described in assay protocol. Supernatants were mixed with gel loading buffer (50 mM Tris pH 6.8, 5% β-ME, 2% SDS, 0.1% Bromophenol Blue, 10% Glycerol) and boiled for 15 minutes. Lysates of approximately equal protein concentrations were loaded on a 15% SDS-PAGE gel and ran at 120V for 90 mins. Gels were transferred onto PVDF membrane at 100V for 60 minutes and then blocked for one hour at room temperature in 4% milk/TBST. The blot was probed with anti- FcγRIIa (R&D Systems – BAF1460) at 1:2000 dilution by rocking overnight in 4% Milk/TBST at 4℃. After washing, blots were probed with an anti-goat IgG IR700 secondary antibody for 1 hour at 1:10,000 dilution at room temperature. Densitometry analysis was performed using Odyssey Image Studio Software (LI-COR Biosciences, Cambridge, UK). Samples were corrected based on blot of loading control anti-actinin-1 (Santacruz H2) and normalised to the average of HC control samples run on the same gel.

4.2.7 Statistical Analysis

All analysis was carried out using IBM SPSS software. Kruskall-Wallis One-Way ANOVA with post-hoc analysis by Bonferroni correction for multiple comparisons was used to assess differences between HC and patients for various parameters. To assess correlation of

relevant individual parameters across all groups and within groups, Spearman's correlation was used. Where categorical data was compared, Chi-Square analysis was used.

4.3 Results

4.3.1 Platelets are Hyper-Activated in MGUS and Multiple Myeloma Patients

Analysis of surface markers of platelet activation revealed that the median level of activated platelets is greater in patient groups for all markers examined. Median PAC-1, CD63 and Annexin V binding were significantly higher in the MGUS group (Figure 4.3.1 A, Supplementary Table 4.3)). In the SM/MM group, median levels of activated platelets were higher than HC, but this was not statistically significant. Additionally, although median P-selectin levels were higher in both patient groups, this did not reach statistical significance.

To further assess the relevance of these findings, a reference range for each platelet surface parameter was established using the 95% range of the HC group assessed and patient results were compared to this range (Figure 4.3.1 B). Patients were grouped according to the number of surface markers of platelet activation which were above the 95% range (Figure 4.3.1 C). Patient age in these groups was not significantly different, as assessed by Kruskall-Wallis One-Way ANOVA (p=0.572, data not shown). In addition, correlation analysis of age versus activation marker levels in HC or patients was non-significant (Supplementary Table 4.2).

Chi-square analysis of the relationship between participant group and the number of elevated activation markers revealed statistically significant dependence (p=0.002). 74% of MGUS patients and 38% of SM/MM patients had one or more elevated marker of platelet activation, while 81% of HC had no elevated markers of activation. Hence a sub-population of patients with hyper-activated platelets exists in the patient groups. Elevation of PAC-1, CD63 and Annexin V was common in both patient groups, while P-selectin was infrequently elevated (Fig 1D, Supplementary Fig 4.1A). There was a significant positive correlation between CD63 and other markers assessed in patients but not in HC (Supplementary Table 4.3 (B)).

Figure 4.3.1

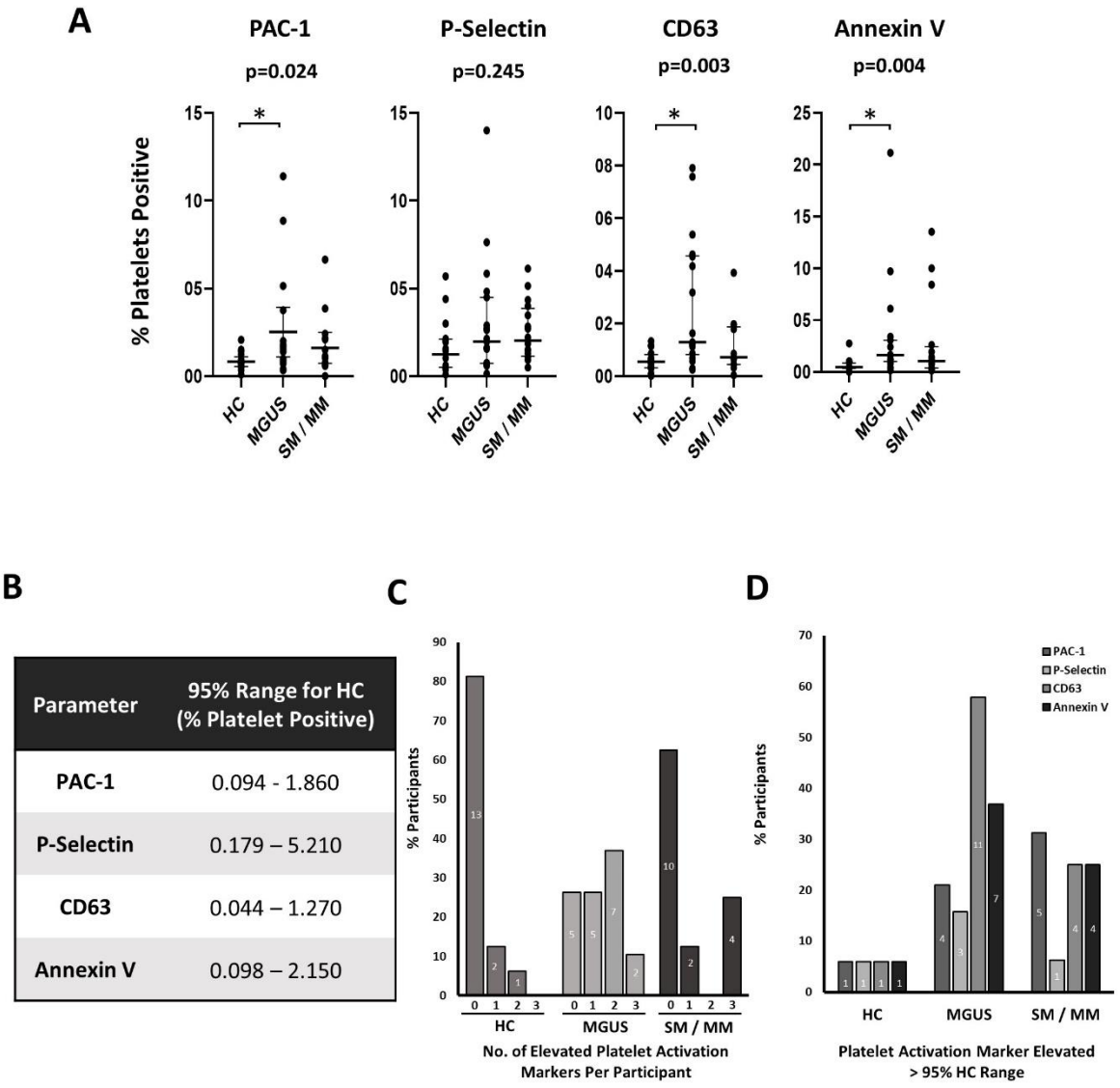

Parameter	95% Range for HC (% Platelet Positive)
PAC-1	0.094 - 1.860
P-Selectin	0.179 – 5.210
CD63	0.044 – 1.270
Annexin V	0.098 – 2.150

Figure 4.3.1 Assessment of resting platelet activation status. (A) Plots of individual values for each platelet activation marker with the median and IQR indicated (thick, wide and thin, narrow horizontal bars respectively). Statistical analysis was carried out using Kruskall–Wallis one-way ANOVA to calculate P-value shown. Asterisks (*) indicate a significant difference (P < 0·05) between healthy controls (HCs) and patient groups by post hoc analysis using Bonferroni correction for multiple comparisons. Sample size was HCs (n = 16), MGUS (n = 19), SM/MM (n = 16) for the measured parameters, with the exception of CD63 assessment. CD63 sample size was HCs (n = 16), MGUS (n = 18), SM/MM (n = 13). (B) 95% range of percentage platelets positive for each activation marker as calculated from analysis of samples from the 16 HCs. Parameters greater than the upper limit of this

95% range were considered elevated in D and E. (C) Comparison of the number of activation markers that were elevated in the HCs and the two patient groups. (D) Comparison of the incidence of elevated values for each marker in the HCs and patient groups. Numbers in white on the bars in D and E indicate the number of patients.

4.3.2 Marker-Specific Changes in Platelet Responsiveness in MGUS and MM Patients.

Platelet responsiveness was assessed by measuring changes in platelet activation markers from baseline levels following *in-vitro* activation with either ADP or TRAP-6 agonist. Platelet responsiveness in terms of PAC-1 binding appeared to decrease with increasing disease severity and surface P-selectin levels were also lower for both patient groups versus HC in response to both agonists (Figure 4.3.2, Supplementary Table 4.4 (A)), being statistically significant for P-selectin levels in MGUS patients with ADP stimulation. Changes in Annexin V and CD63 staining levels in response to both agonists appear low in all groups and no significant difference is apparent. Blood samples from a subset of patients were analysed under arterial flow conditions using a Cone and Plate(let) analyser. The parameters measured also indicated platelet hyporesponsiveness in patient groups, although not statistically significant (Supplementary Table 4.6).

Given the reduced responsiveness of platelets to agonists in patient groups, we assessed whether baseline activation status correlated with decreased P-selectin and PAC-1 levels following ADP and TRAP-6 stimulation using Spearman's correlation analysis. CD63 ($r=-0.300$, $p=0.043$) and Annexin V ($r=-0.332$, $p=0.018$) baseline levels negatively correlated with ADP responsiveness in terms of P-selectin surface expression (n=50) (Supplementary Table 4.4 (B)). Also, distinct changes in individual marker levels were evident as there was a negative correlation between Annexin V levels and PAC-1 and P-selectin levels in response to agonists (Supplementary Table 4.4 (C)).

Figure 4.3.2

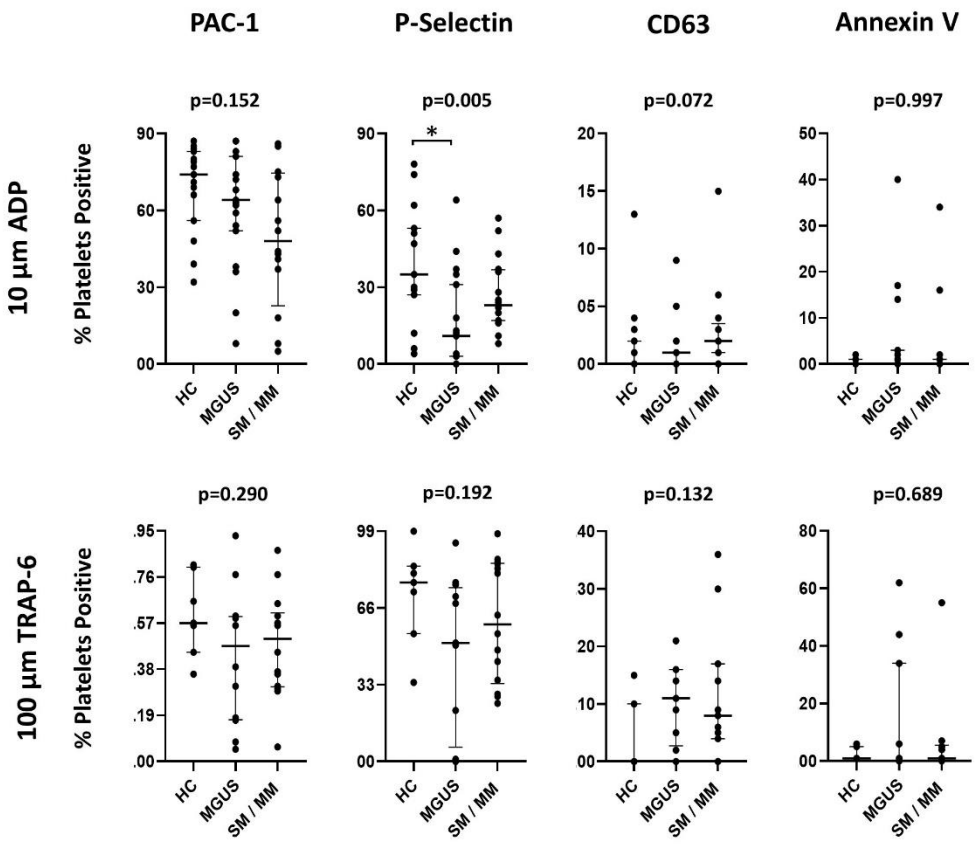

Figure 4.3.2 Assessment of change in platelet activation markers in response to in-vitro activation. *Plots show change in percentage platelets positive for each marker in individual patients in response to ADP (10 µM) or TRAP-6 (100 µM). P-value shown was calculated by Kruskall–Wallis one-way ANOVA. Asterisks (*) indicate a significant difference (P < 0·05) between the healthy controls (HCs) and the patient groups by post hoc analysis using Bonferroni correction for multiple comparisons. The median value and IQR are indicated (thick, wide and thin, narrow horizontal bars respectively). Group sample sizes for ADP reactions were HC (n = 15), MGUS (n = 19), SM/MM (n = 16, except for CD63, n = 13). Group sample sizes for TRAP-6 reactions were HC (n = 7), MGUS (n = 12), SM/MM (n = 14, except for CD63, n = 11).*

4.3.3 Platelet – Leucocyte Aggregates (PLA) and *In-vitro* Formation of PLA are Unaltered in MGUS and Myeloma Patients.

Platelet leucocyte aggregates (PLA) may be a stable indicator of platelet activation as aggregation is facilitated by various factors subsequent to activation, particularly surface expression of P-selectin, which binds to P-selectin Glycoprotein Ligand (PSGL) on leucocytes, and activated αIIbβ3, which binds via fibrinogen to Mac-1, and are elevated in certain pathological conditions (Finsterbusch et al. , 2018). PLA, and the specific leucocytes implicated, were assessed in each patient group and shown to be similar to controls (Fig 3A, Supplementary Table 4.5 (A)). In addition, no clear abnormality in *in-vitro* formation of PLA in response to agonists was seen in patient groups (Supplementary Table 4.5 (B)). P-selectin levels positively correlated with PLA formation *in-vivo* and in response to ADP (Supplementary Table 4.5 (C)).

4.3.4 Increased Platelet-Associated Immunoglobulin (PAIg) in a Subset of MGUS and SM/MM Patients

To investigate possible interactions between paraproteins and platelets we examined PAIg in a subset of study participants. 3 of 6 MGUS patients and 3 of 9 SM/MM patients assessed showed elevation of PAIg (Figure 4.3.3B). The immunoglobulin marker that was elevated in these patients also corresponded with the class of the paraprotein implicated in their disease. Patients with normal and elevated PAIg profiles were compared in terms of platelet count, platelet activation and responsiveness. Numbers were small and no significant difference in baseline activation levels and PLA levels were seen (data not shown). However, reticulated platelet levels and PAC-1 levels in response to ADP were significantly higher ($p=0.029$ & $p=0.008$, respectively) in patients with increased PAIg (Supplementary Figure 4.2 (B)).

Figure 4.3.3

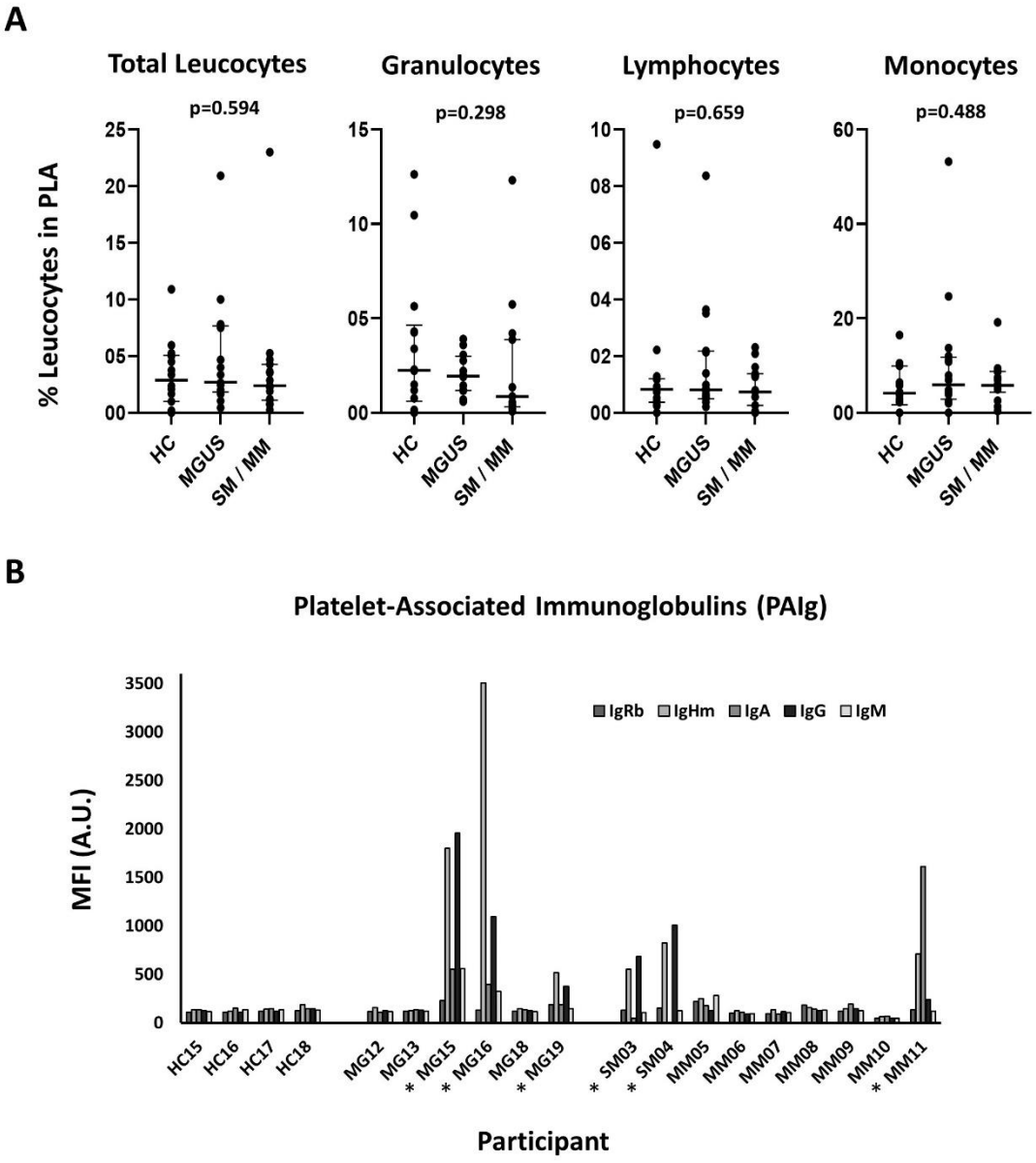

Figure 4.3.3 Assessment of circulating platelet-leucocyte aggregates (PLA) and platelet-associated immunoglobulins (PAIgs) in the resting state. *(A) Plots show individual values for PLA with the median and IQR indicated (thick, wide and thin, narrow horizontal bars respectively). P-value shown was calculated by Kruskall–Wallis one-way ANOVA. Sample size is as follows: healthy controls (HCs; n = 14), MGUS (n = 16), SM/MM (n = 15) (B) Assessment of PAIg in patients. Washed platelet samples were co-stained with anti-CD42a and anti-Ig antibodies. Anti-CD42a positive events were gated and median fluorescence intensity of anti-Ig antibodies are shown. MFI, median fluorescence intensity; A.U., arbitrary*

units; IgRb, anti-rabbit Ig negative control. IgHm, anti-human Ig positive control. Patients with a normal IgRb and elevated IgHm are indicated with an asterisk (*).

4.3.5 SM/MM Patients Have Increased Cleavage of Platelet FcγRIIa Receptor.

Following the identification of PAIg in a subset of patients, the downstream effects of such an interaction were considered. Although rare, there have been several case reports of platelet specific paraproteins being produced in MM patients. One study reported a specificity for glycoprotein IIa (DiMinno et al., 1986), while a number of cases of ITP in MM have been reported, without the specificity of the antibody determined (Gupta et al., 2000; Verdirame et al., 1985). Paraproteins specific for VWF have also been reported in MM causing defective platelet function (Bovill et al., 1986; Mohri et al., 1987; Shinagawa et al., 2005). Immunoglobulins may also interact non-specifically with Fc receptors on platelets and this interaction was explored in this study. A 40 kD Fc receptor with low affinity for monomeric IgG but stronger affinity for dimers to tetramers has been identified on platelets (Rosenfeld et al., 1985). This was later referred to as FcγRIIa (Arman et al., 2015; Qiao et al., 2015). A FcαRI IgA receptor has also been identified on platelets (Qian et al., 2008). Following activation, or stimulation via GPVI, calpain-mediated proteolysis of FcγRIIa occurs to irreversibly inactivate the receptor (Arman et al., 2015). Receptor levels and cleavage levels of the receptor in the washed platelets of HC and patients was investigated by western blotting, as shown in figure 4.3.4.

It was found that there was a significantly increased concentration of cleaved receptor in SM/MM patients versus HC and the amount of total receptor was increased non-significantly (Table 4.2.2). Similar levels of full-length and % cleaved receptor were present in the groups.

Figure 4.3.4

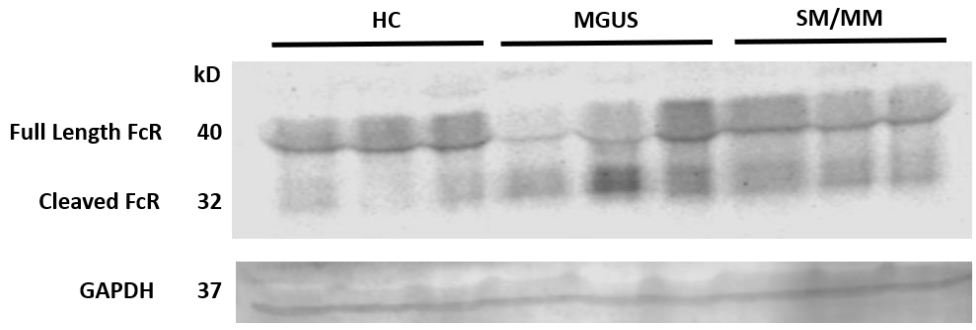

Figure 4.3.4 Representative image of the quantification of platelet FcγRIIa receptor levels and the analysis of receptor cleavage in patients and HC by western blot. *Full length (40 kD) and cleaved (32 kD) receptor are shown. GAPDH is shown as a loading control.*

Table 4.2.2 Quantification of FcγRIIa Receptor Levels and Receptor Cleavage in Washed Platelets

Parameter Mean (SD)	HC (n=14)	MGUS (n=18)	SM / MM (n=16)	P-Value
Relative Full-Length Receptor Quantification	1 (0.67)	1.11 (0.57)	1.29 (0.82)	0.517
Relative Cleaved Receptor Quantification	1 (0.45)	1.46 (0.90)	2.11 (1.57)*	0.027
Relative Total Receptor Quantification	1 (0.52)	1.19 (0.53)	1.59 (0.92)	0.058
% Cleaved Receptor	52.33 (20.17)	54.73 (9.74)	58.99 (9.35)	0.395

Receptor quantification was normalised relative to the average of HC samples on the same gel. Quantities were also corrected by quantification of a loading control (actinin-1). Total receptor was calculated as the sum of the full-length and cleaved receptor. The % cleaved receptor was calculated by the equation (relative cleaved receptor / relative total receptor x 100). Mean (SD) are shown for each group and groups were compared by One-way ANOVA to calculate p-value shown. Asterisks (*) indicate a significant difference (P < 0·05) between HC and patient groups by post hoc analysis using Dunnett's test for multiple comparisons.

As it was hypothesised that the finding of PAIg indicated interaction with and potentially activation of FcγRIIa, patients were grouped according to whether they were positive for PAIg. Only a subset of HC and patients underwent this analysis. Patients with detected PAIg (n=6) had a significantly greater amount of cleaved receptor (p=0.0049) and total receptor (p=0.005) versus HC analysed for PAIg (n=4) (Student's T-test). However, when the patients with no detected PAIg were considered (n=9), a trend for increased total and cleaved receptor levels was present in patients with PAIg but no significant difference between patients and HC was present when the groups were compared by One-way ANOVA (Figure 4.3.5).

Figure 4.3.5

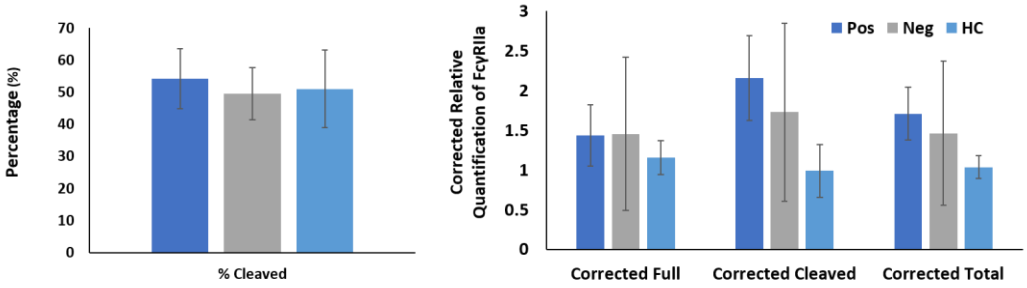

Figure 4.3.5 Comparison of FcγRIIa in patients and HC stratified by PAIg presence. *A subset of participants were analysed for PAIg as described in 4.3.4 and classified as HC (n=4), patients with PAIg (Pos) (n=6) and patients without PAIg (Neg) (n=9). FcγRIIa levels (full length, cleaved, total, % cleaved) were compared in these groups and levels are illustrated by the graph. Quantified FcγRIIa was corrected based on quantified actinin-1 in the same sample and normalised to the average of HC samples in the same blot. Bars represent mean and error bars represent SD. Groups were compared by One-way ANOVA but differences were not significant (p>0.05).*

4.3.6 Fibrinogen Levels Are Elevated in MGUS and MM Patients.

Blood clotting tests, INR and APTT are similar to HC in this study (Table 4.2.3). D-dimer levels were significantly higher in SM/MM patients (Table II). Fibrinogen levels were significantly elevated in both patient groups (Table 4.2.3) and remained elevated when adjusted for age and sex variance between groups (data not shown).

Table 4.2.3: Analysis of non-platelet coagulation parameters reveals raised levels of plasma fibrinogen in patients with MGUS and SM/MM

Parameter Median (IQR)	HC	MGUS	SM / MM	P-Value
INR	1 (1 – 1.08)	1 (1 – 1.1)	1.1 (1 – 1.2)	0.136
APTT (sec)	27 (26 - 28)	27 (25.25 – 27.75)	29.5 (25 – 32.25)	0.264
Fibrinogen (g/L)	2.6 (2.3 – 3.0)	3.5 (3.32 – 4.20)*	3.7 (2.78 – 4.60)*	0.001
D-Dimer (mg/L FEU)	<0.19 (<0.19 – 0.38)	0.37 (0.24 – 0.60)	0.40 (0.21 – 1.67)*	0.029

APTT, Activated partial thromboplastin time; FEU, fibrinogen equivalent units; INR, international normalised ratio. Plasma samples were assessed for non-cellular coagulation parameters in HC and patients, with group medians and IQR shown. Comparison between groups was carried out using Kruskall–Wallis one-way ANOVA. Asterisks (*) indicate a significant difference (P < 0·05) between HC and patient groups by post hoc analysis using Bonferroni correction for multiple comparisons.

4.4 Discussion

The identification of platelet dysregulation in MGUS and MM patients is of clinical importance. If substantiated in future studies, it opens a further opportunity for therapeutic intervention, particularly as antithrombotic therapy choice broadens. Further work is needed to improve our understanding of the pathogenesis of thrombosis in these plasma cell disorders. To date, assessment of platelets in these patients has indicated that hyperactivation is evident in MM and MGUS patients (Robak *et al*., 2012; Egan *et al.*, 2014; Lemancewicz *et al.*, 2014; Guo *et al.*, 2018; Takagi *et al.*, 2018). In this study, we aimed to extend this analysis by using additional, previously unassessed markers of platelet activation (CD63 and Platelet-Leucocyte Aggregates) and by examining the largest cohort of MGUS patients to date, as these patients were under-represented in previous studies.

Here we report that platelet activation markers are elevated *ex-vivo* above the 95% range for HC in a subset of MGUS and SM/MM patients. Unexpectedly, this was seen in a greater number of MGUS patients than SM/MM patients. However, the proportion of SM/MM patients with elevation of three or more markers was greater than for MGUS patients. Although elevated versus HC, cancer patients with relatively lower P-Selectin and PAC-1 binding at diagnosis have been reported to have an increased risk of death within one year and an association with advanced disease (Julia Riedl et al., 2017). This phenomenon could explain the finding of fewer patients with platelet hyperactivation in the SM/MM group.

The use of a panel of activation markers allowed us to evaluate platelet activation profiles in individual patients. Elevation of PAC-1, CD63 and Annexin V but not P-selectin was a common profile in patients, affecting 4 SM / MM patients and 1 MGUS patient (Supplementary Figure 4.1A). This was contrary to previous findings *(Robak et al., 2012; Takagi et al., 2018)* as median P-selectin was not significantly higher than HC for either patient group. It is possible that P-selectin was shed from the platelet surface as soluble P-selectin or as microparticles in these cases (Andre, 2004), and this could be assessed in future studies. Expression levels of these platelet markers varied in response to agonists (Supplementary Figure 4.1B & 4.1C).

In three of four patients with raised platelet P-selectin levels, CD63 levels were also raised. CD63 levels were positively correlated with all other baseline markers in patients, but not in HC. The kinetics and regulation of platelet degranulation is dependent on various factors

reviewed previously (Heijnen *et al.*, 2015; Sharda *et al.*, 2018). Discrepancy in P-selectin and CD63 levels have been noted previously in myeloproliferative disorders *(*Cahill *et al.,* 1996*)*. PAC-1 levels were not raised in these patients, but interestingly three of these patients were the only participants who experienced elevated levels of PAC-1 binding in response to agonist stimulation. Partial platelet activation without αIIbβ3 activation and engagement, followed by *in-vitro* agonist-induced activation of integrin (and PAC-1 binding), may explain this phenomenon (Huang et al., 2019; Shattil, Hoxie, Cunningham, & Brass, 1985). Internalisation of the activated integrin has also been reported (Schober *et al.*, 2003).

Annexin V was the only elevated marker in 3 of the MGUS patients. Annexin V positive platelets are reportedly a pro-thrombotic platelet sub-population *(*Reddy *et al.,* 2020*)*. They may also represent procoagulant microparticles which would be of interest to assess in light of findings of increased thrombin generation in MM (Maeve P. Crowley et al., 2016). Change in Annexin V levels in response to ADP or TRAP-6 was negatively correlated with change in PAC-1 and P-selectin levels in response to the same agonists. This further supports the presence of distinct subpopulations, although both are reported to participate in thrombus formation *(Yakimenko et al., 2012)*. Also, the release of Annexin V positive microparticles may have been stimulated but not accounted for in our analysis *(Södergren et al., 2018)*. Future work in this area could focus on these possibilities. Platelet subpopulations are discussed further in section 1.3.1.1.

The finding of varying profiles of these activation markers suggests that hyperactivation in patients may manifest as elevation of a pro-thrombotic subpopulation alone or a heterogenous profile of pro-thrombotic and aggregatory platelets.

Egan *et al.* (2014) reported platelet hyporesponsiveness to agonists, as assessed by P-selectin, in MM versus MGUS patients (HC were not examined as a reference group). By contrast, while we observe indications of hyporesponsiveness for both patient groups versus HC for P-selectin, no evidence for hyporesponsiveness in MM versus MGUS was apparent for this marker. Platelet responsiveness assessed by PAC-1 binding did show a downward trend with disease progression from HC through MGUS to SM/MM, but this did not reach statistical significance. As has been suggested previously, baseline platelet hyperactivation could conceivably result in hyporesponsiveness, as chronically activated platelets have a diminished response to agonists (Boneu et al., 1984; Mannucci et al., 1989). To examine this hypothesis in this study, baseline platelet activation markers were

correlated with change in PAC-1 and P-Selectin levels following agonist stimulation and a negative trend was apparent, significantly for CD63 and Annexin V (Supplementary Table 4.4 (B)), suggesting that activated platelets are less responsive to *in-vitro* stimulation. Platelet hyporesponsiveness to *in-vitro* stimulation has been associated with increased risk of death and VTE in cancer patients previously (Julia Riedl et al., 2017).

Median age of patients was higher than that of HC in this study in large part because of the exclusion of 4 older HC with unexpected positive paraprotein screens. Their exclusion was critical to allow valid comparison with MGUS patients. While possible age-related changes in platelet function must be kept in mind (Iyer *et al.*, 2019), our analysis suggests that the variations in activation markers reported here are unlikely to be explained by age (Supplementary Table 4.2). Previous study has indicated that platelet aggregation is increased with age (Jones, 2016; Le Blanc *et al.*, 2019), in contrast to our finding of hyporesponsiveness in patients. It has also been reported that no significant difference exists between mid-age and elderly people in terms of P-Selectin and PAC-1 binding following stimulation, although P-selectin levels were slightly reduced following ADP stimulation in older patients (Knight et al., 1997; Wagner et al., 2016). Baseline PAC-1 and P-selectin levels have been reported to negatively correlate with age (Gilstad *et al.*, 2009) and to show no change with age (Wagner et al., 2016). Neither trend was evident in patients in this study, reaffirming that platelet hyperactivation reported here is likely due to a disease-related process. Further study is needed to confirm age-related changes in such markers prior to clinical use.

Monoclonal gammopathies may facilitate platelet activation through a number of mechanisms. Platelet activation and PS exposure, providing a pro-coagulant surface that enhances factors tenase and prothrombinase activity, may be stimulated by VWF and endothelial cell activation, which has been reported as elevated in MM previously (Cosemans et al., 2011; M P Crowley et al., 2015; Fotiou et al., 2018; Takagi et al., 2018). Fibrinogen was elevated in our data in both MGUS and SM/MM groups (Table II), and may bind to platelets and stimulate degranulation and PS exposure (Mattheij et al., 2016). Hyperfibrinogenaemia has been reported in pregnancy, where it is favourable to prevent post-partum haemorrhage (James, 2007; Réger et al., 2013). It is also present in malignancy and has been suggested to impact both thrombotic risk and cancer metastasis in patients with solid tumours (Mei et al., 2017; Tian et al., 2017; Zhang et al., 2017).

We also considered that PAIg might affect platelet activation in MM. PAIg have been reported as increased in subsets of IgG MM patients in several studies (McGrath *et al.*, 1979; Morse *et al.,* 1982; Mueller-Eckhardt *et al.*, 1982; George *et al.,* 1988). Paraproteins with specificity for GPIIa (DiMinno et al., 1986) and VWF (Bovill *et al.*, 1986; Mohri *et al.,* 1987; Shinagawa *et al.,* 2005) have also been reported with platelet function affected. We report elevation of PAIg in a subset of MGUS patients and SM/MM patients. Baseline platelet activation levels were similarly raised in patients with normal and elevated PAIg, indicating that PAIg alone does not cause hyperactivation. Reticulated platelet levels were significantly higher in patients with elevated PAIg possibly due to clearance of platelets after immunoglobulin binding, as has been suggested previously (Fritz et al., 1986). We found that responsiveness in terms of PAC-1 levels after ADP stimulation were significantly increased in patients with elevated PAIg, possibly due to increased levels of reticulated platelets which are more responsive (Mcbane *et al.,* 2014). However, responsiveness was reduced compared with HC, supporting previous findings of reduced platelet aggregation and adhesion in MM patients with PAIg (McGrath et al., 1979). This may be attributed to blockade of specific surface receptors by paraproteins, hindering agonist-receptor interactions (Djunic et al., 2013). Paraprotein binding may also trigger receptor signalling that contributes to platelet hyperactivation.

It was next considered whether our finding of hyperactivation in these patients may involve Fc receptor signalling. FcγRIIa binds the Fc region of IgG with high avidity for IgG immune complexes and IgG opsonized cells (Arman et al., 2015). Aggregated IgGs may also stimulate FcγRIIa receptor signalling, involving integrin activation, degranulation and microparticle formation (Arman *et al.,* 2015). Binding of IgA to the platelet FcαRI receptor has also been demonstrated to stimulate release of pro-inflammatory cytokines, IL-1β and tissue factor (Qian et al., 2008). The finding of PAIg in subsets of SM/MM patients, and PAIg in MGUS patients with relatively low paraprotein levels, supports reports that disease-specific changes affect paraprotein specificity or aggregation to facilitate PAIg (Capra *et al.*, 1970; Benninger *et al.*, 1971; Djunic *et al.*, 2013).

1000-4000 copies of FcγRIIa are expressed on platelets and given their high cell count in the circulation (up to $2x10^{12}$ platelets in an adult with platelet count of 400 x 10^9/L), they are the main source of this receptor in humans (Qiao et al., 2015). Variation in receptor expression exists in the population which is stable over time and independent of age and sex (Rosenfeld et al., 1987). Receptor expression levels are reported to affect aggregation ability in response to aggregated IgG (Rosenfeld et al., 1987) and sensitivity to collagen

stimulation (Calverley et al., 2002). FcγRIIa is also involved in the pathogenesis of several thrombocytopenic and thrombotic disorders, including heparin-induced thrombocytopenia (HIT), immune thrombocytopenia (ITP), systemic lupus erythematosus (SLE) and increased levels of the receptor have been reported in those with diabetes and atherosclerosis (Arman et al., 2015).

It was found in this study that there was a significantly greater amount of cleaved receptor present in SM/MM versus HC. This preliminary finding suggests stimulation of the FcγRIIa receptor may be a source of platelet activation in SM/MM. However activation has also been reported with stimulation by thrombin, ADP and a Thromboxane A_2 analogue (Canobbio et al., 2006). It is thought that FcγRIIa facilitates amplification of platelet activation in response to low level stimulation by release of granule contents including ADP, as higher doses of agonists caused platelet aggregation independent of FcγRIIa (Arman et al., 2015; Canobbio et al., 2006). Hence, further work is needed to confirm whether the finding in this study is due to a direct interaction of paraproteins with FcγRIIa and whether this interaction stimulates platelet activation. The finding of elevated cleaved and total receptor levels in those with PAIg in this study supports the possibility of a direct interaction. The use of patient serum and FcγRIIa blocking antibodies on HC platelets could confirm this in future study.

Although reported as elevated (Gregersen et al., 2011; Kristinsson et al., 2008, 2010; Muslimani et al., 2009; Sallah et al., 2004; Srkalovic et al., 2004), assessing the risk of VTE due to MGUS status is complicated by the frequent presence of co-morbidities in this population due to advanced age. Just one study of VTE risk in MGUS patients used a control population that underwent paraprotein screening (Cohen *et al.*, 2010) and reported a non-significant increase. However, 16% of controls in the study had a malignancy other than MM and thus an increased VTE risk. We also note that no lower limit of paraprotein level was applied to these studies. In our study, the exclusion of patients with paraprotein level <2 g/L and any known renal, cardiac or infection-related co-morbidity, and the use of a control group that underwent paraprotein screening, provides a population where the influence of paraproteins can be interpreted. Although evidence points to a potential increase in VTE risk, further studies of MGUS patients lacking co-morbidities are needed to clarify VTE risk due to MGUS alone. Our finding of platelet hyperactivation in a subset of this group could guide interpretation of VTE risk in future studies.

Conclusion

We have shown that varying profiles of platelet hyperactivation exist in MGUS and SM/MM patients. To assess how these findings contribute to VTE risk, further clinical studies are needed. We also demonstrate the use of a panel of platelet activation markers to assess activation status and platelet responsiveness rapidly by flow cytometry in a clinical setting. Although the activation markers assessed in this study have been reported to be elevated in a variety of clinical settings (Cha et al., 2004; Soma et al., 2016; Toth et al., 2008), large scale study of their use as VTE predictive markers is limited. Further study could identify the predictive and prognostic value of these parameters with follow-up assessment of VTE incidents or progression to malignancy in the MGUS group. If substantiated, anti-platelet agents and assessment of platelet dysregulation may be of value to these patients in assessing and managing thrombotic risk as choices of available antithrombotic agents increase. MGUS patients lacking co-morbidities provide a good model to study the direct effects of paraproteins. Platelet hyperactivation in MM is also of interest in light of recent evidence of their role in MM progression (Takagi et al., 2018). The observation of platelet hyperactivation in this group may point to a further avenue for future research on the possible impact of paraproteins on platelet function and the platelet role in MM.

4.5 Supplementary Results

Supplementary Figure 4.1

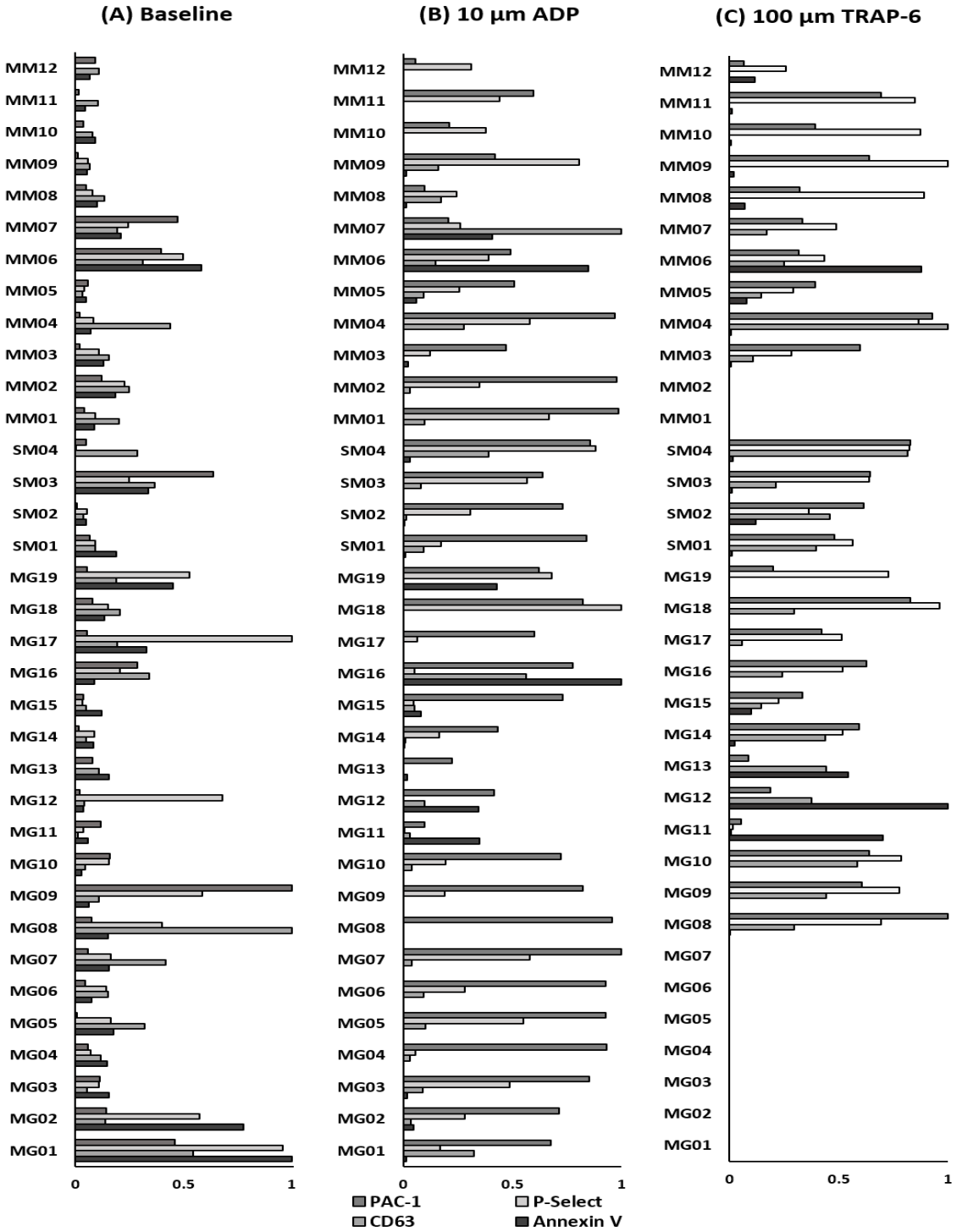

Supplementary Figure 4.1: Illustration of individual patient results for baseline platelet activation and platelet responsiveness assessment. *(A) Baseline percentage platelets positive for activation markers, (B) change in percentage platelet marker levels following stimulation by ADP and (C) TRAP-6. Scale is adjusted for each parameter so that maximum*

patient value obtained for that parameter is 1. MG= MGUS, SM = Smouldering Myeloma, MM = Multiple Myeloma. Note for MM10 - MM12, CD63 was not assessed at baseline or following agonist stimulation. For MG13, baseline CD63 was excluded as an outlier from analysis. MG01-MG07 and MM01-MM02 were not assessed for TRAP-6 responsiveness.

Supplementary Figure 4.2

A

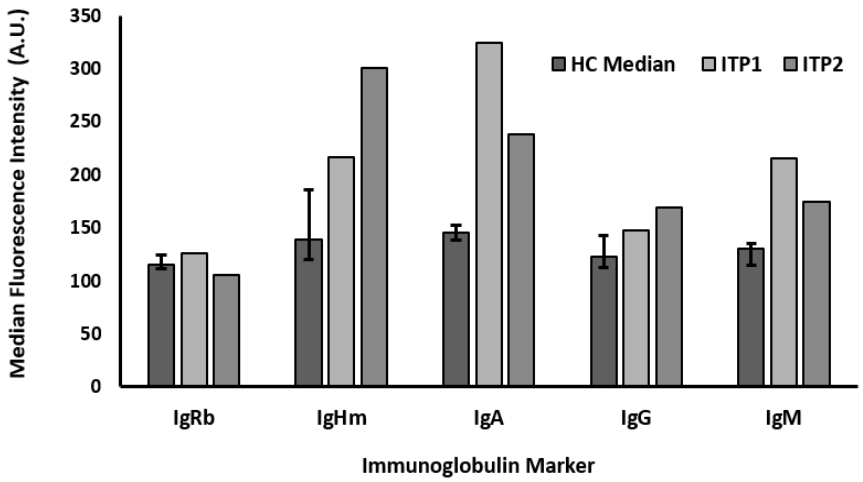

B

Parameter	Normal PAIg	Elevated PAIg	P-Value
MGUS (n)	3	3	NA
SM/MM (n)	6	3	NA
Paraprotein Level (g/L)	16.2 (12.8 – 34.2)	12.8 (6.2 – 30.8)	0.456
Platelet Count x 10^9/L	244 (199 – 322)	219 (173 – 318)	0.388
MPV (fl)	10.1 (9.70- 11.30)	9.95 (9.57 – 11.53)	0.885
% Reticulated Platelets	1.2 (0.46 – 2.28)	3.99 (1.64 – 10.0)	0.029
% PAC-1 positive (ADP)	36.41 (18.14 - 43.62)	59.75 (53.64 – 69.54)	0.008
% PAC-1 positive (TRAP-6)	31.26 (23.44 – 48.21)	59.35 (28.05 – 67.75)	0.328

Supplementary Figure 4.2: Validation of PAIg assay and assessment of patients with elevated PAIg. *(A) Washed platelet samples were co-stained with anti-CD42a and anti-immunoglobulin antibodies. Anti-CD42a positive events were gated for and Median Fluorescence Intensity (MFI) of anti-immunoglobulin antibodies are shown. IgRb = anti-rabbit immunoglobulin negative control. IgHm = anti-human immunoglobulin positive control. HC shows median MFI of 4 HC participants with error bars indicating 95% range. ITP1 and ITP2 are samples from individual immune thrombocytopenia patients. (B) Patients with normal and elevated PAIg were compared by Mann Whitney U test in terms of parameters indicated with p-value shown. Median and IQR of each parameter for each group is shown. MPV = mean platelet volume.*

Supplementary Table 4.1: Assessment of platelet count in patient groups.

Group	Parameter	HC	MGUS	SM / MM	P-Value
Females < 65 years	Median Platelet Count x 10^9 / L	277	311.5	238	0.583
	n	9	4	2	
Females > 65 years	Median Platelet Count x 10^9 / L		241		0.658
	n	1	7	1	
Males < 65 years	Median Platelet Count x 10^9 / L	309.5	289.5	226	0.103
	n	4	2	9	
Males > 65 years	Median Platelet Count x 10^9 / L	250.5	249	201.5	0.839
	n	2	7	4	

Platelet count is shown for four categories differentiated by age and sex (Biino et al., 2013). Sample size is shown for each median to indicate variability in categories which impeded reliable analysis. P-value shown was calculated using Kruskall-Wallis One-Way ANOVA

Supplementary Table 4.2: Correlation of baseline markers of platelet activation with age.

Group	Spearman's Correlation	Paraprotein Level	Baseline parameter correlated with age			
			PAC1	P-selectin	CD63	Annexin V
HC	r	NA	0.270	0.046	-0.156	0.103
	p-value	NA	0.313	0.867	0.564	0.704
MGUS & SM/MM	r	0.074	0.261	-0.051	0.009	0.292
	p-value	0.674	0.130	0.769	0.963	0.089

HC and patients were assessed individually by Spearman's Correlation to determine if age correlated with any marker of platelet activation. For CD63, HC (n=16), MGUS/SM/MM (n=31). For all other parameters HC (n=16) & MGUS/SM/MM (n=35).

Supplementary Table 4.3: Platelet activation status in HC and patients

Parameter	HC	MGUS	SM / MM	P-Value
Sample size	16	19	16	
PAC-1 (%)	0.72 (0.53 – 1.18)	1.7 (0.84 – 2.01)*	1.02 (0.60 – 2.15)	0.024
P-Selectin (%)	1.24 (0.51 – 2.11)	1.97 (0.73 – 4.49)	2.035 (1.15 – 3.87)	0.245
CD63 (%)	0.55 (0.33 – 0.82)	1.29 (0.82 – 4.57)*	0.72 (0.45 – 1.87)	0.003
Annexin V (%)	0.47 (0.34 – 0.87)	1.61 (1.01 – 3.07)*	1.05 (0.40 – 2.44)	0.004

(A) Median and IQR of baseline markers of platelet activation. Median and IQR of the percentage of platelets positive for each activation marker is shown. P-value was calculated by Kruskall-Wallis One Way ANOVA. Asterisk (*) indicates that patient group median was significantly ($p<0.05$) greater than HC in pairwise comparison with correction for multiple comparisons.

		HC					MGUS / SM/ MM			
		PAC1	P-selectin	CD63	Annexin V		PAC1	P-selectin	CD63	Annexin V
PAC-1	**r**	NA	0.468	0.321	0.683	**r**	NA	0.524	0.583	0.415
	p	NA	0.068	0.226	0.004	**p**	NA	0.001	0.001	0.013
	n	NA	16	16	16	**n**	NA	35	31	35
P-selectin	**r**	0.468	NA	0.062	0.549	**r**	0.524	NA	0.430	0.245
	p	0.068	NA	0.820	0.028	**p**	0.001	NA	0.016	0.154
	n	16	NA	16	16	**n**	35	NA	31	35
CD63	**r**	0.321	0.062	NA	0.228	**r**	0.583	0.430	NA	0.498
	p	0.226	0.820	NA	0.395	**p**	0.001	0.016	NA	0.004
	n	16	16	NA	16	**n**	31	31	NA	31
Annexin V	**r**	0.683	0.549	0.228	NA	**r**	0.415	0.245	0.498	NA
	p	0.004	0.028	0.395	NA	**p**	0.013	0.154	0.004	NA
	n	16	16	16	NA	**n**	35	35	31	NA

B) Analysis of correlation between individual markers of platelet activation. HC and patients were assessed individually by Spearman's Correlation to determine if correlation between baseline levels of activation markers existed. Correlation coefficient (r), p-value (p) and sample size (n) are indicated in the table.

Supplementary Table 4.4: Analysis of platelet responsiveness.

Parameter	Agonist	HC	MGUS	SM / MM	P-Value
PAC-1 (%)	ADP	74.22 (55.6 – 82.9)	63.65 (52.4 – 80.9)	48.17 (22.9 – 74.5)	0.152
	TRAP-6	57.02 (44.9 – 79.7)	47.49 (17.7 – 59.3)	50.12 (30.9 – 61.2)	0.290
P-Selectin (%)	ADP	34.85 (26.8 – 53.0)	10.77* (3.0 – 31.4)	23.30 (16.7 – 37.0)	0.005
	TRAP-6	76.56 (55.3 – 84.5)	50.66 (6.6 – 74.7)	58.79 (33.6 – 84.8)	0.192
CD63 (%)	ADP	0.43 (0.09 – 1.98)	0.55 (0 – 1.44)	1.51 (0.89 – 3.46)	0.072
	TRAP-6	0.23 (0 – 9.80)	10.74 (2.87 – 15.99)	7.75 (3.94 – 16.69)	0.132
Annexin V (%)	ADP	0.30 (0.09 – 0.56)	0.23 (0 – 3.23)	0.34 (0 – 1.21)	0. 997
	TRAP-6	1.12 (0.66 – 4.62)	0.28 (0 – 33.86)	0.80 (0.44 – 5.44)	0.689

(A) Median and IQR of markers of platelet responsiveness in response to ADP (10 µM) or TRAP-6 (100 µM). *Results were compared using Kruskall-Wallis One-Way ANOVA and p-values are shown. Group sample sizes for ADP reactions were HC (n=15), MGUS (n=19), SM/MM (For CD63 n=13, all other parameters n=16). Group sample sizes for TRAP-6 reactions were HC (n=7), MGUS (n=12), SM/MM (For CD63 n=11, for all other parameters n=14).*

Agonist	Parameters Correlated		n	r	p-value
ADP	Annexin V	P-selectin	50	-0.484	<0.001
		PAC-1	50	-0.211	0.142
TRAP-6	Annexin V	P-selectin	32	-0.473	0.006
		PAC-1	32	-0.479	0.006

(B) Correlation analysis of platelet PAC-1 and P-Selectin responsiveness to agonists with baseline activation markers. *Spearman's correlation of resting PAC-1, P-Selectin, CD63 and Annexin V with P-selectin and PAC-1 binding in response to ADP or TRAP-6 are shown. Spearman's correlation r and p-value shown. * P<0.05*

Baseline Parameter Correlated	Marker of Responsiveness	Agonist	n	r	p-value
PAC-1	P-selectin	ADP	50	-0.166	0.250
		TRAP-6	33	-0.189	0.292
	PAC-1	ADP	50	-0.020	0.893
		TRAP-6	33	-0.252	0.157
P-Selectin	P-selectin	ADP	50	0.080	0.579
		TRAP-6	33	0.172	0.338
	PAC-1	ADP	50	0.179	0.213
		TRAP-6	33	0.293	0.098
CD63	P-selectin	ADP	46	-0.300	0.043*
		TRAP-6	29	-0.195	0.310
	PAC-1	ADP	46	-0.018	0.904
		TRAP-6	29	-0.144	0.457
Annexin V	P-selectin	ADP	50	-0.332	0.018*
		TRAP-6	33	-0.311	0.078
	PAC-1	ADP	50	-0.147	0.308
		TRAP-6	33	-0.277	0.118

(C) Correlation analysis of individual markers of platelet activation. *Correlation between Annexin V responsiveness and P-Selectin and PAC-1 responsiveness to each agonist was assessed by Spearman's Correlation. Correlation coefficient (r), p-value (p) and sample size (n) are indicated in the table.*

Supplementary Table 4.5: Analysis of Platelet-Leucocyte Aggregates

% Leucocytes in Aggregates	HC	MGUS	SM / MM	P-Value
n	14	16	15	NA
Total Leucocyte - Platelet	2.88 (1.02 – 5.07)	2.69 (1.85 – 7.68)	2.38 (1.12 – 4.28)	0.594
Granulocyte - Platelet	2.26 (0.62 – 4.64)	1.94 (1.18 – 3.0)	0.87 (0.32 – 3.88)	0.298
Lymphocyte - Platelet	0.83 (0.38 – 1.21)	0.82 (0.51 – 2.18)	0.74 (0.26 – 1.38)	0.659
Monocyte - Platelet	4.19 (1.70 – 9.93)	5.92 (2.89 – 11.83)	5.83 (4.38 – 8.78)	0.488

(A) Median percentage and IQR of leucocytes, and individual leucocyte groups, adhered to platelets are shown. *P-Value shown was calculated by Kruskall-Wallis One-Way ANOVA.*

Parameter	Agonist	HC	MGUS	SM / MM	P-Value
Platelet - Leucocyte	ADP	5.37 (3.65 – 9.86)	11.00 (5.41 – 15.71)	8.55 (4.29 – 13.05)	0.157
	TRAP-6	20.54 (4.61 – 41.77)	18.39 (9.64 – 31.52)	27.20 (10.24 – 34.87)	0.852
Platelet - Granulocyte	ADP	5.00 (1.89 – 7.60)	6.35 (2.74 – 15.34)	6.16 (0.60 – 10.54)	0.512
	TRAP-6	20.08 (3.34 – 57.66)	8.92 (4.87 – 38.34)	11.46 (2.25 – 42.20)	0.737
Platelet - Lymphocyte	ADP	1.14 (0.60 – 1.48)	2.17 (1.01 – 4.25)	1.96 (0.85 – 3.60)	0.073
	TRAP-6	4.76 (2.18 – 6.02)	5.89 (3.00 – 17.20)	2.74 (0.91 – 5.16)	0.215
Platelet - Monocyte	ADP	21.83 (10.82 – 32)	20.19 (14.12 – 42.81)	30.75 (15.11 – 45.03)	0.416
	TRAP-6	45.26 (7.04 – 56.1)	26.20 (12.76 – 58.36)	41.42 (20.96 – 61.65)	0.877

(B) Percentage of leucocytes adhered to platelets in whole blood activated in-vitro with 10µM ADP or 100µM TRAP was quantified in participants. *Median and IQR for HC and patient groups is shown. P-value calculated by the Kruskall-Wallis One-Way ANOVA show no evidence of significant differences between groups. Sample size is as follows for ADP reactions HC (n=13), MGUS (n=16), SM/MM (n=15). Sample size for TRAP-6 reactions are reactions HC (n=7), MGUS (n=9), SM/MM (n=13).*

Parameter Correlated with baseline P-selectin levels	Condition	n	r	P-Value
Platelet-Leucocyte	**Rest**	45	0.409	0.005*
Platelet-Granulocyte	**Rest**	45	0.269	0.074
Platelet-Lymphocyte	**Rest**	45	-0.038	0.803
Platelet-Monocyte	**Rest**	45	0.183	0.235
Platelet-Leucocyte	**ADP**	44	0.349	0.019*
Platelet-Granulocyte	**ADP**	44	0.226	0.141
Platelet-Lymphocyte	**ADP**	44	0.334	0.027*
Platelet-Monocyte	**ADP**	44	0.285	0.064
Platelet-Leucocyte	**TRAP-6**	29	0.044	0.816
Platelet-Granulocyte	**TRAP-6**	29	0.011	0.953
Platelet-Lymphocyte	**TRAP-6**	29	0.024	0.902
Platelet-Monocyte	**TRAP-6**	29	0.108	0.583

(C) Correlation analysis by Spearman's Correlation of baseline P-selectin levels with PLA levels at baseline and formation in-vitro in response to ADP (10 µM) or TRAP-6 (100 µM).

Correlation coefficient (r), p-value (p) and sample size (n) are indicated in the table.

Supplementary Table 4.6: Assessment of platelet function under arterial flow conditions.

Parameter (Mean ± SEM)	HC	MGUS	SM / MM	P-Value
Sample size	3	4	6	
Surface Coverage	10.1 ± 0.8	12.17 ± 2.4	8.86 ± 1.2	0.358
	8.03 ± 2.1	**11.98 ± 1.7**	**9.40 ± 1.4**	ns
Average Size	40.67 ± 6.9	45.77 ± 3.1	32.13 ± 5.6	0.222
	46.99 ± 8.9	**40.38 ± 7.3**	**32.47 ± 5.8**	ns
Object Number	1532.33 ± 252	1633.23 ± 248	1478.63 ± 280	0.921
	1345 ± 538	**1674 ± 442**	**1347 ± 350**	ns

Mean and SEM are shown for outputs of the Cone and Plate(let) assay. P-value shown was calculated using One-Way ANOVA. Values shown in bold are corrected for platelet count, fibrinogen and D-dimer levels, where this data was available. Sample size for corrected values are HC=3, MGUS =3, SM/MM = 5. Corrected values are calculated at platelet count = 245, fibrinogen = 3.34 and D-dimer =0.336. ns = non-significant, p-value >0.05. ***. Note this data was collected by co-author G Meade-Murphy.***

5.0 Platelet Hyperactivation and Hyporesponsiveness at Diagnosis in Multiple Myeloma Persists During Treatment Initiation

Chapter 5 details work published in *O'Sullivan LR, Meade-Murphy G, Gilligan OM, Mykytiv V, Cahill MR, Young PW. Platelet hyperactivation and hyporesponsiveness at diagnosis in multiple myeloma persists during treatment initiation. Thromb Res. 2021 Jul;203:186-189. doi: 10.1016/j.thromres.2021.05.004. Epub 2021 May 11. PMID: 34033940*. In the presented work, I designed the study and wrote the published manuscript with co-authors G. Meade-Murphy, P. Young and M.R. Cahill. V. Mykytiv, O. Gilligan and M.R. Cahill recruited and obtained informed consent from patients and healthy controls. I performed all other experiments and data analysis.

5.1 Introduction

Advances in the treatment of Multiple Myeloma (MM) in recent years have improved prognosis and overall survival in patients. However, risk of thrombotic events is high in MM and leads to hospitalisation and increased mortality despite improved anti-cancer therapies. Contemporary initial treatment choices include triplet therapy with Velcade (bortezomib), dexamethasone and Revlimid (lenalidomide) (VRD) or cyclophosphamide (VCD) (Rajkumar, 2019). Use of immunomodulatory agents including lenalidomide without anti-thrombotic therapy was associated with a 23-75% incidence of VTE (Kristinsson et al., 2010) and hence, use of thromboprophylaxis is routine (NICE (National Institute for Health and Care Excellence), 2018; A. Palumbo et al., 2014; Terpos et al., 2015). In spite of thromboprophylaxis, risk of venous thromboembolism (VTE) remains high, with a 7.5–9.2-fold higher risk versus the general population in the year following diagnosis and highest risk in the first months of therapy (Kristinsson et al., 2010). Incidence of arterial thrombosis is also reported to be increased (Kristinsson et al., 2010). A recent review has reported a VTE incidence of 6.2% in patients treated with lenalidomide and dexamethasone with thromboprophylaxis (Chakraborty et al., 2020). Although it has been reported that Bortezomib use reduces lenalidomide-associated VTE incidence (Zangari et al., 2011), further study suggests a non-significant difference in risk (Chakraborty et al., 2020). Various factors contribute to this thrombotic risk and have been reviewed recently (Fotiou et al., 2020). Risk assessment models have been proposed to better identify and treat MM

patients at high risk of VTE, including the IMPEDE VTE score (Sanfilippo et al., 2019) and SAVED score (Li et al., 2019). The ROADMAP-MM-CAT study identified laboratory parameters which were associated with VTE incidence in MM patients, with prolonged procoagulant-PPL significantly associated with higher risk (Fotiou et al., 2018). Platelet-related parameters are assessed in this preliminary study in the context of newly diagnosed MM patients in the initial two months of treatment to address their contribution to this thrombotic risk.

Evidence of platelet hyperactivation in pre-treatment myeloma patients is accumulating with elevated levels of P-selectin (Robak et al., 2012; Takagi *et al.*, 2018), phosphatidylserine (PS) exposure (Guo et al., 2018), platelet-derived microparticles (Nomura et al., 2002), Platelet Factor 4 (PF-4) and β-thromboglobulin reported (E Fritz, Ludwig, Scheithauer, & Sinzinger, 1986). Dysregulated soluble P-selectin may also be a feature of newly diagnosed MM although elevated (Lemancewicz et al., 2014) and reduced (Fotiou et al., 2018) levels have been reported. In a subset of these studies, post-treatment analysis was performed with changes from baseline being reported. Robak et al. showed that treatment with thalidomide and dexamethasone increased P-selectin levels (Robak et al. , 2012). Increased PS exposure due to the same treatments were also reported, although platelets were treated *in-vitro* (Guo et al., 2018). These treatments however have been reported to reduce platelet-derived microparticle levels (Nomura et al., 2002). In patients treated with thalidomide, dexamethasone and cyclophosphamide (CTD) or melphalan, prednisone and thalidomide (MPT), soluble P-selectin levels were reported to decrease (Lemancewicz et al., 2014). In other studies lacking comparison with healthy controls, P-selectin was reported to increase in MM after thalidomide therapy (Dunkley et al., 2007) and soluble P-selectin levels were reported to decrease after dexamethasone and lenalidomide treatment (Rosovsky et al., 2013) and decrease after stem cell transplant (SCT) (Aki et al., 2009). Platelet-monocyte aggregates (PMA) were also reported to decrease after thalidomide and aspirin treatment (Dunkley et al., 2007). Hence, evidence of increased and reduced platelet activation post-treatment exists.

Few studies have addressed platelet responsiveness changes due to MM and treatments used. At diagnosis, extended procoagulant phospholipid-dependent parameters were reported suggesting hypo-responsiveness (Fotiou et al., 2018). Reduced platelet aggregation at diagnosis has also been reported in MM (Fritz *et al.*, 1986; Gorski et al., 1993; Cieslar *et al.*, 2002) and also post treatment with Bortezomib (Rupa-Matysek et al., 2014). PFA-100 closure time has been reported as increased at diagnosis but was reduced

following treatment with thalidomide and dexamethasone (Robak et al., 2012). Responsiveness assessed by flow cytometry has also suggested hyporesponsiveness with reduce PAC-1 binding (Mattheij et al., 2016) and P-selectin levels (Egan et al., 2014; Mattheij et al., 2016) in response to agonists at diagnosis, with an increase seen in MM patients post-treatment (Egan et al., 2014). However, these studies were carried out on a variety of haematology cancer patients (Mattheij et al., 2016), included patients with renal co-morbidities (Cieslar et al., 2002; Rupa-Matysek et al., 2014) or did not compare pre and post treatment data in single patients (Egan et al., 2014), highlighting the need for further study.

Although aspirin or low molecular weight heparin (LMWH) prophylaxis is recommended in patients undergoing treatment with immunomodulatory agents (NICE (National Institute for Health and Care Excellence), 2018), few studies have addressed changes in platelet activation status associated with their use in MM. In a small cohort, aspirin treatment was shown to reduce the thalidomide-induced increases seen in P-selectin and PMA levels (Dunkley et al., 2007).

In addition to VTE risk, thrombocytopenia and bleeding risk complicates management of MM patients. A reduced platelet half-life has been reported in MM patients at diagnosis (Fritz *et al.*, 1986; Gorski et al., 1993) although platelet count was reported in the normal range (E Fritz et al., 1986; Özkurt et al., 2010). Thrombopoietin (TPO) has also been reported as elevated in MM at diagnosis (Kamińska et al., 2014; Lemancewicz et al., 2014; Özkurt et al., 2010). The effect of treatment on these parameters has not been widely investigated. A reduction in TPO with increase in platelet and megakaryocyte count has been reported in a study of patients treated with CTD or MPT therapy (Lemancewicz et al., 2014), while Bortezomib treatment was reported to decrease platelet count (Lonial et al., 2005; Murai et al., 2014; Rupa-Matysek et al., 2014). It has been reported that reticulated platelets are more responsive to agonists and less sensitive to aspirin treatment (Guthikonda et al., 2008), highlighting the need to consider reticulated platelets in the context of MM with dysregulated thrombopoiesis.

In this preliminary study platelet activation status and responsiveness to agonists (ADP, TRAP-6) in MM patients was assessed with an extensive panel of platelet activation markers (PAC-1 binding, P-selectin, CD63, Annexin V, platelet-leucocyte aggregates (PLA)) by flow cytometry in a cohort of patients at diagnosis and at 2 months post initiating treatment. We address treatment with Bortezomib, in combination with dexamethasone

and Revlimid (VRD) or Cyclophosphamide (VCD) for the first time in the context of platelet activation. As antithrombotic agent use is widespread in MM but not often considered in studies of platelet activation, treatment with aspirin will also be considered in patients prescribed it as part of their standard care. Also, as dysregulated thrombopoiesis is reported in association with MM and treatments used, reticulated platelets are quantified and their association with platelet activation and responsiveness considered. By assessing patients in initial months of anti-myeloma and anti-thrombotic treatments, when VTE risk is greatest, we aim to establish a broader understanding of the role of platelets in this risk.

5.2 Methods

5.2.1 Patient Recruitment

Following ethical approval from the local Clinical Research Ethics Committee (CREC) and in accordance with the Declaration of Helsinki, eight newly diagnosed MM patients (untreated) and with no renal, cardiac or infectious co-morbidities, were recruited with informed consent, for participation in this study (from April 2018 - September 2019, Cork University Hospital, Ireland).

Patient Selection

Exclusion Criteria for Participation

2. Anti-myeloma therapy use (prior to start of participation in the study)
3. Current malignancy other than myeloma
4. Known bleeding or thrombotic disorder
5. Abnormal liver or renal function
6. Recent (<1 month prior to collection) surgery or blood transfusion
7. Recent (<2 weeks prior to collection) antithrombotic, antibiotic, antiviral or steroid-based therapy use.

Inclusion Criteria for Participation

2. MM patients: diagnosis based on International Myeloma Working Group diagnostic criteria (Rajkumar et al., 2014).

Healthy Control Selection

Exclusion Criteria for Participation

2. Current or previous malignancy
3. Known bleeding or thrombotic disorder
4. Thrombocytopenia
5. Previous clot (DVT/PE/VTE)
6. Abnormal liver or renal function
7. Recent (<1 month prior to collection) surgery or blood transfusion
8. Recent (<2 weeks prior to collection) antithrombotic, antibiotic, antiviral or steroid-based therapy use.

Inclusion Criteria for Participation

2. Age 45 years or older

Samples were collected from these patients at diagnosis (pre-treatment) and at 2 months after initiating anti-myeloma and antithrombotic treatment, if prescribed (post-treatment). Patients were prescribed (VCD) (n=4), (VRD) (n=2) or VCD with change to VRD (N=1) or (VPD) (n=1). Aspirin was prescribed in a subset of patients (n=5). Samples from eight healthy controls (HC) with no thrombotic, malignant, infectious, renal or cardiac pathologies were also collected during the study period. The median age of patients (64 (IQR 64-73.5)) and controls (59 (IQR 53.5-72)) were non-significantly different (p=0.185). Healthy controls included males (n=4) and females (n=4). As sample size was small, patients were incidentally all males.

5.2.2 Assessment of Platelet Activation Status and Reactivity by Flow Cytometry

Whole blood was collected into 3.2% sodium citrate vacutainers (BD) and stained for flow cytometry within 30 minutes of venepuncture (Pearson et al., 2009). For staining, whole blood was diluted 1:15 in 1% BSA / PBS and stained with anti-CD61- PerCP (BioLegend product no. 336410) or IgG- PerCP isotype control (product no. 400148) and appropriate activation marker. Antibodies used were from Biolegend and as follows : anti-CD41/CD61 (PAC-1)-FITC (product no. 362804), anti-CD63-APC (product no.353008), anti-P-selectin-PE (product no. 304906), anti-Annexin V-FITC (product no. 640906), anti-CD45-FITC (product no. 304006), anti-CD66-APC (product no. 305118), anti-CD14-APC (product no. 367118) or appropriate isotype controls. Staining was carried out for 15 minutes at room temperature. Where platelet reactivity was assessed, whole blood was diluted as described with addition of ADP to final concentration of 10 µM or TRAP-6 (Bachem H7764) to final concentration of 100 µM. *In-vitro* activation was carried out for 15 minutes at room temperature. Following activation and immunolabelling, samples were fixed in sterile filtered 1% paraformaldehyde (PFA)/PBS and analysed using the BD Accuri C6 flow cytometer 30 minutes to 3 hours after fixation.

To analyse platelet activation marker levels, platelets were selected for based on FSC / SSC and CD61-PerCP staining, with the threshold set on FL-3. The selected population was then

assessed in terms of activation marker status. The negative gate for each marker was established using platelets from the same individual stained with isotype controls for each marker. ADP (10 µM) was included in the staining reaction with isotype controls to ensure an accurate negative gate was selected.

To analyse platelet-leucocyte aggregates, leucocytes were selected for based on FSC / SSC and CD45-FITC staining, with the threshold set on FL-1. Granulocytes, monocytes and lymphocytes were gated for based on characteristic FSC / SSC profile and staining for CD66 (granulocytes) and CD14 (monocytes). Each gated population was then assessed in terms of CD61-PerCP positivity, with a negative gate established by staining with a PerCP isotype control.

5.2.3 Washed Platelet Preparation

Washed platelets were prepared from whole blood in 3.2% sodium citrate. Whole blood was diluted 1:1 in wash buffer (36 mM Citric acid, 5 mM Glucose, 5 mM KCl, 2 mM CaCl2, 1 mM MgCl2, 103 mM NaCl pH 6.5) supplemented with Prostaglandin E1 (0.2 µM) (Sigma P5515) at room temperature. Samples were centrifuged at 200 x *g* for 12 minutes without brake. Platelet rich plasma (PRP) was removed from top of the tube, added to a new tube and centrifuged under the same conditions to remove contaminating cells. PRP was removed and diluted 1:1 in wash buffer supplemented with apyrase (0.3 U/mL) (Sigma A6132) and centrifuged at 1500 x *g* for 12 minutes with low brake to pellet platelets. Cells were resuspended in resuspension buffer (10 mM HEPES, 5 mM Glucose, 3 mM KCl, 42 µM $NaHCO_3$, 0.5 mM $MgCl_3$, 140 mM NaCl) for use.

5.2.4 Reticulated Platelet Quantification

Washed platelets (~150 x 10^6 cells per sample) were fixed for 15 minutes in 1% PFA at room temperature. Following fixation, cells were stained with Thiazole Orange (TO) (Sigma – 390062) to quantify reticulated platelets, as described previously (Dale et al., 1995; Kienast & Schmitz, 1990). Cells were pelleted and resuspended in 1 mL TO solution (0.2 µg/mL TO, 2 mM EDTA, PBS) and incubated for 30 minutes in the dark at 37 °C. FL1 staining was assessed using the BD Accuri C6 flow cytometer. Platelets were initially gated for using FSC / SSC. A TO stained and unstained control for each sample was analysed in tandem. Including preliminary analysis, 7 HC samples, with normal platelet count and no known disorder that could affect platelet production, were analysed in total. The gate was

adjusted such that the unstained control was at 0% positive events and HC samples fell within the range 0.5-10.8%. In this data, median (95% range) of %RP was 2.11% (1-10.41%). A gate at <10% for HC is in line with previous data on HC samples (Fujii et al., 2000; Kienast & Schmitz, 1990; Salvagno et al., 2006) and is a gating strategy that practically allowed comparison of samples analysed on different dates. Preliminary analysis demonstrated a reduction in TO signal following treatment with RNAse (data not shown). As an additional verification, a sample from an ITP patient was assessed as described and %RP was 31.95%, in line with previous study (Bonan et al., 1993; Fujii et al., 2000).

5.2.5 Quantification of Thrombopoietin

Thrombopoietin was quantified in serum samples using ELISA kit (Thermo Scientific - EHTHPO).

5.2.6 Statistical Analysis

All analysis was carried out using IBM SPSS software. Kruskall-Wallis One-Way ANOVA with post-hoc analysis by Bonferroni correction for multiple comparisons was used to assess differences between HC and patients for various parameters. To assess correlation of relevant individual parameters across all groups and within groups, Spearman's correlation was used. Where categorical data was compared, Chi-Square analysis was used.

5.3 Results

5.3.1 Platelet Hyperactivation and Hyporesponsiveness Persist Post-Treatment.

Analysis of surface markers of platelet activation revealed significantly elevated median P-selectin and CD63 levels and Annexin V binding at diagnosis (pre-treatment, Figure 5.3.1). Although PAC-1 binding tended to be increased versus HC, this was not statistically significant. Samples taken post-treatment revealed higher median levels of all markers when compared to HC, but these differences were no longer statistically significant. Paired-sample analysis revealed no significant changes in any marker due to treatment. Platelet responsiveness was assessed *in-vitro* by measuring platelet activation markers in response to agonists. When compared to HC, reduced PAC-1 binding and P-selectin levels in response to agonists was evident in patients pre- and post-treatment (Figure 5.3.1). TRAP-6 mediated PAC-1 binding and ADP-mediated P-selectin levels were significantly reduced at diagnosis. Following treatment, PAC-1 binding in response to ADP was also significantly reduced versus HC. Median Fluorescence Intensity (MFI) of these markers was also assessed (Supplementary Table 5.3).

Figure 5.3.1

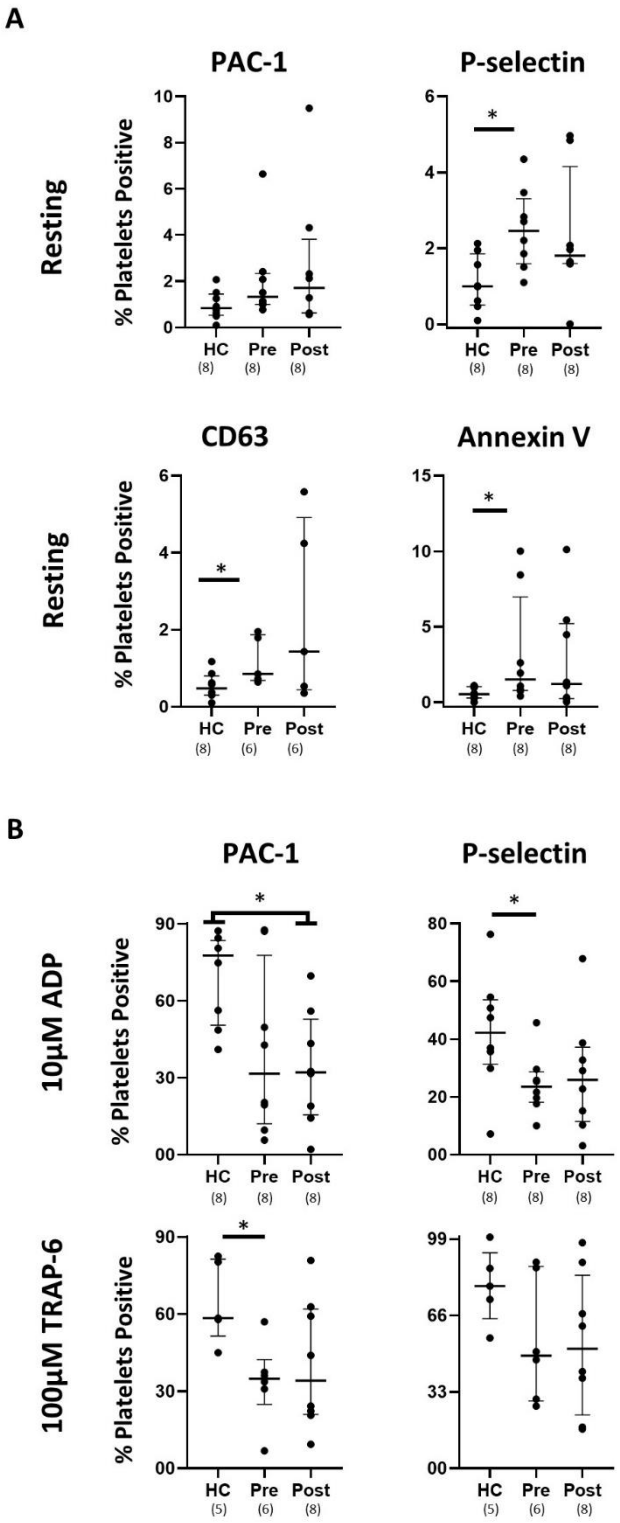

Figure 5.3.1 Platelet activation parameters in healthy controls and Multiple Myeloma patients, pre-treatment and 2 months post initiation of treatment. *Dot-plot graphical representation of percentage of platelets positive for platelet activation parameters in healthy controls (HC), MM patients pre-treatment (Pre) and 2 months post initiation of*

*treatment (Post). Percentage platelets positive for each activation marker are presented as assessed in (**A**) the resting state and (**B**) in response to ADP (10 µM) and TRAP-6 (100 µM). Median and IQR are shown and dots represent individual patients. Statistical analysis was carried out using Mann-Whitney U test to compare HC and patients at each time point. Paired sample analysis of individual patients at both time points was carried out using the Wilcoxon Rank Sign Test. * = P <0.05. P-values for all parameters are detailed in supplementary results. Sample size for each parameter is indicated in brackets below graphs. TRAP-6 = Thrombin Receptor Activating Peptide 6.*

5.3.2 Platelet-Leucocyte Aggregates and Reticulated Platelet Levels Increase Post-Treatment.

Following treatment, paraprotein levels in MM patients were significantly reduced (Table 5.3.1). Clinically reduced red blood cell counts in patients pre- and post-treatment vs HC and reduced haemoglobin levels were noted, although patient haemoglobin levels increased significantly post-treatment (Table 5.3.1). Platelet-leucocyte Aggregates (PLA) occur primarily *via* P-selectin on platelets and P-selectin Glycoprotein Ligand on leucocytes and are an indicator of platelet activation (Finsterbusch et al., 2018). Although normal at diagnosis, we observed a significant increase in total PLA post-treatment (Table 5.3.1). Although no specific leucocyte sub-type appeared significantly increased, a trend towards increased platelet-lymphocyte and platelet-monocyte aggregates (PMA) is noted. No significant abnormality in PLA formation was observed *in-vitro* with agonists (Supplementary Table 5.4).

Platelet count, mean platelet volume and % reticulated platelets (RP) increased in patients post-treatment, with % RP increasing significantly (Table 1). Thrombopoietin levels did not change pre- and post-treatment. INR and APTT were normal in patients at both timepoints (Table 5.3.1). Fibrinogen and D-Dimer levels were significantly increased pre- and post-treatment versus HC, although both tended to decrease post-treatment initiation.

Table 5.3.1 Overview of routine laboratory parameters, platelet-leucocyte aggregates and platelet production parameters in participants.

Parameter Median	Median			P Value		
	HC	Pre	Post	Pre *v* HC	Post *v* HC	Pre *v* Post
Routine Laboratory Parameters						
Paraprotein (g/L)	NA	29	7	NA	NA	0.008
Platelet Count x 10^9 / L	277	195.5	224	*0.038*	*0.083*	*0.195*
Leucocyte Count x 10^9 / L	6.90	5.90	6.00	*0.645*	*0.505*	*1.00*
Red Blood Cell Count x 10^{12} / L	4.61	3.50	3.85	*0.002*	*0.038*	*0.453*
Haemoglobin (g/dL)	13.85	10.15	11.4	*0.003*	*0.004*	*0.039*
% Leucocytes in Platelet-leucocyte Aggregates (PLA)						
Total Leucocyte – Platelet	1.35	2.38	5.84	*0.458*	*0.038*	*0.023*
Granulocyte - Platelet	1.13	0.57	0.90	*0.933*	*0.553*	*0.742*
Lymphocyte - Platelet	0.41	0.72	0.98	*0.423*	*0.185*	*0.762*
Monocyte - Platelet	4.19	5.50	8.71	*0.838*	*0.424*	*0.938*
Platelet-Production Parameters						
Platelet Count x 10^9 / L	277	195.5	224	*0.038*	*0.083*	*0.195*
Mean Platelet Volume (fl)	10.5	10.1	10.75	*0.204*	*0.820*	*0.055*
% Reticulated platelets	3.5	1.82	24.5	*0.460*	*0.032*	*0.031*
Thrombopoietin (pg/mL)	NA	142.14	140.62	*NA*	*NA*	*0.469*
Coagulation Parameters						
INR	1	1.1	1.1	*0.543*	*0.468*	*1*
APTT (sec)	27.5	25	28.5	*0.438*	*0.170*	*0.438*
Fibrinogen (g/L)	2.6	4.9	4.3	*0.006*	*0.002*	*0.531*
D-Dimer (mg/L FEU)	0.19	1.75	0.74	*0.014*	*0.010*	*0.313*

Routine laboratory parameters, median percentage of leucocytes in platelet-leucocyte aggregates (PLA) (CD61/CD45 positive), medians for platelet production and medians for coagulation parameters in healthy controls (HC), MM patients pre-treatment (Pre) and 2 months post-initiating treatment (Post) are shown. Statistical analysis was carried out using Mann-Whitney U test to compare HC and patients at each time point. Paired sample analysis of individual patients at both time points was carried out using the Wilcoxon Rank Sign Test. INR = International Normalised Ratio. APTT = Activated Partial Thromboplastin Test. FEU = Fibrinogen Equivalent Units. Sample size for parameters is as follows: For PLA, platelet count

and mean platelet volume, n=8 for all groups. For % reticulated platelets (RP, RNA-positive platelets), HC n=4, MM pre and post, n=5. For thrombopoietin, MM pre n=8, MM post n=7. For INR and APTT HC n=8, MM pre n=7, MM post n=8. For Fibrinogen, HC n=6, MM pre n=6, MM post n=7. For D-dimer, HC n=7, MM pre n=6, MM post n=7.

5.4 Discussion

In summary, we assessed the activation status of platelets using multiple measurement parameters in newly-diagnosed MM patients in the initial two months of treatment, when VTE risk is reported to be highest (Kristinsson *et al.*, 2010). We investigated these parameters for the first time in patients prescribed systemic anti-cancer therapy in the form of VCD, VRD or VPD and thromboprophylaxis with aspirin. We report that in our cohort of newly-diagnosed MM patients, platelets are hyperactivated, significantly in terms of P-selectin, CD63 and Annexin V, also previously reported for P-selectin (Robak *et al.,* 2012; Takagi *et al.*, 2018) and phosphatidylserine (PS) exposure (Guo *et al.*, 2018). In addition, we report platelet hyporesponsiveness at diagnosis, significantly in terms of PAC-1 binding in response to TRAP-6 and P-selectin levels in response to ADP. This may be indicative of "platelet exhaustion", whereby chronic platelet hyperactivation *in-vivo* results in hyporesponsiveness to agonists (Boneu *et al.*, 1984; Mannucci *et al.*, 1989) and increased baseline levels of activation markers (Cahill *et al.,* 1996). This finding has been reported in cancer patients with advanced disease and elevated VTE risk (Riedl et al., 2017). It is speculated that although responsiveness is reduced *in-vitro*, increased *in-vivo* levels of activated platelets augment thrombotic risk (Baaten et al., 2017). We show for the first time that treatment with VCD, VRD or VPD do not significantly alter this hyperactivated and hyporesponsive state. Although paraprotein levels were significantly reduced during our follow-up study points, patients were not yet in complete remission. It is possible that an extended study period may reveal further changes in these parameters after additional treatment cycles. Analysis of individual patients (Supplementary Figure 2) revealed heterogeneity in terms of activation marker changes, possibly indicative of platelet subpopulations with varying responsiveness (Södergren & Ramström, 2018). It is noted that differences in anti-myeloma therapy and/or aspirin use between patients might contribute to variations in activation markers. While it is not possible to separate out any such effects in this small patient cohort, the possibility merits further investigation in larger studies.

Treatment did impact PLA and RP levels, which increased significantly post-treatment. PLA are a reported marker of thrombo-inflammatory disease with implications in many disease settings, including immune surveillance in liver and lung disease or as an indicator of recurrence in stroke patients (Finsterbusch *et al.*, 2018). In the post-treatment patients, disease burden was reduced and anti-myeloma therapies were being administered.

Thalidomide, from which Revlimid (lenalidomide) is derived, was previously reported to increase PLA (Dunkley et al., 2007). When looking at individual patient results in this study, it appeared that the increases in PLA occurred frequently (4/8 patients) in tandem with decreases in P-selectin. It is possible that P-selectin levels were under-detected in the post-treatment group as P-selectin expressing platelets entered PLA. Aspirin is reported to reduce PLA formation (Dunkley et al., 2007) and in our analysis, this does appear to be the trend as just one of five patients taking aspirin experienced PLA elevation, while all non-users have elevated PLA post treatment, although this was a small cohort (n=3) of patients. Hence, treatments used may have augmented PLA through an activating effect on platelet**s,** however the variation in treatments prescribed limit interpretation of the effect of aspirin alone.

Additionally, reticulated platelet levels are elevated post-treatment. This platelet fraction is reportedly prothrombotic (Bongiovanni et al., 2019) and could contribute to elevated PLA levels. In our post-treatment data, a significant correlation between PLA and reticulated platelet level existed (Pearson's Correlation coefficient = 0.825 (p=0.006)). This platelet fraction may have contributed to elevated PLA.

In relation to the reduction in myeloma disease burden, a role for P-selectin and P-selectin glycoprotein ligand (PSGL) interactions is emerging in myeloma disease progression (Azab et al., 2012; Muz et al., 2015). Platelet interaction with myeloma cells *in-vitro* via P-selectin was also reported (Henderson et al., 2018) and P-selectin levels also were reported to increase with MM disease progression (Takagi et al., 2018). It is possible that a reduction of disease burden in post-treatment patients disrupted disease-associated P-selectin / PSGL interactions contributing to an increased presence of circulating PLA. Further study of the interaction of P-selectin bearing platelets with malignant plasma cells, and the possible effects of aspirin treatment on this interaction, could shed further light on this. Our finding of increased PLA in post-treatment patients could be another feature of this P-selectin / PSGL interaction.

Increased RP levels may be of clinical value as they are reported to have greater propensity for arterial thrombus formation and to be initiators of aggregate formation. (Mcbane *et al.*, 2014; Armstrong *et al.*, 2017). This possibly explains the correlation of parameters. RP are also reported to be less sensitive to antiplatelet agents such as aspirin (Guthikonda *et al.*, 2008) but remain sensitive to antiplatelet agents with longer half-lives, such as ticagrelor (Armstrong *et al.*, 2017). Aspirin schedule also influences efficacy, as a once

daily low-dose regimen has been shown to be sub-optimal for essential thrombocythaemia patients who experience increased platelet production and activation (Rocca *et al.*, 2020). RP changes are also of interest as they may be readily quantified by routine blood count analysers. The finding of increased RP at this time point also correlates with the incidence of thrombotic events in MM patients, with risk being highest in the initial months of treatment (Kristinsson *et al.*, 2010). Elevated TPO levels were not significantly different pre- and post-treatment, despite increases in RP levels only in post-treatment.

Increased TPO levels have been reported previously in MM patients with normal platelet count (Folman et al., 2001; Kamińska et al., 2014; Lemancewicz et al., 2014). This was speculated to be due to increased TPO production by malignant plasma cells or the influence of IL-6 on TPO production. Studies also reported significantly increased IL-6 in newly diagnosed MM patients (Lemancewicz et al., 2014; Özkurt et al., 2010). Increases in IL-6 and TPO are also reported in other inflammatory conditions with increased platelet activity and thrombotic risk (Nagareddy et al. , 2018). Our results are in line with those reported in MM, where increased TPO was present in patients with normal platelet count and features of suppressed haematopoiesis (reduced Hb) (Folman et al., 2001). A reduced megakaryocyte count in the bone marrow was also reported in MM patients at diagnosis (Lemancewicz et al., 2014). Increased TPO is thought to stimulate thrombopoiesis selectively to maintain a normal platelet count despite marrow suppression. Further to this, normal %RP was reported in a small cohort of myeloma patients in peripheral blood previously but relatively higher levels were present in the bone marrow (Stohlawetz et al., 2009). This could explain the finding of unexpectedly low %RP at diagnosis. Platelet count was normal, but slightly suppressed, at this time point in our study and the same finding in %RP is present. MPV was also normal. Hence, it is possible that the combined presence of marrow suppression and increased TPO levels in MM patients at diagnosis resulted in largely unaffected platelet production.

This balance may have been disrupted post treatment, as disease burden was reduced and intermittent myelosuppression was present, whereby treatment delivered in blocks with built in marrow recovery time were delivered before proceeding to each subsequent block. Platelet count and haemoglobin level both increased in patients post treatment in our study, suggesting recovery of haematopoiesis. Although not quite significant ($p=0.055$), MPV in patients was slightly increased post-treatment (10.1 versus 10.75 fl) and %RP increased significantly. MPV has been noted to show only minor differences in disease

states when compared with healthy controls, possibly due to inherent variation in healthy controls and pre-analytical variables (Noris et al., 2016), limiting its widespread use clinically. In this study, the key result of increased MPV in patients post treatment involves the same individuals and pre-analytical factors, and shows a slight increase, consistent with the finding of increased %RP in these patients.

A significant increase in %RP, without significant change in MPV was also reported previously for patients in recovery from aplasia (Salvagno et al., 2006).

Increased platelet production may be due to treatment and marrow recovery from myelosuppression. A study of platelet count and TPO in bortezomib treated patients highlights a relatively stable platelet count and TPO achieved in one myeloma patient treated with weekly bortezomib doses (Lonial et al., 2005). Our study reports the same finding in a larger cohort. A previous study of post-treatment patients (after 6 cycles of treatment) reported a reduction in TPO at this time point and an increase in bone marrow megakaryocytes (Lemancewicz et al., 2014). Our study and that which previously reported maintained TPO levels (Lonial et al., 2005) involved analysis after 2 cycles, possibly explaining the maintained TPO levels. As TPO levels are regulated both by platelet count and megakaryocyte count, it is possible that there is a lag in clearance of malignantly elevated TPO levels as megakaryocyte count returns to normal post treatment. This could be examined further in future studies.

Previous studies have reported varying changes post-treatment with anti-myeloma therapies. Robak *et al*. showed that treatment with thalidomide and dexamethasone increased platelet P-selectin levels (Robak *et al.*, 2012). In an *in-vitro* experiment, increased phosphatidylserine exposure due to the same treatments were also reported (Guo *et al.*, 2018). PAC-1 binding was reported as increased due to thalidomide treatment (Abdullah *et al.,* 2013). However, in another study, thalidomide treatment of human and mouse platelets *in-vitro* and mouse platelets *in-vivo*, did not affect platelet P-selectin levels or PAC-1 binding (Qiao *et al.*, 2017). In a small study cohort, aspirin treatment was shown to reduce thalidomide-induced increases in P-selectin and PMA levels (Dunkley and Gaudry, 2007). In patients treated with thalidomide, dexamethasone and cyclophosphamide (CTD) or melphalan, prednisone and thalidomide (MPT) (Lemancewicz *et al.*, 2014) or dexamethasone and lenalidomide (Rosovsky *et al.*, 2013), soluble plasma P-selectin levels were reported to decrease. Our results show no significant change to the hyperactivated state post-treatment with VCD, VRD or VPD, for the first time. Previous study has

also indicated platelet hyporesponsiveness post-treatment, with reduced PAC-1 binding (Baaten *et al.*, 2018) and P-selectin levels (Egan *et al.*, 2014; Baaten *et al.*, 2018) in response to agonists. Treatment was also reported to increase responsiveness (Egan *et al.*, 2014). However, these studies were carried out on a variety of blood cancer patients (Baaten *et al.*, 2018) or did not compare pre- and post-treatment data in single patients (Egan *et al.*, 2014), highlighting the need for further study. Our data support these findings of platelet hyporesponsiveness post-treatment.

In conclusion, platelet hyperactivation and hyporesponsiveness are present at diagnosis and during treatment initiation in this preliminary cohort of MM patients, while treatment initiation correlated with an elevation of RP levels and PLA. Changes in platelet activation status are relevant in light of previous reports that an increase in mortality is present in cancer patients with reduced P-selectin and PAC-1 binding (Riedl et al., 2017) and Procoagulant-PPL, which indicates platelet or endothelial cell activation, is predictive of VTE risk (Fotiou et al., 2018). Analysis of platelet activation parameters in larger cohorts over a longer study period could expand our understanding of platelet activation as a feature of thrombotic risk and platelet dysregulation during the myeloma disease course.

5.5 Supplementary Results

Supplementary Table 5.1: Baseline platelet activation marker levels in healthy controls and myeloma patients pre and post treatment initiation.

Parameter	Median			*P Value*		
	HC	Pre	Post	Pre V HC	Post V HC	Pre V Post
PAC-1 (%)	0.84	1.33	1.71	*0.069*	*0.169*	*0.779*
P-Selectin (%)	1.00	2.46	1.81	*0.010*	*0.105*	*0.674*
CD63 (%)	0.48	1.32	2.84	*0.020*	*0.059*	*0.116*
Annexin V (%)	0.54	1.51	1.21	*0.038*	*0.139*	*0.575*

Median % platelets positive for each activation marker assessed by flow cytometry is shown. Statistical analysis was carried out using Mann-Whitney U test to compare HC and patients at each time point. Paired sample analysis of individual patients at both time points was carried out using the Wilcoxon Rank Sign Test. HC = Healthy Control.

Supplementary Table 5.2: Platelet responsiveness in healthy controls and myeloma patients pre and post treatment initiation.

Parameter	Agonist	HC	Pre	Post	*Pre V HC*	*Post V HC*	*Pre V Post*
PAC-1 (%)	**ADP**	77.55	31.56	32.04	*0.161*	*0.005*	*0.742*
	TRAP-6	58.50	34.91	34.15	*0.009*	*0.171*	*1*
P-Selectin (%)	**ADP**	42.21	23.49	25.93	*0.028*	*0.130*	*0.742*
	TRAP-6	78.69	48.68	51.69	*0.247*	*0.171*	*0.688*

Median % platelets positive for each activation marker assessed by flow cytometry is shown. Platelets were activated with ADP (10 µM) and TRAP-6 (100 µM) *in-vitro*. Statistical analysis was carried out using Mann-Whitney U test to compare HC and patients at each time point.

Paired sample analysis of individual patients at both time points was carried out using the Wilcoxon Rank Sign Test. HC = Healthy control.

Supplementary Table 5.3 : Median Fluorescent Intensity (MFI) of Activation Markers in Patients and Healthy Controls.

(Resting)

Parameter	Median MFI (AU)			P Value		
	HC	Pre	Post	Pre *v* HC	Post *v* HC	Pre *v* Post
PAC-1	239.5	297	432.5	0.080	0.027*	0.641
P-Selectin	299	312.5	564	0.130	0.038*	0.148
CD63	1096	1276	1455	0.108	0.142	0.463
Annexin V	281.5	360.5	606	0.087	0.019*	0.641

(10 µM ADP)

Parameter	Median change in MFI v Resting (AU)			P Value		
	HC	Pre	Post	Pre *v* HC	Post *v* HC	Pre *v* Post
PAC-1	1798.25	643	405	0.279	0.065	0.313
P-Selectin	787.5	418.78	413.5	0.234	0.505	0.844

(100 µM TRAP-6)

Parameter	Median change in MFI v Resting (AU)			P Value		
	HC	Pre	Post	Pre *v* HC	Post *v* HC	Pre *v* Post
PAC-1	619	550	505	0.246	0.724	0.625
P-Selectin	2411	1946.55	1033	0.841	0.284	0.813

Median fluorescent intensity (MFI) was compared using Mann Whitney U test for healthy controls versus patients at each time point. Patients at each time point were compared using Wilcoxon Sign Rank test. AU = Arbitrary Units.

Supplementary Table 5.4: Measurement of platelet-leucocyte aggregate formation *in-vitro* with agonists in healthy controls and multiple myeloma patients, pre and post treatment initiation.

Parameter	Agonist	Median			P Value		
		HC	Pre	Post	Pre V HC	Post V HC	Pre V Post
Platelet - Leucocyte	**ADP**	4.84	8.42	14.01	*0.574*	*0.065*	*0.313*
	TRAP-6	20.54	15.97	19.31	*0.662*	*0.943*	*1*
Platelet - Granulocyte	**ADP**	3.40	4.56	4.96	*1*	*0.878*	*1*
	TRAP-6	20.08	8.47	8.68	*0.329*	*0.207*	*0.938*
Platelet - Lymphocyte	**ADP**	1.01	1.83	1.30	*0.195*	*0.773*	*0.121*
	TRAP-6	2.71	2.46	1.74	*0.398*	*0.412*	*0.813*
Platelet - Monocyte	**ADP**	20.59	28.85	19.53	*0.463*	*0.959*	*0.297*
	TRAP-6	45.26	30.205	20.67	*0.724*	*1*	*0.063*

Median change in the % of total leucocytes or leucocyte sub-types in platelet-leucocyte aggregates following stimulation with ADP (10 µM) and TRAP-6 (100 µM) *in-vitro* are shown. Statistical analysis was carried out using Mann-Whitney U test to compare HC and patients at each time point. Paired sample analysis of individual patients at both time points was carried out using the Wilcoxon Rank Sign Test. HC = Healthy control.

Supplementary Figure 5.1

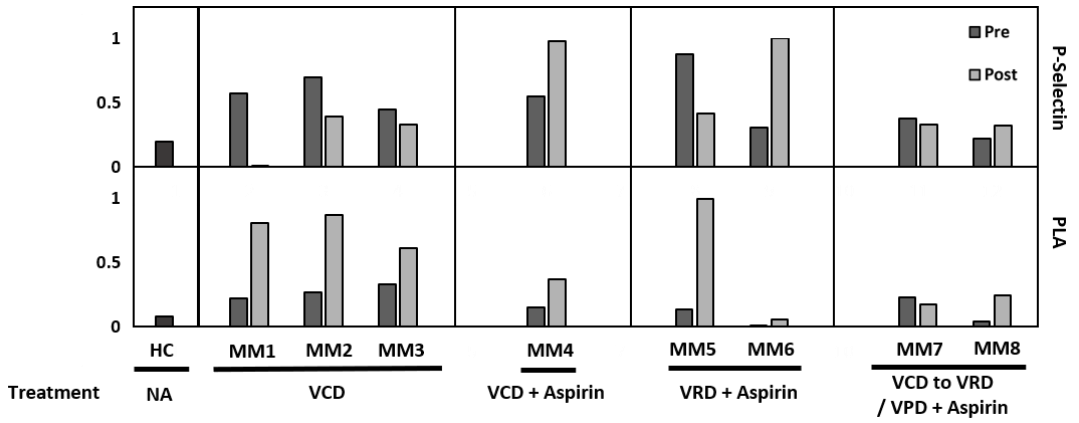

Supplementary Figure 5.1: Analysis of the impact of treatment and aspirin on PLA and P-selectin levels *Figure depicts individual patient PLA and P-Selectin levels. Scale is normalised so that the maximum value obtained for each marker is 1. P-Selectin graph shows % platelets positive for activation marker. PLA=Platelet-leucocyte aggregates, results show % leucocytes positive for platelet marker. Patients are grouped according to the treatment they were prescribed. VCD = Velcade (bortezomib), Cyclophosphamide, Dexamethasone, VRD = Velcade (bortezomib), Revlimid (*lenalidomide*), Dexamethasone, VPD = Velcade (bortezomib), Pomalidomide, Dexamethasone. Pre = pre-treatment, Post = two months post initiating treatment.*

Supplementary Figure 5.2

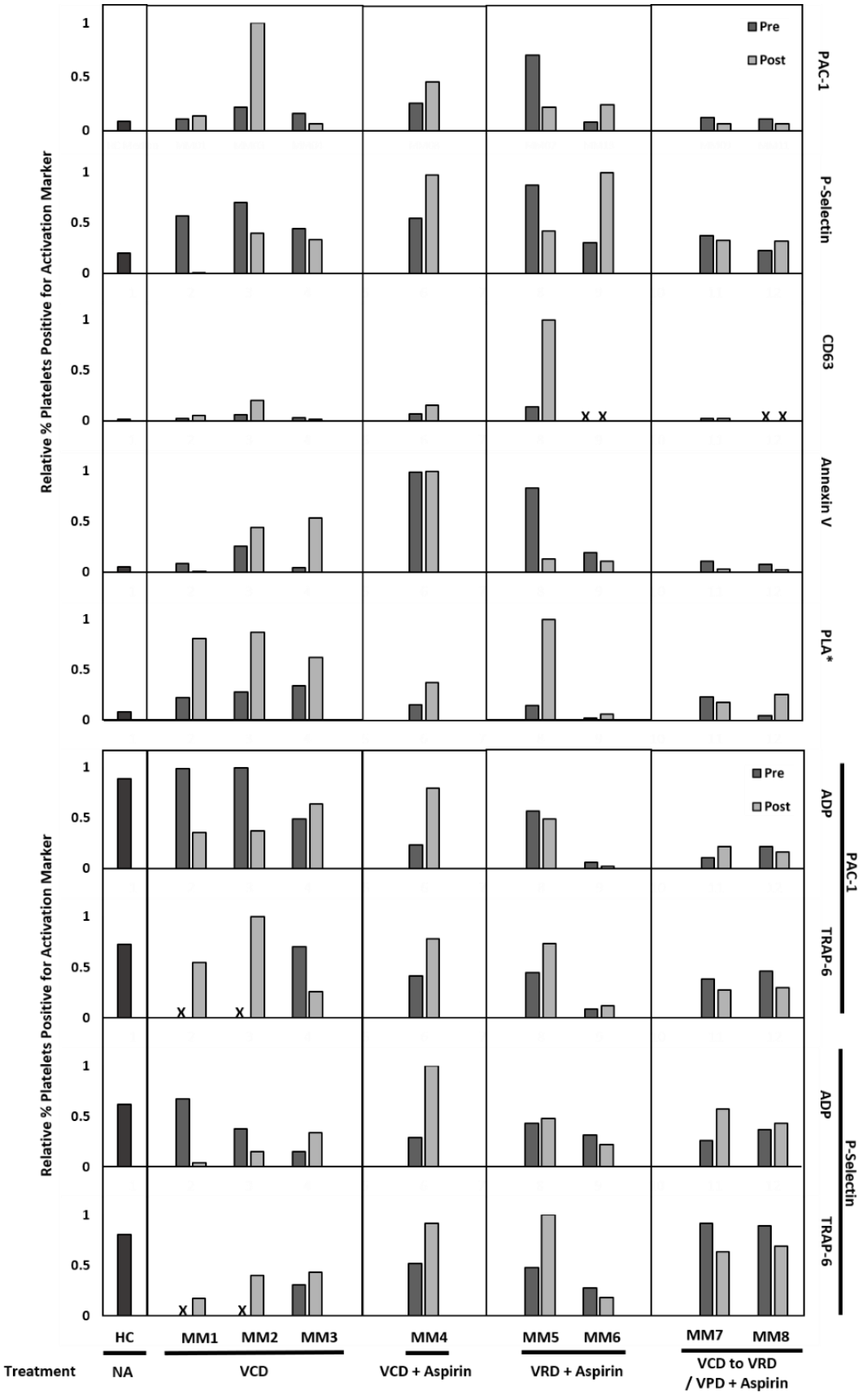

Supplementary Figure 5.2 Individual patient results for activation markers in the resting and activated state. *Individual patient results are shown for baseline and markers post stimulation. Scale is corrected so that maximum value obtained for each marker is 1. Markers show % platelets positive for marker. *PLA=Platelet-leucocyte aggregates, results show % leucocytes positive for platelet marker. X = parameter was not assessed in this patient due to unavailability of TRAP-6 / CD63 reagent. Patients are grouped according to the treatment they were prescribed. VCD = Velcade (bortezomib), Cyclophosphamide, Dexamethasone, VRD = Velcade (bortezomib), Revlimid (*lenalidomide*), Dexamethasone, VPD = Velcade (bortezomib), Pomalidomide, Dexamethasone. Pre = pre-treatment, Post = two months post initiating treatment.*

6.0 Overall Discussion & Conclusion

In this study, I assessed two platelet related disorders. In the assessment of CMTP-causing actinin-1 mutations, it was shown that mutations outside the actin-binding domain also cause an increased ability to bundle F-actin *in-vitro* and increased association with the actin cytoskeleton *in-cellula*. This highlights a regulatory role of the calcium-binding and rod domains on the affinity of actinin for actin. The molecular mechanisms underlying this are speculated upon but further avenues of study are highlighted. This finding also demonstrates a likely common molecular mechanism exists for actinin-1 related CMTP, whereby actinin's affinity for F-actin is increased. This implies that an actinin-1 dependent process in platelet production is sensitive to a tightly regulated actin-actinin interaction.

Identifying the actinin-1 dependent processing in platelet production was an aim of this study and various points of interest were explored. The maturation and structure of megakaryocytes expressing mutant actinin-1 was assessed but no significant disruption was noted, possibly due to the impact of WT actinin-1 which was also expressed and the transient transfection which may have not sufficiently affected the maturation process. Expression of mutant actinin-1 in primary murine megakaryocytes proved technically challenging and prevented the assessment of these mutants in proplatelets and podosomes. However, immunofluorescent staining of these cells highlighted the presence of actinin-1, and also actinin-4, in these structures. Additionally, a known interactor of actinin-1 which is vital in platelet formation and function, integrin αIIβ3, also appeared to interact with actinin-4 or actinin 1/4 heterodimers. It was also found that more actinin-1 was present in platelets and MK cell lines than actinin-4, possibly explaining the tissue specific impact of actinin-1 mutations. Future work may build upon the methods trialled in this study to assess actinin-1 mutants in platelet production. Also the actinin isoform specific functions, specific to actinin-1, actinin-4 or actinin1/4 heterodimers, would be important to clarify, given the isolated impact of actinin-1 mutations on platelets.

In the second part of the project, I studied platelet membrane receptor expression, platelet-leucocyte aggregates, reticulation status and responsiveness *in-vitro* to shed light on platelets and their role in Myeloma and MGUS. It was shown that platelets are hyperactivated and hyporesponsive in MM patients and in premalignant MGUS patients. This is indicative of platelet exhaustion whereby chronic hyperactivation results in reduced responsiveness *in-vitro* and co-exists with increased thrombotic risk. The finding of

hyperactivation in MGUS patients suggests platelet may become dysregulated early in the disease course. Further to this, it was shown that this hyperactive state remains following two months of treatment and a significant reduction in paraprotein levels, possibly due to the impact of treatment. Two additional markers, reticulated platelets and platelet-leucocyte aggregates, were elevated at this timepoint. Current risk assessment and antithrombotic protocols are reportedly inadequate as the incidence of thrombotic events remains high in MM. Although the sample size was small in this study, the extensive panel of platelet markers assessed highlighted that various markers of platelet activation are abnormal in patients and future work may assess the prognostic and predictive nature of these markers, with the view to incorporate parameters into risk assessment models. It remains to be determined how the MM disease state impacts platelets, with the interaction of paraproteins with platelets considered in preliminary analysis in this study. Given the emerging role of platelets in tumour progression and the immune system, various factors may be at play which cause platelet dysregulation in MM. These could be assessed in the context of both thrombotic risk and disease management in MM in future study.

In conclusion, many questions remain in the research of platelet production and the role platelets may play in cancer and this work presents new findings in the areas of actinin-1 related CMTP and platelet dysregulation in MM.

7.0 Bibliography

Abbonante, V., di Buduo, C. A., Gruppi, C., De Maria, C., Spedden, E., de Acutis, A., … Balduini, A. (2017). A new path to platelet production through matrix sensing. *Haematologica*, *102*(7), 1150–1160. https://doi.org/10.3324/haematol.2016.161562

Agbani, E. O., & Poole, A. W. (2017). Procoagulant platelets: Generation, function, and therapeutic targeting in thrombosis. *Blood*, *130*(20), 2171–2179. https://doi.org/10.1182/blood-2017-05-787259

Agbani, E. O., van den Bosch, M. T. J., Brown, E., Williams, C. M., Mattheij, N. J. A., Cosemans, J. M. E. ., … Poole, A. W. (2015). Coordinated Membrane Ballooning and Procoagulant Spreading in Human Platelets. *Circulation*, *132*(15), 1414–1424. https://doi.org/10.1161/CIRCULATIONAHA.114.015036

Agbani, E. O., Williams, C. M., Li, Y., Van Den Bosch, M. T. J., Moore, S. F., Mauroux, A., … Poole, A. W. (2018). Aquaporin-1 regulates platelet procoagulant membrane dynamics and in vivo thrombosis. *JCI Insight*, *3*(10). https://doi.org/10.1172/jci.insight.99062

Agbani, E. O., Zhao, X., Williams, C. M., Aungraheeta, R., Hers, I., Swenson, E. R., & Poole, A. W. (2020). Carbonic Anhydrase Inhibitors suppress platelet procoagulant responses and in vivo thrombosis: Carbonic Anhydrase Inhibitors as Antithrombotics. *Platelets*, *31*(7). https://doi.org/10.1080/09537104.2019.1709632

Aiolfi, R., & Sitia, G. (2015, May 7). Chronic hepatitis B: Role of anti-platelet therapy in inflammation control. *Cellular and Molecular Immunology*, Vol. 12, pp. 264–268. https://doi.org/10.1038/cmi.2014.124

Aki, S. Z., Şucak, G. T., Paşaoğlu, H., Özkurt, Z. N., Yegin, Z. A., Ofluoğlu, E., … Haznedar, R. (2009). Thrombopoietic cytokine and P-selectin levels in patients with multiple myeloma undergoing autologous stem cell transplantation: Decrease in posttransplantation P-selectin levels might predict the degree of maximum response. *Clinical Lymphoma and Myeloma*, *9*(3), 229–233. https://doi.org/10.3816/CLM.2009.n.045

Alard, J. E., Ortega-Gomez, A., Wichapong, K., Bongiovanni, D., Horckmans, M., Megens, R. T. A., … Soehnlein, O. (2015). Recruitment of classical monocytes can be inhibited by disturbing heteromers of neutrophil HNP1 and platelet CCL5. *Science Translational Medicine*, *7*(317). https://doi.org/10.1126/scitranslmed.aad5330

Alfred, T., Ben-Shlomo, Y., Cooper, R., Hardy, R., Cooper, C., Deary, I. J., … Day, I. N. M. (2011). ACTN3 genotype, athletic status, and life course physical capability: Meta-analysis of the published literature and findings from nine studies. *Human Mutation*, *32*(9), 1008–1018. https://doi.org/10.1002/humu.21526

Alonso, A. L., & Cox, D. (2015). Platelet interactions with viruses and parasites. *Platelets*, *26*(4), 317–323. https://doi.org/10.3109/09537104.2015.1025376

Alonso, F., Spuul, P., Daubon, T., Kramer, Ij., & Génot, E. (2019). Variations on the theme of podosomes: A matter of context. *Biochimica et Biophysica Acta - Molecular Cell Research*, *1866*(4), 545–553. https://doi.org/10.1016/j.bbamcr.2018.12.009

Amaya-Amaya, J., Montoya-Sánchez, L., & Rojas-Villarraga, A. (2014). Cardiovascular

involvement in autoimmune diseases. *BioMed Research International*, Vol. 2014. https://doi.org/10.1155/2014/367359

Anderson, D. R., Dunbar, M., Murnaghan, J., Kahn, S. R., Gross, P., Forsythe, M., … Vendittoli, P. A. (2018). Aspirin or rivaroxaban for VTE prophylaxis after hip or knee arthroplasty. *New England Journal of Medicine*, *378*(8), 699–707. https://doi.org/10.1056/NEJMoa1712746

Andre, P. (2004). P-selectin in haemostasis. *British Journal of Haematology*, *126*(3), 298–306. https://doi.org/10.1111/j.1365-2141.2004.05032.x

Andres, O., König, E., Wiegering, E., Klopocki, E., & Schulze, H. (2018). Use of Targeted High-Throughput Sequencing for Genetic Classification of Patients with Bleeding Diathesis and Suspected Platelet Disorder. *TH Open : Companion Journal to Thrombosis and Haemostasis*, *2*(4), e445–e454. https://doi.org/10.1055/S-0038-1676813

Andrews, R. K., & Gardiner, E. E. (2016). *Basic mechanisms of platelet receptor shedding*. https://doi.org/10.1080/09537104.2016.1235690

Angus, D. C., & van der Poll, T. (2013). Severe Sepsis and Septic Shock. *New England Journal of Medicine*, *369*(9), 840–851. https://doi.org/10.1056/NEJMra1208623

Antkowiak, A., Viaud, J., Severin, S., Zanoun, M., Ceccato, L., Chicanne, G., … Gaits-Iacovoni, F. (2016). Cdc42-dependent F-actin dynamics drive structuration of the demarcation membrane system in megakaryocytes. *Journal of Thrombosis and Haemostasis*, *14*(6), 1268–1284. https://doi.org/10.1111/jth.13318

Araki, N., Hatae, T., Yamada, T., & Hirohashi, S. (2000). Actinin-4 is preferentially involved in circular ruffling and macropinocytosis in mouse macrophages: Analysis by fluorescence ratio imaging. *Journal of Cell Science*, *113*(18), 3329–3340.

Arman, M., & Krauel, K. (2015). Human platelet IgG Fc receptor FcγRIIA in immunity and thrombosis. *Journal of Thrombosis and Haemostasis*, *13*(6), 893–908. https://doi.org/10.1111/jth.12905

Armstrong, A. J., Marengo, M. S., Oltean, S., Kemeny, G., Bitting, R. L., Turnbull, J. D., … Garcia-Blanco, M. A. (2011). Circulating tumor cells from patients with advanced prostate and breast cancer display both epithelial and mesenchymal markers. *Molecular Cancer Research*, *9*(8), 997–1007. https://doi.org/10.1158/1541-7786.MCR-10-0490

Asghar, S., Parvaiz, F., & Manzoor, S. (2019). Multifaceted role of cancer educated platelets in survival of cancer cells. *Thrombosis Research*, *177*(October 2018), 42–50. https://doi.org/10.1016/j.thromres.2019.02.026

Assinger, A., Kral, J. B., Yaiw, K. C., Schrottmaier, W. C., Kurzejamska, E., Wang, Y., … Söderberg-Naucler, C. (2014). Human Cytomegalovirus–Platelet Interaction Triggers Toll-Like Receptor 2–Dependent Proinflammatory and Proangiogenic Responses. *Arteriosclerosis, Thrombosis, and Vascular Biology*, *34*(4), 801–809. https://doi.org/10.1161/ATVBAHA.114.303287

Astle, William J., Elding, H., Jiang, T., Allen, D., Ruklisa, D., Mann, A. L., … Soranzo, N. (2016). The Allelic Landscape of Human Blood Cell Trait Variation and Links to Common Complex Disease. *Cell*, *167*(5), 1415-1429.e19. https://doi.org/10.1016/j.cell.2016.10.042

Astle, William John, Team, U. B. T. G., & BLUEPRINT epigenome, C. (2016). A GWAS of

170,000 Individuals Identifies Thousands of Alleles Perturbing Blood Cell Traits, Many of Which Are in Super Enhancers Setting Cell Identity. *Blood*, *128*(22), 2652–2652. https://doi.org/10.1182/blood.v128.22.2652.2652

Ataga, K. I., Kutlar, A., Kanter, J., Liles, D., Cancado, R., Friedrisch, J., … Rother, R. P. (2017). Crizanlizumab for the Prevention of Pain Crises in Sickle Cell Disease. *New England Journal of Medicine*, *376*(5), 429–439. https://doi.org/10.1056/NEJMoa1611770

Ay, C., Dunkler, D., Marosi, C., Chiriac, A. L., Vormittag, R., Simanek, R., … Pabinger, I. (2010). Prediction of venous thromboembolism in cancer patients. *Blood*, *116*(24), 5377–5382. https://doi.org/10.1182/blood-2010-02-270116

Azab, A. K., Quang, P., Azab, F., Pitsillides, C., Thompson, B., Chonghaile, T., … Ghobrial, I. M. (2012). P-selectin glycoprotein ligand regulates the interaction of multiple myeloma cells with the bone marrow microenvironment. *Blood*, *119*(6), 1468–1478. https://doi.org/10.1182/blood-2011-07-368050

Baaten, C. C. F. M. J., Ten Cate, H., Van Der Meijden, P. E. J., & Heemskerk, J. W. M. (2017). *Platelet populations and priming in hematological diseases*. https://doi.org/10.1016/j.blre.2017.07.004

Babaei, M., Rezaieyazdi, Z., Saadati, N., Saghafi, M., Sahebari, M., Naghibzadeh, B., & Esmaily, H. (2016). Serum alpha-actinin antibody status in systemic lupus erythematosus and its potential in the diagnosis of lupus nephritis. *Caspian Journal of Internal Medicine*, *7*(4), 272–277.

Backman, L. (2015). Calcium affinity of human α-actinin 1. *PeerJ*, *3*(e), 944.

Bagnall, R. D., Molloy, L. K., Kalman, J. M., & Semsarian, C. (2014). Exome sequencing identifies a mutation in the ACTN2 gene in a family with idiopathic ventricular fibrillation, left ventricular noncompaction, and sudden death. *BMC Medical Genetics*, *15*(1), 1–9. https://doi.org/10.1186/s12881-014-0099-0

Balduini, C. L., Pecci, A., & Savoia, A. (2011). Recent advances in the understanding and management of MYH9-related inherited thrombocytopenias. *British Journal of Haematology*, *154*(2), 161–174. https://doi.org/10.1111/j.1365-2141.2011.08716.x

Banerjee, M., & Whiteheart, S. W. (2017). The Ins and Outs of Endocytic Trafficking in Platelet Functions. *Current Opinion in Hematology*, *24*(5), 467–474. https://doi.org/10.1097/MOH.0000000000000366.The

Bañuelos, S., Saraste, M., & Carugo, K. D. (1998). Structural comparisons of calponin homology domains: Implications for actin binding. *Structure*, *6*(11), 1419–1431. https://doi.org/10.1016/S0969-2126(98)00141-5

Barbolina, M. V., Adley, B. P., Kelly, D. L., Fought, A. J., Scholtens, D. M., Shea, L. D., & Stack, M. S. (2008). Motility-related actinin alpha-4 is associated with advanced and metastatic ovarian carcinoma. *Laboratory Investigation*, *88*(6), 602–614. https://doi.org/10.1038/labinvest.2008.25

Bariana, T. K., Ouwehand, W. H., Guerrero, J. A., & Gomez, K. (2017). Dawning of the age of genomics for platelet granule disorders: improving insight, diagnosis and management. *British Journal of Haematology*, *176*(5), 705–720. https://doi.org/10.1111/bjh.14471

Baroni, G., Banzato, A., Bison, E., Denas, G., Zoppellaro, G., & Pengo, V. (2017, November 17). The role of platelets in antiphospholipid syndrome. *Platelets*, Vol. 28, pp. 762–

766. https://doi.org/10.1080/09537104.2017.1280150

Battinelli, E., Willoughby, S. R., Foxall, T., Valeri, C. R., & Loscalzo, J. (2001). Induction of platelet formation from megakaryocytoid cells by nitric oxide. *Proceedings of the National Academy of Sciences of the United States of America*, *98*, 14458–14463. https://doi.org/10.1073/pnas.241427398

Bauer, K., Kratzer, M., Otte, M., De Quintana, K. L., Hagmann, J., Arnold, G. J., … Siess, W. (2000). Human CLP36, a PDZ-domain and LIM-domain protein, binds to α-actinin-1 and associates with actin filaments and stress fibers in activated platelets and endothelial cells. *Blood*, *96*(13), 4236–4245. https://doi.org/10.1182/blood.v96.13.4236

Becattini, C., Agnelli, G., Schenone, A., Eichinger, S., Bucherini, E., Silingardi, M., … Prandoni, P. (2012). Aspirin for Preventing the Recurrence of Venous Thromboembolism. *New England Journal of Medicine*, *366*(21), 1959–1967. https://doi.org/10.1056/NEJMoa1114238

Becker-Merok, A., Kalaaji, M., Haugbro, K., Nikolaisen, C., Nilsen, K., Rekvig, O. P., & Nossent, J. C. (2006). Alpha-actinin-binding antibodies in relation to systemic lupus erythematosus and lupus nephritis. *Arthritis Research and Therapy*, *8*(6), 1–8. https://doi.org/10.1186/ar2070

Becker, I. C., Scheller, I., Wackerbarth, L. M., Beck, S., Heib, T., Aurbach, K., … Nieswandt, B. (2020). Actin/microtubule crosstalk during platelet biogenesis in mice is critically regulated by Twinfilin1 and Cofilin1. *Blood Advances*, *4*(10), 2124–2134. https://doi.org/10.1182/bloodadvances.2019001303

Beggs, A. H., Byers, T. J., Knoll, J. H. M., Boyce, F. M., Bruns, G. A. P., & Kunkel, L. M. (1992). Cloning and characterization of two human skeletal muscle α-actinin genes located on chromosomes 1 and 11. *Journal of Biological Chemistry*, *267*(13), 9281–9288.

Behnke, O. (1965). Further studies on microtubules. A marginal bundle in human and rat thrombocytes. *Journal of Ultrasructure Research*, *13*(5–6), 469–477. https://doi.org/10.1016/S0022-5320(65)90009-2

Behnke, O. (1967). Electron microscopic observations on the membrane systems of the rat blood platelet. *The Anatomical Record*, *158*(2), 121–137. https://doi.org/10.1002/ar.1091580203

Bender, M., Giannini, S., Grozovsky, R., Jönsson, T., Christensen, H., Pluthero, F. G., … Falet, H. (2015). Dynamin 2-dependent endocytosis is required for normal megakaryocyte development in mice. *Blood*, *125*(6), 1014–1024. https://doi.org/10.1182/blood-2014-07-587857

Bender, M., Thon, J. N., Ehrlicher, A. J., Wu, S., Mazutis, L., & Deschmann, E. (2015). Microtubule sliding drives proplatelet elongation and is dependent on cytoplasmic dynein. *Blood*, *125*(5), 860–868.

Bennett, J. P., Zaner, K. S., & Stossel, T. P. (1984). Isolation and Some Properties of Macrophage α-Actinin: Evidence that it is not an Actin Gelling Protein. *Biochemistry*, *23*(21), 5081–5086. https://doi.org/10.1021/bi00316a039

Benninger, G. W., & Kreps, S. I. (1971). Aggregation phenomenon in an IgG multiple myeloma resulting in the hyperviscosity syndrome. *The American Journal of Medicine*, *51*(2), 287–293. https://doi.org/10.1016/0002-9343(71)90247-6

Bergmann, C. B., Hefele, F., Unger, M., Huber-Wagner, S., Biberthaler, P., van Griensven, M., & Hanschen, M. (2016). Platelets modulate the immune response following trauma by interaction with CD4+ T regulatory cells in a mouse model. *Immunologic Research*, *64*(2), 508–517. https://doi.org/10.1007/s12026-015-8726-1

Berlanga, O., Bori-Sanz, T., James, J. R., Frampton, J., Davis, S. J., Tomlinson, M. G., & Watson, S. P. (2007). Glycoprotein VI oligomerization in cell lines and platelets. *Journal of Thrombosis and Haemostasis*, *5*(5), 1026–1033. https://doi.org/10.1111/j.1538-7836.2007.02449.x

Berman, Y., & North, K. N. (2010). A gene for speed: The emerging role of α-actinin-3 in muscle metabolism. *Physiology*, *25*(4), 250–259. https://doi.org/10.1152/physiol.00008.2010

Best, M. G., Sol, N., Kooi, I., Tannous, J., Westerman, B. A., Rustenburg, F., … Wurdinger, T. (2015). RNA-Seq of Tumor-Educated Platelets Enables Blood-Based Pan-Cancer, Multiclass, and Molecular Pathway Cancer Diagnostics. *Cancer Cell*, *28*(5), 666–676. https://doi.org/10.1016/j.ccell.2015.09.018

Bhatt, A., Kaverina, I., Otey, C., & Huttenlocher, A. (2002). Regulation of focal complex composition and disassembly by the calcium-dependent protease calpain. *Journal of Cell Science*, *115*(17), 3415–3425.

Bierings, R., & Voorberg, J. (2016). Up or out: polarity of VWF release. *Blood*, *128*(2), 154–155. https://doi.org/10.1182/blood-2016-05-713057

Biino, G., Santimone, I., Minelli, C., Sorice, R., Frongia, B., Traglia, M., … Balduini, C. L. (2013). Age- And Sex-Related Variations in Platelet Count in Italy: A Proposal of Reference Ranges Based on 40987 Subjects' Data. *PLoS ONE*, *8*(1). https://doi.org/10.1371/journal.pone.0054289

Biron, D., & Moses, E. (2004). The Effect of α-Actinin on the Length Distribution of F-Actin. *Biophysical Journal*, *86*(5), 3284–3290. https://doi.org/10.1016/S0006-3495(04)74376-3

Blair, P., Rex, S., Vitseva, O., Beaulieu, L., Tanriverdi, K., Chakrabarti, S., … Freedman, J. E. (2009). Stimulation of Toll-Like Receptor 2 in Human Platelets Induces a Thromboinflammatory Response Through Activation of Phosphoinositide 3-Kinase. *Circulation Research*, *104*(3), 346–354. https://doi.org/10.1161/CIRCRESAHA.108.185785

Blair, T. A., Moore, S. F., & Hers, I. (2015a). Circulating primers enhance platelet function and induce resistance to antiplatelet therapy. *Journal of Thrombosis and Haemostasis*, *13*(8), 1479–1493. https://doi.org/10.1111/jth.13022

Blair, T. A., Moore, S. F., & Hers, I. (2015b). Circulating primers enhance platelet function and induce resistance to antiplatelet therapy. *Journal of Thrombosis and Haemostasis*, *13*(8), 1479–1493. https://doi.org/10.1111/jth.13022

Blair, Thomas A., Moore, S. F., Williams, C. M., Poole, A. W., Vanhaesebroeck, B., & Hers, I. (2014). Phosphoinositide 3-kinases p110α and p110β have differential roles in insulin-like growth factor-1-mediated akt phosphorylation and platelet priming. *Arteriosclerosis, Thrombosis, and Vascular Biology*, *34*(8), 1681–1688. https://doi.org/10.1161/ATVBAHA.114.303954

Blanchard, A., Ohanian, V., & Critchley, D. (1989). The structure and function of alpha-

actinin. *Journal of Muscle Research and Cell Motility*, *10*(4), 280–289. Retrieved from http://www.ncbi.nlm.nih.gov/pubmed/2671039

Blanchoin, L., Boujemaa-Paterski, R., Sykes, C., & Plastino, J. (2014). Actin dynamics, architecture, and mechanics in cell motility. *Physiological Reviews*, *94*(1), 235–263. https://doi.org/10.1152/physrev.00018.2013

Blom, J. W., Doggen, C. J. M., Osanto, S., & Rosendaal, F. R. (2005). Malignancies, prothrombotic mutations, and the risk of venous thrombosis. *Journal of the American Medical Association*, *293*(6), 715–722. https://doi.org/10.1001/jama.293.6.715

Boilard, E., Nigrovic, P. A., Larabee, K., Watts, G. F. M., Coblyn, J. S., Weinblatt, M. E., … Lee, D. M. (2010). Platelets amplify inflammation in arthritis via collagen-dependent microparticle production. *Science*, *327*(5965), 580–583. https://doi.org/10.1126/science.1181928

Boilard, E., Paré, G., Rousseau, M., Cloutier, N., Dubuc, I., Lévesque, T., … Flamand, L. (2014). Influenza virus H1N1 activates platelets through FcγRIIA signaling and thrombin generation. *Blood*, *123*(18), 2854–2863. https://doi.org/10.1182/blood-2013-07-515536

Bois, P. R. J., Borgon, R. A., Vonrhein, C., & Izard, T. (2005). Structural Dynamics of α-Actinin-Vinculin Interactions. *Molecular and Cellular Biology*, *25*(14), 6112–6122. https://doi.org/10.1128/mcb.25.14.6112-6122.2005

Bolshakova, A., Petukhova, O., Turoverova, L., Tentler, D., Babakov, V., Magnusson, K. E., & Pinaev, G. (2007). Extra-cellular matrix proteins induce re-distribution of α-actinin-1 and α-actinin-4 in A431 cells. *Cell Biology International*, *31*(4 SPEC. ISS.), 360–365. https://doi.org/10.1016/j.cellbi.2007.01.021

Bonet, C., MacIver, S. K., & Mozo-Villarías, A. (2010). The regulatory action of α-actinin on actin filaments is enhanced by cofilin. *European Biophysics Journal*, *39*(8), 1143–1153. https://doi.org/10.1007/s00249-009-0566-2

Boneu, B., Bugat, R., Boneu, A., Eche, N., Sie, P., & Combes, P. F. (1984). Exhausted platelets in patients with malignant solid tumors without evidence of active consumption coagulopathy. *European Journal of Cancer and Clinical Oncology*, *20*(7), 899–903. https://doi.org/10.1016/0277-5379(84)90161-5

Bordoli, M. R., Yum, J., Breitkopf, S. B., Thon, J. N., Italiano, J. E., Xiao, J., … Whitman, M. (2014). A secreted tyrosine kinase acts in the extracellular environment. *Cell*, *158*(5), 1033–1044. https://doi.org/10.1016/j.cell.2014.06.048

Borrego-Diaz, E., Kerff, F., Lee, S. H., Ferron, F., Li, Y., & Dominguez, R. (2006). Crystal structure of the actin-binding domain of α-actinin 1: Evaluating two competing actin-binding models. *Journal of Structural Biology*, *155*(2), 230–238. https://doi.org/10.1016/j.jsb.2006.01.013

Bottega, R., Marconi, C., Faleschini, M., Baj, G., Cagioni, C., Pecci, A., … Noris, P. (2014). ACTN1-related thrombocytopenia: identification of novel families for phenotypic characterization. *Blood*, *125*(5), 869–872. https://doi.org/10.1182/blood-2014-08-594531

Bottega, R., Marconi, C., Faleschini, M., Baj, G., Cagioni, C., Pecci, A., … Noris, P. (2015). *ACTN1 -related thrombocytopenia : identi fi cation of novel families for phenotypic characterization*. *125*(5), 869–873. https://doi.org/10.1182/blood-2014-08-

594531.R.B.

Boulaftali, Y., Hess, P. R., Kahn, M. L., & Bergmeier, W. (2014, March 28). Platelet Immunoreceptor Tyrosine-based Activation Motif (ITAM) signaling and vascular integrity. *Circulation Research*, Vol. 114, pp. 1174–1184. https://doi.org/10.1161/CIRCRESAHA.114.301611

Boutroux, H., David, B., Guéguen, P., Frange, P., Vincenot, A., Leverger, G., & Favier, R. (2017). ACTN1-related macrothrombocytopenia: A novel entity in the progressing field of pediatric thrombocytopenia. *Journal of Pediatric Hematology/Oncology*, *39*(8), e515–e518. https://doi.org/10.1097/MPH.0000000000000885

Bovill, E. G., Ershler, W. B., Golden, E. A., Tindle, B. H., & Edson, J. R. (1986). A Human Myeloma-Produced Monoclonal Protein Directed Against the Active Subpopulation of Von Willebrand Factor. *American Journal of Clinical Pathology*, *85*(1), 115–123. https://doi.org/10.1093/ajcp/85.1.115

Bozulic, L., Malik, M., Powell, D., Nanez, A., Link, A., & Ramos, D. (2007). Plasma membrane Ca2+-ATPaseassociates withCLP36, α-actinin andactin in human platelets. *Thrombosis and Haemostasis*, *97*, 587–597. https://doi.org/10.1160/TH06

Brighton, T. A., Eikelboom, J. W., Mann, K., Mister, R., Gallus, A., Ockelford, P., … Simes, J. (2012). Low-Dose Aspirin for Preventing Recurrent Venous Thromboembolism. *New England Journal of Medicine*, *367*(21), 1979–1987. https://doi.org/10.1056/NEJMoa1210384

Brill, A., Fuchs, T. A., Chauhan, A. K., Yang, J. J., De Meyer, S. F., Köllnberger, M., … Wagner, D. D. (2011). Von Willebrand factor-mediated platelet adhesion is critical for deep vein thrombosis in mouse models. *Blood*, *117*(4), 1400–1407. https://doi.org/10.1182/blood-2010-05-287623

Brown, E., Carlin, L. M., Nerlov, C., Lo Celso, C., & Poole, A. W. (2018). Multiple membrane extrusion sites drive megakaryocyte migration into bone marrow blood vessels. *Life Science Alliance*, *1*(2), 1–24. https://doi.org/10.26508/lsa.201800061

Brzeska, H., Venyaminov, S. V., Grabarek, Z., & Drabikowski, W. Comparative studies on thermostability of calmodulin, skeletal muscle troponin C and their tryptic fragments. , 153 FEBS Letters § (1983).

Bunimov, N., Fuller, N., & Hayward, C. M. P. (2013). Genetic loci associated with platelet traits and platelet disorders. *Seminars in Thrombosis and Hemostasis*, *39*(3), 291–305. https://doi.org/10.1055/s-0033-1334466

Burgueño, J., Blake, D. J., Benson, M. A., Tinsley, C. L., Esapa, C. T., Canela, E. I., … Ciruela, F. (2003). The adenosine A2A receptor interacts with the actin-binding protein α-actinin. *Journal of Biological Chemistry*, *278*(39), 37545–37552. https://doi.org/10.1074/jbc.M302809200

Burkhart, J. M., Vaudel, M., Gambaryan, S., Radau, S., Walter, U., Martens, L., … Zahedi, R. P. (2012). The first comprehensive and quantitative analysis of human platelet protein composition allows the comparative analysis of structural and functional pathways. *E-Blood*, *120*(15), 73–82. https://doi.org/10.1182/blood-2012-04-416594.

Burley, K., Westbury, S. K., & Mumford, A. D. (2018, February 17). TUBB1 variants and human platelet traits. *Platelets*, Vol. 29, pp. 209–211. https://doi.org/10.1080/09537104.2017.1411587

Burn, P., Rotman, A., Meyer, R. K., & Burger, M. M. (1985). Diacylglycerol in large α-actinin/actin complexes and in the cytoskeleton of activated platelets. *Nature*, *314*(6010), 469–472. https://doi.org/10.1038/314469a0

Burridge, K. (2017). Focal Adhesions: a personal perspective on a half century of progress. *FEBS*, *284*(20), 3355–3361. https://doi.org/10.1111/febs.14195.Focal

Bury, L., Falcinelli, E., Chiasserini, D., Springer, T. A., Italiano, J. E., & Gresele, P. (2016). Cytoskeletal perturbation leads to platelet dysfunction and thrombocytopenia in variant forms of Glanzmann thrombasthenia. *Haematologica*, *101*(1), 46–56. https://doi.org/10.3324/haematol.2015.130849

Bye, A. P., Unsworth, A. J., & Gibbins, J. M. (2016). Platelet signaling: a complex interplay between inhibitory and activatory networks. *Journal of Thrombosis and Haemostasis : JTH*, *14*(5), 918–930. https://doi.org/10.1111/jth.13302

Cahill, M. R., Macey, M. G., & Newland, A. C. (1996). Correlation of GP53 and P-selectin expression in myeloproliferative disorders and normal controls. *Blood Coagulation and Fibrinolysis*, *7*(2), 169–171. https://doi.org/10.1097/00001721-199603000-00014

Cahill, Mary R. (1995). *Platelet Activation: Measurement and Clinical Significance*. University of London.

Calaminus, S. D. J., Thomas, S., McCarty, O. J. T., Machesky, L. M., & Watson, S. P. (2008). Identification of a novel, actin-rich structure, the actin nodule, in the early stages of platelet spreading. *Journal of Thrombosis and Haemostasis*, *6*(11), 1944–1952. https://doi.org/10.1111/j.1538-7836.2008.03141.x

Calverley, D. C., Brass, E., Hacker, M. R., Tsao-Wei, D. D., Espina, B. M., Pullarkat, V. A., … Groshen, S. (2002). Potential role of platelet FcγRIIA in collagen-mediated platelet activation associated with atherothrombosis. *Atherosclerosis*, *164*(2), 261–267. https://doi.org/10.1016/S0021-9150(02)00179-X

Camerer, E., Qazi, A. A., Duong, D. N., Cornelissen, I., Advincula, R., & Coughlin, S. R. (2004). Platelets, protease-activated receptors, and fibrinogen in hematogenous metastasis. *Blood*, *104*(2), 397–401. https://doi.org/10.1182/blood-2004-02-0434

Canobbio, I., Stefanini, L., Guidetti, G. F., Balduini, C., & Torti, M. (2006). A new role for FcγRIIA in the potentiation of human platelet activation induced by weak stimulation. *Cellular Signalling*, *18*(6), 861–870. https://doi.org/10.1016/j.cellsig.2005.07.014

Caparrós-Pérez, E., Teruel-Montoya, R., Palma-Barquero, V., Torregrosa, J., Blanco, J., Delgado, J., … Ferrer-Marín, F. (2017). Down Regulation of the Munc18b-syntaxin-11 Complex and β1-tubulin Impairs Secretion and Spreading in Neonatal Platelets. *Thrombosis and Haemostasis*, *117*(11), 2079–2091. https://doi.org/10.1160/TH17-04-0241

Capra, J. D., & Kunkel, H. G. (1970). Aggregation of gamma-G3 proteins: relevance to the hyperviscosity syndrome. *The Journal of Clinical Investigation*, *49*(3), 610–621. https://doi.org/10.1172/JCI106272

Case, L. B., & Waterman, C. M. (2015). Integration of actin dynamics and cell dhesion by a three-dimensional, mechanosensitive molecular clutch. *Nature Cell Biology*, *17*(8), 955–963. https://doi.org/10.1038/ncb3191.Integration

Catani, M. V., Savini, I., Tullio, V., & Gasperi, V. (2020). *The " Janus Face " of Platelets in Cancer*.

Cattaneo, M. (2009). New P2Y12 blockers. *Journal of Thrombosis and Haemostasis*, *7*(SUPPL. 1), 262–265. https://doi.org/10.1111/j.1538-7836.2009.03382.x

Cattaneo, Marco. (2006). *P2Y 12 receptor antagonists: a rapidly expanding group of antiplatelet agents*. https://doi.org/10.1093/eurheartj/ehi754

Cesari, F., Marcucci, R., Gori, A. M., Caporale, R., Fanelli, A., Casola, G., … Abbate, R. (2013). Reticulated platelets predict cardiovascular death in acute coronary syndrome patients: Insights from the AMI-florence 2 study. *Thrombosis and Haemostasis*, *109*(5), 846–853. https://doi.org/10.1160/TH12-09-0709

Cha, J.-K., Jo, W.-S., Shin, H. C., Bae, H.-R., Ho, J.-M., & Kim, J. W. (2004). Increased platelet CD63 and P-selectin expression persist in atherosclerotic ischemic stroke. *Platelets*, *15*(1), 3–7. https://doi.org/10.1080/09537100310001644024

Chakraborty, R., Bin Riaz, I., Malik, S. U., Marneni, N., Mejia Garcia, A., Anwer, F., … Majhail, N. S. (2020). Venous thromboembolism risk with contemporary lenalidomide-based regimens despite thromboprophylaxis in multiple myeloma: A systematic review and meta-analysis. *Cancer*, 1–11. https://doi.org/10.1002/cncr.32682

Chan, Y. M., Tong, H. Q., Beggs, A. H., & Kunkel, L. M. (1998). Human skeletal muscle-specific α-actinin-2 and -3 isoforms form homodimers and heterodimers in vitro and in vivo. *Biochemical and Biophysical Research Communications*, *248*(1), 134–139. https://doi.org/10.1006/bbrc.1998.8920

Chiu, C., Bagnall, R. D., Ingles, J., Yeates, L., Kennerson, M., Donald, J. A., … Semsarian, C. (2010). Mutations in Alpha-Actinin-2 Cause Hypertrophic Cardiomyopathy. A Genome-Wide Analysis. *Journal of the American College of Cardiology*, *55*(11), 1127–1135. https://doi.org/10.1016/j.jacc.2009.11.016

Choi, C. K., Vicente-Manzanares, M., Zareno, J., Whitmore, L. A., Mogilner, A., & Horwitz, A. R. (2008). Actin and α-actinin orchestrate the assembly and maturation of nascent adhesions in a myosin II motor-independent manner. *Nature Cell Biology*, *10*(9), 1039–1050. https://doi.org/10.1038/ncb1763

Chowrashi, P., Mittal, B., Sanger, J. M., & Sanger, J. W. (2002). Amorphin is phosphorylase; Phosphorylase is an alpha-actinin-binding protein. *Cell Motility and the Cytoskeleton*, *53*(2), 125–135. https://doi.org/10.1002/cm.10059

Choy, E., Ganeshalingam, K., Semb, A. G., Szekanecz, Z., & Nurmohamed, M. (2014, December 1). Cardiovascular risk in rheumatoid arthritis: Recent advances in the understanding of the pivotal role of inflammation, risk predictors and the impact of treatment. *Rheumatology (United Kingdom)*, Vol. 53, pp. 2143–2154. https://doi.org/10.1093/rheumatology/keu224

Christerson, L. B., Vanderbilt, C. A., & Cobb, M. H. (1999). MEKK1 interacts with α-actinin and localizes to stress fibers and focal adhesion. *Cell Motility and the Cytoskeleton*, *43*(3), 186–198. https://doi.org/10.1002/(SICI)1097-0169(1999)43:3<186::AID-CM2>3.0.CO;2-1

Cieslar, P., Mášová, L., Scheiner, T., Ryšavá, J., Křížová, P., Danzigová, Z., … Tesař, V. (2002). Oxidative stress and platelet function in multiple myeloma and renal insufficiency - Clinical relations of different tests. *Thrombosis Research*, *105*(4), 277–283. https://doi.org/10.1016/S0049-3848(02)00003-8

Clancy, L., Beaulieu, L. M., Tanriverdi, K., & Freedman, J. E. (2017). The role of RNA uptake

in platelet heterogeneity. *Thrombosis and Haemostasis*, *117*(5), 948–961. https://doi.org/10.1160/TH16-11-0873

Clark, K. A., McElhinny, A. S., Beckerle, M. C., & Gregorio, C. C. (2002). Striated muscle cytoarchitecture: An intricate web of form and function. *Annual Review of Cell and Developmental Biology*, Vol. 18, pp. 637–706. https://doi.org/10.1146/annurev.cellbio.18.012502.105840

Clark, S. R., Ma, A. C., Tavener, S. A., McDonald, B., Goodarzi, Z., Kelly, M. M., … Kubes, P. (2007). Platelet TLR4 activates neutrophil extracellular traps to ensnare bacteria in septic blood. *Nature Medicine*, *13*(4), 463–469. https://doi.org/10.1038/nm1565

Cognasse, F., Hamzeh-Cognasse, H., Lafarge, S., Chavarin, P., Cogné, M., Richard, Y., & Garraud, O. (2007). Human platelets can activate peripheral blood B cells and increase production of immunoglobulins. *Experimental Hematology*, *35*(9), 1376–1387. https://doi.org/10.1016/j.exphem.2007.05.021

Cohen, A. L., & Sarid, R. (2010). The relationship between monoclonal gammopathy of undetermined significance and venous thromboembolic disease. *Thrombosis Research*, *125*(3), 216–219. https://doi.org/10.1016/j.thromres.2009.01.004

Colucci, G., Stutz, M., Rochat, S., Conte, T., Pavicic, M., Reusser, M., … Alberio, L. (2014). *The effect of desmopressin on platelet function : a selective enhancement of procoagulant COAT platelets in patients with primary platelet function defects*. *123*(12), 1905–1916. https://doi.org/10.1182/blood-2013-04-497123

Cooper, J. A., & Schafer, D. A. (2000). Control of actin assembly and disassembly at filament ends. *Current Opinion in Cell Biology*, *12*(1), 97–103. https://doi.org/10.1016/S0955-0674(99)00062-9

Corgan, A. M., Singleton, C., Santoso, C. B., & Greenwood, J. A. (2004). Phosphoinositides differentially regulate α-actinin flexibility and function. *Biochemical Journal*, *378*(3), 1067–1072. https://doi.org/10.1042/BJ20031124

Cornelissen, L. L., Caram-Deelder, C., Meier, R. T., Zwaginga, J. J., Evers, D., & Consortium, D. B. T. R. R. (2021). Platelet transfusion and tranexamic acid to prevent bleeding in outpatients with a hematological disease: A Dutch nationwide survey. *European Journal of Haematology*, *106*(3), 362–370. https://doi.org/https://doi.org/10.1111/ejh.13555

Cosemans, J. M. E. M., Schols, S. E. M., Stefanini, L., De Witt, S., Feijge, M. A. H., Hamulyák, K., … Heemskerk, J. W. M. (2011). Key role of glycoprotein Ib/V/IX and von Willebrand factor in platelet activation-dependent fibrin formation at low shear flow. *Blood*, *117*(2), 651–660. https://doi.org/10.1182/blood-2010-01-262683

Coupland, L. A., Chong, B. H., & Parish, C. R. (2012). Platelets and P-selectin control tumor cell metastasis in an organ-specific manner and independently of NK cells. *Cancer Research*, *72*(18), 4662–4671. https://doi.org/10.1158/0008-5472.CAN-11-4010

Cox, S., Rosten, E., Monypenny, J., & Jovanovic-talisman, T. (2012). Bayesian localisation microscopy reveals nanoscale podosome dynamics. *Nature Methods*, *9*(2), 195–200. https://doi.org/10.1038/nmeth.1812.Bayesian

Croquefer, S., Renaudineau, Y., Jousse, S., Gueguen, P., Ansart, S., Saraux, A., & Youinou, P. (2005). The anti-alpha-actinin test completes anti-DNA determination in systemic lupus erythematosus. *Annals of the New York Academy of Sciences*, *1050*, 170–175.

https://doi.org/10.1196/annals.1313.017

Crowley, M P, Quinn, S., Coleman, E., Eustace, J. A., Gilligan, O. M., & O'Shea, S. I. (2015). Differing coagulation profiles of patients with monoclonal gammopathy of undetermined significance and multiple myeloma. *J Thromb Thrombolysis*, *39*(2), 245–249. https://doi.org/10.1007/s11239-014-1140-z

Crowley, Maeve P., Kevane, B., O'shea, S. I., Quinn, S., Egan, K., Gilligan, O. M., & Ní Áinle, F. (2016). Plasma Thrombin Generation and Sensitivity to Activated Protein C Among Patients With Myeloma and Monoclonal Gammopathy of Undetermined Significance. *Clinical and Applied Thrombosis/Hemostasis*, *22*(6), 554–562. https://doi.org/10.1177/1076029615625825

Crowther, G. J., He, P., Rodenbough, P. P., Thomas, A. P., Kovzun, K. V, Leibly, D. J., … Van Voorhis, W. C. (2010). Use of thermal melt curves to assess the quality of enzyme preparations. *Analytical Biochemistry*, *399*(2), 268–275. https://doi.org/10.1016/j.ab.2009.12.018

Cuenca-zamora, E. J., Ferrer-mar, F., & Rivera, J. (2019). *Tubulin in Platelets : When the Shape Matters*. 1–13.

Cuevas, B. D., Abell, A. N., Witowsky, J. A., Yujiri, T., Johnson, N. L., Kesavan, K., … Johnson, G. L. (2003). MEKK1 regulates calpain-dependent proteolysis of focal adhesion proteins for rear-end detachment of migrating fibroblasts. *EMBO Journal*, *22*(13), 3346–3355. https://doi.org/10.1093/emboj/cdg322

Dandapani, S. V., Sugimoto, H., Matthews, B. D., Kolb, R. J., Sinha, S., Gerszten, R. E., … Pollak, M. R. (2007). A-Actinin-4 Is Required for Normal Podocyte Adhesion. *Journal of Biological Chemistry*, *282*(1), 467–477. https://doi.org/10.1074/jbc.M605024200

De Stoppelaar, S. F., Van 't Veer, C., Claushuis, T. A. M., Albersen, B. J. A., Roelofs, J. J. T. H., & Van Der Poll, T. (2014). Thrombocytopenia impairs host defense in gram-negative pneumonia-derived sepsis in mice. *Blood*, *124*(25), 3781–3790. https://doi.org/10.1182/blood-2014-05-573915

DeMali, K. A., Barlow, C. A., & Burridge, K. (2002). Recruitment of the Arp2/3 complex to vinculin: Coupling membrane protrusion to matrix adhesion. *Journal of Cell Biology*, *159*(5), 881–891. https://doi.org/10.1083/jcb.200206043

Deocharan, B., Qing, X., Lichauco, J., & Putterman, C. (2002). α-Actinin Is a Cross-Reactive Renal Target for Pathogenic Anti-DNA Antibodies. *The Journal of Immunology*, *168*(6), 3072–3078. https://doi.org/10.4049/jimmunol.168.6.3072

Deocharan, B., Zhou, Z., Antar, K., Siconolfi-Baez, L., Angeletti, R. H., Hardin, J., & Putterman, C. (2007). α-Actinin Immunization Elicits Anti-Chromatin Autoimmunity in Nonautoimmune Mice. *The Journal of Immunology*, *179*(2), 1313–1321. https://doi.org/10.4049/jimmunol.179.2.1313

Deppermann, C., Cherpokova, D., Nurden, P., Schulz, J. N., Thielmann, I., Kraft, P., … Nieswandt, B. (2013). Gray platelet syndrome and defective thrombo-inflammation in Nbeal2-deficient mice. *Journal of Clinical Investigation*, *123*(8), 3331–3342. https://doi.org/10.1172/JCI69210

Deppermann, C., & Kubes, P. (2018). Start a fire, kill the bug: The role of platelets in inflammation and infection. *Innate Immunity*, *24*(6), 335–348. https://doi.org/10.1177/1753425918789255

Dessen, P., Le Roux, D. T., Kauffmann, A., Robert, T., Larbret, F., Sekkai, D., … Raslova, H. (2006). Interrelation between polyploidization and megakaryocyte differentiation: a gene profiling approach. *Blood*, *109*(8), 3225–3234. https://doi.org/10.1182/blood-2006-07-037838

Diacovo, T. G., DeFougerolles, A. R., Bainton, D. F., & Springer, T. A. (1994). A functional integrin ligand on the surface of platelets: Intercellular adhesion molecule-2. *Journal of Clinical Investigation*, *94*(3), 1243–1251. https://doi.org/10.1172/JCI117442

Diacovo, T. G., Puri, K. D., Warnock, R. A., Springer, T. A., & Von Andrian, U. H. (1996). Platelet-mediated lymphocyte delivery to high endothelial venules. *Science*, *273*(5272), 252–255. https://doi.org/10.1126/science.273.5272.252

DiMinno, G., Coraggio, F., Cerbone, A. M., Capitanio, A. M., Manzo, C., Spina, M., … Mancini, M. (1986). A myeloma paraprotein with specificity for platelet glycoprotein IIIa in a patient with a fatal bleeding disorder. *Journal of Clinical Investigation*, *77*(1), 157–164. https://doi.org/10.1172/JCI112270

Dixson, J. D., Forstner, M. R. J., & Garcia, D. M. (2003). The α-actinin gene family: A revised classification. *Journal of Molecular Evolution*, *56*(1), 1–10. https://doi.org/10.1007/s00239-002-2374-5

Djinovic-Carugo, K., Gautel, M., Ylänne, J., & Young, P. (2002a). The spectrin repeat: A structural platform for cytoskeletal protein assemblies. *FEBS Letters*, *513*(1), 119–123. https://doi.org/10.1016/S0014-5793(01)03304-X

Djinovic-Carugo, K., Gautel, M., Ylänne, J., & Young, P. (2002b). The spectrin repeat: A structural platform for cytoskeletal protein assemblies. *FEBS Letters*, *513*(1), 119–123. https://doi.org/10.1016/S0014-5793(01)03304-X

Djinovic-Carugo, K., Young, P., Gautel, M., & Saraste, M. (1999). Structure of the-Actinin Rod: Molecular Basis for Cross-Linking of Actin Filaments-Actinin is composed of an amino-terminal actin-binding region consisting of two calponin homology (CH) domains, a central rod containing four spectrin-like re. *Cell*, *98*, 537–546.

Djunic, I., Elezovic, I., Vucic, M., Srdic-Rajic, T., Konic-Ristic, A., Ilic, V., … Tomin, D. (2013). Specific binding of paraprotein to platelet receptors as a cause of platelet dysfunction in monoclonal gammopathies. *Acta Haematologica*, *130*(2), 101–107. https://doi.org/10.1159/000345418

Donada, A., Balayn, N., Siwa, D., & Lordier, L. (2019). Disrupted filamin A/αIIbβ3 interaction induces macrothrombocytopenia by increasing RhoA activity. *Blood*, *133*(16), 1778–1788.

Dourdin, N., Bhatt, A. K., Dutt, P., Greer, P. A., Arthur, J. S. C., Elce, J. S., & Huttenlocher, A. (2001). Reduced Cell Migration and Disruption of the Actin Cytoskeleton in Calpain-deficient Embryonic Fibroblasts. *Journal of Biological Chemistry*, *276*(51), 48382–48388. https://doi.org/10.1074/jbc.M108893200

Downey, C., Craig, D. H., & Basson, M. D. (2011). Isoform-specific modulation of pressure-stimulated cancer cell proliferation and adhesion by α-actinin. *American Journal of Surgery*, *202*(5), 520–523. https://doi.org/10.1016/j.amjsurg.2011.06.019

Drmota Prebil, S., Slapšak, U., Pavšic, M., Ilc, G., Puž, V., De Almeida Ribeiro, E., … Djinovic-Carugo, K. (2016). Structure and calcium-binding studies of calmodulin-like domain of human non-muscle α-Actinin-1. *Scientific Reports*, *6*(May), 1–13.

https://doi.org/10.1038/srep27383

Dubernard, Ve ́ronique, Faucher, D., Launay, J. M., & Legrand, C. (1995). Identification of the cytoskeletal protein α-actinin as a platelet thrombospondin-binding protein. *FEBS Letters*, *364*(2), 109–114. https://doi.org/10.1016/0014-5793(95)00362-D

Dubernard, Véronique, Arbeille, B. B., Lemesle, M. B., & Legrand, C. (1997). Evidence for an α-granular pool of the cytoskeletal protein α-actinin in human platelets that redistributes with the adhesive glycoprotein thrombospondin-1 during the exocytotic process. *Arteriosclerosis, Thrombosis, and Vascular Biology*, *17*(10), 2293–2305. https://doi.org/10.1161/01.ATV.17.10.2293

Dubreuil, R. R., & Wang, P. (2000). Genetic analysis of the requirements for α-actinin function. *Journal of Muscle Research and Cell Motility*, *21*(7), 705–713. https://doi.org/10.1023/A:1005699608893

Dunkley, S., & Gaudry, L. (2007). Thalidomide causes platelet activation, which can be abrogated by aspirin [2]. *Journal of Thrombosis and Haemostasis*, *5*(6), 1323–1325. https://doi.org/10.1111/j.1538-7836.2007.02542.x

Ebashi, S., & Ebashi, F. (1964). A new protein factor promoting contraction of actomyosin. *Nature*, Vol. 203, pp. 645–646. https://doi.org/10.1038/203645a0

Eckly, A., Rinckel, J. Y., Proamer, F., Ulas, N., Joshi, S., Whiteheart, S. W., & Gachet, C. (2016). Respective contributions of single and compound granule fusion to secretion by activated platelets. *Blood*, *128*(21), 2538–2549. https://doi.org/10.1182/blood-2016-03-705681

Eckly, A., Scandola, C., Oprescu, A., Michel, D., Rinckel, J. Y., Proamer, F., … Gachet, C. (2020). Megakaryocytes use in vivo podosome-like structures working collectively to penetrate the endothelial barrier of bone marrow sinusoids. *Journal of Thrombosis and Haemostasis*, *18*(11), 2987–3001. https://doi.org/10.1111/jth.15024

Edelstein-Keshet, L., & Ermentrout, G. B. (1998). Models for the length distributions of actin filaments: I. Simple polymerization and fragmentation. *Bulletin of Mathematical Biology*, *60*(3), 449–475. https://doi.org/10.1006/bulm.1997.0011

Edelstein, L. C. (2017, April 3). The role of platelet microvesicles in intercellular communication. *Platelets*, Vol. 28, pp. 222–227. https://doi.org/10.1080/09537104.2016.1257114

Egan, K., Cooke, N., Dunne, E., Murphy, P., Quinn, J., & Kenny, D. (2014). Platelet hyporeactivity in active myeloma. *Thrombosis Research*, *134*(3), 747–749. https://doi.org/10.1016/j.thromres.2014.06.018

Ehrlicher, A. J., Krishnan, R., Guo, M., Bidan, C. M., Weitz, D. A., & Pollak, M. R. (2015). Alpha-actinin binding kinetics modulate cellular dynamics and force generation. *Proceedings of the National Academy of Sciences of the United States of America*, *112*(21), 6619–6624. https://doi.org/10.1073/pnas.1505652112

Eicher, J. D., Lettre, G., & Johnson, A. D. (2018). The genetics of platelet count and volume in humans John. *Platelets*, *29*(2), 125–130. https://doi.org/10.1080/09537104.2017.1317732.The

Elagib, K. E., Rubinstein, J. D., Delehanty, L. L., Ngoh, V. S., Greer, P. A., Li, S., … Goldfarb, A. N. (2013a). Calpain 2 activation of P-TEFb drives megakaryocyte morphogenesis and is disrupted by leukemogenic GATA1 mutation. *Developmental Cell*, *27*(6), 607–620.

https://doi.org/10.1016/j.devcel.2013.11.013

Elagib, K. E., Rubinstein, J. D., Delehanty, L. L., Ngoh, V. S., Greer, P. A., Li, S., … Goldfarb, A. N. (2013b). Calpain 2 activation of P-TEFb drives megakaryocyte morphogenesis and is disrupted by leukemogenic GATA1 mutation. *Developmental Cell*, *27*(6), 607–620. https://doi.org/10.1016/j.devcel.2013.11.013

Elzey, B. D., Tian, J., Jensen, R. J., Swanson, A. K., Lees, J. R., Lentz, S. R., … Ratliff, T. L. (2003). Platelet-mediated modulation of adaptive immunity: A communication link between innate and adaptive immune compartments. *Immunity*, *19*(1), 9–19. https://doi.org/10.1016/S1074-7613(03)00177-8

Engebraaten, O., Trikha, M., Juell, S., Garman-Vik, S., & Fodstad, Ø. (2009). Inhibition of in vivo tumour growth by the blocking of host alpha(v)beta3 and alphaII(b)beta3 integrins. *Anticancer Research*, *29*(1), 131–137. Retrieved from http://www.ncbi.nlm.nih.gov/pubmed/19331142

Escolar, G., Krumwiede, M., & White, J. G. (1986). Organization of the actin cytoskeleton of resting and activated platelets in suspension. *American Journal of Pathology*, *123*(1), 86–94.

Escolar, Gines, Leistikow, E., & White, J. G. (1989). The Fate of the Open Canalicular System in Surface and Suspension-Activated Platelets. In *Blood* (Vol. 74). Retrieved from https://ashpublications.org/blood/article-pdf/74/6/1983/602763/1983.pdf?casa_token=RiXQ-RSrEjkAAAAA:VIwxhC2VgHk9eRStJbjXU6U6dSSJB2h9TrzgN9weVbSe9lcuETN-hdA0kZqw9OdjnSqzXFov

Esue, O., Tseng, Y., & Wirtz, D. (2009). A-Actinin and Filamin Cooperatively Enhance the Stiffness of Actin Filament Networks. *PLoS ONE*, *4*(2), 1–6. https://doi.org/10.1371/journal.pone.0004411

Eynon, N., Hanson, E. D., Lucia, A., Houweling, P. J., Garton, F., North, K. N., & Bishop, D. J. (2013). Genes for elite power and sprint performance: ACTN3 leads the way. *Sports Medicine*, *43*(9), 803–817. https://doi.org/10.1007/s40279-013-0059-4

Faleschini, M., Melazzini, F., Marconi, C., Giangregorio, T., Pippucci, T., Cigalini, E., … Noris, P. (2018). ACTN1 mutations lead to a benign form of platelet macrocytosis not always associated with thrombocytopenia. *British Journal of Haematology*, *183*(2), 276–288. https://doi.org/10.1111/bjh.15531

Falzone, T., Lenz, M., Kovar, D., & Gardel, M. (2013). Assembly Kinetics Determine the Architecture of α-actinin Crosslinked F-actin Networks. *Nature Communications*, (3), 861. https://doi.org/10.1038/ncomms1862.Assembly

Feng, D., DuMontier, C., & Pollak, M. R. (2015). The role of alpha-actinin-4 in human kidney disease. *Cell and Bioscience*, *5*(1), 1–7. https://doi.org/10.1186/s13578-015-0036-8

Feng, D., Notbohm, J., Benjamin, A., He, S., Wang, M., Ang, L.-H., … Pollak, M. R. (2018). Disease-causing mutation in α-actinin-4 promotes podocyte detachment through maladaptation to periodic stretch. *Proceedings of the National Academy of Sciences of the United States of America*, *115*(7), 1517–1522. https://doi.org/10.1073/pnas.1717870115

Feng, S., Reséndiz, J. C., Christodoulides, N., Lu, X., Arboleda, D., Berndt, M. C., & Kroll, M. H. (2002). Pathological shear stress stimulates the tyrosine phosphorylation of alpha-

actinin associated with the glycoprotein Ib-IX complex. *Biochemistry*, *41*(4), 1100–1108. Retrieved from http://www.ncbi.nlm.nih.gov/pubmed/11802708

Feng, Y., Ngu, H., Alford, S. K., Ward, M., Yin, F., & Longmore, G. D. (2013). α-Actinin1 and 4 tyrosine phosphorylation is critical for stress fiber establishment, maintenance and focal adhesion maturation. *Experimental Cell Research*, *319*(8), 1124–1135. https://doi.org/10.1016/j.yexcr.2013.02.009

Ferroni, P., Guadagni, F., Riondino, S., Portarena, I., Mariotti, S., La Farina, F., … Roselli, M. (2014). Evaluation of mean platelet volume as a predictive marker for cancer-associated venous thromboembolism during chemotherapy. *Haematologica*, *99*(10), 1638–1644. https://doi.org/10.3324/haematol.2014.109470

Finsterbusch, M., Schrottmaier, W. C., Kral-Pointner, J. B., Salzmann, M., & Assinger, A. (2018). Measuring and interpreting platelet-leukocyte aggregates. *Platelets*, *29*(7), 677–685. https://doi.org/10.1080/09537104.2018.1430358

Flaumenhaft, R., Dilks, J. R., Rozenvayn, N., Monahan-Earley, R. A., Feng, D., & Dvorak, A. M. (2005). The actin cytoskeleton differentially regulates platelet α-granule and dense-granule secretion. *Blood*, *105*(10), 3879–3887. https://doi.org/10.1182/blood-2004-04-1392

Flood, G., Kahana, E., Gilmore, A. P., Rowe, A. J., Gratzer, W. B., & Critchley, D. R. (1995). Association of structural repeats in the α-actinin rod domain. Alignment of inter-subunit interactions. *Journal of Molecular Biology*, *252*(2), 227–234. https://doi.org/10.1006/jmbi.1995.0490

Flood, G., Rowe, A. J., Critchley, D. R., & Gratzer, W. B. (1997). Further analysis of the role of spectrin repeat motifs in α-actinin dimer formation. *European Biophysics Journal*, *25*(5–6), 431–435. https://doi.org/10.1007/s002490050057

Foley, K. (2013a). *Characterisation of the non- muscle α -actinins*. (January).

Foley, K. (2013b). *Characterisation of the non-muscle α-actinins* (University College Cork). Retrieved from https://cora.ucc.ie/handle/10468/1180

Foley, K. S., & Young, P. W. (2013). An analysis of splicing, actin-binding properties, heterodimerization and molecular interactions of the non-muscle α-actinins. *Biochemical Journal*, *452*(3), 477–488. https://doi.org/10.1042/BJ20121824

Foley, K. S., & Young, P. W. (2014). The non-muscle functions of actinins: an update. *The Biochemical Journal*, *459*, 1–13. https://doi.org/10.1042/BJ20131511

Foss, B., & Bruserud, Ø. (2008, January). Platelet functions and clinical effects in acute myelogenous leukemia. *Thrombosis and Haemostasis*, Vol. 99, pp. 27–37. https://doi.org/10.1160/TH07-04-0240

Fotiou, D., Gavriatopoulou, M., Ntanasis-Stathopoulos, I., Migkou, M., Dimopoulos, M. A., & Terpos, E. (2019, May 4). Updates on thrombotic events associated with multiple myeloma. *Expert Review of Hematology*, Vol. 12, pp. 355–365. https://doi.org/10.1080/17474086.2019.1604214

Fotiou, D., Gavriatopoulou, M., & Terpos, E. (2020). Multiple myeloma and thrombosis: Prophylaxis and risk prediction tools. *Cancers*, *12*(1). https://doi.org/10.3390/cancers12010191

Fotiou, D., Sergentanis, T. N., Papageorgiou, L., Stamatelopoulos, K., Gavriatopoulou, M.,

Kastritis, E., … Gerotziafas, G. T. (2018). Longer procoagulant phospholipid-dependent clotting time, lower endogenous thrombin potential and higher tissue factor pathway inhibitor concentrations are associated with increased VTE occurrence in patients with newly diagnosed multiple myeloma: results. *Blood Cancer Journal*, *8*(11), 102. https://doi.org/10.1038/s41408-018-0135-y

Fraley, T. S., Pereira, C. B., Tran, T. C., Singleton, C. A., & Greenwood, J. A. (2005). Phosphoinositide binding regulates α-actinin dynamics: Mechanism for modulating cytoskeletal remodeling. *Journal of Biological Chemistry*, *280*(15), 15479–15482. https://doi.org/10.1074/jbc.M500631200

Fraley, T. S., Tran, T. C., Corgan, A. M., Nash, C. A., Hao, J., Critchley, D. R., & Greenwood, J. A. (2003). Phosphoinositide binding inhibits α-actinin bundling activity. *Journal of Biological Chemistry*, *278*(26), 24039–24045. https://doi.org/10.1074/jbc.M213288200

Franzot, G., Sjöblom, B., Gautel, M., & Carugo, K. D. (2005). The crystal structure of the actin binding domain from α-actinin in its closed conformation: Structural insight into phospholipid regulation of α-actinin. *Journal of Molecular Biology*, *348*(1), 151–165. https://doi.org/10.1016/j.jmb.2005.01.002

Freson, K., & Turro, E. (2017). High-throughput sequencing approaches for diagnosing hereditary bleeding and platelet disorders. *Journal of Thrombosis and Haemostasis*, *15*(7), 1262–1272. https://doi.org/10.1111/jth.13681

Freynhofer, M. K., Gruber, S. C., Grove, E. L., Weiss, T. W., Wojta, J., & Huber, K. (2015). Antiplatelet drugs in patients with enhanced platelet turnover: Biomarkers versus platelet function testing. *Thrombosis and Haemostasis*, *114*(3), 459–468. https://doi.org/10.1160/TH15-02-0179

Fritz, E, Ludwig, H., Scheithauer, W., & Sinzinger, H. (1986). Shortened platelet half-life in multiple myeloma. *Blood*, *68*(2), 514–520. Retrieved from http://www.ncbi.nlm.nih.gov/pubmed/3730614

Fritz, Elke, Ludwig, H., Scheithauer, W., & Sinzinger, H. (1986). Shortened Platelet Half-life in Multiple Myeloma. *Blood*, *68*(2), 514–520. Retrieved from http://www.ncbi.nlm.nih.gov/pubmed/3730614

Fujiwara, K., Porter, M. E., & Pollard, T. D. (1978). FURROW DURING These observations prompted us to investigate Cells and Staining Preparation o f Fluorescein Labeled Antibodies Biochemical Methods Downloaded from jcb . rupress . org on July 2 , 2010 Purification o f Alpha- Actinin Antibodies Characterizat. *October*, *79*(October).

Fukami, K., Endo, T., Imamura, M., & Takenawa, T. (1994). α-Actinin and vinculin are PIP2-binding proteins involved in signaling by tyrosine kinase. *Journal of Biological Chemistry*, *269*(2), 1518–1522.

Fukami, K., Sawada, N., Endo, T., & Takenawa, T. (1996). Identification of a phosphatidylinositol 4,5-bisphosphate-binding site in chicken skeletal muscle α-actinin. *Journal of Biological Chemistry*, *271*(5), 2646–2650. https://doi.org/10.1074/jbc.271.5.2646

Fukumoto, M., Kurisu, S., Yamada, T., & Takenawa, T. (2015). α-Actinin-4 Enhances Colorectal Cancer Cell Invasion by Suppressing Focal Adhesion Maturation. *PLOS ONE*, *10*(4), e0120616. https://doi.org/10.1371/journal.pone.0120616

Fukushima, S., Yoshida, A., Honda, K., Maeshima, A. M., Narita, Y., Yamada, T., … Tsuda, H. (2014). Immunohistochemical actinin-4 expression in infiltrating gliomas: Association with WHO grade and differentiation. *Brain Tumor Pathology*, *31*(1), 11–16. https://doi.org/10.1007/s10014-013-0139-z

Full, S. J., Deinzer, M. L., Ho, P. S., & Greenwood, J. A. (2007). Phosphoinositide binding regulates α-actinin CH2 domain structure: Analysis by hydrogen/deuterium exchange mass spectrometry. *Protein Science*, *16*(12), 2597–2604. https://doi.org/10.1110/ps.073146807

Funk, C. D., & FitzGerald, G. A. (2007). COX-2 Inhibitors and Cardiovascular Risk. *Journal of Cardiovascular Pharmacology*, *50*(5). Retrieved from https://journals.lww.com/cardiovascularpharm/Fulltext/2007/11000/COX_2_Inhibitors_and_Cardiovascular_Risk.2.aspx

Furman, M. I., Barnard, M. R., Krueger, L. A., Fox, M. L., Shilale, E. A., Lessard, D. M., … Michelson, A. D. (2001). Circulating monocyte-platelet aggregates are an early marker of acute myocardial infarction. *Journal of the American College of Cardiology*, *38*(4), 1002–1006. https://doi.org/10.1016/S0735-1097(01)01485-1

Gache, Y., Landon, F., Touitou, H., & Olomucki, A. (1984). Susceptibility of platelet α-actinin to a Ca2+-activated neutral protease. *Biochemical and Biophysical Research Communications*, *124*(3), 877–881. https://doi.org/10.1016/0006-291X(84)91039-8

Galkin, V. E., Orlova, A., Salmazo, A., Djinović-Carugo, K., & Egelman, E. (2010). Opening of tandem calponin homology domains regulates their affinity for F-actin. *Nat Struct Mol Biol.*, *17*(5), 614–616. https://doi.org/10.1038/nsmb.1789.Opening

Gardiner, E. E., Karunakaran, D., Shen, Y., Arthur, J. F., Andrews, R. K., & Berndt, M. C. (2007). Controlled shedding of platelet glycoprotein (GP)VI and GPIb-IX-V by ADAM family metalloproteinases. *Journal of Thrombosis and Haemostasis*, *5*(7), 1530–1537. https://doi.org/10.1111/j.1538-7836.2007.02590.x

Garton, F. C., Houweling, P. J., Vukcevic, D., Meehan, L. R., Lee, F. X. Z., Lek, M., … North, K. N. (2018). The Effect of ACTN3 Gene Doping on Skeletal Muscle Performance. *American Journal of Human Genetics*, *102*(5), 845–857. https://doi.org/10.1016/j.ajhg.2018.03.009

Gautel, M., & Djinović-Carugo, K. (2016). The sarcomeric cytoskeleton: From molecules to motion. *Journal of Experimental Biology*, *219*(2), 135–145. https://doi.org/10.1242/jeb.124941

Gay, L. J., & Felding-Habermann, B. (2011, February). Contribution of platelets to tumour metastasis. *Nature Reviews Cancer*, Vol. 11, pp. 123–134. https://doi.org/10.1038/nrc3004

George, J. N., & Saucerman, S. (1988). Platelet IgG, IgA, IgM, and Albumin: Correlation of Platelet and Plasma Concentrations in Normal Subjects and in Patients With ITP or Dysproteinemia. In *Blood* (Vol. 72). Retrieved from https://ashpublications.org/blood/article-pdf/72/1/362/599810/362.pdf?casa_token=eUdhdDvGin8AAAAA:EtQKki668wgBJ9B7yteH5W0jq_u1OPyW_fh5D70syhpJxAWkDXBZ6RT_RlEFnnuPGHG0o_o6

Gerdes, N., Zhu, L., Ersoy, M., Hermansson, A., Hjemdahl, P., Hu, H., … Nailin, L. (2011). Platelets regulate CD4 + T-cell differentiation via multiple chemokines in humans. *Thrombosis and Haemostasis*, *106*(2), 353–362. https://doi.org/10.1160/TH11-01-

0020

Gerrard, J., Schollmeyer, J., Phillips, D., & White, J. (1979). Actinin deficiency in thrombasthenia. *American Journal of Path*, *94*(3), 509–523.

Ghasemzadeh, M., Kaplan, Z. S., Alwis, I., Schoenwaelder, S. M., Ashworth, K. J., Westein, E., … Jackson, S. P. (2013). The CXCR1/2 ligand NAP-2 promotes directed intravascular leukocyte migration through platelet thrombi. *Blood*, *121*(22), 4555–4566. https://doi.org/10.1182/blood-2012-09-459636

Gieger, C., Radhakrishnan, A., Cvejic, A., Tang, W., Porcu, E., Pistis, G., … Soranzo, N. (2011). New gene functions in megakaryopoiesis and platelet formation. *Nature*, *480*(7376), 201–208. https://doi.org/10.1038/nature10659

Gilstad, J. R., Gurbel, P. A., & Andersen, R. E. (2009). Relationship between age and platelet activation in patients with stable and unstable angina. *Archives of Gerontology and Geriatrics*, *48*(2), 155–159. https://doi.org/10.1016/j.archger.2007.12.006

Girolami, F., Iascone, M., Tomberli, B., Bardi, S., Benelli, M., Marseglia, G., … Olivotto, I. (2014). Novel α-actinin 2 variant associated with familial hypertrophic cardiomyopathy and juvenile atrial arrhythmias: A massively parallel sequencing study. *Circulation: Cardiovascular Genetics*, *7*(6), 741–750. https://doi.org/10.1161/CIRCGENETICS.113.000486

Glück, U., & Ben-Ze'ev, A. (1994). Modulation of α-actinin levels affects cell motility and confers tumorigenicity on 3T3 cells. *Journal of Cell Science*, *107*(7), 1773–1782.

Gluck, U., Kwiatkowski, D. J., & Ben-Ze'ev, A. (1993). Suppression of tumorigenicity in simian virus 40-transformed 3T3 cells transfected with α-actinin cDNA. *Proceedings of the National Academy of Sciences of the United States of America*, *90*(2), 383–387. https://doi.org/10.1073/pnas.90.2.383

Gogstad, G., Olav Solum, N., & Hagen, I. (1981). Platelet Glycoprotein III and a-actinin are different proteins. *Thrombosis Research*, *24*, 157–162.

Golji, J., Collins, R., & Mofrad, M. R. K. (2009). Molecular mechanics of the α-actinin rod domain: Bending, torsional, and extensional behavior. *PLoS Computational Biology*, *5*(5). https://doi.org/10.1371/journal.pcbi.1000389

Gomez, K., Anderson, J., Baker, P., Biss, T., Jennings, I., Lowe, G., & Platton, S. (2021). Clinical and laboratory diagnosis of heritable platelet disorders in adults and children: a British Society for Haematology Guideline. *British Journal of Haematology*, *195*, 46–72.

Good, J. M., Fellmann, F., Bhuiyan, Z. A., Rotman, S., Pruvot, E., & Schläpfer, J. (2020). ACTN2 variant associated with a cardiac phenotype suggestive of left-dominant arrhythmogenic cardiomyopathy. *HeartRhythm Case Reports*, *6*(1), 15–19. https://doi.org/10.1016/j.hrcr.2019.10.001

Gorski, J., Luka, K., & Czestochowska, E. (1993). Platelet function and survival in multiple myeloma. *Haematologia*, *25*(2), 131–135. Retrieved from http://www.ncbi.nlm.nih.gov/pubmed/8244200

Greenwood, J. A., Theibert, A. B., Prestwich, G. D., & Murphy-Ullrich, J. E. (2000). Restructuring of focal adhesion plaques by PI 3-kinase: Regulation by PtdIns (3,4,5)-P3 binding to α-actinin. *Journal of Cell Biology*, *150*(3), 627–641. https://doi.org/10.1083/jcb.150.3.627

Gregersen, H., Nørgaard, M., Severinsen, M. T., Engebjerg, M. C., Jensen, P., & Sørensen, H. T. (2011). Monoclonal gammopathy of undetermined significance and risk of venous thromboembolism. *European Journal of Haematology*, *86*(2), 129–134. https://doi.org/10.1111/j.1600-0609.2010.01539.x

Gremmel, T., Iii, A. L. F., & Michelson, A. D. (2016). *Platelet Physiology*.

Gresele, P., Harrison, P., Bury, L., Falcinelli, E., Gachet, C., Hayward, C. P., … Cattaneo, M. (2014). Diagnosis of suspected inherited platelet function disorders: Results of a worldwide survey. *Journal of Thrombosis and Haemostasis*, *12*(9), 1562–1569. https://doi.org/10.1111/jth.12650

Grozovsky, R., Giannini, S., Falet, H., & Hoffmeister, K. M. (2015). Regulating billions of blood platelets: Glycans and beyond. *Blood*, *126*(16), 1877–1884. https://doi.org/10.1182/blood-2015-01-569129

Guéguen, P., Dalekos, G., Nousbaum, J.-B., Zachou, K., Chaim, P., Pierre, Y., & Renaudineau, Y. (2006). Double reactivity against actin and α-actinin defines a severe form of autoimmune hepatitis type 1. *Journal of Clinical Immunology*, *26*(6), 495–505. https://doi.org/10.1007/s10875-006-9045-z

Guéguen, P., Rouault, K., Chen, J. M., Raguénès, O., Fichou, Y., Hardy, E., … Férec, C. (2013). A Missense Mutation in the Alpha-Actinin 1 Gene (ACTN1) Is the Cause of Autosomal Dominant Macrothrombocytopenia in a Large French Family. *PLoS ONE*, *8*(9), 1–8. https://doi.org/10.1371/journal.pone.0074728

Guo, L., Tong, D., Yu, M., Zhang, Y., Li, T., Wang, C., … Shi, J. (2018). Phosphatidylserine-exposing cells contribute to the hypercoagulable state in patients with multiple myeloma. *International Journal of Oncology*, *52*(6), 1981–1990. https://doi.org/10.3892/ijo.2018.4354

Gupta, S., Donati, A., & Reviakine, I. (2016). Differences in intracellular calcium dynamics cause differences in α-granule secretion and phosphatidylserine expression in platelets adhering on glass and TiO_2. *Biointerphases*, *11*(2), 029807. https://doi.org/10.1116/1.4947047

Gupta, V., Hegde, U. M., Parameswaran, R., & Newland, A. C. (2000). Multiple myeloma and immune thrombocytopenia. *Clinical and Laboratory Haematology*, *22*(4), 239–242. https://doi.org/10.1046/j.1365-2257.2000.00125.x

Gupta, Vandana, Discenza, M., Guyon, J. R., Kunkel, L. M., & Beggs, A. H. (2012). α-Actinin-2 deficiency results in sarcomeric defects in zebrafish that cannot be rescued by α-actinin-3 revealing functional differences between sarcomeric isoforms. *The FASEB Journal*, *26*(5), 1892–1908. https://doi.org/10.1096/fj.11-194548

Guthikonda, S., Alviar, C. L., Vaduganathan, M., Arikan, M., Tellez, A., DeLao, T., … Lev, E. I. (2008). Role of Reticulated Platelets and Platelet Size Heterogeneity on Platelet Activity After Dual Antiplatelet Therapy With Aspirin and Clopidogrel in Patients With Stable Coronary Artery Disease. *Journal of the American College of Cardiology*, *52*(9), 743–749. https://doi.org/10.1016/j.jacc.2008.05.031

Guvakova, M. A., Adams, J. C., & Bettiger, D. (2002, November 1). Functional role of α-actinin, Pl 3-kinase and MEK1/2 in insulin-like growth factor I receptor kinase regulated motility of human breast carcinoma cells. *Journal of Cell Science*, Vol. 115, pp. 4149–4165. https://doi.org/10.1242/jcs.00104

Haemmerle, M., Stone, R. L., Menter, D. G., Afshar-Kharghan, V., & Sood, A. K. (2018). The Platelet Lifeline to Cancer: Challenges and Opportunities. *Cancer Cell*, *33*(6), 965–983. https://doi.org/10.1016/j.ccell.2018.03.002

Halvorsen, S., Andreotti, F., Ten Berg, J. M., Cattaneo, M., Coccheri, S., Marchioli, R., … De Caterina, R. (2014, July 22). Aspirin therapy in primary cardiovascular disease prevention: A position paper of the european society of cardiology working group on thrombosis. *Journal of the American College of Cardiology*, Vol. 64, pp. 319–327. https://doi.org/10.1016/j.jacc.2014.03.049

Hamill, K. J., Hiroyasu, S., Colburn, Z. T., Ventrella, R. V., Hopkinson, S. B., & Jones, J. C. R. (2015). Alpha actinin-1 regulates cell-matrix adhesion organization in keratinocytes: consequences for skin cell motility. *J Invest Dermatol.*, *135*(4), 1043–1052. https://doi.org/10.1038/jid.2014.505.Alpha

Hamill, K. J., Hopkinson, S. B., Skalli, O., & Jones, J. C. R. (2013). Actinin-4 in keratinocytes regulates motility via an effect on lamellipodia stability and matrix adhesions. *FASEB Journal*, *27*(2), 546–556. https://doi.org/10.1096/fj.12-217406

Hampton, C. M., Taylor, D. W., & Taylor, K. A. (2007). Novel Structures for α-Actinin:F-Actin Interactions and their Implications for Actin-Membrane Attachment and Tension Sensing in the Cytoskeleton. *Journal of Molecular Biology*, *368*(1), 92–104. https://doi.org/10.1016/j.jmb.2007.01.071

Hanjaya-Putra, D., Haller, C., Wang, X., Dai, E., Lim, B., Liu, L., … Chaikof, E. L. (2018). Platelet-targeted dual pathway antithrombotic inhibits thrombosis with preserved hemostasis. *JCI Insight*, *3*(15). https://doi.org/10.1172/jci.insight.99329

Hardy, A. R., Jones, M. L., Mundell, S. J., & Poole, A. W. (2004). Reciprocal cross-talk between P2Y1 and P2Y12 receptors at the level of calcium signaling in human platelets. *Blood*, *104*(6), 1745–1752. https://doi.org/10.1182/blood-2004-02-0534

Harris, A. R., Belardi, B., Jreij, P., Wei, K., Shams, H., Bausch, A., & Fletcher, D. A. (2019). Steric regulation of tandem calponin homology domain actin-binding affinity. *Molecular Biology of the Cell*, *30*(26), 3112–3122. https://doi.org/10.1091/mbc.E19-06-0317

Harsfalvi, J., Fesus, L., Tarcsa, E., Laczko, J., & Loewy, A. G. (1991). The presence of a covalently cross-linked matrix in human platelets. *BBA - General Subjects*, *1073*(2), 268–274. https://doi.org/10.1016/0304-4165(91)90131-Y

Hartwig, J. H., & DeSisto, M. (1991). The cytoskeleton of the resting human blood platelet: Structure of the membrane skeleton and its attachment to actin filaments. *Journal of Cell Biology*, *112*(3), 407–425. https://doi.org/10.1083/jcb.112.3.407

Hathcock, J. J. (2006). Flow Effects on Coagulation and Thrombosis. *Arteriosclerosis, Thrombosis, and Vascular Biology*, *26*(8), 1729–1737. https://doi.org/10.1161/01.ATV.0000229658.76797.30

Hayashida, Y., Honda, K., Idogawa, M., Ino, Y., Ono, M., Tsuchida, A., … Yamada, T. (2005). E-cadherin regulates the association between β-catenin and actinin-4. *Cancer Research*, *65*(19), 8836–8845. https://doi.org/10.1158/0008-5472.CAN-05-0718

Haydon, G. B., & Taylor, D. A. (1965). Microtubules in hamster platelets. *The Journal of Cell Biology*, *26*(2), 673–676. https://doi.org/10.1083/jcb.26.2.673

Haywood, N. J., Wolny, M., Rogers, B., Trinh, C. H., Shuping, Y., Edwards, T. A., & Peckham,

M. (2016). Hypertrophic cardiomyopathy mutations in the calponin-homology domain of ACTN2 affect actin binding and cardiomyocyte Z-disc incorporation. *Biochemical Journal*, *473*(16), 2485–2493. https://doi.org/10.1042/BCJ20160421

Heemskerk, J. W. M., Bevers, E. M., & Lindhout, T. (2002). Platelet Activation and Blood Coagulation. In *Thromb Haemost* (Vol. 88).

Heemskerk, J. W. M., Kuijpers, M. J. E., Munnix, I. C. A., & Siljander, P. R. M. (2005). Platelet Collagen Receptors and Coagulation. A Characteristic Platelet Response as Possible Target for Antithrombotic Treatment. *Trends in Cardiovascular Medicine*, *15*(3), 86–92. https://doi.org/10.1016/j.tcm.2005.03.003

Heijnen, H., & van der Sluijs, P. (2015). Platelet secretory behaviour: as diverse as the granules … or not? *Journal of Thrombosis and Haemostasis*, *13*(12), 2141–2151. https://doi.org/10.1111/jth.13147

Henderson, J. M., Al-Waheeb, S., Weins, A., Dandapani, S. V., & Pollak, M. R. (2008). Mice with altered α-actinin-4 expression have distinct morphologic patterns of glomerular disease. *Kidney International*, *73*(6), 741–750. https://doi.org/10.1038/sj.ki.5002751

Ho-Tin-Noé, B., Boulaftali, Y., & Camerer, E. (2018, January 18). Platelets and vascular integrity: How platelets prevent bleeding in inflammation. *Blood*, Vol. 131, pp. 277–288. https://doi.org/10.1182/blood-2017-06-742676

Hodohara, K., Fujii, N., Yamamoto, N., & Kaushansky, K. (2000). Stromal cell-derived factor-1 (SDF-1) acts together with thrombopoietin to enhance the development of megakaryocytic progenitor cells (CFU-MK). *Blood*, *95*(3), 769–775. https://doi.org/10.1182/blood.v95.3.769.003a49_769_775

Hogarth, M. W., Houweling, P. J., Thomas, K. C., Gordish-Dressman, H., Bello, L., Pegoraro, E., … North, K. N. (2017). Evidence for ACTN3 as a genetic modifier of Duchenne muscular dystrophy. *Nature Communications*, *8*. https://doi.org/10.1038/ncomms14143

Honda, K. (2015). The biological role of actinin-4 (ACTN4) in malignant phenotypes of cancer. *Cell and Bioscience*, *5*(1), 1–9. https://doi.org/10.1186/s13578-015-0031-0

Honda, K., Yamada, T., Endo, R., Ino, Y., Gotoh, M., Tsuda, H., … Hirohashi, S. (1998). Actinin-4, a novel actin-bundling protein associated with cell motility and cancer invasion. *Journal of Cell Biology*, *140*(6), 1383–1393. https://doi.org/10.1083/jcb.140.6.1383

Honn, K. V., Tang, D. G., & Crissman, J. D. (1992). Platelets and cancer metastasis: A causal relationship? *Cancer and Metastasis Reviews*, *11*(3–4), 325–351. https://doi.org/10.1007/BF01307186

Hosseini, K., Sbosny, L., Poser, I., & Fischer-Friedrich, E. (2020). Binding Dynamics of α-Actinin-4 in Dependence of Actin Cortex Tension. *Biophysical Journal*, *119*(6), 1091–1107. https://doi.org/10.1016/J.BPJ.2020.07.031

Hotulainen, P., & Lappalainen, P. (2006). Stress fibers are generated by two distinct actin assembly mechanisms in motile cells. *Journal of Cell Biology*, *173*(3), 383–394. https://doi.org/10.1083/jcb.200511093

Hoyt, C. H., & Lerea, K. M. (1995). Aggregation-Dependent Signaling in Human Platelets Is Sensitive to Protein Serine/Threonine Phosphatase Inhibitors. *Biochemistry*, *34*(29), 9565–9570. https://doi.org/10.1021/bi00029a033

Hsu, C. P., Moghadaszadeh, B., Hartwig, J. H., & Beggs, A. H. (2018). Sarcomeric and nonmuscle α-actinin isoforms exhibit differential dynamics at skeletal muscle Z-lines. *Cytoskeleton*, *75*(5), 213–228. https://doi.org/10.1002/cm.21442

Hu, H., Zhu, L., Huang, Z., Ji, Q., Chatterjee, M., Zhang, W., & Li, N. (2010). Platelets enhance lymphocyte adhesion and infiltration into arterial thrombus. *Thrombosis and Haemostasis*, *104*(6), 1184–1192. https://doi.org/10.1160/TH10-05-0308

Hu, S., Grobe, H., Guo, Z., Wang, Y. H., Doss, B. L., Pan, M., … Zaidel-Bar, R. (2019). Reciprocal regulation of actomyosin organization and contractility in nonmuscle cells by tropomyosins and alpha-actinins. *Molecular Biology of the Cell*, *30*(16), 2025–2036. https://doi.org/10.1091/mbc.E19-02-0082

Hua, V. M., Abeynaike, L., Glaros, E., Campbell, H., Pasalic, L., Hogg, P. J., & Chen, V. M. Y. (2015). Necrotic platelets provide a procoagulant surface during thrombosis. *Blood*, *126*(26), 2852–2862. https://doi.org/10.1182/blood-2015-08-663005

Huang, J., Li, X., Shi, X., Zhu, M., Wang, J., Huang, S., … Jin, J. (2019, March 7). Platelet integrin αIIbβ3: Signal transduction, regulation, and its therapeutic targeting. *Journal of Hematology and Oncology*, Vol. 12, pp. 1–22. https://doi.org/10.1186/s13045-019-0709-6

Huynh, K., & Partch, C. L. (2015). Analysis of protein stability and ligand interactions by thermal shift assay. *Current Protocols in Protein Science*, *2015*, 19.26.1-19.26.14. https://doi.org/10.1002/0471140864.ps1926s79

Iannacone, M. (2016). Platelet-mediated modulation of adaptive immunity. *Seminars in Immunology*, *28*(6), 555–560. https://doi.org/10.1016/j.smim.2016.10.008

Ibrahim, H., Schutt, R. C., Hannawi, B., DeLao, T., Barker, C. M., & Kleiman, N. S. (2014). Association of immature platelets with adverse cardiovascular outcomes. *Journal of the American College of Cardiology*, *64*(20), 2122–2129. https://doi.org/10.1016/j.jacc.2014.06.1210

Icli, A., Aksoy, F., Nar, G., Kaymaz, H., Alpay, M. F., Nar, R., … Dogan, A. (2015). Increased Mean Platelet Volume in Familial Hypercholesterolemia. *Angiology*, *67*(2), 146–150. Retrieved from https://www.unboundmedicine.com/medline/citation/25859052/Increased_Mean_Platelet_Volume_in_Familial_Hypercholesterolemia_

Ikura, M. (1996). Calcium binding and conformational response in EF-hand proteins. *Trends in Biochemical Sciences*, *21*(1), 14–17. https://doi.org/10.1016/S0968-0004(06)80021-6

Imamura, M., Endo, T., Kuroda, M., Tanaka, T., & Masaki, T. (1988). Substructure and higher structure of chicken smooth muscle alpha-actinin molecule. *The Journal of Biological Chemistry*, *263*(16), 7800–7805.

Inada, M., Benten, D., Cheng, K., Joseph, B., Berishvili, E., Badve, S., … Gupta, S. (2008). Stage-specific regulation of adhesion molecule expression segregates epithelial stem/progenitor cells in fetal and adult human livers. *Hepatology International*, *2*(1), 50–62. https://doi.org/10.1007/s12072-007-9023-4

Isakari, Y, Harada, Y., Ishikawa, D., Matsumura-Takeda, K., Sogo, S., Ishida, T., … Kiwada, H. (2007). Efficient gene expression in megakaryocytic cell line using nucleofection. *Int.J.Pharm.*, *338*(0378-5173 (Print)), 157–164.

Isakari, Yoshimasa, Harada, Y., Ishikawa, D., Matsumura-Takeda, K., Sogo, S., Ishida, T., … Kiwada, H. (2007). Efficient gene expression in megakaryocytic cell line using nucleofection. *International Journal of Pharmaceutics*, *338*(1–2), 157–164. https://doi.org/10.1016/j.ijpharm.2007.01.042

Italiano Jr., J. E., Lecine, P., Shivdasani, R. A., & Hartwig, J. H. (1999). Blood platelets are assembled principally at the ends of proplatelet processes produced by differentiated megakaryocytes. *J Cell Biol*, *147*(6), 1299–1312. Retrieved from https://www.ncbi.nlm.nih.gov/pmc/articles/PMC2168104/pdf/9909028.pdf

Italiano, J. E., Richardson, J. L., Patel-Hett, S., Battinelli, E., Zaslavsky, A., Short, S., … Klement, G. L. (2008). Angiogenesis is regulated by a novel mechanism: Pro- and antiangiogenic proteins are organized into separate platelet α granules and differentially released. *Blood*, *111*(3), 1227–1233. https://doi.org/10.1182/blood-2007-09-113837

Iyer, K. S., & Dayal, S. (2019). Modulators of platelet function in aging. *Platelets*. https://doi.org/10.1080/09537104.2019.1665641

Izaguirre, G, Aguirre, L., Ji, P., Aneskievich, B., & Haimovich, B. (1999). Tyrosine phosphorylation of alpha-actinin in activated platelets. *The Journal of Biological Chemistry*, *274*(52), 37012–37020. https://doi.org/10.1074/jbc.274.52.37012

Izaguirre, Gonzalo, Aguirre, L., Hu, Y. P., Lee, H. Y., Schlaepfer, D. D., Aneskievich, B. J., & Haimovich, B. (2001a). The Cytoskeletal/Non-musele Isoform of α-Actinin Is Phosphorylated on Its Actin-binding Domain by the Focal Adhesion Kinase. *Journal of Biological Chemistry*, *276*(31), 28676–28685. https://doi.org/10.1074/jbc.M101678200

Izaguirre, Gonzalo, Aguirre, L., Hu, Y. P., Lee, H. Y., Schlaepfer, D. D., Aneskievich, B. J., & Haimovich, B. (2001b). The Cytoskeletal/Non-musele Isoform of α-Actinin Is Phosphorylated on Its Actin-binding Domain by the Focal Adhesion Kinase. *Journal of Biological Chemistry*, *276*(31), 28676–28685. https://doi.org/10.1074/jbc.M101678200

Jain, S., Russell, S., & Ware, J. (2009). Platelet glycoprotein VI facilitates experimental lung metastasis in syngenic mouse models. *Journal of Thrombosis and Haemostasis*, *7*(10), 1713–1717. https://doi.org/10.1111/j.1538-7836.2009.03559.x

James, A. H. (2007). Prevention and Management of Venous Thromboembolism in Pregnancy. *American Journal of Medicine*, *120*(10 suppl. 2). https://doi.org/10.1016/j.amjmed.2007.08.011

Janowska-Wieczorek, A., Majka, M., Kijowski, J., Baj-Krzyworzeka, M., Reca, R., Robert Turner, A., … Ratajczak, M. Z. (2001). Platelet-derived microparticles bind to hematopoietic stem/progenitor cells and enhance their engraftment. *Blood*, *98*(10), 3143–3149. https://doi.org/10.1182/blood.V98.10.3143

Jasalava, R., Martinez, H., Thumar, J., Andaya, A., Gingras, A. C., Eng, J. K., … Wright, M. E. (2007). Identification of putative androgen receptor interaction protein modules: Cytoskeleton and endosomes modulate androgen receptor signaling in prostate cancer cells. *Molecular and Cellular Proteomics*, *6*(2), 252–271. https://doi.org/10.1074/mcp.M600169-MCP200

Jayadev, R., Kuk, C. Y., Low, S. H., & Murata-Hori, M. (2012). Calcium sensitivity of α-actinin is required for equatorial actin assembly during cytokinesis. *Cell Cycle*, *11*(10), 1929–

1937. https://doi.org/10.4161/cc.20277

Jenne, C. N., & Kubes, P. (2015). Platelets in inflammation and infection. *Platelets*, *26*(4), 286–292. https://doi.org/10.3109/09537104.2015.1010441

Jensvoll, H., Blix, K., Braekkan, S. K., & Hansen, J. B. (2014). Platelet Count Measured Prior to Cancer Development Is a Risk Factor for Future Symptomatic Venous Thromboembolism: The Tromso Study. *PLoS ONE*, *9*(3). https://doi.org/10.1371/journal.pone.0092011

Jia, Y., & Kuroda, M. (2011). Limited digestion of α-actinin in the presence of F-actin. *Biophysics*, *7*, 29–34. https://doi.org/10.2142/biophysics.7.29

Jones, C. I. (2016, August 1). Platelet function and ageing. *Mammalian Genome*, Vol. 27, pp. 358–366. https://doi.org/10.1007/s00335-016-9629-8

Josefsson, E. C., Burnett, D. L., Lebois, M., Debrincat, M. A., White, M. J., Henley, K. J., … Kile, B. T. (2014). Platelet production proceeds independently of the intrinsic and extrinsic apoptosis pathways. *Nature Communications*, *5*. https://doi.org/10.1038/ncomms4455

Joshi, S., & Whiteheart, S. W. (2017, February 17). The nuts and bolts of the platelet release reaction. *Platelets*, Vol. 28, pp. 129–137. https://doi.org/10.1080/09537104.2016.1240768

Jung, S. M., Tsuji, K., & Moroi, M. (2009). Glycoprotein (GP) VI dimer as a major collagen-binding site of native platelets: Direct evidence obtained with dimeric GPVI-specific Fabs. *Journal of Thrombosis and Haemostasis*, *7*(8), 1347–1355. https://doi.org/10.1111/j.1538-7836.2009.03496.x

Jurk, K., Clemetson, K. J., de Groot, P. G., Brodde, M. F., Steiner, M., Savion, N., … Kehrel, B. E. (2003). Thrombospondin-1 mediates platelet adhesion at high shear via glycoprotein Ib (GPIb): an alternative/backup mechanism to von Willebrand factor. *The FASEB Journal : Official Publication of the Federation of American Societies for Experimental Biology*, *17*(11), 1490–1492. https://doi.org/10.1096/fj.02-0830fje

Jurk, K., Jahn, U.-R., Van Aken, H., Schriek, C., Droste, D. W., Ritter, M. A., … Kehrel, B. E. (2004). Platelets in patients with acute ischemic stroke are exhausted and refractory to thrombin, due to cleavage of the seven-transmembrane thrombin receptor (PAR-1). *Thrombosis and Haemostasis*, *91*(2), 334–344. https://doi.org/10.1160/TH03-01-0044

Kamińska, J., Koper, O. M., Mantur, M., Matowicka-Karna, J., Sawicka-Powierza, J., Sokołowski, J., … Kemona, H. (2014). Does thrombopoiesis in multiple myeloma patients depend on the stage of the disease? *Advances in Medical Sciences*, *59*(2), 166–171. https://doi.org/10.1016/J.ADVMS.2013.12.006

Kanhai, D., Mulder, R., Amstel, H. K. P. van, Schutgens, R., Lukens, M., & Tamminga, R. Y. J. (2018). Familial macrothrombocytopenia due to a double mutation in cis in the alpha-actinin 1 gene (ACTN1), previously considered to be chronic immune thrombocytopenic purpura. *Pediatric Blood & Cancer*, *65*(12), e27418. https://doi.org/10.1002/PBC.27418

Kao, H.-Y., Zhang, C., Wan, P., Pasha, Z., Guaiquil, V., Liu, A., … Rosenblatt, M. I. (2015). The actinin family proteins: biological function and clinical implications. *Cell & Bioscience*, *5*(1), 48. https://doi.org/10.1186/s13578-015-0039-5

Kaplan, J. M., Kim, S. H., North, K. N., Rennke, H., Correia, L. A., Tong, H. Q., … Pollak, M. R. (2000). Mutations in ACTN4, encoding α-actinin-4, cause familial focal segmental glomerulosclerosis. *Nature Genetics*, *24*(3), 251–256. https://doi.org/10.1038/73456

Karim, S., Habib, A., Lévy-Toledano, S., & Maclouf, J. (1996). Cyclooxygenase-1 and -2 of endothelial cells utilize exogenous or endogenous arachidonic acid for transcellular production of thromboxane. *The Journal of Biological Chemistry*, *271*(20), 12042–12048. https://doi.org/10.1074/jbc.271.20.12042

Karpatkin, S. (1969). Heterogeneity of human platelets. I. Metabolic and kinetic evidence suggestive of young and old platelets. *The Journal of Clinical Investigation*, *48*(6), 1073–1082. https://doi.org/10.1172/JCI106063

Kaser, A., Brandacher, G., Steurer, W., Kaser, S., Offner, F. A., Zoller, H., … Tilg, H. (2001). Interleukin-6 stimulates thrombopoiesis through thrombopoietin: Role in inflammatory thrombocytosis. *Blood*, *98*(9), 2720–2725. https://doi.org/10.1182/blood.V98.9.2720

Kashiwagi, H., Shiraga, M., Honda, S., Kosugi, S., Kamae, T., Kato, H., … Tomiyama, Y. (2004). Activation of integrin ??IIb??3 in the glycoprotein lb-high population of a megakaryocytic cell line, CMK, by inside-out signaling. *Journal of Thrombosis and Haemostasis*, *2*(1), 177–186. https://doi.org/10.1111/j.1538-7836.2003.00529.x

Kelly, M., & Semsarian, C. (2009, April). Multiple mutations in genetic cardiovascular disease a marker of disease severity? *Circulation: Cardiovascular Genetics*, Vol. 2, pp. 182–190. https://doi.org/10.1161/CIRCGENETICS.108.836478

Kemp, J. P., & Brieher, W. M. (2018). The actin filament bundling protein α-actinin-4 actually suppresses actin stress fibers by permitting actin turnover. *Journal of Biological Chemistry*, *293*(37), 14520–14533. https://doi.org/10.1074/jbc.RA118.004345

Keularts, I. M. L. W., Van Gorp, R. M. A., Feijge, M. A. H., Vuist, W. M. J., & Heemskerk, J. W. M. (2000). α(2A)-Adrenergic receptor stimulation potentiates calcium release in platelets by modulating cAMP levels. *Journal of Biological Chemistry*, *275*(3), 1763–1772. https://doi.org/10.1074/jbc.275.3.1763

Khorana, A. A., Francis, C. W., Culakova, E., Kuderer, N. M., & Lyman, G. H. (2007, March). Thromboembolism is a leading cause of death in cancer patients receiving outpatient chemotherapy. *Journal of Thrombosis and Haemostasis*, Vol. 5, pp. 632–634. https://doi.org/10.1111/j.1538-7836.2007.02374.x

Khurana, S., Chakraborty, S., Lam, M., Liu, Y., Su, Y. T., Zhao, X., … Kao, H. Y. (2012). Familial focal segmental glomerulosclerosis (FSGS)-linked α-actinin 4 (ACTN4) protein mutants lose ability to activate transcription by nuclear hormone receptors. *Journal of Biological Chemistry*, *287*(15), 12027–12035. https://doi.org/10.1074/jbc.M112.345421

Kikuchi, S., Honda, K., Tsuda, H., Hiraoka, N., Imoto, I., Kosuge, T., … Yamada, T. (2008). Expression and gene amplification of actinin-4 in invasive ductal carcinoma of the pancreas. *Clinical Cancer Research*, *14*(17), 5348–5356. https://doi.org/10.1158/1078-0432.CCR-08-0075

Kim, Y. J., Borsig, L., Varki, N. M., & Varki, A. (1998). P-selectin deficiency attenuates tumor growth and metastasis. *Proceedings of the National Academy of Sciences of the United States of America*, *95*(16), 9325–9330. https://doi.org/10.1073/pnas.95.16.9325

King, S. M., & Reed, G. L. (2002). Development of platelet secretory granules. *Seminars in Cell and Developmental Biology*, *13*(4), 293–302. https://doi.org/10.1016/S1084952102000599

Kleinschnitz, C., Pozgajova, M., Pham, M., Bendszus, M., Nieswandt, B., & Stoll, G. (2007). Targeting platelets in acute experimental stroke: Impact of glycoprotein Ib, VI, and IIb/IIIa blockade on infarct size, functional outcome, and intracranial bleeding. *Circulation*, *115*(17), 2323–2330. https://doi.org/10.1161/CIRCULATIONAHA.107.691279

Klinger, M. H. F., & Jelkmann, W. (2002). Role of blood platelets in infection and inflammation. *Journal of Interferon and Cytokine Research*, *22*(9), 913–922. https://doi.org/10.1089/10799900260286623

Knight, C. J., Panesar, M., Wright, C., Clarke, D., Butowski, P. S., Patel, D., … Goodall, A. H. (1997). Altered platelet function detected by flow cytometry: Effects of coronary artery disease and age. *Arteriosclerosis, Thrombosis, and Vascular Biology*, *17*(10), 2044–2053. https://doi.org/10.1161/01.ATV.17.10.2044

Knudsen, K. A., Soler, A. P., Johnson, K. R., & Wheelock, M. J. (1995). Interaction of α-actinin with the cadherin/catenin cell-cell adhesion complex via α-catenin. *Journal of Cell Biology*, *130*(1), 67–77. https://doi.org/10.1083/jcb.130.1.67

Koga, H., Sugiyama, S., Kugiyama, K., Fukushima, H., Watanabe, K., Sakamoto, T., … Ogawa, H. (2006). Elevated levels of remnant lipoproteins are associated with plasma platelet microparticles in patients with type-2 diabetes mellitus without obstructive coronary artery disease. *European Heart Journal*, *27*(7), 817–823. https://doi.org/10.1093/eurheartj/ehi746

Komatsu, N., Suda, T., Moroi, M., Tokuyama, N., Sakata, Y., Okada, M., … Fuse, A. (1989). Growth and differentiation of a human megakaryoblastic cell line, CMK. *Blood*, *74*(1), 42–48. https://doi.org/10.1182/blood.v74.1.42.42

Kopp, H. G., Placke, T., & Salih, H. R. (2009). Platelet-derived transforming growth factor-β down-regulates NKG2D thereby inhibiting natural killer cell antitumor reactivity. *Cancer Research*, *69*(19), 7775–7783. https://doi.org/10.1158/0008-5472.CAN-09-2123

Kos, C. H., Le, T. C., Sinha, S., Henderson, J. M., Kim, S. H., Sugimoto, H., … Pollak, M. R. (2003). Mice deficient in α-actinin-4 have severe glomerular disease. *Journal of Clinical Investigation*, *111*(11), 1683–1690. https://doi.org/10.1172/jci200317988

Kostrubiec, M., Łabyk, A., Pedowska-Włoszek, J., Hrynkiewicz-Szymańska, A., Pacho, S., Jankowski, K., … Pruszczyk, P. (2010). Mean platelet volume predicts early death in acute pulmonary embolism. *Heart*, *96*(6), 460–465. https://doi.org/10.1136/hrt.2009.180489

Koupenova, M., Clancy, L., Corkery, H. A., & Freedman, J. E. (2018). Circulating Platelets as Mediators of Immunity, Inflammation, and Thrombosis. *Circulation Research*, *122*(2), 337–351. https://doi.org/10.1161/CIRCRESAHA.117.310795

Koupenova, M., Vitseva, O., MacKay, C. R., Beaulieu, L. M., Benjamin, E. J., Mick, E., … Freedman, J. E. (2014). Platelet-TLR7 mediates host survival and platelet count during viral infection in the absence of platelet-dependent thrombosis. *Blood*, *124*(5), 791–802. https://doi.org/10.1182/blood-2013-11-536003

Kovac, B., Teo, J. L., Mäkelä, T. P., & Vallenius, T. (2013). Assembly of non-contractile dorsal stress fibers requires α-actinin-1 and Rac1 in migrating and spreading cells. *Journal of Cell Science*, *126*(1), 263–273. https://doi.org/10.1242/jcs.115063

Kowata, S., Isogai, S., Murai, K., Ito, S., Tohyama, K., Ema, M., … Ishida, Y. (2014). Platelet demand modulates the type of intravascular protrusion of megakaryocytes in bone marrow. *Thrombosis and Haemostasis*, *112*(4), 743–756. https://doi.org/10.1160/TH14-02-0123

Krishnamurti, L., Neglia, J. P., Nagarajan, R., Berry, S. A., Lohr, J., Hirsch, B., & White, J. G. (2001). Paris-Trousseau syndrome platelets in a child with Jacobsen's syndrome. *American Journal of Hematology*, *66*(4), 295–299. https://doi.org/10.1002/ajh.1061

Kristinsson, S. Y., Fears, T. R., Gridley, G., Turesson, I., Mellqvist, U. H., Björkholm, M., & Landgren, O. (2008). Deep vein thrombosis after monoclonal gammopathy of undetermined significance and multiple myeloma. *Blood*, *112*(9), 3582–3586. https://doi.org/10.1182/blood-2008-04-151076

Kristinsson, S. Y., Pfeiffer, R. M., Björkholm, M., Goldin, L. R., Schulman, S., Blimark, C., … Landgren, O. (2010). Arterial and venous thrombosis in monoclonal gammopathy of undetermined significance and multiple myeloma: A population-based study. *Blood*, *115*(24), 4991–4998. https://doi.org/10.1182/blood-2009-11-252072

Kristinsson, Y., Kristinsson, S. Y., Cesarman-Maus, G., Braggio, E., & Fonseca, R. (2010). Thrombosis in Multiple Myeloma. *Hematology*, *2010*(1), 437–444. https://doi.org/10.1179/102453312X13336169156933

Kunicki, T. J. (1989). Platelet membrane glycoproteins and their function: An overview. *Blut*, *59*(1), 30–34. https://doi.org/10.1007/BF00320245

Kunishima, S., Okuno, Y., Yoshida, K., Shiraishi, Y., Sanada, M., Muramatsu, H., … Ogawa, S. (2013). *ACTN1 Mutations Cause Congenital Macrothrombocytopenia*. *92*(3), 431–438. https://doi.org/10.1016/j.ajhg.2013.01.015

Kunishima, S., & Saito, H. (2006). Congenital macrothrombocytopenias. *Blood Reviews*, *20*(2), 111–121. https://doi.org/10.1016/j.blre.2005.08.001

Labberton, L., Kenne, E., Long, A. T., Nickel, K. F., Di Gennaro, A., Rigg, R. A., … Renné, T. (2016). Neutralizing blood-borne polyphosphate in vivo provides safe thromboprotection. *Nature Communications*, *7*(1), 1–14. https://doi.org/10.1038/ncomms12616

Labelle, M., Begum, S., & Hynes, R. O. (2011). Direct Signaling between Platelets and Cancer Cells Induces an Epithelial-Mesenchymal-Like Transition and Promotes Metastasis. *Cancer Cell*, *20*(5), 576–590. https://doi.org/10.1016/j.ccr.2011.09.009

Landgren, O., Graubard, B. I., Kumar, S., Kyle, R. A., Katzmann, J. A., Murata, K., … Rajkumar, S. V. (2017). Prevalence of myeloma precursor state monoclonal gammopathy of undetermined significance in 12372 individuals 10-49 years old: a population-based study from the National Health and Nutrition Examination Survey. *Blood Cancer Journal*, *7*(10), e618. https://doi.org/10.1038/bcj.2017.97

Landon, F., Gache, Y., Touitou, H., & Olomucki, a. (1985). Properties of two isoforms of human blood platelet alpha-actinin. *European Journal of Biochemistry / FEBS*, *153*(2), 231–237. Retrieved from http://www.ncbi.nlm.nih.gov/pubmed/2934249

Landon, F., & Olomucki, A. (1983). Isolation and physico-chemical properties of blood

platelet alpha-actinin. *Biochimica et Biophysica Acta*, *742*(1), 129–134. Retrieved from http://www.ncbi.nlm.nih.gov/pubmed/6824676

Langer, Barbara, Leung, L., Gonnella, P., Nachmias, V., Nachmant, R. L., & Pepe, F. A. (1982). a-Actinin and membrane glycoprotein IIIa are different proteins in human blood platelets. *Proceedings of the National Academy of Sciences*, *79*(January), 432–435.

Langer, BG, Gonnella, P., & Nachmias, V. (1984). alpha-Actinin and vinculin in normal and thrombasthenic platelets. *Blood*, *63*(3). Retrieved from http://www.bloodjournal.org/content/63/3/606.long?sso-checked=true

Laporte, D., Ojkic, N., Vavylonis, D., & Wu, J. Q. (2012). α-actinin and fimbrin cooperate with myosin II to organize actomyosin bundles during contractile-ring assembly. *Molecular Biology of the Cell*, *23*(16), 3094–3110. https://doi.org/10.1091/mbc.E12-02-0123

Läubli, H., Spanaus, K. S., & Borsig, L. (2009). Selectin-mediated activation of endothelial cells induces expression of CCL5 and promotes metastasis through recruitment of monocytes. *Blood*, *114*(20), 4583–4591. https://doi.org/10.1182/blood-2008-10-186585

Le Blanc, J., & Lordkipanidzé, M. (2019). Platelet Function in Aging. *Frontiers in Cardiovascular Medicine*, *6*(109). https://doi.org/10.3389/fcvm.2019.00109

Le Clainche, C., & Carlier, M. F. (2008). Regulation of actin assembly associated with protrusion and adhesion in cell migration. *Physiological Reviews*, *88*(2), 489–513. https://doi.org/10.1152/physrev.00021.2007

Le, S., Hu, X., Yao, M., Chen, H., Yu, M., Xu, X., … Yan, J. (2017). Mechanotransmission and Mechanosensing of Human alpha-Actinin 1. *Cell Reports*, *21*(10), 2714–2723. https://doi.org/10.1016/j.celrep.2017.11.040

Lê, V. B., Schneider, J. G., Boergeling, Y., Berri, F., Ducatez, M., Guerin, J. L., … Riteau, B. A. (2015). Platelet activation and aggregation promote lung inflammation and influenza virus pathogenesis. *American Journal of Respiratory and Critical Care Medicine*, *191*(7), 804–819. https://doi.org/10.1164/rccm.201406-1031OC

Lee, F. X. Z., Houweling, P. J., North, K. N., & Quinlan, K. G. R. (2016). How does α-actinin-3 deficiency alter muscle function? Mechanistic insights into ACTN3, the "gene for speed." *Biochimica et Biophysica Acta - Molecular Cell Research*, *1863*(4), 686–693. https://doi.org/10.1016/j.bbamcr.2016.01.013

Lee, S. H., Weins, A., Hayes, D. B., Pollak, M. R., & Dominguez, R. (2008). Crystal Structure of the Actin-Binding Domain of α-Actinin-4 Lys255Glu Mutant Implicated in Focal Segmental Glomerulosclerosis. *Journal of Molecular Biology*, *376*(2), 317–324. https://doi.org/10.1016/j.jmb.2007.11.084

Lefrançais, E., Ortiz-Muñoz, G., Caudrillier, A., Mallavia, B., Liu, F., Sayah, D. M., … Looney, M. R. (2017). The lung is a site of platelet biogenesis and a reservoir for hematopoietic progenitors HHS Public Access. *Nature*, *544*(7648), 105–109. https://doi.org/10.1038/nature21706

Leinoe, E. B., Hoffmann, M. H., Kjaersgaard, E., & Johnsen, H. E. (2004). Multiple platelet defects identified by flow cytometry at diagnosis in acute myeloid leukaemia. *British Journal of Haematology*, *127*(1), 76–84. https://doi.org/10.1111/j.1365-2141.2004.05156.x

Leinøe, E., Zetterberg, E., Kinalis, S., Østrup, O., Kampmann, P., Norström, E., … Rossing, M. (2017). Application of whole-exome sequencing to direct the specific functional testing and diagnosis of rare inherited bleeding disorders in patients from the Öresund Region, Scandinavia. *British Journal of Haematology*, *179*(2), 308–322. https://doi.org/10.1111/bjh.14863

Lek, M., MacArthur, D. G., Yang, N., & North, K. N. (2010). Phylogenetic analysis of gene structure and alternative splicing in α-Actinins. *Molecular Biology and Evolution*, *27*(4), 773–780. https://doi.org/10.1093/molbev/msp268

Lek, M., Quinlan, K. G. R., & North, K. N. (2010). The evolution of skeletal muscle performance: gene duplication and divergence of human sarcomeric Î±-actinins. *BioEssays*, *32*(1), 17–25. https://doi.org/10.1002/bies.200900110

Lemancewicz, D., Bolkun, L., Mantur, M., Semeniuk, J., Kloczko, J., & Dzieciol, J. (2014). Bone marrow megakaryocytes, soluble P-selectin and thrombopoietic cytokines in multiple myeloma patients. *Platelets*, *25*(3), 181–187. https://doi.org/10.3109/09537104.2013.805405

Leo, V. C., Morgan, N. V., Bem, D., Jones, M. L., Lowe, G. C., Lordkipanidzé, M., … Daly, M. E. (2015). Use of next-generation sequencing and candidate gene analysis to identify underlying defects in patients with inherited platelet function disorders. *Journal of Thrombosis and Haemostasis*, *13*(4), 643–650. https://doi.org/10.1111/jth.12836

Lev, E. I. (2016). *Immature Platelets*. 987–988. https://doi.org/10.1160/TH15-02-0179.3.

Leven, R., & Nachmias, V. (1982). Cultured Megakaryocytes: Changes in the Cytoskeleton after ADP-Induced Spreading. *The Journal of Cell Biology*, *92*, 313–325.

Levin, J., & Conley, C. L. (1964). Thrombocytosis Associated With Malignant Disease. *Archives of Internal Medicine*, *114*(4), 497–500. https://doi.org/10.1001/archinte.1964.03860100079008

Li, A., Wu, Q., Luo, S., Warnick, G. S., Zakai, N. A., Libby, E. N., … Sanfilippo, K. M. (2019). Derivation and validation of a risk assessment model for immunomodulatory drug-associated thrombosis among patients with multiple myeloma. *JNCCN Journal of the National Comprehensive Cancer Network*, *17*(7), 840–847. https://doi.org/10.6004/jnccn.2018.7273

Li, N. (2013, February 28). CD4+ T cells in atherosclerosis: Regulation by platelets. *Thrombosis and Haemostasis*, Vol. 109, pp. 980–990. https://doi.org/10.1160/TH12-11-0819

LI, N., JI, Q., & HJEMDAHL, P. (2006). Platelet-lymphocyte conjugation differs between lymphocyte subpopulations. *Journal of Thrombosis and Haemostasis*, *4*(4), 874–881. https://doi.org/10.1111/j.1538-7836.2006.01817.x

Li, X., & Cong, H. (2009). Platelet-derived microparticles and the potential of glycoprotein IIb/IIIa antagonists in treating acute coronary syndrome. *Texas Heart Institute Journal*, Vol. 36, pp. 134–139. Retrieved from /pmc/articles/PMC2676586/?report=abstract

Lickert, S., Sorrentino, S., Studt, J.-D., Medalia, O., Vogel, V., & Schoen, I. (2018). Morphometric analysis of spread platelets identifies integrin αIIbβ3-specific contractile phenotype. *Scientific Reports*, *8*(1), 5428. https://doi.org/10.1038/s41598-018-23684-w

Lim, J. P., & Gleeson, P. A. (2011). Macropinocytosis: An endocytic pathway for internalising

large gulps. *Immunology and Cell Biology*, *89*(8), 836–843. https://doi.org/10.1038/icb.2011.20

Lin, S. Y., Raval, S., Zhang, Z., Deverill, M., Siminovitch, K. A., Branch, D. R., & Haimovich, B. (2004). The protein-tyrosine phosphatase SHP-1 regulates the phosphorylation of α-actinin. *Journal of Biological Chemistry*, *279*(24), 25755–25764. https://doi.org/10.1074/jbc.M314175200

Linder, S., & Wiesner, C. (2016). Feel the force: Podosomes in mechanosensing. *Experimental Cell Research*, *343*(1), 67–72. https://doi.org/10.1016/j.yexcr.2015.11.026

Lippross, S., Moeller, B., Haas, H., Tohidnezhad, M., Steubesand, N., Wruck, C. J., … Varoga, D. (2011). Intraarticular injection of platelet-rich plasma reduces inflammation in a pig model of rheumatoid arthritis of the knee joint. *Arthritis and Rheumatism*, *63*(11), 3344–3353. https://doi.org/10.1002/art.30547

Lischke, S., & Schneider, D. J. (2011). Recent developments in the use of antiplatelet agents to prevent cardiovascular events. *Future Cardiology*, *7*(3), 403–413. https://doi.org/10.2217/fca.11.8

Liu, J., Taylor, D. W., & Taylor, K. A. (2004a). A 3-D reconstruction of smooth muscle α-actinin by CryoEm reveals two different conformations at the actin-binding region. *Journal of Molecular Biology*, *338*(1), 115–125. https://doi.org/10.1016/j.jmb.2004.02.034

Liu, J., Taylor, D. W., & Taylor, K. A. (2004b). A 3-D reconstruction of smooth muscle α-actinin by CryoEm reveals two different conformations at the actin-binding region. *Journal of Molecular Biology*, *338*(1), 115–125. https://doi.org/10.1016/j.jmb.2004.02.034

Liu, Y., & Robinson, D. (2018). Recent advances in cytokinesis: Understanding the molecular underpinnings [version 1; referees: 2 approved]. *F1000Research*, *7*(0). https://doi.org/10.12688/f1000research.16502.1

Lonial, S., Waller, E. K., Richardson, P. G., Jagannath, S., Orlowski, R. Z., Giver, C. R., … SUMMIT/CREST Investigators. (2005). Risk factors and kinetics of thrombocytopenia associated with bortezomib for relapsed, refractory multiple myeloma. *Blood*, *106*(12), 3777–3784. https://doi.org/10.1182/blood-2005-03-1173

Lonsdorf, A. S., Krämer, B. F., Fahrleitner, M., Schönberger, T., Gnerlich, S., Ring, S., … Langer, H. F. (2012). Engagement of αIIbβ3 (GPIIb/IIIa) with αvβ3 integrin mediates interaction of melanoma cells with platelets: A connection to hematogenous metastasis. *Journal of Biological Chemistry*, *287*(3), 2168–2178. https://doi.org/10.1074/jbc.M111.269811

Lopez, E., Bermejo, N., Berna-Erro, A., Alonso, N., Salido, G. M., Redondo, P. C., & Rosado, J. A. (2015). Relationship between calcium mobilization and platelet α- And δ-granule secretion. A role for TRPC6 in thrombin-evoked δ-granule exocytosis. *Archives of Biochemistry and Biophysics*, *585*, 75–81. https://doi.org/10.1016/j.abb.2015.09.012

Lornage, X., Romero, N. B., Grosgogeat, C. A., Donkervoort, S., Marchetti, M. M., Neuhaus, S. B., … Hospital, R. P. (2019). ACTN2 mutations cause “Multiple structured Core Disease” (MsCD). *Acta Neuropathol.*, *137*(3), 501–519. https://doi.org/10.1007/s00401-019-01963-8.ACTN2

Low, S. H., Mukhina, S., Srinivas, V., Ng, C. Z., & Murata-Hori, M. (2010). Domain analysis of α-actinin reveals new aspects of its association with F-actin during cytokinesis. *Experimental Cell Research*, *316*(12), 1925–1934. https://doi.org/10.1016/j.yexcr.2010.03.004

Lozano, M. L., Cook, A., Bastida, J. M., Paul, D. S., Iruin, G., Cid, A. R., … Rivera, J. (2016). Novel mutations in RASGRP2, which encodes CalDAG-GEFI, abrogate Rap1 activation, causing platelet dysfunction. *Blood*, *128*(9), 1282–1289. https://doi.org/10.1182/blood-2015-11-683102

Łukasik, Z. M., Makowski, M., & Makowska, J. S. (2018). From blood coagulation to innate and adaptive immunity: the role of platelets in the physiology and pathology of autoimmune disorders. *Rheumatology International*, *38*(6), 959–974. https://doi.org/10.1007/s00296-018-4001-9

Lundahl, T. H., Petersson, J., Fagerberg, I. H., Berg, S., & Lindahl, T. L. (1998). Impaired platelet function correlates with multi-organ dysfunction. A study of patients with sepsis. *Platelets*, *9*(3–4), 223–225. https://doi.org/10.1080/09537109876735

Luo, F.-M., Fan, L.-L., Sheng, Y., Dong, Y., & Liu, L. (2021). Case Report: Exome Sequencing Identified a Novel Frameshift Mutation of α-Actin 1 in a Chinese Family With Macrothrombocytopenia and Mild Bleeding. *Frontiers in Pediatrics*, *9*(June). https://doi.org/10.3389/fped.2021.679279

Luo, T., Mohan, K., Iglesias, P. A., & Robinson, D. N. (2013). Molecular mechanisms of cellular mechanosensing. *Nature Materials*, *12*(11), 1064–1071. https://doi.org/10.1038/nmat3772

Macarthur, D. G., Seto, J. T., Chan, S., Quinlan, K. G. R., Raftery, J. M., Turner, N., … North, K. N. (2008). An Actn3 knockout mouse provides mechanistic insights into the association between α-actinin-3 deficiency and human athletic performance. *Human Molecular Genetics*, *17*(8), 1076–1086. https://doi.org/10.1093/hmg/ddm380

MacArthur, D. G., Seto, J. T., Raftery, J. M., Quinlan, K. G., Huttley, G. A., Hook, J. W., … North, K. N. (2007). Loss of ACTN3 gene function alters mouse muscle metabolism and shows evidence of positive selection in humans. *Nature Genetics*, *39*(10), 1261–1265. https://doi.org/10.1038/ng2122

Machesky, L. M. (2008). Lamellipodia and filopodia in metastasis and invasion. *FEBS Letters*, *582*(14), 2102–2111. https://doi.org/10.1016/j.febslet.2008.03.039

Machlus, K. R., & Italiano, J. E. (2013). The incredible journey: From megakaryocyte development to platelet formation. *Journal of Cell Biology*, *201*(6), 785–796. https://doi.org/10.1083/jcb.201304054

Machlus, K. R., Thon, J. N., & Italiano, J. E. (2014). Interpreting the developmental dance of the megakaryocyte: A review of the cellular and molecular processes mediating platelet formation. *British Journal of Haematology*, *165*(2), 227–236. https://doi.org/10.1111/bjh.12758

Mackman, N. (2008, February 21). Triggers, targets and treatments for thrombosis. *Nature*, Vol. 451, pp. 914–918. https://doi.org/10.1038/nature06797

Manhart, A., Icheva, T. A., Guerin, C., Klar, T., Boujemaa-Paterski, R., Thery, M., … Mogilner, A. (2019). Quantitative regulation of the dynamic steady state of actin networks. *ELife*, *8*, 1–37. https://doi.org/10.7554/eLife.42413

Mannucci, P. M., Cattaneo, M., Teresa Canciani, M., Maniezzo, M., Vaglini, M., & Cascinelli, N. (1989). Early presence of activated ('exhausted') platelets in malignant tumors (breast adenocarcinoma and malignant melanoma). *European Journal of Cancer and Clinical Oncology*, *25*(10), 1413–1417. https://doi.org/10.1016/0277-5379(89)90098-9

Manson, J. J., Ma, A., Rogers, P., Mason, L. J., Berden, J. H., van der Vlag, J., … Rahman, A. (2009). Relationship between anti-dsDNA, anti-nucleosome and anti-alpha-actinin antibodies and markers of renal disease in patients with lupus nephritis: A prospective longitudinal study. *Arthritis Research and Therapy*, *11*(5), 1–9. https://doi.org/10.1186/ar2831

Marcondes, S., Cardoso, M., Morganti, R., Thomazzi, S., Lilla, S., Murad, F., … Antunes, E. (2005). Cyclic GMP-independent mechanisms contribute to the inhibition of platelet adhesion by nitric oxide donor: A role for actinin nitration. *PNAS*, *103*(9), 3434–3439.

Maron, B. J., Gardin, J. M., Flack, J. M., Gidding, S. S., Kurosaki, T. T., & Bild, D. E. (1995). Prevalence of hypertrophic cardiomyopathy in a general population of young adults: Echocardiographic analysis of 4111 subjects in the CARDIA study. *Circulation*, *92*(4), 785–789. https://doi.org/10.1161/01.CIR.92.4.785

Maruyama, K., & Ebashi, S. (1965). a-Actinin, a New Structural Protein from Striated Muscle. *The Journal of Biochemistry*, *58*(1), 13–19.

Mattheij, N. J. A., Swieringa, F., Mastenbroek, T. G., Berny-Lang, M. A., May, F., Baaten, C. C. F. M. J., … Cosemans, J. M. E. M. (2016). Coated platelets function in platelet-dependent fibrin formation via integrin αIIbβ3 and transglutaminase factor XIII. *Haematologica*, *101*(4), 427–436. https://doi.org/10.3324/haematol.2015.131441

Maugeri, N., Rovere-Querini, P., Evangelista, V., Covino, C., Capobianco, A., Bertilaccio, M. T. S., … Manfredi, A. A. (2009). Neutrophils phagocytose activated platelets in vivo: A phosphatidylserine, P-selectin, and β2 integrin-dependent cell clearance program. *Blood*, *113*(21), 5254–5265. https://doi.org/10.1182/blood-2008-09-180794

May, J. A., Glenn, J. R., Spangenberg, P., & Heptinstall, S. (1996). The composition of the platelet cytoskeleton following activation by ADP: Effects of various agents that modulate platelet function. *Platelets*, *7*(3), 159–168. https://doi.org/10.3109/09537109609023575

May, R. C., & Machesky, L. M. (2001). Phagocytosis and the actin cytoskeleton. *Journal of Cell Science*, *114*(6), 1061–1077.

Maynard, D. M., Heijnen, H. F. G., Horne, M. K., White, J. G., & Gahl, W. A. (2007). Proteomic analysis of platelet α-granules using mass spectrometry. *Journal of Thrombosis and Haemostasis*, *5*(9), 1945–1955. https://doi.org/10.1111/j.1538-7836.2007.02690.x

Mazzi, S., Lordier, L., Debili, N., Raslova, H., & Vainchenker, W. (2018). Megakaryocyte and polyploidization. *Experimental Hematology*, *57*, 1–13. https://doi.org/10.1016/j.exphem.2017.10.001

Mcbane, R. D., Gonzalez, C., Hodge, D. O., & Wysokinski, W. E. (2014). Propensity for young reticulated platelet recruitment into arterial thrombi. *Journal of Thrombosis and Thrombolysis*, *37*(2), 148–154. https://doi.org/10.1007/s11239-013-0932-x

McCarty, O. J. T., Mousa, S. A., Bray, P. F., & Konstantopoulos, K. (2000). Immobilized platelets support human colon carcinoma cell tethering, rolling, and firm adhesion

under dynamic flow conditions. *Blood*, *96*(5), 1789–1797. https://doi.org/10.1182/blood.v96.5.1789.h8001789_1789_1797

McFadyen, J. D., Schaff, M., & Peter, K. (2018, March 1). Current and future antiplatelet therapies: Emphasis on preserving haemostasis. *Nature Reviews Cardiology*, Vol. 15, pp. 181–191. https://doi.org/10.1038/nrcardio.2017.206

McGough, A., Way, M., & DeRosier, D. (1994). Determination of the α-actinin-binding site on actin filaments by cryoelectron microscopy and image analysis. *Journal of Cell Biology*, *126*(2), 433–443. https://doi.org/10.1083/jcb.126.2.433

McGrath, K. M., Stuart, J. J., Richards, F., Grath, K. M., Stuart, J. J., & Richards, F. (1979). Correlation between Serum IgG, Platelet Membrane IgG, and Platelet Function in Hypergammaglobulinaemic States. *British Journal of Haematology*, *42*(4), 585–591. https://doi.org/10.1111/j.1365-2141.1979.tb01171.x

Meacci, G., Wolfenson, H., Liu, S., Stachowiak, M. R., Iskratsch, T., Mathur, A., … Sheetz, M. P. (2016). α-Actinin links extracellular matrix rigidity-sensing contractile units with periodic cell-edge retractions. *Molecular Biology of the Cell*, *27*(22), 3471–3479. https://doi.org/10.1091/mbc.E16-02-0107

Megy, K., Downes, K., Simeoni, I., Bury, L., Morales, J., Mapeta, R., … Freson, K. (2019). Curated disease-causing genes for bleeding, thrombotic, and platelet disorders: Communication from the SSC of the ISTH. *Journal of Thrombosis and Haemostasis : JTH*, *17*(8), 1253–1260. https://doi.org/10.1111/jth.14479

Mei, Y., Liu, H., Sun, X., Li, X., Zhao, S., & Ma, R. (2017). Plasma fibrinogen level may be a possible marker for the clinical response and prognosis of patients with breast cancer receiving neoadjuvant chemotherapy. *Tumor Biology*, *39*(6). https://doi.org/10.1177/1010428317700002

Menez, J., Chansac, B. L. M., Dorothée, G., Vergnon, I., Jalil, A., Carlier, M.-F., … Mami-Chouaib, F. (2004). Mutant α-actinin-4 promotes tumorigenicity and regulates cell motility of a human lung carcinoma. *Oncogene*, *23*(15), 2630–2639. https://doi.org/10.1038/sj.onc.1207347

Meng, R., Wu, J., Harper, D. C., Wang, Y., Kowalska, M. A., Abrams, C. S., … Marks, M. S. (2015). Defective release of α granule and lysosome contents from platelets in mouse Hermansky-Pudlak syndrome models. *Blood*, *125*(10), 1623–1632. https://doi.org/10.1182/blood-2014-07-586727

Meyer, R. K., & Aebi, U. (1990). Bundling of actin filaments by α-actinin depends on its molecular length. *Journal of Cell Biology*, *110*(6), 2013–2024. https://doi.org/10.1083/jcb.110.6.2013

Meyer, S. C., Keller, M. D., Woods, B. A., Lafave, L. M., Bastian, L., Kleppe, M., … Levine, R. L. (2014). Genetic studies reveal an unexpected negative regulatory role for jak2 in thrombopoiesis. *Blood*, *124*(14), 2280–2284. https://doi.org/10.1182/blood-2014-03-560441

Michael, J. V., Wurtzel, J. G. T., Mao, G. F., Rao, A. K., Kolpakov, M. A., Sabri, A., … Goldfinger, L. E. (2017). Platelet microparticles infiltrating solid tumors transfer miRNAs that suppress tumor growth. *Blood*, *130*(5), 567–580. https://doi.org/10.1182/blood-2016-11-751099

Michaud, J. L.R., Chaisson, K. M., Parks, R. J., & Kennedy, C. R. J. (2006). FSGS-associated α-

actinin-4 (K256E) impairs cytoskeletal dynamics in podocytes. *Kidney International*, *70*(6), 1054–1061. https://doi.org/10.1038/sj.ki.5001665

Michaud, Jean Louis R., Hosseini-Abardeh, M., Farah, K., & Kennedy, C. R. J. (2009). Modulating α-actinin-4 dynamics in podocytes. *Cell Motility and the Cytoskeleton*, *66*(3), 166–178. https://doi.org/10.1002/cm.20339

Michelson, A. D., Barnard, M. R., Krueger, L. A., Valeri, C. R., & Furman, M. I. (2001). Circulating Monocyte-Platelet Aggregates Are a More Sensitive Marker of In Vivo Platelet Activation Than Platelet Surface P-Selectin: Studies in Baboons, Human Coronary Intervention, and Human Acute Myocardial Infarction. *Circulation*, *104*(13), 1533–1537. https://doi.org/10.1161/hc3801.095588

Middleton, E. A., He, X.-Y., Denorme, F., Campbell, R. A., Ng, D., Salvatore, S. P., … Yost, C. C. (2020). Neutrophil extracellular traps contribute to immunothrombosis in COVID-19 acute respiratory distress syndrome. *Blood*, *136*(10), 1169–1179. https://doi.org/10.1182/blood.2020007008

Mills, M. A., Yang, N., Weinberger, R., Vander Woude, D. L., Beggs, A. H., Easteal, S., & North, K. N. (2001). Differential expression for the actin-binding proteins, α-actinin-2 and -3, in different species: Implications for the evolution of functional redundancy. *Human Molecular Genetics*, *10*(13), 1335–1346. https://doi.org/10.1093/hmg/10.13.1335

Mimura, N., & Asano, A. (1978). Actin-related gelation of Ehrlich tumour cell extracts is reversibly inhiited by low concentrations of Ca2+. *Nature*, *272*, 273–276.

Mirabelli, F., Salis, A., Vairetti, M., Bellomo, G., Thor, H., & Orrenius, S. (1989). Cytoskeletal alterations in human platelets exposed to oxidative stress are mediated by oxidative and Ca2+-dependent mechanisms. *Archives of Biochemistry and Biophysics*, *270*(2), 478–488. https://doi.org/10.1016/0003-9861(89)90529-8

Miyamoto, S., Teramoto, H., Coso, O. A., Gutkind, J. S., Burbelo, P. D., Akiyama, S. K., & Yamada, K. M. (1995). Integrin function: Molecular hierarchies of cytoskeletal and signaling molecules. *Journal of Cell Biology*, *131*(3), 791–805. https://doi.org/10.1083/jcb.131.3.791

Miyanaga, A., Honda, K., Tsuta, K., Masuda, M., Yamaguchi, U., Fujii, G., … Yamada, T. (2013). Diagnostic and prognostic significance of the alternatively spliced ACTN4 variant in high-grade neuroendocrine pulmonary tumours. *Annals of Oncology*, *24*(1), 84–90. https://doi.org/10.1093/annonc/mds215

Miyata, H., Yasuda, R., & Kinosita, K. (1996). Strength and lifetime of the bond between actin and skeletal muscle α-actinin studied with an optical trapping technique. *Biochimica et Biophysica Acta - General Subjects*, *1290*(1), 83–88. https://doi.org/10.1016/0304-4165(96)00003-7

Moeckel, D., Jeong, S. S., Sun, X., Broekman, M. J., Nguyen, A., Drosopoulos, J. H. F., … Abendschein, D. (2014). Optimizing human apyrase to treat arterial thrombosis and limit reperfusion injury without increasing bleeding risk. *Science Translational Medicine*, *6*(248). https://doi.org/10.1126/scitranslmed.3009246

Mohapatra, B., Jimenez, S., Lin, J. H., Bowles, K. R., Coveler, K. J., Marx, J. G., … Bowles, N. E. (2003). Mutations in the muscle LIM protein and α-actinin-2 genes in dilated cardiomyopathy and endocardial fibroelastosis. *Molecular Genetics and Metabolism*, *80*(1–2), 207–215. https://doi.org/10.1016/S1096-7192(03)00142-2

Möhle, R., Green, D., Moore, M. A. S., Nachman, R. L., & Rafii, S. (1997). Constitutive production and thrombin-induced release of vascular endothelial growth factor by human megakaryocytes and platelets. *Proceedings of the National Academy of Sciences of the United States of America*, *94*(2), 663–668. https://doi.org/10.1073/pnas.94.2.663

Mohri, H., Noguchi, T., Kodama, F., Itoh, A., & Ohkubo, T. (1987). Acquired von Willebrand Disease Due to Inhibitor of Human Myeloma Protein Specific for von Willebrand Factor. *American Journal of Clinical Pathology*, *87*(5), 663–668. https://doi.org/10.1093/ajcp/87.5.663

Montoro-García, S., Schindewolf, M., Stanford, S., Larsen, O. H., & Thiele, T. (2016). The role of platelets in venous thromboembolism. *Seminars in Thrombosis and Hemostasis*, *42*(3), 242–251. https://doi.org/10.1055/s-0035-1570079

Moore, C., Sambrook, J., Walker, M., Tolkien, Z., Kaptoge, S., Allen, D., … Danesh, J. (2014). The INTERVAL trial to determine whether intervals between blood donations can be safely and acceptably decreased to optimise blood supply: Study protocol for a randomised controlled trial. *Trials*, *15*(1). https://doi.org/10.1186/1745-6215-15-363

Morowski, M., Vögtle, T., Kraft, P., Kleinschnitz, C., Stoll, G., & Nieswandt, B. (2013). Only severe thrombocytopenia results in bleeding and defective thrombus formation in mice. *Blood*, *121*(24), 4938–4947. https://doi.org/10.1182/blood-2012-10-461459

Morrow, D. A., Braunwald, E., Bonaca, M. P., Ameriso, S. F., Dalby, A. J., Fish, M. P., … Murphy, S. A. (2012). Vorapaxar in the Secondary Prevention of Atherothrombotic Events. *New England Journal of Medicine*, *366*(15), 1404–1413. https://doi.org/10.1056/NEJMoa1200933

Morse, B. S., Giuliani, D., & Nussbaum, M. (1982). A rapid quantitation of platelet-associated igg by nephelometry. *American Journal of Hematology*, *12*(3), 271–275. https://doi.org/10.1002/ajh.2830120309

Mostoslavsky, G., Fischel, R., Yachimovich, N., Yarkoni, Y., Rosenmann, E., Monestier, M., … Eilat, D. (2001). Lupus anti-DNA autoantibodies cross-react with a glomerular structural protein: A case for tissue injury by molecular mimicry. *European Journal of Immunology*, *31*(4), 1221–1227. https://doi.org/10.1002/1521-4141(200104)31:4<1221::AID-IMMU1221>3.0.CO;2-P

Mott, P. J., & Lazarus, A. H. (2013). CD44 Antibodies and Immune Thrombocytopenia in the Amelioration of Murine Inflammatory Arthritis. *PLoS ONE*, *8*(6), e65805. https://doi.org/10.1371/journal.pone.0065805

Mueller-Eckhardt, C., Mueller-Eckhardt, G., Kayser, W., Voss, R. M., and, J. W., & Küenzlen, E. (1982). Platelet associated IgG, platelet survival, and platelet sequestration in thrombocytopenic states. *British Journal of Haematology*, *52*(1), 49–58. https://doi.org/10.1111/j.1365-2141.1982.tb03860.x

Mukhina, S., Wang, Y., & Murata-Hori, M. (2007). α-Actinin Is Required for Tightly Regulated Remodeling of the Actin Cortical Network during Cytokinesis. *Developmental Cell*, *13*(4), 554–565. https://doi.org/10.1016/J.DEVCEL.2007.08.003

Munnix, I. C. A., Kuijpers, M. J. E., Auger, J., Thomassen, C. M. L. G. D., Panizzi, P., Van Zandvoort, M. A. M., … Heemskerk, J. W. M. (2007). Segregation of platelet aggregatory and procoagulant microdomains in thrombus formation: Regulation by transient integrin activation. *Arteriosclerosis, Thrombosis, and Vascular Biology*,

27(11), 2484–2490. https://doi.org/10.1161/ATVBAHA.107.151100

Murai, K., Kowata, S., Shimoyama, T., Yashima-Abo, A., Fujishima, Y., Ito, S., & Ishida, Y. (2014). Bortezomib induces thrombocytopenia by the inhibition of proplatelet formation of megakaryocytes. *European Journal of Haematology*, *93*(4), 290–296. https://doi.org/10.1111/ejh.12342

Murphy, A. C. H., Lindsay, A. J., McCaffrey, M. W., Djinovic-Carugo, K., & Young, P. W. (2016). Congenital macrothrombocytopenia-linked mutations in the actin-binding domain of alpha-actinin-1 enhance F-actin association. *FEBS Letters*, *590*(6), 685–695. https://doi.org/10.1002/1873-3468.12101

Murphy, A. C. H., & Young, P. W. (2015). The actinin family of actin cross-linking proteins - A genetic perspective. *Cell and Bioscience*, *5*(1), 1–9. https://doi.org/10.1186/s13578-015-0029-7

Muslimani, A. A., Spiro, T. P., Chaudhry, A. A., Taylor, H. C., Jaiyesimi, I., & Daw, H. A. (2009). Venous thromboembolism in patients with monoclonal gammopathy of undetermined significance. *Clinical Advances in Hematology and Oncology*, *7*(12), 827–832.

N, Y., DG, M., JP, G., AG, H., AH, B., & S, E. (2003). ACTN3 Genotype Is Associated with Human Elite Athletic Performance. *Am J Hum Genet.*, *73*(3), 627–631.

Nagy, M., Mastenbroek, T. G., Mattheij, N. J. A., de Witt, S., Clemetson, K. J., Kirschner, J., … Heemskerk, J. W. M. (2018). Variable impairment of platelet functions in patients with severe, genetically linked immune deficiencies. *Haematologica*, *103*(3), 540–549. https://doi.org/10.3324/haematol.2017.176974

Nazi, I., Arnold, D. M., Smith, J. W., Horsewood, P., Moore, J. C., Warkentin, T. E., … Kelton, J. G. (2013). FcγRIIa proteolysis as a diagnostic biomarker for heparin-induced thrombocytopenia. *Journal of Thrombosis and Haemostasis*, *11*(6), 1146–1153. https://doi.org/10.1111/jth.12208

Nazi, I., Smith, J. W., Arnold, D. M., Horsewood, P., Moore, J. C., Warkentin, T. E., & Kelton, J. G. (2011). The association between platelet activation and FcγRIIa proteolysis. *Journal of Thrombosis and Haemostasis*, *9*(4), 885–887. https://doi.org/10.1111/j.1538-7836.2011.04239.x

Neunert, C. E., Buchanan, G. R., Imbach, P., Bolton-Maggs, P. H. B., Bennett, C. M., Neufeld, E. J., … Kühne, T. (2008). Severe hemorrhage in children with newly diagnosed immune thrombocytopenic purpura. *Blood*, *112*(10), 4003–4008. https://doi.org/10.1182/blood-2008-03-138487

Ng, A. P., Kauppi, M., Metcalf, D., Hyland, C. D., Josefsson, E. C., Lebois, M., … Alexander, W. S. (2014). Mpl expression on megakaryocytes and platelets is dispensable for thrombopoiesis but essential to prevent myeloproliferation. *Proceedings of the National Academy of Sciences of the United States of America*, *111*(16), 5884–5889. https://doi.org/10.1073/pnas.1404354111

Niazi, H., Zoghdani, N., Couty, L., Leuci, A., Nitzsche, A., Allende, M. L., … Camerer, E. (2019). Murine platelet production is suppressed by S1P release in the hematopoietic niche, not facilitated by blood S1P sensing. *Blood Advances*, *3*(11), 1702–1713. https://doi.org/10.1182/bloodadvances.2019031948

NICE (National Institute for Health and Care Excellence). (2018). Venous thromboembolism

in over 16s: reducing the risk of hospital-acquired deep vein thrombosis or pulmonary embolism. Retrieved from https://www.nice.org.uk/guidance/ng89/chapter/Recommendations#interventions-for-people-with-cancer

Nieset, J. E., Redfield, A. R., Jin, F., Knudsen, K. A., Johnson, K. R., & Wheelock, M. J. (1997). Characterization of the interactions of alpha-catenin with alpha-actinin and beta-catenin/plakoglobin. *Journal of Cell Science*, *1106*, 1013–1022. Retrieved from http://jcs.biologists.org/content/joces/110/8/1013.full.pdf

Nieswandt, B., Hafner, M., Echtenacher, B., & Männel, D. N. (1999). Lysis of Tumor Cells by Natural Killer Cells in Mice Is Impeded by Platelets. *Cancer Research*, *59*(6), 1295–1300.

Nikolopoulos, S. N., Spengler, B. A., Kisselbach, K., Evans, A. E., Biedler, J. L., & Ross, R. A. (2000). The human non-muscle α-actinin protein encoded by the ACTN4 gene suppresses tumorigenicity of human neuroblastoma cells. *Oncogene*, *19*(3), 380–386. https://doi.org/10.1038/sj.onc.1203310

Nomura, S., Imamura, A., Okuno, M., Kamiyama, Y., Fujimura, Y., Ikeda, Y., & Fukuhara, S. (2000). Platelet-derived microparticles in patients with arteriosclerosis obliterans: Enhancement of high shear-induced microparticle generation by cytokines. *Thrombosis Research*, *98*(4), 257–268. https://doi.org/10.1016/S0049-3848(00)00186-9

Nomura, S., Kanazawa, S., & Fukuhara, S. (2002). Effects of efonidipine on platelet and monocyte activation markers in hypertensive patients with and without type 2 diabetes mellitus. *Journal of Human Hypertension*, *16*(8), 539–547. https://doi.org/10.1038/sj.jhh.1001447

Nomura, S., Ozaki, Y., & Ikeda, Y. (2008). Function and role of microparticles in various clinical settings. *Thrombosis Research*, Vol. 123, pp. 8–23. https://doi.org/10.1016/j.thromres.2008.06.006

Nonne, C., Lenain, N., Hechler, B., Mangin, P., Cazenave, J.-P., Gachet, C., & Lanza, F. (2005). Importance of platelet phospholipase Cgamma2 signaling in arterial thrombosis as a function of lesion severity. *Arteriosclerosis, Thrombosis, and Vascular Biology*, *25*(6), 1293–1298. https://doi.org/10.1161/01.ATV.0000163184.02484.69

Nørgaard, M., Severinsen, M. T., Lund Maegbaek, M., Jensen, A. Ø., Cha, S., & Sørensen, H. T. (2012). Risk of arterial thrombosis in patients with primary chronic immune thrombocytopenia: a Danish population-based cohort study. *British Journal of Haematology*, *159*(1), 109–111. https://doi.org/10.1111/j.1365-2141.2012.09231.x

North, K. N., Yang, N., Wattanasirichaigoon, D., Mills, M., Easteal, S., & Beggs, A. H. (1999). A common nonsense mutation results in α-actinin-3 deficiency in the general population [1]. *Nature Genetics*, *21*(4), 353–354. https://doi.org/10.1038/7675

Novotny, W. F., Girard, T. J., Miletich, J. P., & Broze, G. J. (1988). Platelets secrete a coagulation inhibitor functionally and antigenically similar to the lipoprotein associated coagulation inhibitor. *Blood*, *72*(6), 2020–2025. Retrieved from http://www.ncbi.nlm.nih.gov/pubmed/3143429

Nurden, A. T., & Nurden, P. (2015). Inherited disorders of platelet function: Selected updates. *Journal of Thrombosis and Haemostasis*, *13*(S1), S2–S9. https://doi.org/10.1111/jth.12898

Nürnberg, S. T., Rendon, A., Smethurst, P. A., Paul, D. S., Voss, K., Thon, J. N., … Ouwehand, W. H. (2012). AGWAS sequence variant for platelet volume marks an alternative DNM3 promoter in megakaryocytes near a MEIS1 binding site. *Blood*, *120*(24), 4859–4868. https://doi.org/10.1182/blood-2012-01-401893

O'Sullivan, L. R., Cahill, M. R., & Young, P. W. (2021). The Importance of Alpha-Actinin Proteins in Platelet Formation and Function, and Their Causative Role in Congenital Macrothrombocytopenia. *International Journal of Molecular Sciences*, *22*(17). https://doi.org/10.3390/ijms22179363

O'Sullivan, L. R., Praburam Ajaykumar, A., Dembicka, K. M., Murphy, A., Grennan, E. P., & Young, P. W. (2019). Investigation of calmodulin-like and rod domain mutations suggests common molecular mechanism for α-actinin-1-linked congenital macrothrombocytopenia. *FEBS Letters*, 1873-3468.13562. https://doi.org/10.1002/1873-3468.13562

Ogura, M., Morishima, Y., Okumura, M., Hotta, T., Takamoto, S., Ohno, R., … Saito, H. (1988). Functional and Morphological Differentiation Induction of a Human Megakaryoblastic Leukaemia Cell Line (MEG-01s) by Phorbol Diesters. *Blood*, *72*(1), 49–60.

Olie, R. H., van der Meijden, P. E. J., & ten Cate, H. (2018). The coagulation system in atherothrombosis: Implications for new therapeutic strategies. *Research and Practice in Thrombosis and Haemostasis*, *2*(2), 188–198. https://doi.org/10.1002/rth2.12080

Oliver, A. E., Tablin, F., Walker, N. J., & Crowe, J. H. (1999). The internal calcium concentration of human platelets increases during chilling. *Biochimica et Biophysica Acta (BBA) - Biomembranes*, *1416*(1–2), 349–360. https://doi.org/10.1016/S0005-2736(98)00239-9

Onlamoon, N., Noisakran, S., Hsiao, H. M., Duncan, A., Villinger, F., Ansari, A. A., & Perng, G. C. (2010). Dengue virus - Induced hemorrhage in a nonhuman primate model. *Blood*, *115*(9), 1823–1834. https://doi.org/10.1182/blood-2009-09-242990

Otey, C. A., & Carpen, O. (2004). α-Actinin Revisited: A Fresh Look at an Old Player. *Cell Motility and the Cytoskeleton*, *111*(February), 104–111. https://doi.org/10.1002/cm.20007

Otey, C. A., Pavalko, F. M., & Burridge, K. (1990). An interaction between α-actinin land the β1 integrin subunit in vitro. *Journal of Cell Biology*, *111*(2), 721–729. https://doi.org/10.1083/jcb.111.2.721

Otey, C. A., Vasquez, G. B., Burridge, K., & Erickson, B. W. (1993). Mapping of the ??-actinin binding site within the ??1 integrin cytoplasmic domain. *Journal of Biological Chemistry*, *268*(28), 21193–21197.

Özkurt, Z. N., Yağci, M., Sucak, G. T., Kirazli, Ş., Haznedar, R., Yağci, M., … Haznedar, R. (2010). Thrombopoietic cytokines and platelet count in multiple myeloma. *Platelets*, *21*(1), 33–36. https://doi.org/10.3109/09537100903360007

Paavilainen, V. O., Bertling, E., Falck, S., & Lappalainen, P. (2004). Regulation of cytoskeletal dynamics by actin-monomer-binding proteins. *Trends in Cell Biology*, *14*(7), 386–394. https://doi.org/10.1016/j.tcb.2004.05.002

Pacaud, M., & Harricane, M. C. (1993). Macrophage α-Actinin Is Not a Calcium-Modulated Actin-Binding Protein. *Biochemistry*, *32*(1), 363–374.

https://doi.org/10.1021/bi00052a045

Palumbo, A., Rajkumar, S. V., San Miguel, J. F., Larocca, A., Niesvizky, R., Morgan, G., … Orlowski, R. Z. (2014). International Myeloma Working Group consensus statement for the management, treatment, and supportive care of patients with myeloma not eligible for standard autologous stem-cell transplantation. *Journal of Clinical Oncology*, *32*(6), 587–600. https://doi.org/10.1200/JCO.2013.48.7934

Palumbo, J. S., Talmage, K. E., Massari, J. V., La Jeunesse, C. M., Flick, M. J., Kombrinck, K. W., … Degen, J. L. (2005). Platelets and fibrin(ogen) increase metastatic potential by impeding natural killer cell-mediated elimination of tumor cells. *Blood*, *105*(1), 178–185. https://doi.org/10.1182/blood-2004-06-2272

Pasquet, J M, Gross, B. S., Gratacap, M. P., Quek, L., Pasquet, S., Payrastre, B., … Watson, S. P. (2000). Thrombopoietin potentiates collagen receptor signaling in platelets through a phosphatidylinositol 3-kinase-dependent pathway. *Blood*, *95*(11), 3429–3434. Retrieved from http://www.ncbi.nlm.nih.gov/pubmed/10828025

Pasquet, Jean Max, Quek, L., Pasquet, S., Poole, A., Matthews, J. R., Lowell, C., & Watson, S. P. (2000). Evidence of a role for SHP-1 in platelet activation by the collagen receptor glycoprotein VI. *Journal of Biological Chemistry*, *275*(37), 28526–28531. https://doi.org/10.1074/jbc.M001531200

Patel-Hett, S., Wang, H., Begonja, A. J., Thon, J. N., Alden, E. C., Wandersee, N. J., … Italiano, J. E. J. (2011). The spectrin-based membrane skeleton stabilizes mouse megakaryocyte membrane systems and is essential for proplatelet and platelet formation. *Blood*, *118*(6), 1641–1652. https://doi.org/10.1182/blood-2011-01-330688

Patrono, C., Morais, J., Baigent, C., Collet, J. P., Fitzgerald, D., Halvorsen, S., … Vilahur, G. (2017, October 3). Antiplatelet Agents for the Treatment and Prevention of Coronary Atherothrombosis. *Journal of the American College of Cardiology*, Vol. 70, pp. 1760–1776. https://doi.org/10.1016/j.jacc.2017.08.037

Pavalko, F. M., & Otey, C. A. (1991). *α-Actinin : a direct link between actin and integrins Focal adhesions are a model for studying actin-membrane interactions In vitro identification of an α-actinin-*.

Petersen, R., Lambourne, J. J., Javierre, B. M., Grassi, L., Kreuzhuber, R., Ruklisa, D., … Frontini, M. (2017). Platelet function is modified by common sequence variation in megakaryocyte super enhancers. *Nature Communications*, *8*(1), 1–12. https://doi.org/10.1038/ncomms16058

Philippe, C., Philippe, B., Fouqueray, B., Perez, J., Lebret, M., & Baud, L. (1993). Protection from tumor necrosis factor-mediated cytolysis by platelets. *American Journal of Pathology*, *143*(6), 1713–1723. Retrieved from /pmc/articles/PMC1887257/?report=abstract

Pickering, C., & Kiely, J. (2017). ACTN3: More than just a gene for speed. *Frontiers in Physiology*, *8*(DEC), 1–9. https://doi.org/10.3389/fphys.2017.01080

Placke, T., Örgel, M., Schaller, M., Jung, G., Rammensee, H. G., Kopp, H. G., & Salih, H. R. (2012). Platelet-derived MHC class I confers a pseudonormal phenotype to cancer cells that subverts the antitumor reactivity of natural killer immune cells. *Cancer Research*, *72*(2), 440–448. https://doi.org/10.1158/0008-5472.CAN-11-1872

Pleines, I., Lebois, M., Gangatirkar, P., Au, A. E., Lane, R. M., Henley, K. J., … Josefsson, E. C.

(2018). Intrinsic apoptosis circumvents the functional decline of circulating platelets but does not cause the storage lesion. *Blood*, *132*(2), 197–209. https://doi.org/10.1182/blood-2017-11-816355

PM, M., & A, T. (2012). Hemostatic defects in liver and renal dysfunction. *Hematology. American Society of Hematology. Education Program*, *2012*. https://doi.org/10.1182/ASHEDUCATION-2012.1.168

Pollard, T. D., Blanchoin, L., & Mullins, R. D. (2000). Molecular Mechanisms Controlling Actin Filament Dynamics In Nonmuscle Cells. *Annual Review of Physiology*, *29*, 545–576.

Postea, O., Vasina, E. M., Cauwenberghs, S., Projahn, D., Liehn, E. A., Lievens, D., … Koenen, R. R. (2012). Contribution of Platelet CX $_3$ CR1 to Platelet–Monocyte Complex Formation and Vascular Recruitment During Hyperlipidemia. *Arteriosclerosis, Thrombosis, and Vascular Biology*, *32*(5), 1186–1193. https://doi.org/10.1161/ATVBAHA.111.243485

Poulter, N. S., Pollitt, A. Y., Davies, A., Malinova, D., Nash, G. B., Hannon, M. J., … Thomas, S. G. (2015). Platelet actin nodules are podosome-like structures dependent on Wiskott-Aldrich syndrome protein and ARP2/3 complex. *Nature Communications*, *6*. https://doi.org/10.1038/ncomms8254

Poulter, N. S., & Thomas, S. G. (2015). Cytoskeletal regulation of platelet formation: Coordination of F-actin and microtubules. *International Journal of Biochemistry and Cell Biology*, *66*, 69–74. https://doi.org/10.1016/j.biocel.2015.07.008

Powers, M. E., Becker, R. E. N., Sailer, A., Turner, J. R., & Bubeck Wardenburg, J. (2015). Synergistic Action of Staphylococcus aureus α-Toxin on Platelets and Myeloid Lineage Cells Contributes to Lethal Sepsis. *Cell Host and Microbe*, *17*(6), 775–787. https://doi.org/10.1016/j.chom.2015.05.011

Prebil, S. D., Slapšak, U., Pavšič, M., Ilc, G., Puž, V., Ribeiro, E. de A., … Djinović-Carugo, K. (2016). Structure and calcium-binding studies of calmodulin-like domain of human non-muscle α-actinin-1. *Scientific Reports*, *6*, 27383. https://doi.org/10.1038/SREP27383

Prodan, C. I., Joseph, P. M., Vincent, A. S., & Dale, G. L. (2008). Coated-platelets in ischemic stroke: Differences between lacunar and cortical stroke. *Journal of Thrombosis and Haemostasis*, *6*(4), 609–614. https://doi.org/10.1111/j.1538-7836.2008.02890.x

Pruliere, G., D'Albis, A., & Der Terrossian, E. (1986). Effect of tropomyosin on the interactions of actin with actin-binding proteins isolated from pig platelets. *European Journal of Biochemistry*, *159*(3), 535–547. https://doi.org/10.1111/j.1432-1033.1986.tb09920.x

Qian, K., Xie, F., Gibson, A. W., Edberg, J. C., Kimberly, R. P., & Wu, J. (2008). Functional expression of IgA receptor FcαRI on human platelets. *Journal of Leukocyte Biology*, *84*(6), 1492–1500. https://doi.org/10.1189/jlb.0508327

Qiao, J., Al-Tamimi, M., Baker, R. I., Andrews, R. K., & Gardiner, E. E. (2015, November 1). The platelet Fc receptor, FcγRIIa. *Immunological Reviews*, Vol. 268, pp. 241–252. https://doi.org/10.1111/imr.12370

Quick, Q., & Skalli, O. (2010). α-Actinin 1 and α-actinin 4: Contrasting roles in the survival, motility, and RhoA signaling of astrocytoma cells. *Experimental Cell Research*, *316*(7),

1137–1147. https://doi.org/10.1016/j.yexcr.2010.02.011

Rajkumar, S. V. (2019). Multiple myeloma: Every year a new standard? *Hematological Oncology*, *37*(S1), 62–65. https://doi.org/10.1002/hon.2586

Rajkumar, S. V., Dimopoulos, M. A., Palumbo, A., Blade, J., Merlini, G., Mateos, M. V., … Miguel, J. F. S. (2014, November 1). International Myeloma Working Group updated criteria for the diagnosis of multiple myeloma. *The Lancet Oncology*, Vol. 15, pp. e538–e548. https://doi.org/10.1016/S1470-2045(14)70442-5

Rakus, D., Mamczur, P., Gizak, A., Dus, D., & Dzugaj, A. (2003). Colocalization of muscle FBPase and muscle aldolase on both sides of the Z-line. *Biochemical and Biophysical Research Communications*, *311*(2), 294–299. https://doi.org/10.1016/j.bbrc.2003.09.209

Ramakrishnan, V., DeGuzman, F., Bao, M., Hall, S. W., Leung, L. L., & Phillips, D. R. (2001). A thrombin receptor function for platelet glycoprotein Ib-IX unmasked by cleavage of glycoprotein V. *Proceedings of the National Academy of Sciences of the United States of America*, *98*(4), 1823–1828. https://doi.org/10.1073/pnas.98.4.1823

Ramos, P. S., Williams, A. H., Ziegler, J. T., Comeau, M. E., Guy, R. T., Lessard, C. J., … Moser, K. L. (2011). Genetic analyses of interferon pathway-related genes reveal multiple new loci associated with systemic lupus erythematosus. *Arthritis and Rheumatism*, *63*(7), 2049–2057. https://doi.org/10.1002/art.30356

Rand, M. L., Reddy, E. C., & Israels, S. J. (2018). Laboratory diagnosis of inherited platelet function disorders. *Transfusion and Apheresis Science*, *57*(4), 485–493. https://doi.org/10.1016/j.transci.2018.07.009

Rasband, W. S. (n.d.). *ImageJ, U. S. National Institutes of Health, Bethesda, Maryland, USA*. Retrieved from https://imagej.nih.gov/ij/, 1997-2018.

Reddy, E. C., & Rand, M. L. (2020). Procoagulant Phosphatidylserine-Exposing Platelets in vitro and in vivo. *Frontiers in Cardiovascular Medicine*, *7*(15). https://doi.org/10.3389/fcvm.2020.00015

Redondo, P. C., Harper, A. G. S., Harper, M. T., Brownlow, S. L., Rosado, J. A., & Sage, S. O. (2007). hTRPC1-associated α-actinin, and not hTRPC1 itself, is tyrosine phosphorylated during human platelet activation. *Journal of Thrombosis and Haemostasis*, *5*(12), 2476–2483. https://doi.org/10.1111/j.1538-7836.2007.02773.x

Réger, B., Péterfalvi, Á., Litter, I., Pótó, L., Mózes, R., Tóth, O., … Losonczy, H. (2013). Challenges in the evaluation of D-dimer and fibrinogen levels in pregnant women. *Thrombosis Research*, *131*(4), 183–187. https://doi.org/10.1016/j.thromres.2013.02.005

Reichl, E. M., & Robinson, D. N. (2007). Putting the Brakes on Cytokinesis with α-Actinin. *Developmental Cell*, *13*(4), 460–462. https://doi.org/10.1016/j.devcel.2007.09.010

Renaudineau, Y., Dalekos, G. N., Guéguen, P., Zachou, K., & Youinou, P. (2008). Anti-α-actinin antibodies cross-react with anti-ssDNA antibodies in active autoimmune hepatitis. *Clinical Reviews in Allergy and Immunology*, *34*(3), 321–325. https://doi.org/10.1007/s12016-007-8050-1

Renaudineau, Y., Deocharan, B., Jousse, S., Renaudineau, E., Putterman, C., & Youinou, P. (2007). Anti-alpha-actinin antibodies: A new marker of lupus nephritis. *Autoimmunity Reviews*, *6*(7), 464–468. https://doi.org/10.1016/j.autrev.2007.02.001

Reséndiz, J C, Feng, S., Ji, G., & Kroll, M. H. (2004). von Willebrand factor binding to platelet glycoprotein Ib-IX-V stimulates the assembly of an alpha-actinin-based signaling complex. *Journal of Thrombosis and Haemostasis : JTH*, *2*(1), 161–169. Retrieved from http://www.ncbi.nlm.nih.gov/pubmed/14717980

Reséndiz, Julio C., Feng, S., Ji, G., & Kroll, M. H. (2004). Von Willebrand factor binding to platelet glycoprotein Ib-IX-V stimulates the assembly of an α-actinin-based signaling complex. *Journal of Thrombosis and Haemostasis*, *2*(1), 161–169. https://doi.org/10.1111/j.1538-7836.2003.00497.x

Revollo, L., Merrill-Skoloff, G., Ceunynck, K. De, Dilks, J. R., Bordoli, M., Peters, C. G., … Flaumenhaft, R. (2021). The secreted tyrosine kinase VLK is essential for normal platelet activation and thrombus formation. *BioRxiv*, 2021.01.24.427281. https://doi.org/10.1101/2021.01.24.427281

Ribeiro, E. D. A., Pinotsis, N., Ghisleni, A., Salmazo, A., Konarev, P. V., Kostan, J., … Djinović-Carugo, K. (2014). The structure and regulation of human muscle α-Actinin. *Cell*, *159*(6), 1447–1460. https://doi.org/10.1016/j.cell.2014.10.056

Ribeiro, E. de A., Pinotsis, N., Ghisleni, A., Salmazo, A., Konarev, P. V, Kostan, J., … Djinović-Carugo, K. (2014). The structure and regulation of human muscle α-actinin. *Cell*, *159*(6), 1447–1460. https://doi.org/10.1016/j.cell.2014.10.056

Riedl, J., Pabinger, I., & Ay, C. (2014). Platelets in cancer and thrombosis. *Hamostaseologie*, *34*(1), 54–62. https://doi.org/10.5482/HAMO-13-10-0054

Riedl, Julia, Kaider, A., Marosi, C., Prager, G. W., Eichelberger, B., Assinger, A., … Ay, C. (2017). Decreased platelet reactivity in patients with cancer is associated with high risk of venous thromboembolism and poor prognosis. *Thrombosis and Haemostasis*, *117*(1), 90–98. https://doi.org/10.1160/TH16-02-0123

Robak, M., Treliński, J., & Chojnowski, K. (2012). Hemostatic changes after 1 month of thalidomide and dexamethasone therapy in patients with multiple myeloma. *Medical Oncology*, *29*(5), 3574–3580. https://doi.org/10.1007/s12032-012-0290-0

Roberts, H. R., Monroe, D. M., & White, G. C. (2004). The use of recombinant factor VIIa in the treatment of bleeding disorders. *Blood*, *104*(13), 3858–3864. https://doi.org/10.1182/blood-2004-06-2223

Robison, A. J., Bass, M. A., Jiao, Y., MacMillan, L. B., Carmody, L. C., Bartlett, R. K., & Colbran, R. J. (2005). Multivalent interactions of calcium/calmodulin-dependent protein kinase II with the postsynaptic density proteins NR2B, densin-180, and α-actinin-2. *Journal of Biological Chemistry*, *280*(42), 35329–35336. https://doi.org/10.1074/jbc.M502191200

Roca-Cusachs, P., Del Rio, A., Puklin-Faucher, E., Gauthier, N. C., Biais, N., & Sheetz, M. P. (2013). Integrin-dependent force transmission to the extracellular matrix by α-actinin triggers adhesion maturation. *Proceedings of the National Academy of Sciences of the United States of America*, *110*(15). https://doi.org/10.1073/pnas.1220723110

Romo, G. M., Dong, J. F., Schade, A. J., Gardiner, E. E., Kansas, G. S., Li, C. Q., … López, J. A. (1999). The glycoprotein Ib-IX-V complex is a platelet counterreceptor for P- selectin. *Journal of Experimental Medicine*, *190*(6), 803–813. https://doi.org/10.1084/jem.190.6.803

Rosa, J. P., Raslova, H., & Bryckaert, M. (2019). Filamin A: Key actor in platelet biology.

Blood, *134*(16), 1279–1288. https://doi.org/10.1182/blood.2019000014

Rosenberg, S., Stracher, a, & Burridge, K. (1981). Isolation and characterization of a calcium-sensitive alpha-actinin-like protein from human platelet cytoskeletons. *The Journal of Biological Chemistry*, *256*(24), 12986–12991. Retrieved from http://www.pubmedcentral.nih.gov/articlerender.fcgi?artid=1158224&tool=pmcentrez&rendertype=abstract

Rosenfeld, S. I., Looney, R. J., Leddy, J. P., Phipps, D. C., Abraham, G. N., & Anderson, C. L. (1985). Human platelet Fc receptor for immunoglobulin G. Identification as a 40,000-molecular-weight membrane protein shared by monocytes. *Journal of Clinical Investigation*, *76*(6), 2317–2322. https://doi.org/10.1172/JCI112242

Rosenfeld, S. I., Ryan, D. H., Looney, R. J., Anderson, C. L., Abraham, G. N., & Leddy, J. P. (1987). Human Fc gamma receptors: stable inter-donor variation in quantitative expression on platelets correlates with functional responses. *Journal of Immunology (Baltimore, Md. : 1950)*, *138*(9), 2869–2873. Retrieved from http://www.ncbi.nlm.nih.gov/pubmed/2952726

Rosovsky, R., Hong, F., Tocco, D., Connell, B., Mitsiades, C., Schlossman, R., … Richardson, P. (2013). Endothelial stress products and coagulation markers in patients with multiple myeloma treated with lenalidomide plus dexamethasone: An observational study. *British Journal of Haematology*, *160*(3), 351–358. https://doi.org/10.1111/bjh.12152

Rossaint, J., Margraf, A., & Zarbock, A. (2018). Role of platelets in leukocyte recruitment and resolution of inflammation. *Frontiers in Immunology*, *9*(NOV), 1–13. https://doi.org/10.3389/fimmu.2018.02712

Rottner, K., & Schaks, M. (2019). Assembling actin filaments for protrusion. *Current Opinion in Cell Biology*, *56*, 53–63. https://doi.org/10.1016/j.ceb.2018.09.004

Rottner, K., & Stradal, T. E. B. (2011). Actin dynamics and turnover in cell motility. *Current Opinion in Cell Biology*, *23*(5), 569–578. https://doi.org/10.1016/j.ceb.2011.07.003

Rupa-Matysek, J., Gil, L., Wojtasińska, E., Nowicki, A., Dytfeld, D., Kaźmierczak, M., & Komarnicki, M. (2014). Inhibitory effects of bortezomib on platelet aggregation in patients with multiple myeloma. *Thrombosis Research*, *134*(2), 404–411. https://doi.org/10.1016/j.thromres.2014.05.032

Ruzgys, P., Jakutavičiūtė, M., Šatkauskienė, I., Čepurnienė, K., & Šatkauskas, S. (2019). Effect of electroporation medium conductivity on exogenous molecule transfer to cells in vitro. *Scientific Reports*, *9*(1), 1–9. https://doi.org/10.1038/s41598-018-38287-8

Sabri, S., Foudi, A., Boukour, S., Franc, B., Charrier, S., Jandrot-Perrus, M., … Vainchenker, W. (2006). Deficiency in the Wiskott-Aldrich protein induces premature proplatelet formation and platelet production in the bone marrow compartment. *Blood*, *108*(1), 134–140. https://doi.org/10.1182/blood-2005-03-1219

Sallah, S., Husain, A., Wan, J., Vos, P., & Nguyen, N. P. (2004). The risk of venous thromboembolic disease in patients with monoclonal gammopathy of undetermined significance. *Annals of Oncology*, *15*(10), 1490–1494. https://doi.org/10.1093/annonc/mdh385

Sanfilippo, K. M., Luo, S., Wang, T.-F., Fiala, M., Schoen, M., Wildes, T. M., … Gage, B. F. (2019). Predicting venous thromboembolism in multiple myeloma: development and

validation of the IMPEDE VTE score. *American Journal of Hematology*. https://doi.org/10.1002/ajh.25603

Sangaletti, S., Tripodo, C., Chiodoni, C., Guarnotta, C., Cappetti, B., Casalini, P., … Colombo, M. P. (2012). Neutrophil extracellular traps mediate transfer of cytoplasmic neutrophil antigens to myeloid dendritic cells toward ANCA induction and associated autoimmunity. *Blood*, *120*(15), 3007–3018. https://doi.org/10.1182/blood-2012-03-416156

Sanger, J. M., Mittal, B., Pochapin, M. B., & Sanger, J. W. (1987). Stress fiber and cleavage furrow formation in living cells microinjected with fluorescently labeled α-actinin. *Cell Motility and the Cytoskeleton*, *7*(3), 209–220. https://doi.org/10.1002/cm.970070304

Sarma, J., Laan, C. A., Alam, S., Jha, A., Fox, K. A. A., & Dransfield, I. (2002). Increased platelet binding to circulating monocytes in acute coronary syndromes. *Circulation*, *105*(18), 2166–2171. https://doi.org/10.1161/01.CIR.0000015700.27754.6F

Sato, T., Fuse, A., Eguchi, M., Hayashi, Y., Ryo, R., Adachi, M., … Nakajima, H. (1989). Establishment of a human leukaemic cell line (CMK) with megakaryocytic characteristics from a Down's syndrome patient with acute megakaryoblastic leukaemia. *British Journal of Haematology*, *72*(2), 184–190. https://doi.org/10.1111/j.1365-2141.1989.tb07681.x

Savarese, M., Palmio, J., Poza, J. J., Weinberg, J., Olive, M., Cobo, A. M., … Udd, B. (2019). Actininopathy: A new muscular dystrophy caused by ACTN2 dominant mutations. *Annals of Neurology*, *85*(6), 899–906. https://doi.org/10.1002/ana.25470

Schachtner, H., Calaminus, S. D. J., Sinclair, A., Monypenny, J., Blundell, M. P., Leon, C., … Machesky, L. M. (2013). Megakaryocytes assemble podosomes that degrade matrix and protrude through basement membrane. *Blood*, *121*(13), 2542–2552. https://doi.org/10.1182/blood-2012-07-443457

Schick, U. M., Jain, D., Hodonsky, C. J., Morrison, J. V., Davis, J. P., Brown, L., … Reiner, A. P. (2016). Genome-wide Association Study of Platelet Count Identifies Ancestry-Specific Loci in Hispanic/Latino Americans. *American Journal of Human Genetics*, *98*(2), 229–242. https://doi.org/10.1016/j.ajhg.2015.12.003

Schiffhauer, E. S. S., Luo, T., Mohan, K., Srivastava, V., Qian, X., Griffis, E. R. R., … Robinson, D. N. N. (2016). Mechanoaccumulative Elements of the Mammalian Actin Cytoskeleton. *Current Biology*, *26*(11), 1473–1479. https://doi.org/10.1016/j.cub.2016.04.007

Schober, J. M., Lam, S. C.-T., & Wencel-Drake, J. D. (2003). Effect of cellular and receptor activation on the extent of integrin alphaIIbbeta3 internalization. *Journal of Thrombosis and Haemostasis*, *1*(11), 2404–2410. https://doi.org/10.1046/j.1538-7836.2003.00417.x

Schollmeyer, J. V., Rao, G. H. R., & White, J. G. (1978). An actin-binding protein in human platelets. Interactions with α-actinin on gelatin of actin and the influence of cytochalasin B. *American Journal of Pathology*, *93*(2), 433–446.

Schwarz, H., Heeb, M., Wencel-Drake, J., & Griffin, J. (1985). Identification and quantitation of protein S in human platelets. *Blood*, *66*(6), 1452–1455. Retrieved from https://europepmc.org/article/med/2933098

Schweinfurth, N., Hohmann, S., Deuschle, M., Lederbogen, F., & Schloss, P. (2010). Valproic

acid and all trans retinoic acid differentially induce megakaryopoiesis and platelet-like particle formation from the megakaryoblastic cell line MEG-01. *Platelets*, *21*(8), 648–657. https://doi.org/10.3109/09537104.2010.513748

Schwertz, H., Köster, S., Kahr, W. H. A., Michetti, N., Kraemer, B. F., Weitz, D. A., … Weyrich, A. S. (2010). Anucleate platelets generate progeny. *Blood*, *115*(18), 3801–3809. https://doi.org/10.1182/blood-2009-08-239558

Seano, G., & Primo, L. (2015). Podosomes and invadopodia: Tools to breach vascular basement membrane. *Cell Cycle*, *14*(9), 1370–1374. https://doi.org/10.1080/15384101.2015.1026523

Selvadurai, M. V, Hamilton, J. R., Selvadurai, M. V, & Hamilton, J. R. (2018). *Structure and function of the open canalicular system – the platelet ' s specialized internal membrane network Structure and function of the open canalicular system – the platelet ' s specialized internal membrane network*. *7104*. https://doi.org/10.1080/09537104.2018.1431388

Semeniak, D., Kulawig, R., Stegner, D., Meyer, I., Schwiebert, S., Bösing, H., … Schulze, H. (2016). Proplatelet formation is selectively inhibited by collagen type I through Syk-independent GPVI signaling. *Journal of Cell Science*, *129*(18), 3473–3484. https://doi.org/10.1242/jcs.187971

Semple, J. W., Italiano, J. E., & Freedman, J. (2011, April). Platelets and the immune continuum. *Nature Reviews Immunology*, Vol. 11, pp. 264–274. https://doi.org/10.1038/nri2956

Sen, S., Dong, M., & Kumar, S. (2009). Isoform-specific contributions of α-actinin to glioma cell mechanobiology. *PLoS ONE*, *4*(12), 8427. https://doi.org/10.1371/journal.pone.0008427

Senger, F., Pitaval, A., Ennomani, H., Kurzawa, L., Blanchoin, L., & Théry, M. (2019). Spatial integration of mechanical forces by α-actinin establishes actin network symmetry. *Journal of Cell Science*, *132*(22). https://doi.org/10.1242/jcs.236604

Shams, H., Golji, J., Garakani, K., & Mofrad, M. R. K. (2016). Dynamic Regulation of α-Actinin's Calponin Homology Domains on F-Actin. *Biophysical Journal*, *110*(6), 1444–1455. https://doi.org/10.1016/j.bpj.2016.02.024

Shams, H., Golji, J., & Mofrad, M. R. K. (2012a). A Molecular Trajectory of α-Actinin Activation. *Biophysical Journal*, *103*(10), 2050–2059. https://doi.org/10.1016/j.bpj.2012.08.044

Shams, H., Golji, J., & Mofrad, M. R. K. (2012b). A Molecular Trajectory of α-Actinin Activation. *Biophysical Journal*, *103*(10), 2050–2059. https://doi.org/10.1016/j.bpj.2012.08.044

Shams, H., & Mofrad, M. R. K. (2017). α-Actinin Induces a Kink in the Transmembrane Domain of β3-Integrin and Impairs Activation via Talin. *Biophysical Journal*, *113*(4), 948–956. https://doi.org/10.1016/j.bpj.2017.06.064

Shao, H., Li, S., Watkins, S. C., & Wells, A. (2014). α-Actinin-4 is required for amoeboid-type invasiveness of melanoma cells. *Journal of Biological Chemistry*, *289*(47), 32717–32728. https://doi.org/10.1074/jbc.M114.579185

Shao, H., Travers, T., Camacho, C., & Wells, A. (2013). The Carboxyl Tail of Alpha-Actinin-4 Regulates Its Susceptibility to m-Calpain and thus Functions in Cell Migration and

Spreading. *International Journal of Biochemistry and Cell Biology*, *45*(6), 1051–1063. https://doi.org/10.1016/j.biocel.2013.02.015

Shao, H., Wang, A., Lauffenburger, D., & Wells, A. (2018). Tyro3-mediated phosphorylation of ACTN4 at tyrosines is FAK-dependent and decreases susceptibility to cleavage by m-Calpain. *International Journal of Biochemistry and Cell Biology*, *95*, 73–84. https://doi.org/10.1016/j.biocel.2017.12.014

Shao, H., Wang, J. H.-C., Pollak, M. R., & Wells, A. (2010). α-Actinin-4 Is Essential for Maintaining the Spreading, Motility and Contractility of Fibroblasts. *PLoS ONE*, *5*(11), e13921. https://doi.org/10.1371/journal.pone.0013921

Shao, H., Wingert, B., Weins, A., Pollak, M. R., Camacho, C., & Wells, A. (2019). Focal segmental glomerulosclerosis ACTN4 mutants binding to actin: regulation by phosphomimetic mutations. *Scientific Reports*, *9*(1), 1–12. https://doi.org/10.1038/s41598-019-51825-2

Shao, H., Wu, C., & Wells, A. (2010). Phosphorylation of α-actinin 4 upon epidermal growth factor exposure regulates its interaction with actin. *Journal of Biological Chemistry*, *285*(4), 2591–2600. https://doi.org/10.1074/jbc.M109.035790

Sharda, A., & Flaumenhaft, R. (2018). The life cycle of platelet granules. *F1000Research*, Vol. 7. https://doi.org/10.12688/f1000research.13283.1

Shattil, S. J., Hoxie, J. A., Cunningham, M., & Brass, L. F. (1985). Changes in the platelet membrane glycoprotein IIb.IIIa complex during platelet activation. *Journal of Biological Chemistry*, *260*(20), 11107–11114.

Shekhonin, B. V, Domogatsky, S. P., Muzykantov, V. R., Idelson, G. L., & Rukosuev, V. S. (1985). Distribution of type I, III, IV and V collagen in normal and atherosclerotic human arterial wall: immunomorphological characteristics. *Collagen and Related Research*, *5*(4), 355–368. https://doi.org/10.1016/s0174-173x(85)80024-8

Shi, D. S., Smith, M. C. P., Campbell, R. A., Zimmerman, P. W., Franks, Z. B., Kraemer, B. F., … Weyrich, A. S. (2014). Proteasome function is required for platelet production. *Journal of Clinical Investigation*, *124*(9), 3757–3766. https://doi.org/10.1172/JCI75247

Shih, L., Kaplan, D., Kraiss, L. W., Casper, T. C., Pendleton, R. C., Peters, C. L., … Rondina, M. T. (2016). Platelet-Monocyte Aggregates and C-Reactive Protein are Associated with VTE in Older Surgical Patients. *Scientific Reports*, *6*, 27478–27478. https://doi.org/10.1038/srep27478

Shinagawa, A., Kojima, H., Berndt, M. C., Kaneko, S., Suzukawa, K., Hasegawa, Y., … Nagasawa, T. (2005). Characterization of a myeloma patient with a life-threatening hemorrhagic diathesis: Presence of a lambda dimer protein inhibiting shear-induced platelet aggregation by binding to the A1 domain of von Willebrand factor. *Thrombosis and Haemostasis*, *93*(5), 889–896. https://doi.org/10.1160/TH04-03-0193

Simeoni, I., Stephens, J. C., Hu, F., Deevi, S. V. V., Megy, K., Bariana, T. K., … Turro, E. (2016). A high-throughput sequencing test for diagnosing inherited bleeding, thrombotic, and platelet disorders. *Blood*, *127*(23), 2791–2803. https://doi.org/10.1182/blood-2015-12-688267

Simon, D. I., Chen, Z., Xu, H., Li, C. Q., Dong, J. F., McIntire, L. V., … López, J. A. (2000). Platelet glycoprotein Ibα is a counterreceptor for the leukocyte integrin Mac-1 (CD11b/CD18). *Journal of Experimental Medicine*, *192*(2), 193–204.

https://doi.org/10.1084/jem.192.2.193

Simon, L. M., Edelstein, L. C., Nagalla, S., Woodley, A. B., Chen, E. S., Kong, X., … Bray, P. F. (2014). Human platelet microRNA-mRNA networks associated with age and gender revealed by integrated plateletomics. *Blood*, *123*(16). https://doi.org/10.1182/blood-2013-12-544692

Sixma, J. J., Schiphorst, M. E., Verhoeckx, C., & Jockusch, B. M. (1982). Peripheral and integral proteins of human blood platelet membranes α-actinin is not identical to glycoprotein III. *Biochimica et Biophysica Acta (BBA)/Protein Structure and Molecular*, *704*(2), 333–344. https://doi.org/10.1016/0167-4838(82)90163-7

Sjöblom, B., Salmazo, A., & Djinović-Carugo, K. (2008). α-Actinin structure and regulation. *Cellular and Molecular Life Sciences*, *65*(17), 2688–2701. https://doi.org/10.1007/s00018-008-8080-8

Smethurst, P., & Cardigan, R. (2021). Current challenges in platelet transfusion. *Platelets*, *0*(0), 1–10. https://doi.org/10.1080/09537104.2021.1961711

Sobue, K., & Kanda, K. (1989). α-Actinins, Calspectin (Brain Spectrin or Fodrin), and Actin Participate in Adhesion and Movement of Growth Cones. *Neuron*, *3*(3), 311–319. https://doi.org/10.1016/0896-6273(89)90255-9

Södergren, A. L., & Ramström, S. (2018). Platelet subpopulations remain despite strong dual agonist stimulation and can be characterised using a novel six-colour flow cytometry protocol. *Scientific Reports*, *8*(1441). https://doi.org/10.1038/s41598-017-19126-8

Solari, F. A., Mattheij, N. J. A., Burkhart, J. M., Swieringa, F., Collins, P. W., Cosemans, J. M. E. M., … Zahedi, R. P. (2016). Combined quantification of the global proteome, phosphoproteome, and proteolytic cleavage to characterize altered platelet functions in the human scott syndrome. *Molecular and Cellular Proteomics*, *15*(10), 3154–3169. https://doi.org/10.1074/mcp.M116.060368

Solh, T., Botsford, A., & Solh, M. (2015). Glanzmann's thrombasthenia: pathogenesis, diagnosis, and current and emerging treatment options. *Journal of Blood Medicine*, *6*, 219–227. https://doi.org/10.2147/JBM.S71319

Soma, P., Swanepoel, A. C., du Plooy, J. N., Mqoco, T., & Pretorius, E. (2016). Flow cytometric analysis of platelets type 2 diabetes mellitus reveals "angry" platelets. *Cardiovascular Diabetology*, *15*(52). https://doi.org/10.1186/s12933-016-0373-x

Sorrentino, S., Studt, J., Bokstad, M., Medalia, O., & Sapra, K. T. (2016). Toward correlating structure and mechanics of platelets. *Cell Adhesion & Migration*, *10*(5), 568–575. https://doi.org/10.1080/19336918.2016.1173803

Sorrentino, S., Studt, J. D., Medalia, O., & Tanuj Sapra, K. (2015). Roll, adhere, spread and contract: Structural mechanics of platelet function. *European Journal of Cell Biology*, *94*(3–4), 129–138. https://doi.org/10.1016/j.ejcb.2015.01.001

Sprague, C. R., Fraley, T. S., Hyo, S. J., Lal, S., & Greenwood, J. A. (2008). Phosphoinositide binding to the substrate regulates susceptibility to proteolysis by calpain. *Journal of Biological Chemistry*, *283*(14), 9217–9223. https://doi.org/10.1074/jbc.M707436200

Srkalovic, G., Cameron, M. G., Rybicki, L., Deitcher, S. R., Kattke-Marchant, K., & Hussein, M. A. (2004). Monoclonal gammopathy of undetermined significance and multiple myeloma are associated with an increased incidence of venothromboembolic disease.

Cancer, *101*(3), 558–566. https://doi.org/10.1002/cncr.20405

Stalker, T. J., Welsh, J. D., Tomaiuolo, M., Wu, J., Colace, T. V., Diamond, S. L., & Brass, L. F. (2014). A systems approach to hemostasis: 3. Thrombus consolidation regulates intrathrombus solute transport and local thrombin activity. *Blood*, *124*(11), 1824–1831. https://doi.org/10.1182/blood-2014-01-550319

Stegner, D., Vaneeuwijk, J. M. M., Angay, O., Gorelashvili, M. G., Semeniak, D., Pinnecker, J., … Heinze, K. G. (2017). Thrombopoiesis is spatially regulated by the bone marrow vasculature. *Nature Communications*, *8*(1), 1–11. https://doi.org/10.1038/s41467-017-00201-7

Stenberg, P. E., Shuman, M. A., Levine, S. P., & Bainton, D. F. (1984). Redistribution of alpha-granules and their contents in thrombin-stimulated platelets. *Journal of Cell Biology*, *98*(2), 748–760. https://doi.org/10.1083/jcb.98.2.748

Stevens, H., & McFadyen, J. D. (2019). Platelets as Central Actors in Thrombosis - Reprising an Old Role and Defining a New Character. *Seminars in Thrombosis and Hemostasis*, *45*(8), 802–809. https://doi.org/10.1055/s-0039-1698829

Stickel, S., & Wang, Y. (1988). Vinculin from the Sites of Focal Contacts. *The Journal of Cell Biology*, *107*(September), 1231–1239.

Stocker, T. J., Ishikawa-Ankerhold, H., Massberg, S., & Schulz, C. (2017). Small but mighty: Platelets as central effectors of host defense. *Thrombosis and Haemostasis*, *117*(4), 651–661. https://doi.org/10.1160/TH16-12-0921

Stritt, S., Thielmann, I., Dütting, S., Stegner, D., & Nieswandt, B. (2014). Phospholipase D is a central regulator of collagen I-induced cytoskeletal rearrangement and podosome formation in megakaryocytes. *Journal of Thrombosis and Haemostasis*, *12*(8), 1364–1371. https://doi.org/10.1111/jth.12623

Suarez, C., & Kovar, D. R. (2016). Internetwork competition for monomers governs actin cytoskeleton organization. *Nature Reviews Molecular Cell Biology*, *17*(12), 799–810. https://doi.org/10.1038/nrm.2016.106

Sugiyama, T., Kohara, H., Noda, M., & Nagasawa, T. (2006). Maintenance of the Hematopoietic Stem Cell Pool by CXCL12-CXCR4 Chemokine Signaling in Bone Marrow Stromal Cell Niches. *Immunity*, *25*(6), 977–988. https://doi.org/10.1016/j.immuni.2006.10.016

Swieringa, F., Spronk, H. M. H., Heemskerk, J. W. M., & van der Meijden, P. E. J. (2018). Integrating platelet and coagulation activation in fibrin clot formation. *Research and Practice in Thrombosis and Haemostasis*, *2*(3), 450–460. https://doi.org/10.1002/rth2.12107

Tadokoro, S., Nakazawa, T., Kamae, T., Kiyomizu, K., Kashiwagi, H., Honda, S., … Tomiyama, Y. (2011). A potential role for -actinin in inside-out IIb 3 signaling. *Blood*, *117*(1), 250–258. https://doi.org/10.1182/blood-2009-10-246751

Tadokoro, Seiji, Nakazawa, T., Kamae, T., Kiyomizu, K., Kashiwagi, H., Honda, S., … Tomiyama, Y. (2011). Apotential role for α-actinin in inside-out αIIbβ3 signaling. *Blood*, *117*(1), 250–258. https://doi.org/10.1182/blood-2009-10-246751

Takagi, S., Tsukamoto, S., Park, J., Johnson, K. E., Kawano, Y., Moschetta, M., … Ghobrial, I. M. (2018). Platelets enhance multiple myeloma progression via il-1b upregulation. *Clinical Cancer Research*, *24*(10), 2430–2439. https://doi.org/10.1158/1078-0432.CCR-

17-2003

Takeuchi, K., Satoh, M., Kuno, H., Yoshida, T., Kondo, H., & Takeucni, M. (1998). Platelet-like particle formation in the human megakaryoblastic leukaemia cell lines, MEG-01 and MEG-01s. *British Journal of Haematology*, Vol. 100, pp. 436–444. https://doi.org/10.1046/j.1365-2141.1998.00576.x

Takubo, T, Hino, M., Suzuki, K., & Tatsumi, N. (1999). Relative distribution of myosin, actin, and alpha-actinin in adherent monocytes. *European Journal of Histochemistry : EJH*, *43*(1), 71–77. Retrieved from http://www.ncbi.nlm.nih.gov/pubmed/10340146

Takubo, Takayuki, Hino, M., Suzuki, K., & Tatsumi, N. (1998). Localization of myosin, actin, α-actinin, tropomyosin and vinculin in surface-activated, spreading human platelets. *Biotechnic and Histochemistry*, *73*(6), 310–315. https://doi.org/10.3109/10520299809141124

Talior-Volodarsky, I., Randhawa, V. K., Zaid, H., & Klip, A. (2008). α-actinin-4 is selectively required for insulin-induced GLUT4 translocation. *Journal of Biological Chemistry*, *283*(37), 25115–25123. https://doi.org/10.1074/jbc.M801750200

Tang, J., Taylor, D. W., & Taylor, K. A. (2001). The three-dimensional structure of α-actinin obtained by cryoelectron microscopy suggests a model for Ca2+-dependent actin binding. *Journal of Molecular Biology*, *310*(4), 845–858. https://doi.org/10.1006/jmbi.2001.4789

Tang, V. W., & Brieher, W. M. (2012). α-Actinin-4/FSGS1 is required for Arp2/3-dependent actin assembly at the adherens junction. *Journal of Cell Biology*, *196*(1), 115–130. https://doi.org/10.1083/jcb.201103116

Tardif, J. C., Tanguay, J. F., Wright, S. S., Duchatelle, V., Petroni, T., Grégoire, J. C., … L'Allier, P. L. (2013). Effects of the P-selectin antagonist inclacumab on myocardial damage after percutaneous coronary intervention for non-st-segment elevation myocardial infarction: Results of the SELECT-ACS trial. *Journal of the American College of Cardiology*, *61*(20), 2048–2055. https://doi.org/10.1016/j.jacc.2013.03.003

Tarone, G., Cirillo, D., Giancotti, F. G., Comoglio, P. M., & Marchisio, P. C. (1985). Rous sarcoma virus-transformed fibroblasts adhere primarily at discrete protrusions of the ventral membrane called podosomes. *Experimental Cell Research*, *159*(1), 141–157. https://doi.org/10.1016/S0014-4827(85)80044-6

Taylor, K. A., & Taylor, D. W. (1993). Projection Image of smooth muscle α-actinin from two-dimensional crystals formed on positively chargedlipid layers. *Journal of Molecular Biology*, *230*(1), 196–205. https://doi.org/10.1006/jmbi.1993.1136

Tentler, D., Lomert, E., Novitskaya, K., & Barlev, N. A. (2019). Role of ACTN4 in Tumorigenesis, Metastasis, and EMT. *Cells*, *8*(11), 1–16. https://doi.org/10.3390/cells8111427

Terpos, E., Kleber, M., Engelhardt, M., Zweegman, S., Gay, F., Kastritis, E., … Palumbo, A. (2015). European myeloma network guidelines for the management of multiple myeloma-related complications. *Haematologica*, *100*(10), 1254–1266. https://doi.org/10.3324/haematol.2014.117176

Tharabenjasin, P., Pabalan, N., & Jarjanazi, H. (2019). Association of the ACTN3 R577X (rs1815739) polymorphism with elite power sports: A meta-analysis. *PLoS ONE*, *14*(5), 1–20. https://doi.org/10.1371/journal.pone.0217390

The International Mouse Phenotyping Consortium. (n.d.). Retrieved October 6, 2020, from https://www.mousephenotype.org/data/genes/MGI:2137706

Thomas, D. G., & Robinson, D. N. (2017). The fifth sense: Mechanosensory regulation of alpha-actinin-4 and its relevance for cancer metastasis. *Seminars in Cell and Developmental Biology*, *71*, 68–74. https://doi.org/10.1016/j.semcdb.2017.05.024

Thomas, S. G., Poulter, N. S., Bem, D., Finney, B., Machesky, L. M., & Watson, S. P. (2017). The actin binding proteins cortactin and HS1 are dispensable for platelet actin nodule and megakaryocyte podosome formation. *Platelets*, *28*(4), 372–379. https://doi.org/10.1080/09537104.2016.1235688

Thon, J. N., Montalvo, A., Patel-Hett, S., Devine, M. T., Richardson, J. L., Ehrlicher, A., … Italiano, J. E. (2010). Cytoskeletal mechanics of proplatelet maturation and platelet release. *Journal of Cell Biology*, *191*(4), 861–874. https://doi.org/10.1083/jcb.201006102

Tian, Y., Hong, M., Jing, S., Liu, X., Wang, H., Wang, X., … Wang, Z. (2017). Clinical and Prognostic Effect of Plasma Fibrinogen in Renal Cell Carcinoma: A Meta-Analysis. *BioMed Research International*, Vol. 2017. https://doi.org/10.1155/2017/9591506

Tímár, J., Tóvári, J., Rásó, E., Mészáros, L., Bereczky, B., & Lapis, K. (2005). Platelet-Mimicry of Cancer Cells: Epiphenomenon with Clinical Significance. *Oncology*, *69*(3), 185–201. https://doi.org/10.1159/000088069

Timo Rademakers, Marieke Goedhart, Mark Hoogenboezem, Alexander García Ponce, Jos van Rijssel, Maryna Samus, … Jaap D van Buul. (2020). Hematopoietic stem and progenitor cells use podosomes to transcellularly cross the bone marrow endothelium. *Haematologica*, *105*(12), 2746–2756. https://doi.org/10.3324/haematol.2018.196329

Toth, B., Liebhardt, S., Steinig, K., Ditsch, N., Rank, A., Bauerfeind, I., … Reininger, A. J. (2008). Platelet-derived microparticles and coagulation activation in breast cancer patients. *Thrombosis and Haemostasis*, *100*(4), 663–669. https://doi.org/10.1160/TH07-10-0602

Travers, T., Shao, H., Joughin, B. A., Lauffenburger, D. A., Wells, A., & Camacho, C. J. (2015). Tandem phosphorylation within an intrinsically disordered region regulates ACTN4 function. *Science Signaling*, *8*(378), 1–10. https://doi.org/10.1126/scisignal.aaa1977

Travers, T., Shao, H., Wells, A., & Camacho, C. J. (2013). Modeling the assembly of the multiple domains of α-actinin-4 and its role in actin cross-linking. *Biophysical Journal*, *104*(3), 705–715. https://doi.org/10.1016/j.bpj.2012.12.003

Tricoci, P., Huang, Z., Held, C., Moliterno, D. J., Armstrong, P. W., Van De Werf, F., … Mahaffey, K. W. (2012). Thrombin-receptor antagonist vorapaxar in acute coronary syndromes. *New England Journal of Medicine*, *366*(1), 20–33. https://doi.org/10.1056/NEJMoa1109719

Trovati, M., Mularoni, E. M., Burzacca, S., Ponziani, M. C., Massucco, P., Mattiello, L., … Anfossi, G. (1995). Impaired insulin-induced platelet antiaggregating effect in obesity and in obese NIDDM patients. *Diabetes*, *44*(11), 1318–1322. https://doi.org/10.2337/diab.44.11.1318

Ts'ao, C. (1971). Rough Endoplasmic Reticulum and Ribosomes in Blood Platelets. *Scandinavian Journal of Haematology*, *8*(2), 134–140. https://doi.org/10.1111/J.1600-

0609.1971.TB01964.X

Tsai, A. W., Cushman, M., Rosamond, W. D., Heckbert, S. R., Tracy, R. P., Aleksic, N., & Folsom, A. R. (2002). Coagulation factors, inflammation markers, and venous thromboembolism: The longitudinal investigation of thromboembolism etiology (LITE). *American Journal of Medicine*, *113*(8), 636–642. https://doi.org/10.1016/S0002-9343(02)01345-1

Tsukada, N., Ackerley, C. A., & Phillips, M. J. (1995). The structure and organization of the bile canalicular cytoskeleton with special reference to actin and actin-binding proteins. *Hepatology*, *21*(4), 1106–1113. https://doi.org/10.1016/0270-9139(95)90262-7

van den Dries, K., Nahidiazar, L., Slotman, J. A., Meddens, M. B. M., Pandzic, E., Joosten, B., … Cambi, A. (2019). Modular actin nano-architecture enables podosome protrusion and mechanosensing. *Nature Communications*, *10*(1), 1–16. https://doi.org/10.1038/s41467-019-13123-3

van den Dries, K., Schwartz, S. L., Byars, J., Meddens, M. B. M., Bolomini-Vittori, M., Lidke, D. S., … Cambi, A. (2013). Dual-color superresolution microscopy reveals nanoscale organization of mechanosensory podosomes. *Molecular Biology of the Cell*, *24*(13), 2112–2123. https://doi.org/10.1091/mbc.E12-12-0856

van der Meijden, P. E. J., & Heemskerk, J. W. M. (2019, March 1). Platelet biology and functions: new concepts and clinical perspectives. *Nature Reviews Cardiology*, Vol. 16, pp. 166–179. https://doi.org/10.1038/s41569-018-0110-0

Van Gestel, M. A., Heemskerk, J. W. M., Slaaf, D. W., Heijnen, V. V. T., Sage, S. O., Reneman, R. S., & Oude Egbrink, M. G. A. (2002). Real-time detection of activation patterns in individual platelets during thromboembolism in vivo: Differences between thrombus growth and embolus formation. *Journal of Vascular Research*, *39*(6), 534–543. https://doi.org/10.1159/000067208

Van Nispen Tot Pannerden, H., De Haas, F., Geerts, W., Posthuma, G., Van Dijk, S., & Heijnen, H. F. G. (2010). The platelet interior revisited: Electron tomography reveals tubular α-granule subtypes. *Blood*, *116*(7), 1147–1156. https://doi.org/10.1182/blood-2010-02-268680

Varon, D., & Shai, E. (2015). Platelets and their microparticles as key players in pathophysiological responses. *Journal of Thrombosis and Haemostasis*, *13*(S1), S40–S46. https://doi.org/10.1111/jth.12976

Vasina, E. M., Cauwenberghs, S., Staudt, M., Feijge, M. A., Weber, C., Koenen, R. R., & Heemskerk, J. W. (2013). Aging- and activation-induced platelet microparticles suppress apoptosis in monocytic cells and differentially signal to proinflammatory mediator release. *American Journal of Blood Research*, *3*(2), 107–123. Retrieved from http://www.ncbi.nlm.nih.gov/pubmed/23675563%0Ahttp://www.pubmedcentral.nih.gov/articlerender.fcgi?artid=PMC3649808

Vasina, E., W.M. Heemskerk, J., Weber, C., & R. Koenen, R. (2010). Platelets and Platelet-Derived Microparticles in Vascular Inflammatory Disease. *Inflammation & Allergy - Drug Targets*, *9*(5), 346–354. https://doi.org/10.2174/187152810793938008

Verdirame, J., Feagler, J., & Commers, J. (1985). Multiple Myeloma Associated With Immune Thrombocytopenic Purpura. *Cancer*, *56*(5). https://doi.org/10.1002/1097-0142(19850901)56:5<1199::AID-CNCR2820560539>3.0.CO;2-8

Vicic, W. J., & Weiss, H. J. (1983). Evidence That Platelet Alpha-Granules Are a Major Determinant of Platelet Density: Studies in Storage Pool Deficiency. *Thrombosis and Haemostasis*, *50*(4), 878–880.

Vijey, P., Posorske, B., & Machlus, K. R. (2018). In vitro culture of murine megakaryocytes from fetal liver-derived hematopoietic stem cells. *Platelets*, *29*(6), 583–588. https://doi.org/10.1080/09537104.2018.1492107

Vincenot, A. et al. (2019). Novel ACTN1 variants in cases of thrombocytopenia. *Human Mutation*. https://doi.org/10.1002/humu.23840

Virel, A., & Backman, L. (2004). Molecular evolution and structure of α-actinin. *Molecular Biology and Evolution*, *21*(6), 1024–1031. https://doi.org/10.1093/molbev/msh094

Volkmer Ward, S. M., Weins, A., Pollak, M. R., & Weitz, D. A. (2008). Dynamic viscoelasticity of actin cross-linked with wild-type and disease-causing mutant α-actinin-4. *Biophysical Journal*, *95*(10), 4915–4923. https://doi.org/10.1529/biophysj.108.131722

Von Wichert, G., Haimovich, B., Feng, G. S., & Sheetz, M. P. (2003). Force-dependent integrin-cytoskeleton linkage formation requires downregulation of focal complex dynamics by Shp2. *EMBO Journal*, *22*(19), 5023–5035. https://doi.org/10.1093/emboj/cdg492

Wachsstock, D. H., Schwartz, W. H., & Pollard, T. D. (1993). Affinity of alpha-actinin for actin determines the structure and mechanical properties of actin filament gels. *Biophysical Journal*, *65*(1), 205–214. https://doi.org/10.1016/S0006-3495(93)81059-2

Wagner, H., Lood, C., Borna, C., Gidlöf, O., Truedsson, L., Brown, P., … Erlinge, D. (2016). Prasugrel 5 mg inhibits platelet P-selectin and GPIIb–IIIa expression in very elderly and non elderly: results from the GENERATIONS trial, a pharmacodynamic study in stable CAD patients. *Journal of Thrombosis and Thrombolysis*, *42*(3), 369–375. https://doi.org/10.1007/s11239-016-1372-1

Wang, G., Huang, W., Li, W., Chen, S., Chen, W., Zhou, Y., … Gu, W. (2018). TFPI-2 suppresses breast cancer cell proliferation and invasion through regulation of ERK signaling and interaction with actinin-4 and myosin-9. *Scientific Reports*, *8*(1), 1–12. https://doi.org/10.1038/s41598-018-32698-3

Wang, R., Stone, R. L., Kaelber, J. T., Rochat, R. H., Nick, A. M., Vijayan, K. V., … Chiu, W. (2015). Electron cryotomography reveals ultrastructure alterations in platelets from patients with ovarian cancer. *Proceedings of the National Academy of Sciences of the United States of America*, *112*(46), 14266–14271. https://doi.org/10.1073/pnas.1518628112

Wang, Yanhua, Sun, Y., Li, D., Zhang, L., Wang, K., Zuo, Y., … Liu, J. (2013). Platelet P2Y12 Is Involved in Murine Pulmonary Metastasis. *PLoS ONE*, *8*(11), e80780. https://doi.org/10.1371/journal.pone.0080780

Wang, Yunmei, Gao, H., Shi, C., Erhardt, P. W., Pavlovsky, A., Soloviev, D. A., … Simon, D. I. (2017). Leukocyte integrin Mac-1 regulates thrombosis via interaction with platelet GPIbα. *Nature Communications*, *8*. https://doi.org/10.1038/ncomms15559

Way, M., Pope, B., & Weeds, A. G. (1992). Evidence for functional homology in the F-actin binding domains of gelsolin and α-actinin: Implications for the requirements of severing and capping. *Journal of Cell Biology*, *119*(4), 835–842. https://doi.org/10.1083/jcb.119.4.835

Weins, A., Schlondorff, J. S., Nakamura, F., Denker, B. M., Hartwig, J. H., Stossel, T. P., & Pollak, M. R. (2007). Disease-associated mutant α-actinin-4 reveals a mechanism for regulating its F-actin-binding affinity. *Proceedings of the National Academy of Sciences of the United States of America*, *104*(41), 16080–16085. https://doi.org/10.1073/pnas.0702451104

Welsch, T., Keleg, S., Bergmann, F., Bauer, S., Hinz, U., & Schmidt, J. (2009). Actinin-4 Expression in Primary and Metastasized Pancreatic Ductal Adenocarcinoma. *Pancreas*, *38*(8), 968–976. https://doi.org/10.1097/MPA.0b013e3181b28d6f

Wendt, B., Hofmann, T., Martin, S. R., Bayley, P., Brodin, P., Grundstrom, T., … Forsen, S. (1988). Effect of amino acid substitutions and deletions on the thermal stability, the pH stability and unfolding by urea of bovine calbindin D9k. *FEBS*, *175*, 439–445. Retrieved from https://febs.onlinelibrary.wiley.com/doi/pdf/10.1111/j.1432-1033.1988.tb14214.x

Westbury, S. K., Shoemark, D. K., & Mumford, A. D. (2017). *ACTN1* variants associated with thrombocytopenia. *Platelets*, *28*(6), 625–627. https://doi.org/10.1080/09537104.2017.1356455

Westbury, S. K., Turro, E., Greene, D., Lentaigne, C., Kelly, A. M., Bariana, T. K., … Freson, K. (2015). Human phenotype ontology annotation and cluster analysis to unravel genetic defects in 707 cases with unexplained bleeding and platelet disorders. *Genome Medicine*, *7*(1), 36. https://doi.org/10.1186/s13073-015-0151-5

White, J. G. (1969). The submembrane filaments of blood platelets. *American Journal of Pathology*, *56*(2), 267–277.

White, James G. (2002). Electron dense chains and clusters in human platelets. *Platelets*, *13*(5–6), 317–325. https://doi.org/10.1080/0953770021000007267

White, James G, & Krumwiede, M. (1987). Further Studies of the Secretory Pathway in Thrombin-Stimulated Human Platelets. In *Blood* (Vol. 69). Retrieved from https://ashpublications.org/blood/article-pdf/69/4/1196/595973/1196.pdf?casa_token=7ZB2-NYbzpcAAAAA:0tmjKEouRdpjdHcEhN47yLcCVoVAHW4av4OyzkcotjZzZAnHWutMyRTmc2Rp8ScipCqhdUtB

Winkler, J., Lünsdorf, H., & Jockusch, B. M. (1997). Flexibility and fine structure of smooth-muscle α-actinin. *European Journal of Biochemistry*, *248*(1), 193–199. https://doi.org/10.1111/j.1432-1033.1997.00193.x

Wong, C. H. Y., Jenne, C. N., Petri, B., Chrobok, N. L., & Kubes, P. (2013). Nucleation of platelets with blood-borne pathogens on Kupffer cells precedes other innate immunity and contributes to bacterial clearance. *Nature Immunology*, *14*(8), 785–792. https://doi.org/10.1038/ni.2631

Wu, J.-Q., Rg Bähler, J., & Pringle, J. R. (2001). Roles of a Fimbrin and an-Actinin-like Protein in Fission Yeast Cell Polarization and Cytokinesis. In *Molecular Biology of the Cell* (Vol. 12).

Wyszynski, M., Kharazia, V., Shanghvi, R., Rao, A., Beggs, A. H., Craig, A. M., … Sheng, M. (1998). Differential regional expression and ultrastructural localization of α- actinin-2, a putative NMDA receptor-anchoring protein, in rat brain. *Journal of Neuroscience*, *18*(4), 1383–1392. https://doi.org/10.1523/jneurosci.18-04-01383.1998

Xu, J., Tseng, Y., & Wirtz, D. (2000). Strain hardening of actin filament networks: Regulation by the dynamic cross-linking protein α-actinin. *Journal of Biological Chemistry*, *275*(46), 35886–35892. https://doi.org/10.1074/jbc.M002377200

Yadav, S., & Storrie, B. (2017, February 17). The cellular basis of platelet secretion: Emerging structure/function relationships. *Platelets*, Vol. 28, pp. 108–118. https://doi.org/10.1080/09537104.2016.1257786

Yakimenko, A. O., Verholomova, F. Y., Kotova, Y. N., Ataullakhanov, F. I., & Panteleev, M. A. (2012). Identification of different proaggregatory abilities of activated platelet subpopulations. *Biophysical Journal*, *102*(10), 2261–2269. https://doi.org/10.1016/j.bpj.2012.04.004

Yamada, S., Yanamoto, S., Yoshida, H., Yoshitomi, I., Kawasaki, G., Mizuno, A., & Nemoto, T. K. (2010). RNAi-mediated down-regulation of α-actinin-4 decreases invasion potential in oral squamous cell carcinoma. *International Journal of Oral and Maxillofacial Surgery*, *39*(1), 61–67. https://doi.org/10.1016/j.ijom.2009.10.003

Yamaguchi, H., & Condeelis, J. (2007, May 1). Regulation of the actin cytoskeleton in cancer cell migration and invasion. *Biochimica et Biophysica Acta - Molecular Cell Research*, Vol. 1773, pp. 642–652. https://doi.org/10.1016/j.bbamcr.2006.07.001

Yamaguchi, H., Ito, Y., Miura, N., Nagamura, Y., Nakabo, A., Fukami, K., … Sakai, R. (2017). Actinin-1 and actinin-4 play essential but distinct roles in invadopodia formation by carcinoma cells. *European Journal of Cell Biology*, *96*(7), 685–694. https://doi.org/10.1016/j.ejcb.2017.07.005

Yamamoto, S., Tsuda, H., Honda, K., Kita, T., Takano, M., Tamai, S., … Matsubara, O. (2007). Actinin-4 expression in ovarian cancer: a novel prognostic indicator independent of clinical stage and histological type. *Modern Pathology*, *20*(12), 1278–1285. https://doi.org/10.1038/modpathol.3800966

Yamamoto, S., Tsuda, H., Honda, K., Takano, M., Tamai, S., Imoto, I., … Matsubara, O. (2012). ACTN4 gene amplification and actinin-4 protein overexpression drive tumour development and histological progression in a high-grade subset of ovarian clear-cell adenocarcinomas. *Histopathology*, *60*(7), 1073–1083. https://doi.org/10.1111/j.1365-2559.2011.04163.x

Yan, Q., Sun, W., Kujala, P., Lotfi, Y., Vida, T. A., & Bean, A. J. (2005). CART: An hrs/actinin-4/BERP/myosin V protein complex required for efficient receptor recycling. *Molecular Biology of the Cell*, *16*(5), 2470–2482. https://doi.org/10.1091/mbc.E04-11-1014

Yang, Xinrui, Pang, Y., Zhang, J., Shi, J., Zhang, X., Zhang, G., … Fu, L. (2019). High expression levels of ACTN1 and ACTN3 indicate unfavorable prognosis in acute myeloid leukemia. *Journal of Cancer*, *10*(18), 4286–4292. https://doi.org/10.7150/jca.31766

Yang, Xinyu, Wang, H., Zhang, M., Liu, J., Lv, B., & Chen, F. (2015, August 6). HMGB1: A novel protein that induced platelets active and aggregation via Toll-like receptor-4, NF-κB and cGMP dependent mechanisms. *Diagnostic Pathology*, Vol. 10. https://doi.org/10.1186/s13000-015-0348-3

Yao, J., Le, T. C., Kos, C. H., Henderson, J. M., Allen, P. G., Denker, B. M., & Pollak, M. R. (2004). α-Actinin-4-Mediated FSGS: An Inherited Kidney Disease Caused by an Aggregated and Rapidly Degraded Cytoskeletal Protein. *PLoS Biology*, *2*(6), e167. https://doi.org/10.1371/journal.pbio.0020167

Yasutomi, M., Kunishima, S., Okazaki, S., Tanizawa, A., Tsuchida, S., & Ohshima, Y. (2015). ACTN1 rod domain mutation associated with congenital macrothrombocytopenia. *Annals of Hematology*, *95*(1), 141–144. https://doi.org/10.1007/s00277-015-2517-6

Ye, N., Verma, D., Meng, F., Davidson, M. W., Suffoletto, K., & Hua, S. Z. (2014). Direct observation of α-actinin tension and recruitment at focal adhesions during contact growth. *Experimental Cell Research*, *327*(1), 57–67. https://doi.org/10.1016/j.yexcr.2014.07.026

Yin, H. L., & Janmey, P. A. (2003). Phosphoinositide Regulation of the Actin Cytoskeleton. *Annual Review of Physiology*, Vol. 65, pp. 761–789. https://doi.org/10.1146/annurev.physiol.65.092101.142517

Ylänne, J, Scheffzek, K., Young, P., & Saraste, M. (2001). Crystal structure of the alpha-actinin rod reveals an extensive torsional twist. *Structure (London, England : 1993)*, *9*(7), 597–604. Retrieved from http://www.ncbi.nlm.nih.gov/pubmed/11470434

Ylänne, Jari, Scheffzek, K., Young, P., & Saraste, M. (2001). Crystal structure of the α-actinin rod reveals an extensive torsional twist. *Structure*, *9*(7), 597–604. https://doi.org/10.1016/S0969-2126(01)00619-0

Yoon, K. J., Phelps, D. A., Bush, R. A., Remack, J. S., Billups, C. A., & Khoury, J. D. (2008). ICAM-2 Expression Mediates a Membrane-Actin Link, Confers a Nonmetastatic Phenotype and Reflects Favorable Tumor Stage or Histology in Neuroblastoma. *PLoS ONE*, *3*(11), e3629. https://doi.org/10.1371/journal.pone.0003629

Young, P, & Gautel, M. (2000). The interaction of titin and alpha-actinin is controlled by a phospholipid-regulated intramolecular pseudoligand mechanism. *The EMBO Journal*, *19*(23), 6331–6340. https://doi.org/10.1093/emboj/19.23.6331

Young, Paul, Ferguson, C., Bañuelos, S., & Gautel, M. (1998). Molecular structure of the sarcomeric Z-disk: Two types of titin interactions lead to an asymmetrical sorting of α-actinin. *EMBO Journal*, *17*(6), 1614–1624. https://doi.org/10.1093/emboj/17.6.1614

Young, Paul, & Gautel, M. (2000). *The interaction of titin and a -actinin is controlled by a phospholipid-regulated intramolecular pseudoligand mechanism*. *19*(23), 6331–6340.

Youssefian, T., Drouin, A., Massé, J. M., Guichard, J., & Cramer, E. M. (2002). Host defense role of platelets: Engulfment of HIV and Staphylococcus aureus occurs in a specific subcellular compartment and is enhanced by platelet activation. *Blood*, *99*(11), 4021–4029. https://doi.org/10.1182/blood-2001-12-0191

Zachou, K., Oikonomou, K., Renaudineau, Y., Chauveau, A., Gatselis, N., Youinou, P., & Dalekos, G. N. (2012). Anti-α actinin antibodies as new predictors of response to treatment in autoimmune hepatitis type 1. *Alimentary Pharmacology and Therapeutics*, *35*(1), 116–125. https://doi.org/10.1111/j.1365-2036.2011.04908.x

Zaid, Y., Puhm, F., Allaeys, I., Naya, A., Oudghiri, M., Khalki, L., … Boilard, E. (2020). Platelets Can Associate with SARS-Cov-2 RNA and Are Hyperactivated in COVID-19. *Circulation Research*, *127*(11), 1404–1418. https://doi.org/10.1161/CIRCRESAHA.120.317703

Zangari, M., Fink, L., Zhan, F., & Tricot, G. (2011). Low venous thromboembolic risk with bortezomib in multiple myeloma and potential protective effect with thalidomide/lenalidomide-based therapy: Review of data from phase 3 trials and studies of novel combination regimens. *Clinical Lymphoma, Myeloma and Leukemia*, *11*(2), 228–236. https://doi.org/10.1016/j.clml.2011.03.006

Zarbock, A., Singbartl, K., & Ley, K. (2006). Complete reversal of acid-induced acute lung injury by blocking of platelet-neutrophil aggregation. *Journal of Clinical Investigation*, *116*(12), 3211–3219. https://doi.org/10.1172/JCI29499

Zhan, X., Haudenschild, C. C., Ni, Y., Smith, E., & Huang, C. (1997). Upregulation of cortactin expression during the maturation of megakaryocytes. *Blood*, *89*(2), 457–464. https://doi.org/10.1182/blood.v89.2.457

Zhang, F., Wang, Y., Sun, P., Wang, Z. Q., Wang, D. S., Zhang, D. S., … Li, Y. H. (2017). Fibrinogen promotes malignant biological tumor behavior involving epithelial–mesenchymal transition via the p-AKT/p-mTOR pathway in esophageal squamous cell carcinoma. *Journal of Cancer Research and Clinical Oncology*, *143*(12), 2413–2424. https://doi.org/10.1007/s00432-017-2493-4

Zhang, J., Somani, A. K., & Siminovitch, K. A. (2000). Roles of the SHP-1 tyrosine phosphatase in the negative regulation of cell signalling. *Seminars in Immunology*, *12*(4), 361–378. https://doi.org/10.1006/smim.2000.0223

Zhang, W. H., Pan, H. F., Zhao, X. F., Ye, D. Q., Li, X. P., & Xu, J. H. (2010). Anti-α-actinin antibodies in relation to new-onset systemic lupus erythematosus and lupus nephritis. *Molecular Biology Reports*, *37*(3), 1341–1345. https://doi.org/10.1007/s11033-009-9513-7

Zhang, Y. Y., Tabataba, H., Liu, X. Y., Wang, J. Y., Yan, X. G., Farrelly, M., … Jin, L. (2018). ACTN4 regulates the stability of RIPK1 in melanoma. *Oncogene*, *37*(29), 4033–4045. https://doi.org/10.1038/s41388-018-0260-x

Zhao, X., Khurana, S., Charkraborty, S., Tian, Y., Sedor, J. R., Bruggman, L. A., & Kao, H. Y. (2017). α actinin 4 (ACTN4) regulates glucocorticoid receptor-mediated transactivation and transrepression in podocytes. *Journal of Biological Chemistry*, *292*(5), 1637–1647. https://doi.org/10.1074/jbc.M116.755546

Zhao, Z., Deocharan, B., Scherer, P. E., Ozelius, L. J., & Putterman, C. (2006). Differential Binding of Cross-Reactive Anti-DNA Antibodies to Mesangial Cells: The Role of α-Actinin. *The Journal of Immunology*, *176*(12), 7704–7714. https://doi.org/10.4049/jimmunol.176.12.7704

Zhou, J.-K., Fan, X., Cheng, J., Liu, W., & Peng, Y. (2021). PDLIM1: Structure, function and implication in cancer. *Cell Stress*, *5*(8), 119–127. https://doi.org/10.15698/cst2021.08.254

Zou, X., Qu, M., Fang, F., Fan, Z., Chen, L., Yue, W., … Pei, X. (2017). Small molecule supplements improve cultured megakaryocyte polyploidization by modulating multiple cell cycle regulators. *BioMed Research International*, *2017*. https://doi.org/10.1155/2017/2320519

Zucoloto, A. Z., & Jenne, C. N. (2019). Platelet-Neutrophil Interplay: Insights Into Neutrophil Extracellular Trap (NET)-Driven Coagulation in Infection. *Frontiers in Cardiovascular Medicine*, *6*(June), 1–8. https://doi.org/10.3389/fcvm.2019.00085

8.0 Appendix

Actinin-1 and Actinin-4 constructs used

For all experiments where full-length actinin-1 or actinin-4 were used. The non-muscle, exon 19a-containing, calcium-sensitive splice variant of human actinin-1 sequence was used (Accession no. NM_001102). The non-muscle, calcium-sensitive human actinin-4 sequence was used (Accession no. NM_004924).

Appendix Table 6.1 Antibodies Used for Immunofluorescent Staining

Antibody	**Manufacturer – Product No.**	**Dilution**
Vinculin	Sigma – V9131	1:200
MHCIIA	Biolegend - 909801	1:500
WASP	Santa Cruz Biotechnology – SC-13139	1:50
Phalloidin Rhodamine	Sigma - 77418	1:2000
Actinin (BM75.2)	Sigma – A5044	1:500
Actinin-4	Immunoglobe – 0042-05	1:250
CD61	Biolegend - 336402	1:100
CD29	Biolegend - 303001	1:100
β-Tubulin	Sigma – T5293	1:100
α-Rabbit-488	Jackson Immunoresearch – 711-545-152	1:1000
α-Mouse-488	Jackson Immunoresearch – 715-545-150	1:1000
α-Rabbit-Cy3	Jackson Immunoresearch – 711-165-152	1:1000
α-Mouse-Cy3	Jackson Immunoresearch – 715-165-150	1:1000

Appendix Table 6.2 Antibodies Used for Blotting

Antibody	**Manufacturer**	**Dilution**
β-Actin	Sigma – A5441	1:3000
GAPDH (Ms)	Sigma – G8795	1:2000
GAPDH (Rb)	Sigma – G9545	1:3000
His Tag	Genscript – A00186	1:5000
GST	Sigma – G1160	1:2000
GFP	Abcam – ab290	1:2000
FLAG	Sigma – F3156	1:2000
Actinin (H-2)	Santa Cruz Biotechnology – sc-17829	1:500
Actinin (H-300)	Santa Cruz Biotechnology – sc-15335	1:750
Actinin-4	Immunoglobe – 0042-05	1:1000
Phophotyrosine (PY20)	Biolegend - 309301	1:500
CD61	Biolegend - 336402	1:1000
FcγRIIa/CD32a	R&D Systems – AF-1875-SP	1:2000
Anti-Mouse IR700	Rockland Antibodies & Assays – 610-130-121	1:10,000
Anti-Mouse IR800	Li-Cor Biosciences – 926 32210	1:10,000
Anti-Rabbit IR700	Rockland Antibodies & Assays – 611-130-122	1:10,000
Anti-Rabbit IR800 (Gt polyclonal)	Li-Cor Biosciences – 926 32213	1:10,000
Anti-Rabbit IR800 (Dk)	Li-Cor Biosciences – 926 32211	1:10,000
TrueBlot Anti-mouse IgG	Rockland Antibodies & Assays – 18-8817-33	1:1000
TrueBlot Anti-rabbit IgG	Rockland Antibodies & Assays – 18-8816-31	1:1000
Anti-Human HRP	Jackson Immunoresearch – 109-035-190	1:1500
Anti- Rabbit HRP (Gt)	Jackson Immunoresearch – 111-035-003	1:1500
Anti-Mouse HRP (Gt)	Jackson Immunoresearch – 115-035-003	1:1500

Appendix Figure 6.1 Assessment of actinin antibody specificity for immunofluorescent staining of actinin-1 and actinin-4

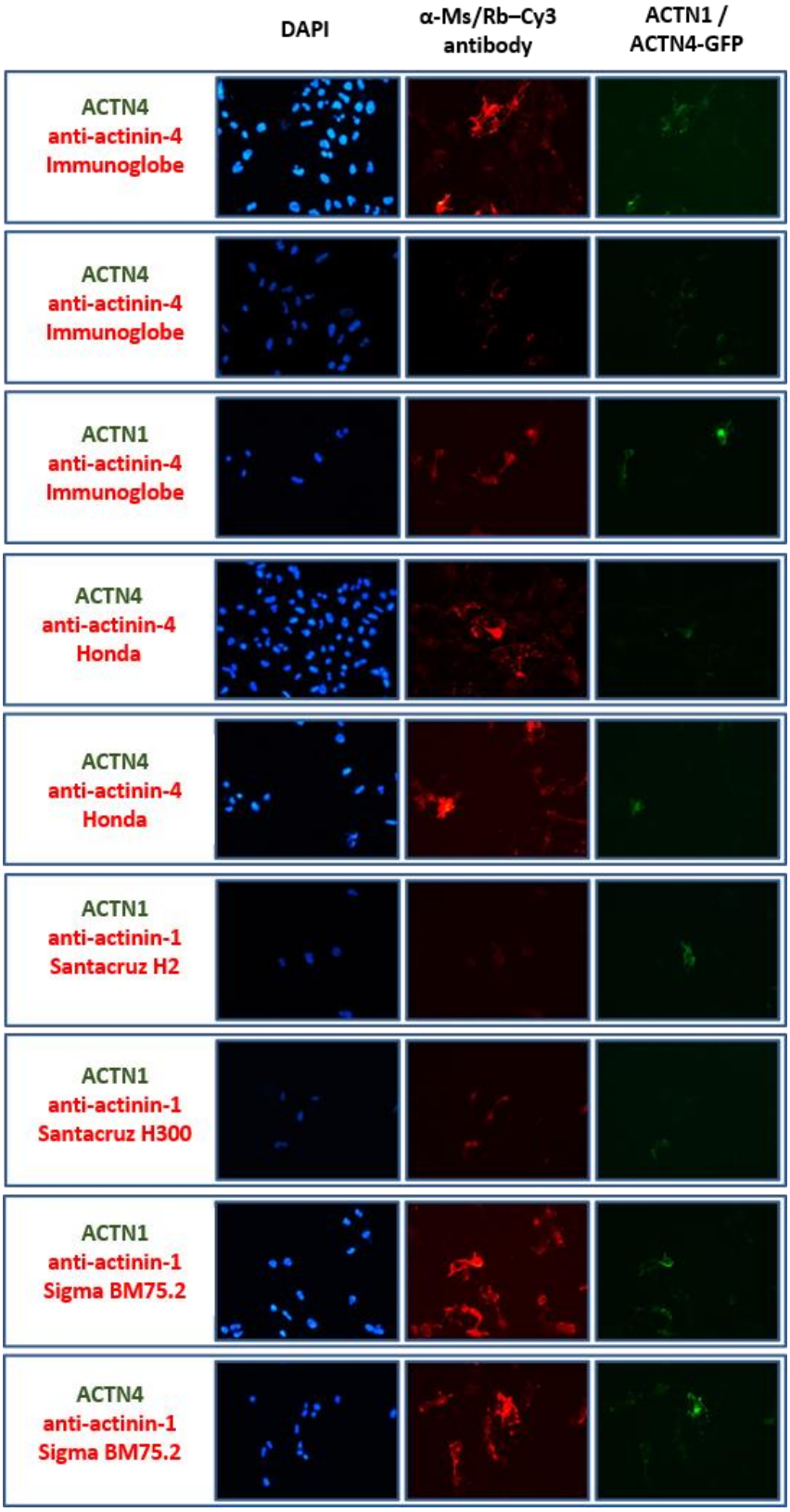

Appendix Figure 6.1 Assessment of actinin antibody specificity for immunofluorescent staining of actinin-1 and actinin-4. *HEK-293 cells expressing either actinin-1-GFP or actinin-*

4-GFP were stained with the indicated anti-actinin antibodies. Actinin-GFP expressing cells are imaged in the green channel. Anti-mouse or anti-rabbit Cy3-tagged secondary antibodies were used as appropriate to detect primary anti-actinin antibody staining in the same field, imaged in the red channel. DAPI shows nuclear staining. In each row, the actinin isoform being expressed by cells is indicated in green text. The antibodies used, including proposed specificity and supplier, are indicated in red text. Note for Honda antibody, the antibody was generously provided by Kaufumi Honda (Honda et al., 1998). Further details of the antibody staining protocol are available in Table 3.2.4.

Appendix Figure 6.2 Lentivirus plasmid maps

A. VSV-G

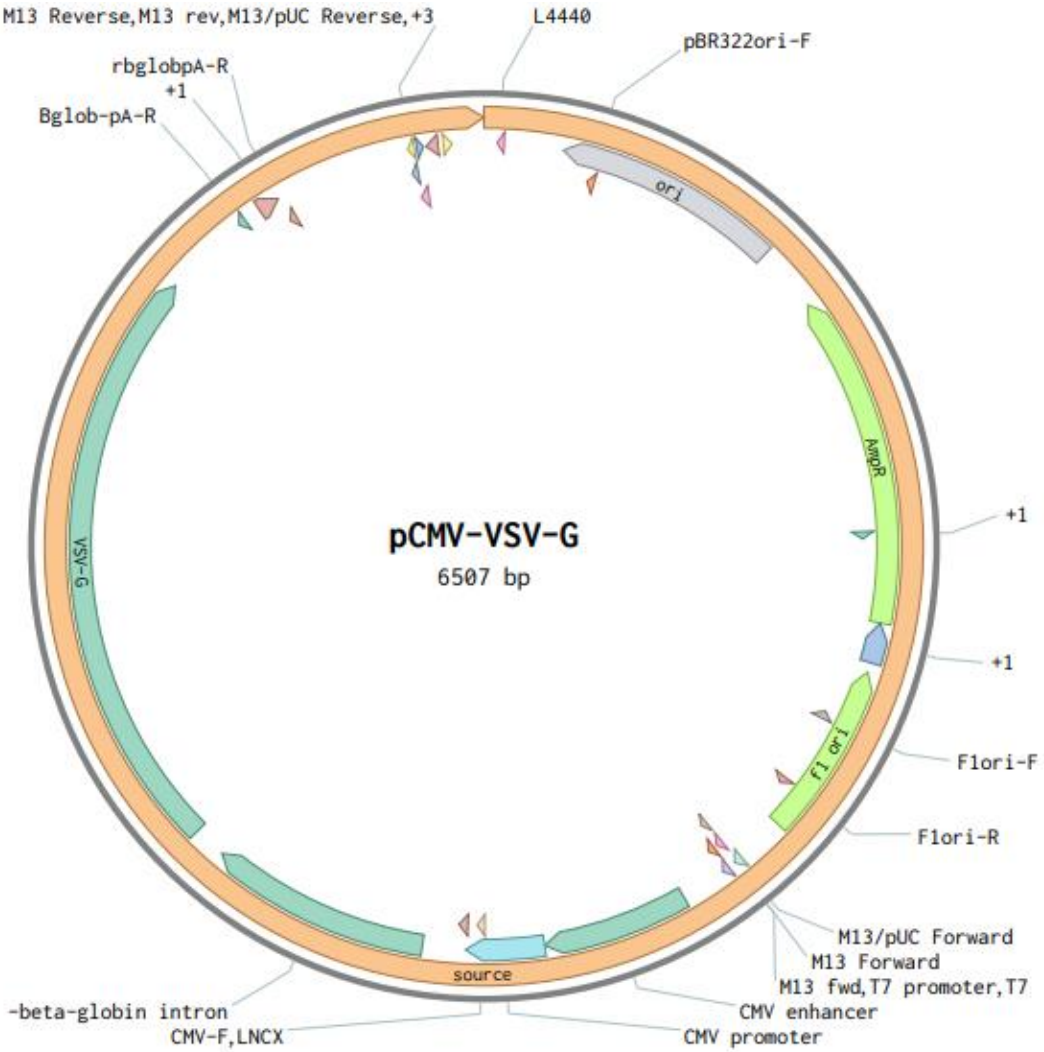

B. Δ8.9

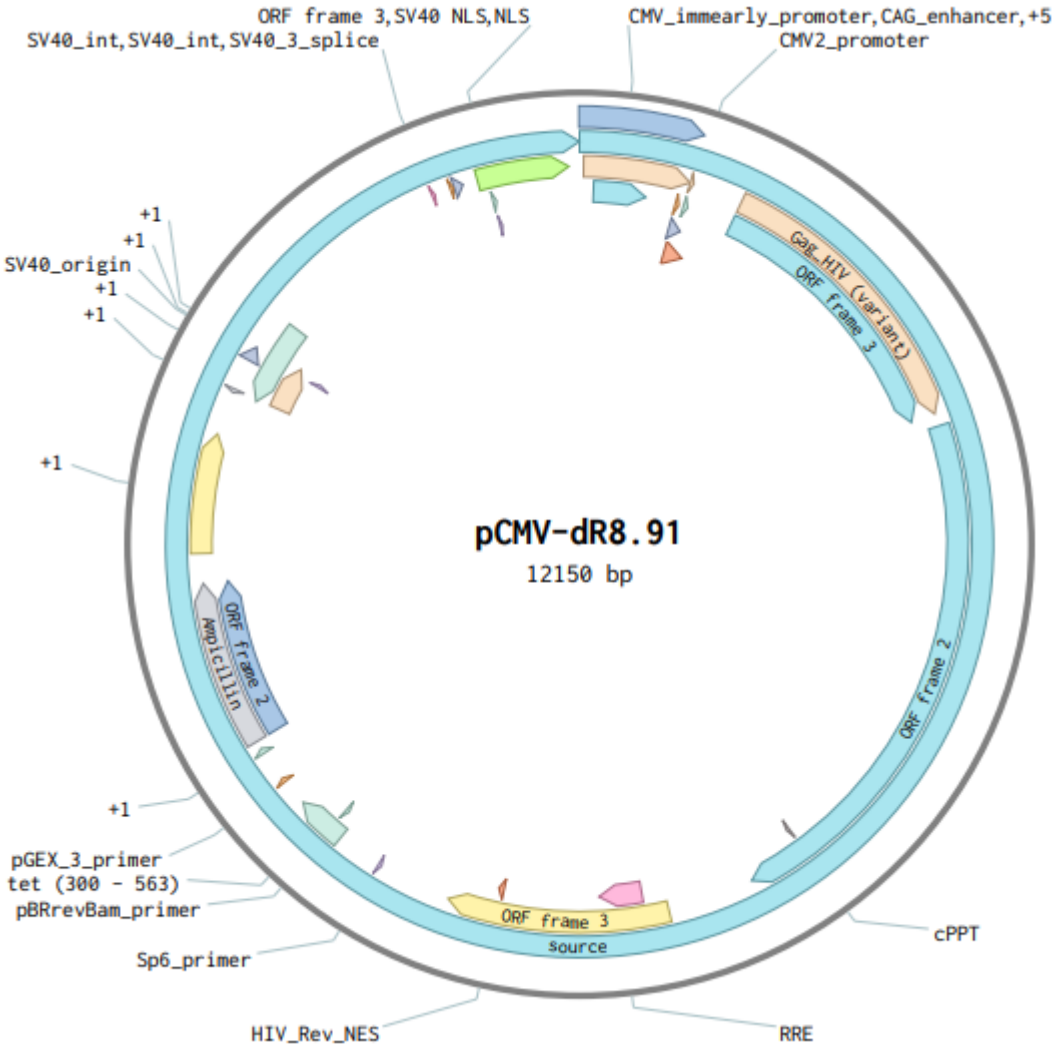
ORF frame 3,SV40 NLS,NLS
SV40_int,SV40_int,SV40_3_splice
CMV_immearly_promoter,CAG_enhancer,+5
CMV2_promoter
+1
+1
SV40_origin
+1
+1
+1
Gag_HIV (variant)
ORF frame 3
pCMV-dR8.91
12150 bp
ORF frame 2
Ampicillin
ORF frame 2
+1
pGEX_3_primer
tet (300 - 563)
pBRrevBam_primer
ORF frame 3
source
cPPT
Sp6_primer
HIV_Rev_NES
RRE

C. FUGW

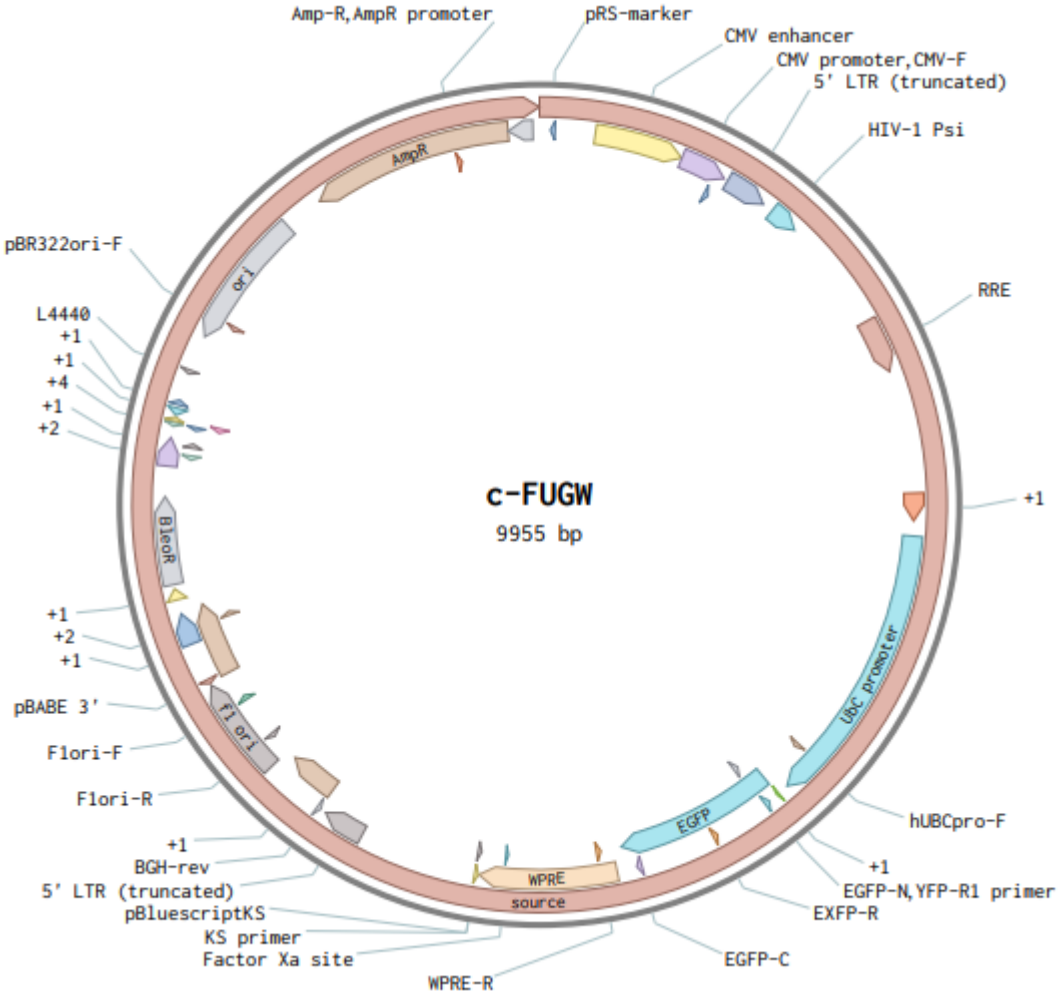
Amp-R,AmpR promoter
pRS-marker
CMV enhancer
CMV promoter,CMV-F
5' LTR (truncated)
HIV-1 Psi
RRE
+1
hUBCpro-F
+1
EGFP-N,YFP-R1 primer
EXFP-R
EGFP-C
WPRE-R
Factor Xa site
KS primer
pBluescriptKS
5' LTR (truncated)
+1
BGH-rev
F1ori-R
F1ori-F
pBABE 3'
+1
+2
+1
+1
+2
+1
+4
+1
+1
L4440
pBR322ori-F
AmpR
ori
BleoR
F1 ori
WPRE
source
EGFP
UbC promoter
c-FUGW
9955 bp